

Novel biocatalytic strategies for the synthesis of *N*-functionalised amino acids

Julia Hyslop

PhD thesis

Department of Pure and Applied Chemistry

University of Strathclyde in collaboration with GSK

2018

This thesis is the result of the author's original research. It has been composed by the author and has not been previously submitted for examination which has led to the award of a degree.

The copyright of this thesis belongs to GSK in accordance with the author's contract of engagement with GSK under the terms of the United Kingdom Copyright Acts. Due acknowledgement must always be made of the use of any material contained in, or derived from, this thesis.

Signed:

A handwritten signature in black ink, appearing to be 'J. S. L.' with a stylized flourish at the end.

Date:

29 May 2018

Contents

1. Introduction.....	21
1.1. N-Functionalised amino acids.....	21
1.2. Chemical synthesis of N-functionalised amino acids.....	24
1.2.1. N-Alkylation.....	25
1.2.2. Mitsunobu reaction.....	28
1.2.3. Reductive amination.....	29
1.2.4. Palladium catalysis.....	30
1.3. Enzymatic synthesis of N-functionalised amino acids.....	32
1.3.1. Opine dehydrogenases (ODHs).....	36
1.3.2. Ammonia lyases (ALs).....	40
1.3.3. Amino acid dehydrogenases (AADHs).....	41
1.3.4. Amine dehydrogenases (AmDHs).....	42
1.3.5. N-methyl transferases (NMTs).....	43
1.3.6. Imine reductases (IREDs).....	44
1.3.7. N-Methyl amino acid dehydrogenases (NMAADHs).....	48
1.3.8. Ketimine reductases (KIREDs).....	54
1.3.9. Pyrroline-5-carboxylate reductases (P5CRs).....	56
1.4. Conclusions.....	58
2. Objectives.....	59
3. Results and Discussion.....	62
3.1. Enzymes selection.....	62
3.2. Enzymes expression and purification.....	66
3.3. Reaction optimisation.....	69
3.3.1. pH profile and buffer impact.....	70
3.3.2. Substrate and catalyst loading.....	75
3.3.3. Enzyme formulation.....	79

3.4.	Enzyme screening.....	81
3.4.1.	Synthesis of product standards.....	82
3.4.2.	Screening plates assay.....	85
3.4.3.	Keto acid scope screening.....	87
3.4.4.	Amine scope screening	90
3.4.5.	Expanding the substrate scope	98
3.5.	Scale-up enzymatic reactions	104
3.6.	Molecular Docking.....	106
3.6.1.	Characterisation and crystal structure	106
3.6.2.	Rationalisation of the stereoselectivity	110
3.7.	Enzymatic cascades using NMAADHs for N-alkylation.....	112
3.7.1.	DAADH expression and purification.....	114
3.7.2.	DAADH activity assay.....	114
3.7.1.	DAADH formulation	116
3.7.2.	Enzymatic cascade optimisation	119
4.	Conclusions	123
5.	Future work	125
5.1.	Identification of other reductive amination biocatalysts	125
5.2.	Make improvements to the enzyme via mutagenesis	125
5.3.	Investigation of enzyme mechanism	127
5.4.	Correlation of conversions and imine formation.....	127
5.5.	Improvement to the N-alkylation cascade process.....	128
6.	Experimental	129
6.1.	Equipment	129
6.2.	Enzymes	130
6.2.1.	Enzyme selection	130
6.2.2.	Enzyme Expression.....	132
6.2.3.	Enzyme Purification.....	134
6.3.	Reaction optimisation.....	140

6.3.1.	Determination of pH optima	140
6.3.2.	Buffer concentration.....	141
6.3.3.	D-Glucose loading	141
6.3.4.	Amine and enzyme loading.....	142
6.3.5.	Enzyme formulation.....	143
6.4.	Method development	144
6.4.1.	Liquid chromatography	144
6.4.2.	Gas chromatography	148
6.4.3.	Spectrophotometric assay.....	148
6.5.	Screening	151
6.5.1.	General procedure for preparation of racemic N-alkylated amino acid standards.....	151
6.5.2.	General procedure for the synthesis of L-amino acid standards	157
6.5.3.	Small scale amine substrate scope screening	157
6.5.4.	Analysis of expressed recombinant protein for IRED plate screening	158
6.5.5.	General procedure for screening of IRED plate ⁵⁵	159
6.6.	Biocatalytic large scale reactions	160
6.6.1.	Scale-up procedure for 2-(methylamino)-3-phenylpropanoic acid based on literature conditions	78 160
6.6.2.	Scale-up procedure.....	161
6.7.	Molecular docking and crystal structure	162
6.7.1.	Screening of commercial crystallisation kits	162
6.7.2.	Optimisation of crystallisation conditions	162
6.7.3.	Co-crystallisation protocols	163
6.8.	Enzymatic cascade.....	164
6.8.1.	DAADH expression	164
6.8.2.	DAADH screening reaction	165
6.8.3.	Cascade protocol	165

7. References	166
8. Appendix	173
8.1. Buffer and solution ingredients	173
8.2. Experimental data	179

Table of figures

Figure 1. Disconnections used to synthesise N-methyl amino acids.	24
Figure 2. Sequential similarity of reductive amination enzymes.	35
Figure 3. Natural reactions of the enzyme classes that can carry out reductive aminations.	36
Figure 4. Examples of reactivity with different opine dehydrogenases.	39
Figure 5. Proposed mechanism of action for NMAADH.	50
Figure 6. Crystal structure of <i>P. syringae</i> NMAADH.	53
Figure 7. Three domains in NMAADH enzymes.	54
Figure 8. pH profile of <i>N. crassa</i> P5CR. ¹⁰⁵	57
Figure 9. Areas of substrate scope exploration	60
Figure 10. Structures of different enzyme classes.	65
Figure 11. Purification of En02 shown on gel electrophoresis.	66
Figure 12. SDS-PAGE gel showing expression of NMAADHs in BL21(DE3).	68
Figure 13. Comparison of activity levels in enzymes stored in buffer, without glycerol, before and after freezing.	69
Figure 14. pH profile of three NMAADHs (En01-03) based on initial rate.	71
Figure 15. Conversion over time using En01, without pH adjustment.	72
Figure 16. pH profile of En04-06 based on initial rate.	73
Figure 17. pH profile of En07 based on initial rate.	73
Figure 18. Effect of Tris HCl buffer (pH 8.5) concentration on conversion using En01.	74
Figure 19. Reaction mixture and reactor used for large scale reaction (3 g scale). ...	75
Figure 20. Reaction profile of large scale production of N-methyl phenylalanine 78 with En01.	75
Figure 21. NADPH consumption assay demonstration with controls.	77
Figure 22. Conversion to A desired product N-methyl phenylalanine 78 and B undesired product 3-phenyl lactic acid 138.	78
Figure 23. Conversion to A desired product N-methyl phenylalanine 78 and B undesired product 3-phenyl lactic acid 138.	79
Figure 24. Activity of lysate over time when refrigerated.	80
Figure 25. Product profile of En01 lysate versus lyophilised powder.	81

Figure 26. SDS-PAGE gel showing expression levels of En01-07 when grown in a 96 well plate.	86
Figure 27. Plate map of IRED panel.	99
Figure 28. Heat map representing conversion of 1-(4-fluorophenyl)propan-2-one 184 and methylamine 76 (10 equiv) at pH 7.0 after 24 h.	99
Figure 29. Heat map representing conversion of 1-(4-fluorophenyl)propan-2-one 184 and methylamine 76 (10 equiv) at pH 9.0.	100
Figure 30. Heat map representing conversion of 1-(4-fluorophenyl)propan-2-one 184 and methylamine 76 (1.1 equiv) at pH 9.0.	100
Figure 31. Heat map representing enantioselectivity of 1-(4-fluorophenyl)propan-2-one 184 and methylamine 76 (1.1 equiv) at pH 9.0.	101
Figure 32. Heat map representing conversion of 1-(4-fluorophenyl)propan-2-one 184 at pH 9.0 with 1.1 equivalent of amine 146.	101
Figure 33. Heat map representing conversion of 1-(4-fluorophenyl)propan-2-one 184 at pH 9.0 with 1.1 equivalent of amine 146.	102
Figure 34. Heat map representing conversion of 1-(4-fluorophenyl)propan-2-one 184 at pH 9.0 with 1.1 equivalent of amine 142.	102
Figure 35. Heat map representing conversion of phenyl pyruvate 122 at pH 7.0 with 10 equivalent of methylamine 76.	103
Figure 36. Heat map representing conversion of phenyl pyruvate 122 at pH 9.0 with 10 equivalent of methylamine 76.	104
Figure 37. Model of the crystal structure of NMAADH from <i>P. syringae</i> with the substrate phenyl pyruvate 122 docked.	107
Figure 38. A. <i>P. putida</i> NMAADH crystal giving the best resolution. B. Newly acquired crystal structure of <i>P. putida</i> NMAADH.	108
Figure 39. Comparison of new crystal structure of En01 (green) with existing structure of En02 (pink, 2CWH).	109
Figure 40. Model of En01 active site with product N-methyl phenylalanine 78 (yellow).	110
Figure 41. Model of En05 active site with compound N-methyl phenylalanine 78 (yellow).	111

Figure 42. Model of En07 active site with compound N-methyl phenylalanine 78 (yellow).	112
Figure 43. SDS Page gel showing the total and soluble expression of the two DAADH selected.	114
Figure 44. Reaction profile at different concentrations of methylamine.	116
Figure 45. Cascade reaction using purified enzyme and crude lysate combinations.	119
Figure 46. Cascade reaction profile using purified protein and catalytic co-factor, showing conversion to N-methylphenylalanine 78.	120
Figure 47. Cascade reaction profile, showing conversion to N-methylphenylalanine 78, with the addition of further DAADH, or both enzymes and co-factor at 210 h.	121
Figure 48. Heat maps showing the differences in conversion over time for different loadings of En08 (A) and En01 (B).	122
Figure 49. Active site of En01, with large residues that could be mutated to expand the active site highlighted in purple.	126
Figure 50. En01 purification SDS-PAGE.	135
Figure 51. En02 purification SDS-PAGE.	135
Figure 52. En03 purification SDS-PAGE.	136
Figure 53. En04 purification SDS-PAGE.	136
Figure 54. En05 purification SDS-PAGE.	137
Figure 55. En06 purification SDS-PAGE.	137
Figure 56. En07 purification SDS-PAGE.	138
Figure 57. En08 purification SDS-PAGE.	138
Figure 58. BSA calibration curve.	139
Figure 59. Calculated concentration of purified protein En01-08.	140
Figure 60. Plate layout for NMAADH pH optima determination.	141
Figure 61. Results of lowering glucose loading.	142
Figure 62. Plate layout for amine and enzyme loading screening.	143
Figure 63. Freeze dry recipe for lyophilisation of En01.	143
Figure 64. NADPH and NADP ⁺ absorbance between 200 and 800 nm.	149
Figure 65. Absorbance of reaction components (1 mM) between 200 and 800 nm.	150
Figure 66. Calibration of concentration of co-factor with absorbance.	151

Figure 67. Plate map for substrate scope screening.	158
Figure 68. Capillary electrophoresis analysis showing the profile of soluble protein extracts from E. coli expressing recombinant IREDs from the panel.....	159
Figure 69. Plate map of first optimisation screen.	163
Figure 70. Plate map of second optimisation screen.....	163

Table of tables

Table 1. Examples of secondary amines substrates in enzyme catalysed reductive amination. ⁸⁸	46
Table 2. Examples of secondary amines substrates in enzyme catalysed reductive amination. ⁵⁵	47
Table 3. Examples of reductive aminase catalysed reactions. ⁵⁴	48
Table 4. Range of keto acids and their relative activities (relative to reaction of pyruvate 58 and methylamine 76) when screened against <i>P. putida</i> NMAADH. ⁹² ...	51
Table 5. Variety of amines and their relative activities (relative to reaction of methyl pyruvate 58 and methylamine 76) when screened against <i>P. putida</i> NMAADH.....	52
Table 6. N-functionalised amino acids synthesised using a KIREd.	56
Table 7. Enzymes selected for screening.	63
Table 8. Percentage similarity of En01-07calculated using MOE v2015 software. ..	64
Table 9. Concentration of purified proteins calculated using Bradford assay	67
Table 10. Racemic standards preparation.	84
Table 11. L-enantiomers synthesised as product standards.	85
Table 12. Results of amine screening against hit plate.	87
Table 13. NMAADHs in reaction with several keto acids.....	88
Table 14. Other accepted keto acid substrates.	90
Table 15. Comparison of reductive amination activity between phenyl pyruvate 122 with different amines.....	93
Table 16. Comparison of reductive amination activity between phenyl pyruvate 122 with different amines.....	95
Table 17. Enantioselectivity of reactions between phenyl pyruvate 122 and different amines.	97
Table 18. Demonstration of NMAADH, KIREd and P5CR enzymes on a 200 mg scale.....	105
Table 19. DAADH and NMAADH catalysed reactions.	117
Table 20. Preparation of BSA stock solutions.	139
Table 21. Final concentrations calculated from Bradford assay.	140
Table 22. Reaction set up for D-glucose concentration reaction.	142

Table 23. Sample calculation for the conversion of lysate volume to lyophilised powder mass.....	144
Table 24. HPLC method 1.	145
Table 25. HPLC method 2.	145
Table 26. HPLC method 3.	146
Table 27. HPLC method 4.	147
Table 28. LCMS Method 5.	147
Table 29. LCMS Method 6.	147
Table 30. Mass directed auto preparation methods.....	148
Table 31. GC Chiral Method 7.....	148
Table 32. Molarity and absorbance of NADPH solutions.	150

Table of schemes

Scheme 1. Biologically active peptides containing N-functionalised amino acids. ..	22
Scheme 2. Example of naturally produced N-methylated peptide, thaxtomin A 5....	24
Scheme 3. Examples of N-methyl amino acid bio-active small molecules.	24
Scheme 4. Route to N-methyl amino acids via α -bromo esters.	25
Scheme 5. Examples of amino acid coupling using triflate leaving group. ^{32, 33}	26
Scheme 6. Examples of base mediated N-alkylation. ³⁸	27
Scheme 7. SPPS N-alkylation technique using an oNBS protecting group. ³⁶	27
Scheme 8. Mitsunobu/oNBS approach to N-alkylation in SPPS. ⁴²	28
Scheme 9. Example of Mitsunobu reaction employed in SPPS peptide synthesis for N-methylation. ⁴¹	29
Scheme 10. Example of reductive amination utilised to synthesise an N-methyl amino acid. ²⁷	29
Scheme 11. Example of Leuckart reaction used to synthesise N-methyl amino acids. ⁴⁵	30
Scheme 12. An example of N-methylation via a protecting group strategy. ⁴⁷	30
Scheme 13. SPPS N-alkylation technique using palladium catalysis. ³⁶	31
Scheme 14. Example of Buchwald-Hartwig coupling to synthesise an amino acid-flavone hybrid.	32
Scheme 15. Anthrobacter sp. opine dehydrogenase applied to the synthesis of phenylalanine. ⁶⁰	37
Scheme 16. An example of an octopine dehydrogenase catalysed reaction. ⁵⁹	37
Scheme 17. Alanopine dehydrogenase catalysed reaction.....	38
Scheme 18. Other opine dehydrogenase substrates.	38
Scheme 19. Examples of reactions possibly carried out by evolved opine dehydrogenases. ⁶⁵	40
Scheme 20. Generic ammonia lyase reaction.	41
Scheme 21. Example of PAL from <i>P. crispum</i> accepting N-methyl phenylalanine ..	41
Scheme 22. Alanine dehydrogenase catalysed reaction.....	42
Scheme 23. Step in Atazanavir synthesis, using a leucine dehydrogenase. ⁷²	42
Scheme 24. Engineered amine dehydrogenase catalysed reaction. ⁷⁶	43
Scheme 25. Example of an N-methyl transferase catalysed reaction. ²⁹	44

Scheme 26. Substrates of specific N-methyl transferases.....	44
Scheme 27. RIR and SIR imine reductases. ⁸⁵	45
Scheme 28. Lysine degradation pathway steps incorporating NMAADHs.....	49
Scheme 29. Reduction of pyrroline-2-carboxylate 117, a natural substrates of NMAADHs. ⁹¹	49
Scheme 30. General scheme of reactions shown in Table 4.....	51
Scheme 31. General scheme of reactions shown in Table 5.....	51
Scheme 32. Role of ketimine reductase in lysine metabolism. ⁹¹	55
Scheme 33. Sulfur containing imino acids accepted by ketimine reductases. ¹⁰⁴	55
Scheme 34. General scheme for the reaction of substrates in Table 6.....	56
Scheme 35. Reaction catalysed by P5CR enzymes. ¹⁰⁵	57
Scheme 36. Model biocatalytic reaction to investigate reductive amination potential of NMAADHs, KIREds and P5CRs	59
Scheme 37. Model reaction used for reaction optimisation.....	70
Scheme 38. Side reaction of the NMAADHs.	76
Scheme 39. Synthesis of racemic product standards.	82
Scheme 40. Synthesis of single enantiomer product standards.....	84
Scheme 41. Amine scope screening reaction used in Table 12.....	86
Scheme 42. Screening of alternative chain length keto acids.	88
Scheme 43. Wider scope of ketones screened.	89
Scheme 44. Reaction investigated in Table 15.	91
Scheme 45. Reaction shown in Table 16.	94
Scheme 46. Model reaction using 1-(4-fluorophenyl)propan-2-one 184 and methylamine 76 to synthesise amphetamine-like compound 185.	99
Scheme 47. Extension of the amine scope screened to include propargylamine 146.	101
Scheme 48. Extension of the amine scope screened to include amine 146.	102
Scheme 49. Examination of utility of IRED panel to synthesize N-methyl amino acids.	103
Scheme 50. Postulated N-methylation cascade.....	113
Scheme 51. DAADH catalysed reaction in the reductive direction.....	115
Scheme 52. Proposed route to the mixture of products generated in the cascade. ..	118

Scheme 53. Reaction being investigated in Figure 44.	121
Scheme 54. N-alkylation cascade process.	128
Scheme 55. Potential racemase step that could be incorporated into the active site.	128

Acknowledgments

I have been very fortunate to have the support of many wonderful people throughout my PhD, all of whom I would like to show my appreciation.

My GSK supervisors have provided important input to this project; Dr Peter W. Sutton, who started the project and gave me much constructive criticism, Dr Sarah L. Lovelock, who helped me through a difficult time and set me on the right track, and Dr Gheorghe-Doru Roiban, who was enthusiastic, encouraging and helped me give shape to the final product. My Strathclyde supervisor, Dr Allan J. B. Watson, provided excellent advice and rapid feedback.

There have been many people in the Synthetic Biochemistry team who have contributed expertise, taught me more about biocatalysis or helped improve my writing, to whom I am very grateful. I would also like to thank Dr Angela Bridges, Dr Colin Edge and Dr Marcelo Kern for passing on knowledge in their respective fields, and Dr Kristen Brown and Dr Chun-wa Chung for their contribution to the crystallography and modelling component of this project. Darrian Hollywood carried out the crystallisation screening experiments, and her experimental contribution was greatly appreciated.

Dr Harry Kelly and Dr William Kerr, the PhD programme coordinators, who have been continually involved and supportive, and enabled me to attend conferences. I appreciate my fellow PhD students, who have always been interested and provided honest feedback. There are also a number of people across the wider chemistry community at GSK Stevenage, all of whom have contributed to my time there.

I am thankful for the friends who have helped me, put up with me and stayed in touch in the last four years. My brother, who always has something to cheer me up, and my parents, who gave me every advantage.

Finally, I do not believe I could have gotten this far without the unending, tireless support of my fiancée Catherine. She has given me an endless supply of encouragement, despite the distance between us.

Abbreviations

Abbreviation	Definition
AADH	Amino acid dehydrogenase
AL	Ammonia lyase
AL	Ammonia lyase
Ala	Alanine
AlaDH	Alanine dehydrogenase
AMU	Atomic mass units
Arg	Arginine
BINAP	2,2-Bis(diphenylphosphino)-1,1-binaphthalene,
BLOSUM62	Blocks substitution matrix 62
Boc	<i>tert</i> -Butyloxycarbonyl
BSA	Bovine serum albumin
BuLi	Butyl lithium
CLANS	Cluster analysis of sequences
COSY	Homonuclear correlation spectroscopy
DAADH	D-Amino acid dehydrogenase
Db	Dibenzylideneacetone
DBU	1,8-Diazabicyclo(5,4,0)undec-7-ene
DCM	Dichloromethane
DEAD	Diethylazodicarboxylate
DIAD	Diisopropylazodicarboxylate
DMA	Dimethylacetamide
DMF	Dimethylformamide
DMSO	Dimethyl sulfoxide
DNA	Deoxyribonucleic acid
DTT	Dithiothreitol
EC	Enzyme classification
EC	Enzyme classification
EDTA	Ethylenediaminetetraacetic acid
FA	Formic acid

FID	Flame ionisation detector
Fmoc	Fluorenylmethyloxycarbonyl
GC	Gas chromatography
GDH	Glucose dehydrogenase
Gly	Glycine
HCl	Hydrochloric acid
HIV	Human immunodeficiency virus
HMBC	Heteronuclear multiple bond correlation
HPLC	High performance liquid chromatography
HRMS	High resolution mass spectroscopy
HSQC	Heteronuclear single quantum coherence
IPTG	Isopropyl β -D-1-thiogalactopyranoside
IRED	Imine reductase
KIRED	Ketimine reductase
LB	Luria-Bertani
LCMS	Liquid chromatography mass spectrometry
MDAP	Mass directed auto-purification
MeOH	Methanol
MIO	4-methylideneimidazole-5-one
MOE	Molecular operating environment
NAD ⁺	Nicotinamide adenine dinucleotide
NADH	Nicotinamide adenine dinucleotide hydride
NADP ⁺	Nicotinamide adenine dinucleotide phosphate
NADPH	Nicotinamide adenine dinucleotide phosphate hydride
NC	Negative control
Ni-NTA	Nickel nitrilotriacetic acid
NMAADH	<i>N</i> -Methyl amino acid dehydrogenase
NMDA	<i>N</i> -Methyl-D-aspartate
NMR	Nuclear magnetic resonance
NMT	<i>N</i> -Methyl transferase
NRPS	Non-ribosomal peptide synthase
ODH	Opine dehydrogenase

<i>o</i> NBS	<i>o</i> -Nitrobenzenesulfonyl
OpDH	Octopine dehydrogenase
P5CR	Pyrroline-5-carboxylate reductase
PAL	Phenylalanine ammonia lyase
PDB	Protein databank
PEG	Polyethylene glycol
RIR	(<i>R</i>)-imine reductase
SAM	<i>S</i> -Adenosyl methionine
SDS-PAGE	Sodium dodecyl sulfate polyacrylamide gel electrophoresis
SEASS	Seven-stranded anti-parallel β -sheet
SIR	(<i>S</i>)-imine reductase
SOC	Super optimal catabolite broth
SPPS	Solid phase peptide synthesis
StrDH	Strombine dehydrogenases
Tau	Taurine
TFA	Trifluoroacetic acid
THF	Tetrahydrofuran
Tris HCl	Tris(hydroxymethyl)aminomethane hydrochloride
UPLC	Ultra-performance liquid chromatography
UV	Ultraviolet
β -Ala	β -Alanine
β -AlaDH	β -Alanine dehydrogenase

Abstract

Chiral unnatural amino acids represent a class of building blocks that has gained significant attention within the pharmaceutical and agrochemical industries in recent years. Therefore, the availability of synthetic methods for novel unnatural *N*-protected α -amino acid derivatives is critical. Their synthesis has attracted considerable interest, however access to *N*-protected amino acids often requires the use of toxic reagents and hazardous solvents or stoichiometric quantities of hazardous hydrides.

A number of biocatalytic approaches to chiral amino acids have been reported in recent years that provide access to this class of compounds using greener, less hazardous methodologies, however the identification of enzyme classes that could carry out reactions efficiently under industrially applicable conditions with a large substrate scope still represents a challenge. To this end, the development of a panel of novel biocatalysts to carry out reductive amination reactions for use in large scale drug synthesis has been attempted in this project.

This entailed an examination of the existing wild type enzymes from three different classes (*N*-methylamino acid dehydrogenases, ketimine reductases and Δ^1 -pyrroline-5-carboxylate reductases), which required expression and screening. A variety of substrates were tested to determine the substrate scope of the enzymes. Additionally, a set of racemic product standards was selected and synthesised by chemical methods for comparison with the enzymatic products. This allowed the identification of new substrates that could be accepted for reductive amination, allowing for the synthesis of *N*-functionalised amino acids not previously accessible by enzyme catalysis.

Chapter 1: Introduction

NADPH Oxido-reductases and their role in the synthesis of *N*-functionalised amino acids

1. Introduction

The pharmaceutical industry, as all other manufacturing sectors, is increasingly concerned with the environmental impact of their processes.¹ Various technologies have been invested in and explored to achieve improved eco-friendliness in medicine manufacturing processes. Biocatalysis is one of the approaches that can be used, contributing several factors often associated with environmental friendliness. These include: use of water rather than other solvents, operation at ambient or near ambient temperatures and atmospheric pressure.¹

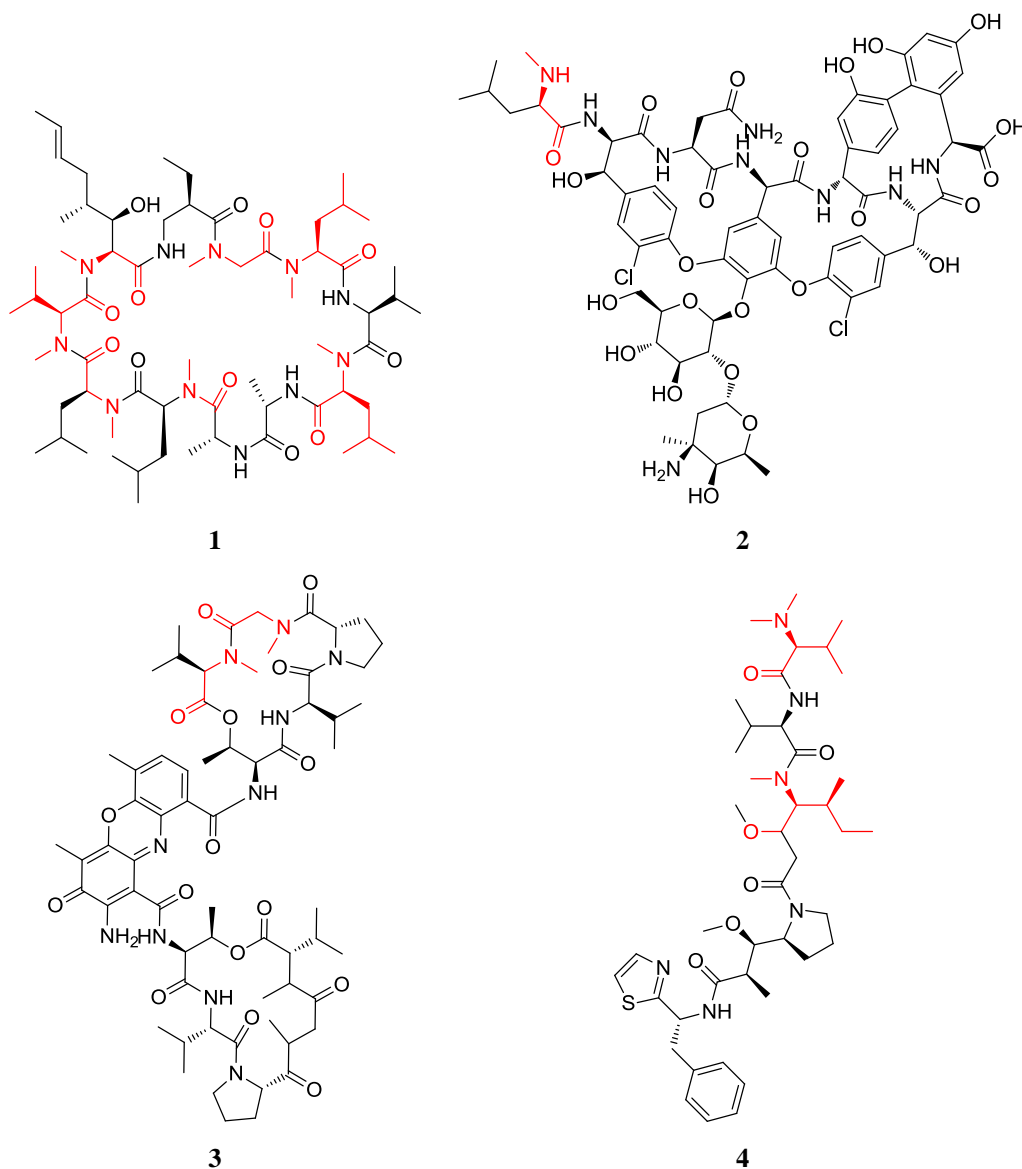
This project aims to characterise enzymes that can be used to synthesise *N*-functionalised amino acids. While there are currently a variety of methods to synthesise amino acids enzymatically, there are no approaches to make *N*-functionalised amino acids (as most enzymes can only incorporate ammonia as an amine). If a method could be developed, this would provide a useful strategy for making peptide building blocks in an environmentally friendly manner.

1.1. *N*-Functionalised amino acids

Unnatural chiral amino acids, as a class of building blocks, are highly important to the pharmaceutical and agrochemical industries.² Peptides have a high potential to be used as medicines, as there are many highly active peptide natural products that contain unnatural amino acids, such as cyclosporins (e.g. **1**), vancomycin **2**, actinomycins (e.g. **3**) and dolastatins (e.g. **4**) (**Scheme 1**). These compounds are non-ribosomal peptides (NRPs), small molecules involved in metabolism or with antibiotic or toxic effects.^{3, 4} They often incorporate non-proteinogenic amino acids, and there are examples of these NRPs being *N*- or *C*-methylated. Due to their complex structure peptide molecules can exist in multiple conformations, only one of which provides the desired activity.⁵ *N*-alkylation can help to fix the conformation, though in natural peptides *N*-methylation is the most common.⁶ This conformational biasing can affect the physical properties of the drug, as well as ensuring the desired conformation is achieved.

An example of the conformation being biased to the desired shape is cyclosporin A **1**, which has seven *N*-methylated amide bonds and four intramolecular hydrogen bonds that limit the number of possible conformations to the active structure, resulting in a

highly effective immunosuppressant.⁶ Vancomycin **2** is a highly effective, *N*-methyl group containing antibiotic, which binds to peptides and prevents cross-linking in cell wall formation in Gram positive bacteria.⁷ The *N*-methyl group increases the hydrophobicity of vancomycin and improves the binding to the peptides.⁸



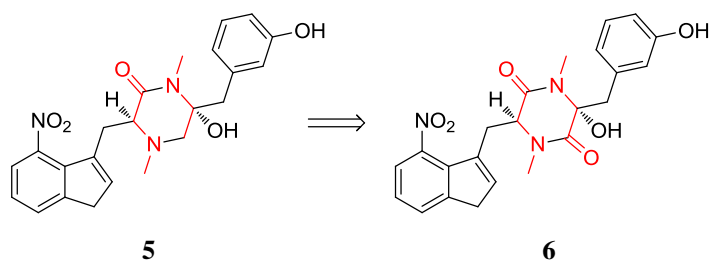
Scheme 1. Biologically active peptides containing *N*-functionalised amino acids. *N*-functionalised amino acids highlighted in red.^{7, 9-11}

Dolastatins are natural products noted for their anti-cancer activity, several of these compounds (such as **4**) contain *N*-methyl groups.¹⁰ While no dolastatins have been approved for clinical use, a derivative compound monomethyl auristatin E (which also

contains two *N*-methyl groups) has been approved for the treatment of a variety of cancers.¹²

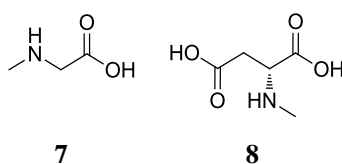
As has been briefly touched on in the preceding paragraph, *N*-functionalisation can increase the lipophilicity of the drug molecule. This can help improve the interaction with the receptor, if there is a hydrophobic pocket. *N*-Methylation can also affect the potency of peptides either positively or negatively. In one study Haviv *et al.* *N*-methylated all of the possible peptide bonds in several luteinising hormone releasing agonists and in all cases this resulted in reduced potency.¹³ However, there are several examples of peptides having vastly improved potency (in some cases greater than 200-fold improvement).^{14, 15}

Additionally, peptide drugs often have poor oral bioavailability and membrane permeability, due to their non-compliance with Lipinski's rules, as they are often high in molecular weight and replete with hydrogen bond donors and acceptors.¹⁶ These properties can be improved by *N*-methylation or alkylation as this will increase the lipophilicity and reduce the number of hydrogen bond donors.⁶ Gordon *et al.* were able to demonstrate that an *N*-methylated anti-amyloid peptide showed thirty-fold improved solubility, compared to the non-methylated counterpart, and was able to permeate phospholipid bi-layers far more effectively.¹⁷ Other examples were shown by White *et al.* with the methylation of a range of cyclic peptides, with the methylated derivatives showing significant improvement in solubility regardless of the position of the methyl group.¹⁸⁻²¹ *N*-methylation also reduces the susceptibility of NRPs to proteolytic cleavage, such as thaxtomins (for example thaxtomin A **5**, which is derived from **6**, **Scheme 2**).^{22, 23}



Scheme 2. Example of naturally produced *N*-methylated peptide, thaxtomin A **5**.

In addition to NRPs, there are also other small molecule drugs that incorporate *N*-alkylated amino acids. Examples of bioactive small molecules include sarcosine (*N*-methylglycine) **7** and *N*-methyl-D-aspartate (NMDA) **8** (Scheme 3).



Scheme 3. Examples of *N*-methyl amino acid bio-active small molecules.

It has been suggested that sarcosine could be used to treat depression and schizophrenia.²⁴ NDMA has been implicated in neural development and calcium channels, though neither of these compounds has been approved for clinical use.²⁵

1.2. Chemical synthesis of *N*-functionalised amino acids



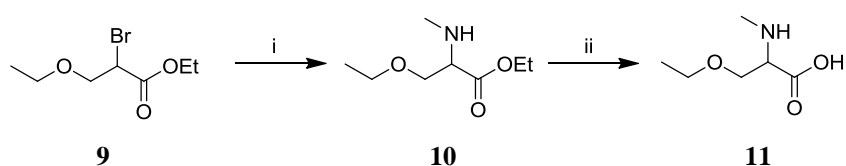
Figure 1. Disconnections used to synthesise *N*-methyl amino acids.

The availability of synthetic methods for novel unnatural *N*-protected α -amino acid derivatives is critical and their synthesis has attracted considerable interest.²⁶ There are two basic disconnections used to synthesise *N*-methyl amino acids (**Figure 1**), either by alkylating the primary amino acid (**A**) or by carrying out a substitution using an amine nucleophile (**B**). However, access to *N*-protected amino acids through *N*-alkylation or arylation often requires the use of toxic reagents and hazardous solvents.

Reductive aminations, the formation of an imine from a carbonyl and an amine with subsequent reduction, are a common method for installing alkyl groups. These are normally performed using stoichiometric quantities of hazardous hydrides, which are often flammable, require complex work-up procedures and generate high levels of waste.^{27, 28} Numerous chemical asymmetric approaches to reductive amination have been reported, but they have limitations such as the requirement to pre-form the imine (to avoid ketone reduction), narrow substrate range, the use of heavy metals or the use of ligands that are difficult to recover and recycle.^{29, 30}

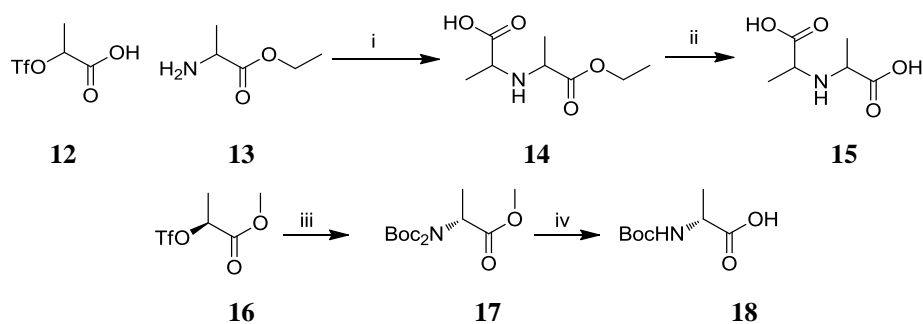
1.2.1. *N*-Alkylation

N-Alkylation is an atom efficient method of synthesising *N*-functionalised amino acids. There are various leaving groups that can be installed alpha to the acid. These include a limited number of examples incorporating the use of α -bromo esters and nucleophilic substitution with primary amines (**Scheme 4**), however these tend to result in low yields and high rates of racemization and are largely restricted to earlier syntheses.^{6, 31}



Scheme 4. Route to *N*-methyl amino acids via α -bromo esters. Reaction conditions: (i) ethyl-2-bromo-3-ethoxypropanoate (0.18 mol), methylamine (1.6 mol), 33% ethanol, 12 h, 100 °C, sealed tube. Yield: 52%. (ii) Excess hydrobromic acid (48%).³¹

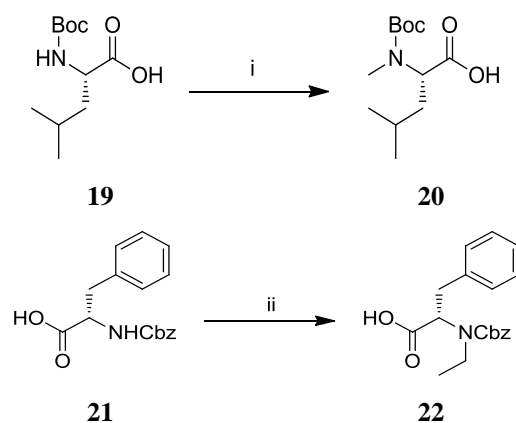
There are also examples where a triflate leaving group has been utilised, reducing the degree of racemization observed.³² As triflate is an effective leaving group lower temperatures are required for alkylation. Examples are shown in **Scheme 5**, demonstrating the lower temperatures needed, however this does require the α -hydroxy acid starting material.



Scheme 5. Examples of amino acid coupling using triflate leaving group.^{32,33} **Reaction conditions:** (i) THF 0 °C. (ii) HCl, NEt₃, yield 86-89%. (iii) Boc₂NH, BuLi, THF, 0 °C. (iv) TFA (1.5 equiv), DCM. Overall yield: 83%.

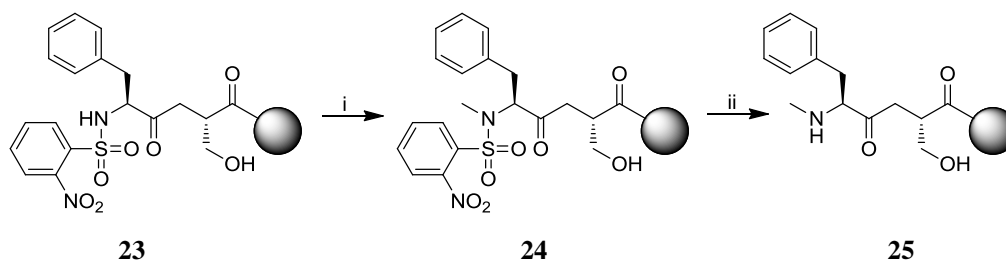
Another approach is to alkylate an *N*-protected amino acid. A note on protecting groups, as mono-alkylation can be difficult to achieve, the use of protecting groups can be required. It is common to carry out *N*-alkylation in the presence of a sulfonamide protecting group. These protecting groups, such as tosyl and nosyl, can be easily installed via the relevant chloride, but they require harsh conditions for their removal after methylation.³⁴ Other sulfonamide groups, such as ortho-nitrobenzene sulfonamide (*o*NBS) have become increasingly popular, particularly for use in solid phase peptide synthesis (SPPS) and can be cleaved with mercaptoethanol and other thiols.^{35,36} Alternatively carbamate protecting groups, such as *tert*-butyloxycarbonyl (Boc) and fluorenylmethyloxycarbonyl (Fmoc), are also frequently utilised and the different groups have a variety of cleavage conditions.³⁷

Base mediated alkylation can be used to install alkyl groups onto amino acids. This can be done in solution (**Scheme 6**) or as part of a SPPS (**Scheme 7**). Various bases can be employed for the deprotonation of amino acids, and these generally proceed with low levels of racemization.⁶



Scheme 6. Examples of base mediated N-alkylation.³⁸ Reaction conditions: (i) substrate **19** (5 mmol), sodium hydride (60% dispersion in mineral oil; 2 equiv), dimethyl sulfate (1.8 equiv), THF (22 mL), 17-20 °C, 2 h. Yield: 91%. (ii) substrate **21** (200 mM), ethyl iodide (8 equiv), sodium hydride (50% dispersion in mineral oil; 3 equiv), 0 to 60 °C, 48 h. Yield: 64%.³⁹

The use of sulfonamide protecting groups enhances the acidity of the amino acid NH, easing the deprotonation.⁶ A variety of methyl or alkyl sources can be used, such as the methyl nitrobenzene sulfonate shown in **Scheme 7**.³⁵

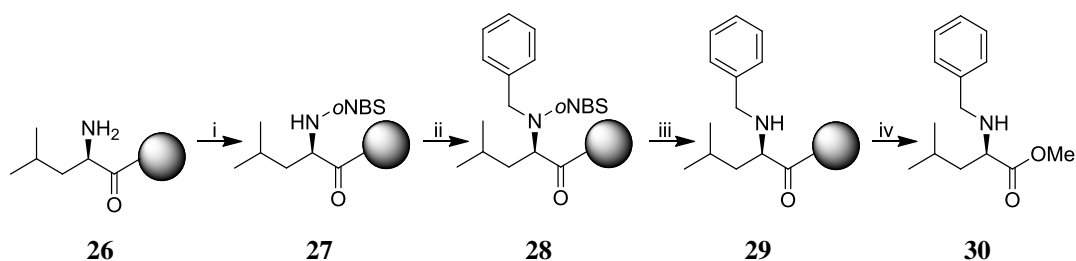


Scheme 7. SPPS N-alkylation technique using an *o*NBS protecting group.³⁶ Reaction conditions: (i) methyl 4-nitrobenzenesulfonate (4 equiv.), 7-methyl triazabicyclodec-5-ene (3 equiv), DMA, 30 min. (ii) 2-mercaptoethanol (10 equiv), DBU (5 equiv), DMF, 30 min. Synthesis on polystyrene residue.

Miller and co-workers attempted to employ sulfonamide protecting group strategy in conjunction with the Mitsunobu reaction discussed in the following section. They attempted both standard conditions and the modification shown by Tsunoda *et al.*, but were unsuccessful.^{35, 40} Therefore, they made use of the nucleophilic substitution approach shown in **Scheme 7**, and this sulphonamide is frequently employed in SPPS.³⁵

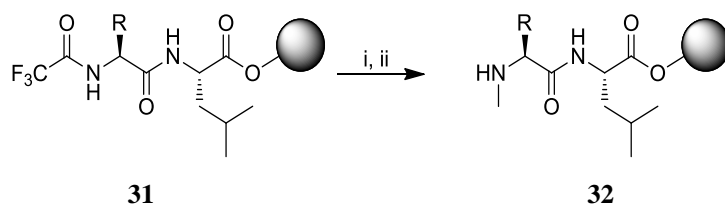
1.2.2. Mitsunobu reaction

Subsequent to the attempts of Miller *et al.* mentioned above, others have been successful in employing Mitsunobu reactions in the synthesis of *N*-alkyl amino acids, which is the standard method employed for *N*-alkylation in SPPS, in conjunction with *o*NBS protection (**Scheme 8**).⁴¹ This methodology, developed by Reichwein *et al.*, resulted from their finding that *N*-alkylated peptides were difficult to couple using standard amide coupling methods (such as *N,N'*-Diisopropylcarbodiimide (DIC) and benzotriazol-1-yloxytris (dimethylamino) phosphonium hexafluorophosphate (BOP)).⁴² This route allows for protection, deprotection and alkylation under mild conditions, but does use diethyl azodicarboxylate (DEAD) to carry out the reaction, which is both highly toxic and explosive.



Scheme 8. Mitsunobu/*o*NBS approach to *N*-alkylation in SPPS.⁴² Reaction conditions: (i) *o*NBS-C1 (5 equiv), DiPEA (5 equiv), DMF, 0.5 h. (ii) PPh₃ (5 equiv), EtOH (5 equiv), DEAD (5 equiv), DCM, 0.5 h. (iii) *t*-BuOK (3 equiv), PhSH (5 equiv), DMF, 0.5 h (iv) NaCN (catalytic), MeOH, 16 h. Overall yield: 57%.

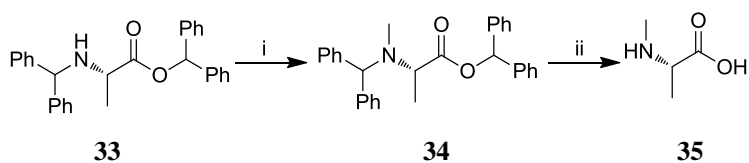
There are also examples of Mitsunobu alkylations being used for the synthesis of *N*-functionalised amino acids, with other protecting groups or in a non-solid supported reaction.⁴³ More recently this approach has been employed using the more environmentally friendly diisopropyl azodicarboxylate (DIAD) coupling agent and a trifluoroacetamide protecting group (**Scheme 9**), which could be cleaved using sodium borohydride.



Scheme 9. Example of Mitsunobu reaction employed in SPPS peptide synthesis for *N*-methylation.
⁴¹ Reaction conditions: R = natural amino acid side chains. (i) PPh₃ (750 mM, 5 equiv), DIAD (750 mM), MeOH (1500 mM), rt, 30 min. Yields: >95%. (ii) NaBH₄ (1500 mM), rt, 30 min, quantitative.

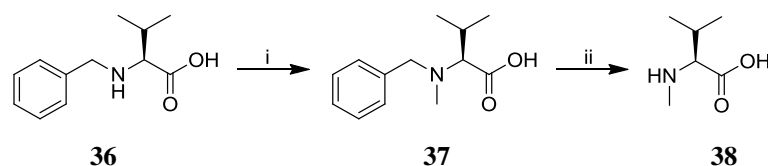
1.2.3. Reductive amination

Reductive aminations are often employed for the synthesis of C-N bonds and involve the use of a carbonyl and amine to form an imine or Schiff base, which can then be reduced to give the final product. Reductive aminations are normally performed using stoichiometric quantities of hazardous hydrides, which are often flammable and generate high levels of waste.^{6, 26, 27} An example is shown in **Scheme 10**, using formaldehyde to incorporate a methyl group.²⁷



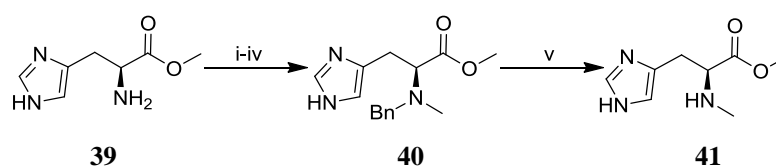
Scheme 10. Example of reductive amination utilised to synthesise an *N*-methyl amino acid.²⁷
 Reaction conditions: (i) formaldehyde, NaBH₃CN, pH-5-7. Yield: 77%. (ii). H₂, Pd/C, MeOH. Yield: 91%.

A variety of hydride reducing agents can be employed, with varying efficiency, to carry out the imine reduction step. However, ease of imine formation is substrate dependant and reductive amination can vary in efficacy dependant on substrate type. This was shown by McGonagle *et al.*, who carried out an analysis of the conversion of a variety of carbonyl and amine classes in different solvents and with different reducing agents.⁴⁴ While this paper is a useful tool for predicting reductive amination success, it does not distinguish between the ease of imine formation and the impact of solvent and reducing agent. The substrates will have an impact on the ease of imine formation, through a combination of the steric and electronic effects of both reactants.



Scheme 11. Example of Leuckart reaction used to synthesise *N*-methyl amino acids.⁴⁵ Reaction conditions: (i) formic acid (150 mmol, 3 equiv.), formaldehyde (60 mmol, 1.2 equiv.). (ii) Pd/C, H₂. Yield: 36%.

The Leuckart reaction is also used to methylate amino acids, with a palladium catalysed hydrogenolysis step. This synthesis was first demonstrated by Quitt and co-workers, and shown to be applicable to a wide range of *N*-methyl amino acids by Ebata *et al.* in yields between 3 and 42% (**Scheme 11**).^{45, 46}

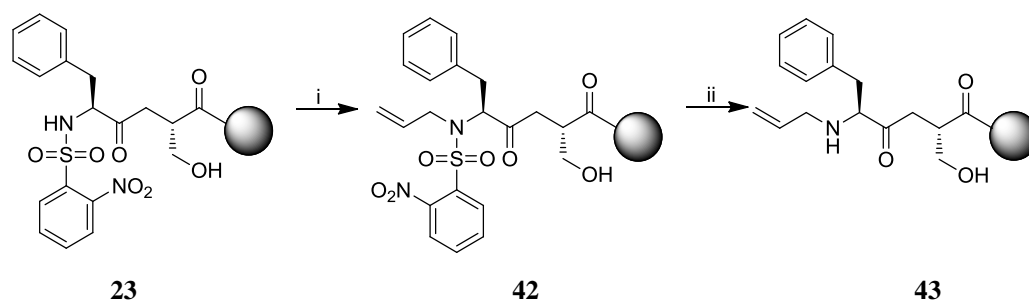


Scheme 12. An example of *N*-methylation via a protecting group strategy.⁴⁷ Reaction conditions: (i) Substrate 39 (100 mM), benzaldehyde (105 mM), methanol, 1 h. (ii) NaBH₃CN (105 mM), 18 h. (iii) paraformaldehyde (105 mM), until dissolved. (iv) NaBH₃CN (105 mM), 18 h. (v) 40 (100 mM), Pd(OH)₂ (0.5 weight equiv), H₂ (55 psi), 18 h. Yield: 98%.

Another example of reductive amination applied to *N*-methylated amino acid synthesis is demonstrated by White *et al.* (**Scheme 12**).⁴⁷ This makes use of benzyl protected amino acids prior to *N*-methylation with paraformaldehyde. While this route does have multiple steps, steps i-iv can be telescoped. However, while the publication claims a diverse range of amino acids, only naturally occurring D- and L-amino acid have been demonstrated.

1.2.4. Palladium catalysis

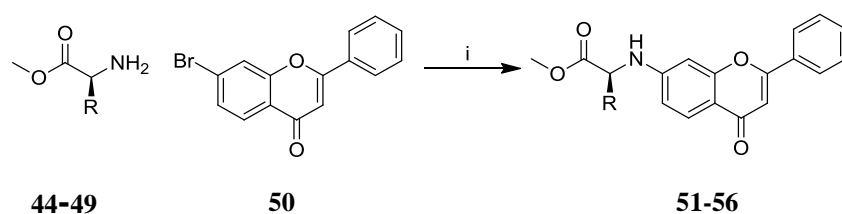
Palladium catalysed cross coupling can also be used to incorporate alkyl groups. The example shown in **Scheme 13** is an alternative route from Miller *et al.* as shown in **Scheme 7**, which incorporates an allyl group via palladium cross coupling.³⁶

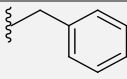
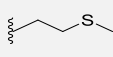
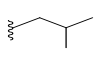
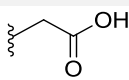

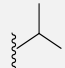


Scheme 13. SPPS *N*-alkylation technique using palladium catalysis.³⁶ Reaction conditions: (i) allyl methyl carbonate (15 equiv.), Pd₂dba₃ (10 mol%), PPh₃ (80mol%), THF, 2 h; (ii) 2-mercaptoethanol (10 equiv.), DBU (5 equiv.), DMF, 30 min. Synthesis on polystyrene resin. Yield: 98%.

This process allows an allyl group to be incorporated at 10 mol% palladium loading. Again, in this instance the *o*NBS protecting group increases the acidity of the NH of the amino acid and is compatible with the palladium cross-coupling. While the researchers achieved this reaction in very high yield (98%), they found that the product could not be coupled effectively through SPPS. When this was attempted with HATU and Fmoc-phenylalanine a yield of only 5% resulted, somewhat reducing the usefulness of this derivatives.³⁶

While Buchwald-Hartwig chemistry is frequently applied to the synthesis of alkyl or arylamino substituted cycles, there are very few examples of amino acid functionalisation.^{48, 49} The majority of these examples deal with the synthesis of flavone derivatives, which are known to inhibit cyclin-dependant kinases. It has been suggested that this inhibition could be used in chemotherapy for treatment of breast cancer.⁵⁰ As cyclin dependant kinases are involved in cell cycle regulation. If they can be selectively inhibited in cancer cells it will result in cell death, and therefore the mitigation of the cancer.⁵⁰



R=	Yield [%]	ee [%]	R=	Yield [%]	ee [%]
	74	75		75	87
	66	93		30	56
	65	86		37	98

Scheme 14. Example of Buchwald-Hartwig coupling to synthesise an amino acid-flavone hybrid. Reaction conditions: (i) Amino acid methyl ester **44-49** (110 mM), bromoflavone **50** (110 mM, 1 equiv), Pd(OAc)₂ (10 mol%), BINAP (15 mol%), Cs₂CO₃ (285 mM, 2.6 equiv), pressure tube, 3 h, 110°C.

A recent paper from Konya *et al.* noted that this method was limited by a high degree of racemisation (ee < 10%) and poor regioselectivity on the flavone component.⁴⁹ The example shown in **Scheme 14**, represents a more recent synthesis, which has overcome the racemization problem by carrying out a base and ligand screen to speed up the reductive elimination step and avoid β-hydride elimination.⁴⁸ However, even with these improved conditions, the ee is only high for some compounds. Aspartate **46** gave only 56% ee, while valine **48** resulted in 98% ee, so these findings appear to be substrate dependant.

1.3. Enzymatic synthesis of *N*-functionalised amino acids

Several biocatalytic approaches to the synthesis of chiral amino acids have been reported in recent years, which provide access to this class of compounds using greener, less hazardous methodologies. While there are a number of enzymes that can carry out reductive amination, there are very few examples that can be applied to amino

acids. The members of the common enzyme classes and their relationship in theoretical sequence space are shown in

Figure 2.

These enzymes have been analysed using a technique called cluster analysis of sequences (CLANs), this allows for large numbers of protein sequences to be analysed and visualised in a practical manner.⁵¹ Representation of this volume data as a phylogenetic tree is not practical and difficult to interpret, whereas the plots generated from CLANs allows the visualisation seen in

Figure 2.⁵² This software operates by grouping enzymes based on both their annotations (which are assigned by researchers to indicate proposed enzymatic function) and sequence.⁵² However, as this plot is generated in three dimensions, for representation here this figure has been compressed into a two-dimensional image.

Each cluster (indicated by a black oval in

Figure 2) is composed of a sample of enzymes (each represented by a small sphere) in that class, which have a high sequence homology. An enlargement of each cluster is also shown in

Figure 2, for clarity. The distance between these clusters shows that they are sequentially distinct from each other and have a low homology. The large grey sphere represents the theoretical sequence space in which these enzymes fall. This theoretical sequence space is generated based on the sequences used in the generation of this figure and does not represent the entirety of enzyme space.

There are several enzyme classes that can accept amines in an NAD(P)H dependent reductive amination manner and provide amino acids. The different enzyme clusters (shown in

Figure 2) are sequentially very diverse, suggesting they do not share a common ancestor. While the reactivity of the different clusters appears similar, the sequences and fold patterns are different and the homology between these clusters is low.

The only related clusters shown in

Figure 2 are the NMAADHs and lactate dehydrogenases. Lactate dehydrogenases are not discussed here as they do not synthesise amino acids, but they are structurally similar to NMAADHs. This has led to some NMAADHs being mis-classified as lactate dehydrogenases (as this class was established earlier than the NMAADH super-

family). Lactate dehydrogenases reduce carbonyl groups to alcohols and this has implications on the activity of the NMAADHs, which will be discussed in later sections.

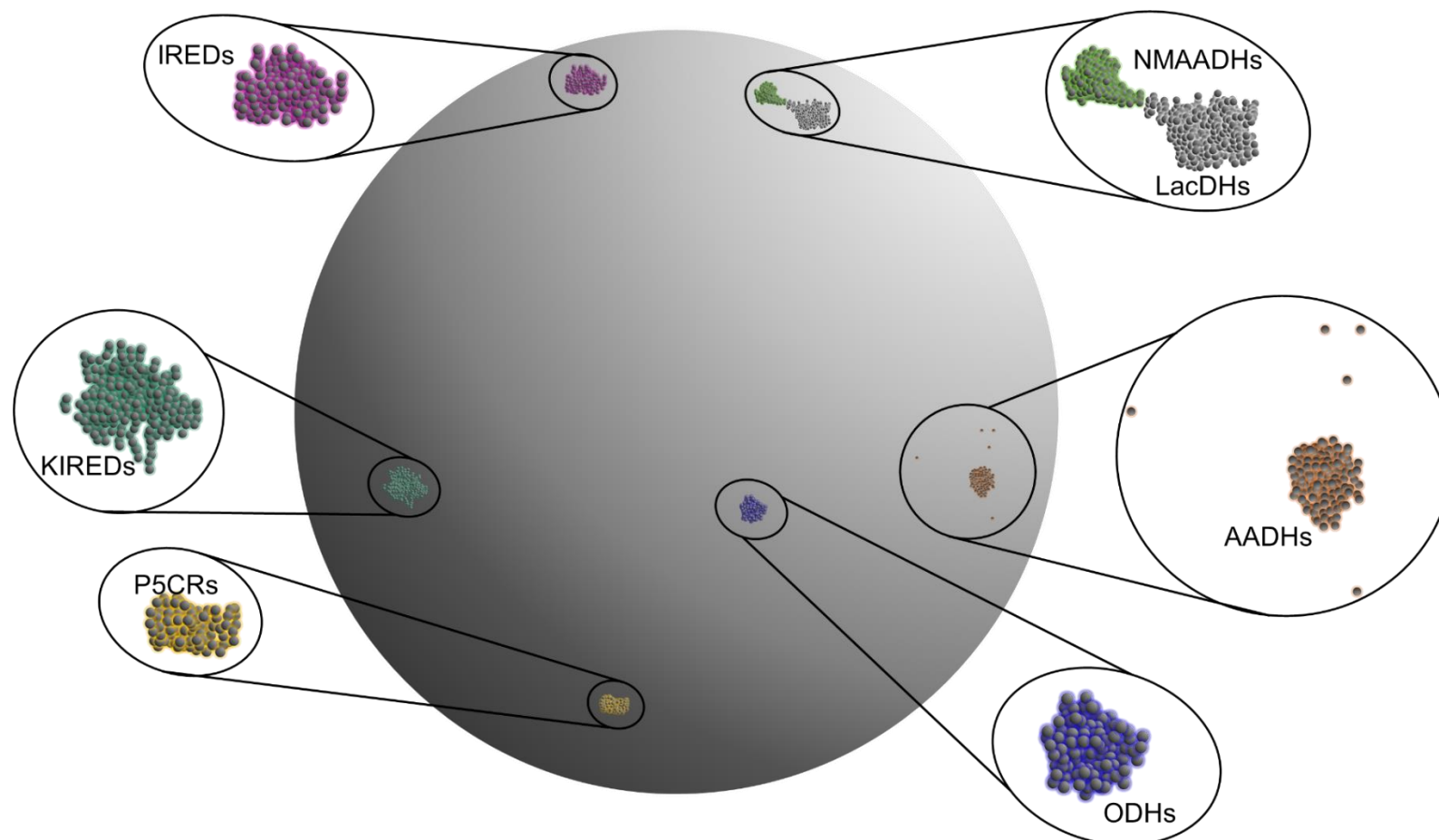


Figure 2. Sequential similarity of reductive amination enzymes. Imine reductases (IREDs), *N*-methylamino acid dehydrogenases (NMAADHs), ketimine reductases (KIREDs), opine dehydrogenases (ODHs), amino acid dehydrogenases (AADHs), fungal pyrroline-5-carboxylate reductases (P5CRs) and lactate dehydrogenases (LacDHs).

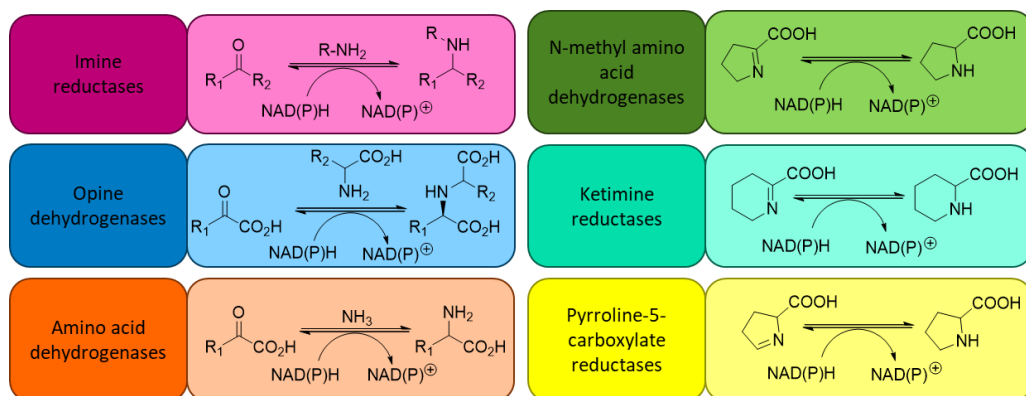


Figure 3. Natural reactions of the enzyme classes that can carry out reductive aminations.

The activities of these enzyme classes appear similar, and are shown in **Figure 3**. The clusters include opine dehydrogenases (ODHs), which are capable of effecting the reductive amination of α -amino acids with α -keto acids, however there is only one example incorporating an alkyl amine and only after extensive engineering.⁵³ Despite the recent advances in the field of imine reductases (IREDs), the only example of an IRED catalysed reductive amination of a keto acid refers to the reaction of pyruvate with an excess of propargylamine or methylamine which yielded conversions <4%.⁵⁴ ⁵⁵ *N*-Methyl amino acid dehydrogenases (NMAADHs) have been employed to synthesise *N*-alkylated amino acids, using a range of keto acids and straight chain amines.⁵⁶ There is a single example of a ketimine reductase (KIREd) being used as a reductive amination biocatalyst, but these enzymes have never been extensively utilised.⁵⁷ In addition pyrroline-5-carboxylate reductase (P5CR) enzymes have never been employed as biocatalysts. This section will endeavour to explore the use of biocatalysts in *N*-functionalised amino acid synthesis, by examining these different enzyme classes.

1.3.1. Opine dehydrogenases (ODHs)

Opine dehydrogenases (ODHs) are a class of oxidoreductases that in nature catalyse the synthesis of a class of compounds known informally as opines, that result from the condensation of an amino acid and a pyruvate or sugar.⁵⁸ As is the case with many of the enzyme classes detailed here, these enzymes exist as homodimers with a Rossmann fold NAD(P)H binding site.⁵⁹ The best characterised example was isolated from

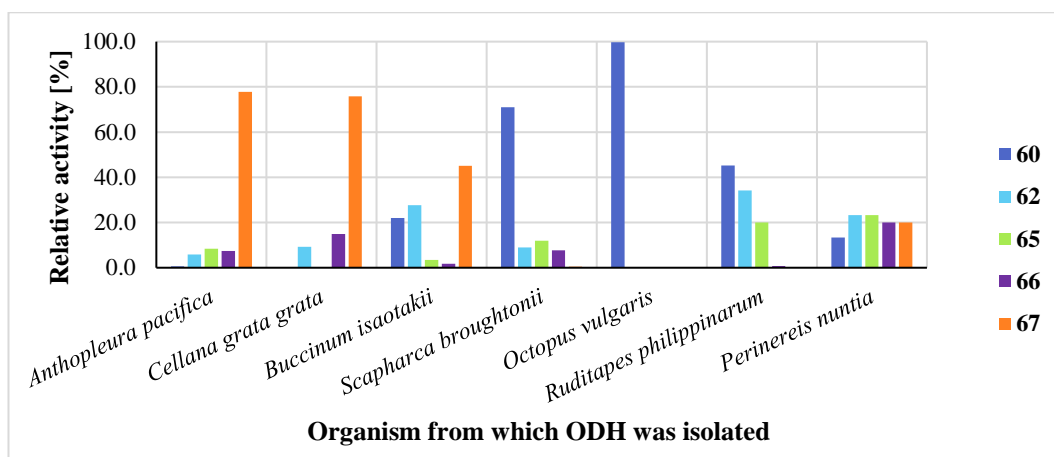
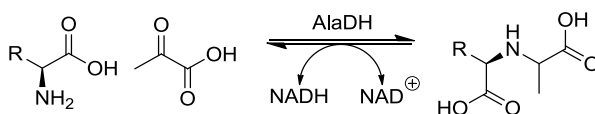
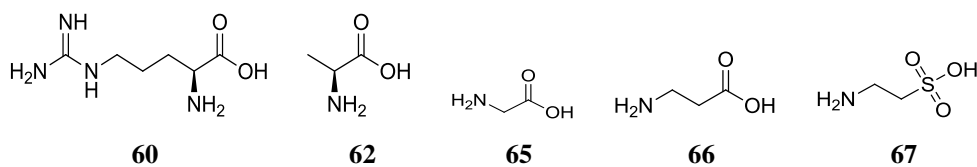
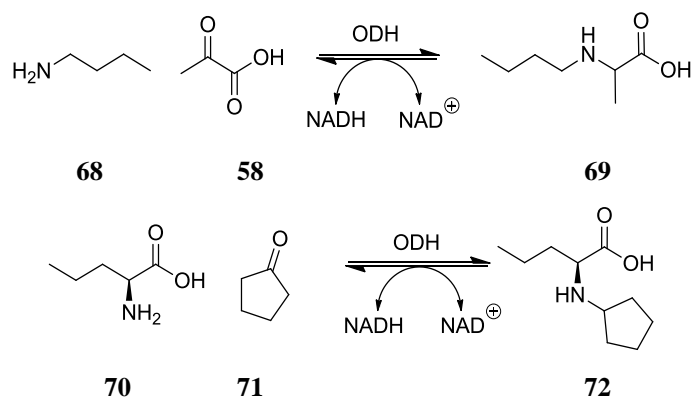


Figure 4. Examples of reactivity with different opine dehydrogenases. This data was selected from Sato *et al.* with 4 amino acids arginine 60 (Arg), alanine 62 (Ala), glycine 65 (Gly) and β -alanine 66 (β -Ala), as well as taurine 67 (Tau).⁵⁸

While there are a variety of wild type opine dehydrogenases, none of them can incorporate amine sources aside from amino acids, and very few examples employ other keto acids.⁶⁵ Any alternative α -keto acids (to 2-oxopropanoic acid) tested tend to be 2-oxobutanoic acid or 2-oxopentanoic acid.^{59, 60} Chen *et al.* carried out extensive engineering on *Anthrobacter sp.* opine dehydrogenase to expand the accepted substrate scope.⁶⁵



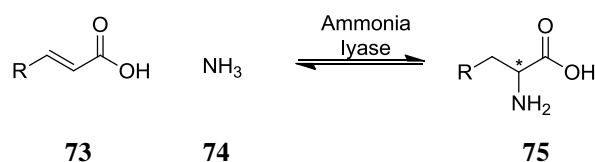
Scheme 19. Examples of reactions possibly carried out by evolved opine dehydrogenases.⁶⁵ The patent does not disclose which, if any, of the mutants have activity for these reactions.

The reactions encompassed by their mutants include pyruvate **58** and butylamine **68**, which is the only example of an alkyl amine being coupled with pyruvate by an opine dehydrogenase. Additionally there are several examples where ketone substrates (such as **71**) other than keto acids are incorporated.⁶⁵ However as these findings have not been disclosed outside of a patent neither the level of activity nor the exact sequences of the enzyme mutants is known.

1.3.2. Ammonia lyases (ALs)

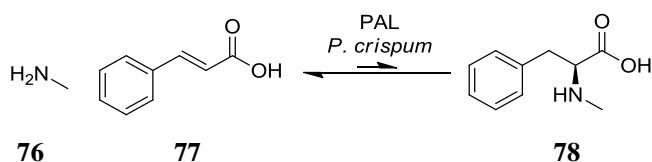
Ammonia lyases (EC 4.3.1) are enzymes commonly found in plants and fungi, which carry out either the deamination of amino acids to α,β -unsaturated carboxylic acids and ammonia **74** or the reverse amination process (**Scheme 20**).⁶⁶ Unlike the other enzyme classes discussed in this section, ammonia lyases are not NAD(P)H dependant. These enzymes use a 4-methylideneimidazole-5-one (MIO) co-factor, which is formed from amino acids in the enzyme cross-linking. This class of enzymes is therefore mechanistically very different from the other classes discussed, as well as being sequentially and structurally different.

There are seven different classes, which accept different amino acid functionalities (R groups).⁶⁷ There are also examples of ammonia lyases accepting unnatural amino acids, for example phenylalanine ammonia lyases (PALs, EC 4.3.1.24) are able to accept other cycles or substituted phenyl rings.^{66, 68, 69}



Scheme 20. Generic ammonia lyase reaction. R = phenylalanine, tyrosine, histidine, aspartate, serine, threonine, lysine, and tryptophan side chains.

However, these enzymes accept ammonia as their amine source, and there are very few examples of any other amines being accepted. Viergutz *et al.* demonstrated that a wild type PAL (from *P. crispum*) was able to deaminate *N*-methyl phenylalanine **78**, but did not carry out the reverse reaction at a detectable rate (**Scheme 21**).⁷⁰ Additionally this PAL did not accept 4-nitro-*N*-methyl phenylalanine or 4-nitro-*N,N*-dimethyl phenylalanine in either direction.⁷⁰

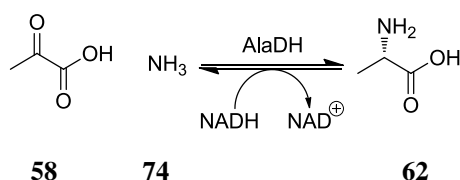


Scheme 21. Example of PAL from *P. crispum* accepting *N*-methyl phenylalanine

While these enzymes could potentially be evolved to accept other amines, this class does not currently represent the most feasible synthesis route for *N*-functionalised amino acids.

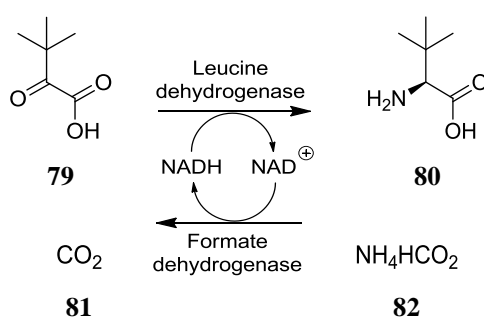
1.3.3. Amino acid dehydrogenases (AADHs)

There are a number of amino acid dehydrogenases (EC 1.4.1) that have been isolated from a variety of bacteria and are involved in the metabolism of amino acids.⁷¹ These are classified by the amino acid that is their best accepted substrate, and can be specific for either L- or D-amino acids.⁷¹ AADHs only accept ammonia as the amine substrate (**Scheme 22**), most are NADH dependant, but there are also some NADPH dependant examples.²



Scheme 22. Alanine dehydrogenase catalysed reaction.

An example of the use of an amino acid dehydrogenases in industry, is in the synthesis of Atazanavir (an anti-viral HIV treatment), which involves the reduction of a α -keto acid using a leucine dehydrogenase (**Scheme 23**). This was carried out on a large scale as a whole cell process using *E. coli* expressing leucine dehydrogenase and the co-factor recycling formate dehydrogenase enzyme.⁷²

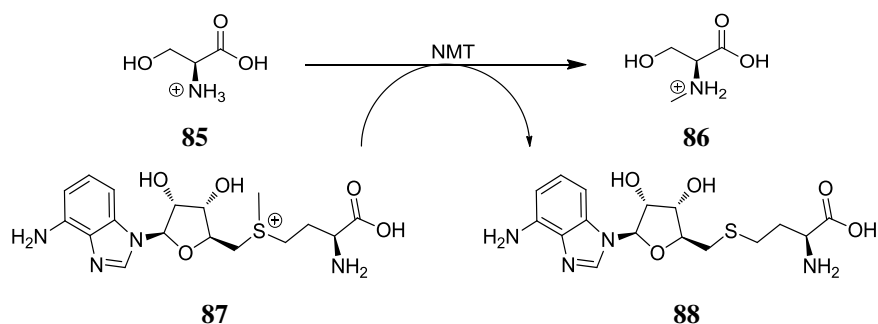


Scheme 23. Step in Atazanavir synthesis, using a leucine dehydrogenase.⁷² Reaction conditions: 3,3-dimethyl-2-oxobutanoic acid **79** (900 mM), ammonium formate **82** (2500 mM), NADH (1 mM), whole cell (*E. coli* BW3110) containing leucine dehydrogenase and formate dehydrogenase.

Amino acid dehydrogenases are clearly a very useful class of enzymes, but their widespread use is limited as their substrate specificity is restricted to α -keto acids and ammonia.

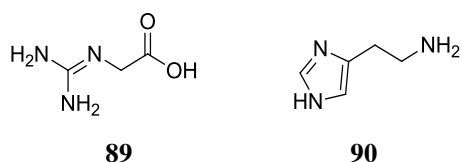
1.3.4. Amine dehydrogenases (AmDHs)

Amine dehydrogenases (EC 1.4.9) exist in nature, and carry out the oxidative cleavage of simple alkyl or aryl amines.⁷³ These are copper containing enzymes, and examples include methylamine dehydrogenases and aromatic AmDH, which can act on amines such as phenylethylamine.^{74,75} There are more recent examples of a highly engineered AmDH, which was evolved from phenylalanine dehydrogenase. While this allowed for the reductive amination of several ketones (**Scheme 24**), it reduced the activity for the natural phenylalanine substrate to undetectable levels.^{76,77}



Scheme 25. Example of an *N*-methyl transferase catalysed reaction.²⁹

Examples of specific *N*-methyl transferases include guanidinoacetate *N*-methyl transferases (EC 2.1.1.2) and histamine *N*-methyl transferases (EC 2.1.1.8), which operate on **89** and **90** respectively (**Scheme 26**).^{81, 82}



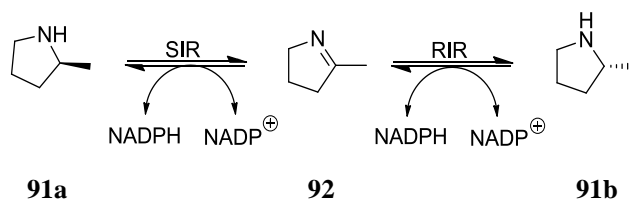
Scheme 26. Substrates of specific *N*-methyl transferases.

While these enzymes have the potential to be evolved to carry out *N*-methylation on a wider range of substrates, there are currently no examples of evolved enzymes being used. This may be due to the added complication of synthesising the relevant SAM analogues, but at present these enzymes do not provide a method to synthesise *N*-functionalised amino acids.

1.3.6. Imine reductases (IREDs)

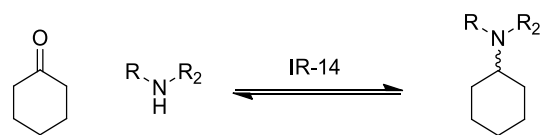
Imine reductases are known to carry out the reduction of cyclic imines, however there are a rapidly increasing number of examples of imine reductases being used to carry out reductive aminations.⁵⁴ Certain substrates are better accepted for IRED catalysed reductive aminations, such as acetophenone and cyclohexanone, while other substrates, such as amino acids, are not accepted.^{54, 55} Early IREDs capable of carrying out stereoselective reactions were identified and isolated by Mitsukura.⁸³ These were isolated from *Streptomyces* bacteria and could carry out the transformation shown in **Scheme 27** efficiently, but they did not have a wide substrate scope, and other imines

screened (mainly acyclic) were not accepted by these enzymes.⁸⁴ **Scheme 27** shows the use of (*S*)-selective IRED (SIR) and (*R*)-selective IRED (RIR) with the most active substrate.^{84, 85} The work of Ghislieri *et al.*⁸⁶ and Scheller *et al.*⁸⁷ has further investigated the use of IREDs to reduce cyclic imines. Their studies showed a wider range of applicability, including five-, six- and seven-membered rings containing imines.



Scheme 27. RIR and SIR imine reductases.⁸⁵

In the last five years the number of IREDs known to act in a reductive amination fashion has expanded dramatically. Scheller *et al.* demonstrated reductive amination with methylamine and acetophenone, but did not demonstrate any other amine substrates and only one other ketone substrate (benzaldehyde).⁸⁷



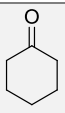
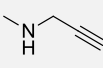
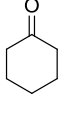
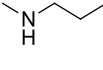
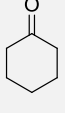
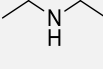
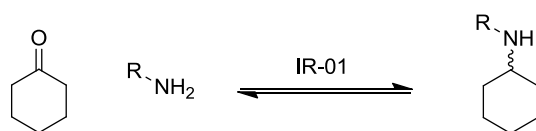
Ketone	Amine	Conversion [%]
 93	 94	83
 93	 95	9
 93	 96	0

Table 1. Examples of secondary amines substrates in enzyme catalysed reductive amination.⁸⁸ Reaction conditions: Cyclohexanone **93 (10 mM), amine **94-96** (500 mM), NADPH (0.5 mM), glucose (60 mM), 0.5 mg/mL purified IRED (“IR-14”), 0.1 mg/mL GDH, pH 9.5, 30 °C, 90 h.**

Matzel *et al.* and Roiban *et al.* both showed screening of a panel of IREDs with a range of substrates.^{55, 88} Both papers demonstrate the ability of a large number of IREDs to act on amines other than methylamine and a range of ketones. Cyclohexanone seems to be a very active substrate for most IREDs, but neither paper shows any use of α -keto acids. Matzel *et al.* were able to present some of the only known examples of the use of secondary amines in enzymatic reductive amination (**Table 1**). However, this publication used 50 equivalents of amine with these and all other examples in this paper, while Roiban *et al.* achieved a 1:1.1 stoichiometry between the amine and ketone. Roiban’s paper also uses cyclohexanone **93**, but demonstrated IREDs catalysing reactions with heterocyclic amines (**Table 2**) another class of amines less commonly seen in biocatalytic reductive aminations.⁵⁵



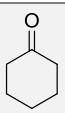
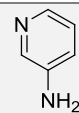
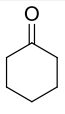
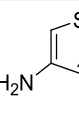
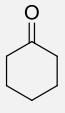
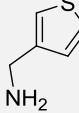
Ketone	Amine	Conversion [%]
 93	 97	19
 93	 98	62
 93	 99	97

Table 2. Examples of secondary amines substrates in enzyme catalysed reductive amination.⁵⁵ Reaction conditions: Cyclohexanone **93 (29 mM), amine **97-99** (32 mM), NADPH (1.5 mM), glucose (63 mM), crude lysate (“IR-01”), 0.3 mg/mL GDH, potassium phosphate buffer (100 mM), pH 7.0, 30 °C, 4 h.**

It is also worth commenting on the reductive aminase identified by Aleku *et al.* that catalyses the coupling of a variety of amines and ketones (**Table 3**).⁵⁴ This reductive aminase has moderate to high conversions across all substrates shown in **Table 3**, however a variety of amine to ketone ratios are required to achieve these conversions. In the case of benzaldehyde **108** and acetophenone **111** large excesses of amine were required to achieve high conversions. Whether this enzyme is genuinely a different class to IREDs is debatable, as it can achieve low amine to ketone ratios with some substrates, but needs a large excess of amines in other examples. Regardless of the semantics, this is an effective example of an enzyme catalysed reductive amination. Again, there are no examples capable of catalysing reactions to make amino acid substrates.

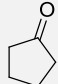
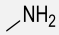
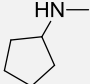
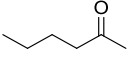
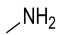
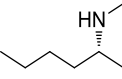
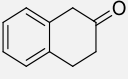
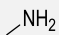
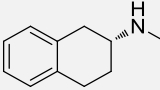
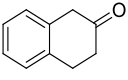
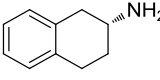
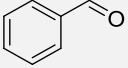
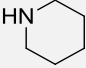
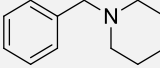
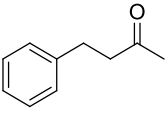
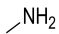
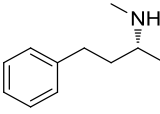
Ketone	Amine	Equivalents of amine	Product	Conversion [%]	Ee [%]
 100	 76	4	 101	81	-
 102	 76	2	 103	72	98
 104	 76	5	 105	39	88
 106	NH_3 74	20	 107	37	97
 108	 109	20	 110	40	-
 111	 76	50	 112	97	85

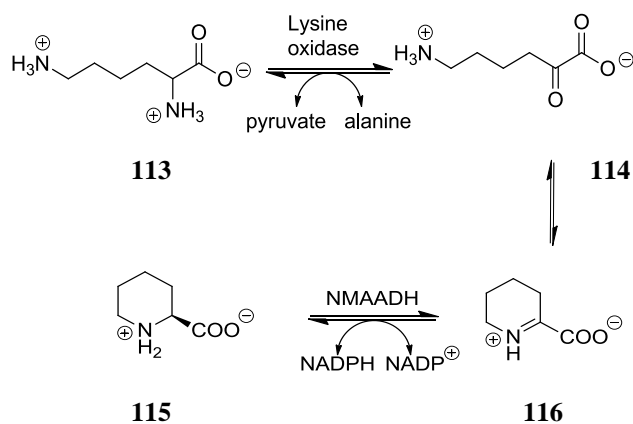
Table 3. Examples of reductive aminase catalysed reactions.⁵⁴ Reaction conditions: ketone/aldehyde (5 mM), amine (2 to 50 eq.), AspRedAm (1 mg/mL), NADP⁺ (1 mM), GDH (0.2 mg/mL), glucose (30 mM), Tris HCl buffer (100 mM, pH 9.0), 25 °C, 24 h. Conversions determined by HPLC or GC-FID analysis.

Research in imine reductases has increased the scope of known enzyme catalysed reductive aminations significantly. They both allow for the reduction of a multitude of cyclic imines, but also can accommodate a variety of aldehydes and ketones in reductive amination with various amines. However, they do not accept α -keto acids as substrates, which means that they cannot be used for amino acid synthesis.

1.3.7. *N*-Methyl amino acid dehydrogenases (NMAADHs)

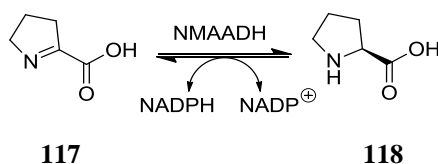
Bacterial *N*-methyl amino acid dehydrogenases (NMAADHs, EC 1.5.1.1 and EC 1.5.1.21), which are also known as dPKAs or Δ^1 -piperidine-2-carboxylate (Pyr2CR)/

Δ^1 -pyrrolidine-2-carboxylate reductases (Pip2CR), are responsible for the reduction of cyclic imino acids.⁸⁹ First isolated by Lin and Wagner in 1975, they were shown to be part of the lysine degradation pathway (**Scheme 28**).⁹⁰



Scheme 28. Lysine degradation pathway steps incorporating NMAADHs.

While reduction of this type of cyclic imino acid **116**, as well as the five-membered ring analogue **117** (as shown in **Scheme 29**) are the natural reaction of these enzymes, they have been repurposed for reductive amination.



Scheme 29. Reduction of pyrroline-2-carboxylate 117, a natural substrate of NMAADHs.⁹¹

The catalytic triad of NMAADHs consists of an asparagine, a serine and a histidine is involved in hydrogen bonding the substrate (**Figure 5**). There is an active site in each of the monomeric units of the enzyme. The hydride attack from the co-factor occurs while the substrate is hydrogen bonded into position, allowing the enantioselective reductive amination to take place.

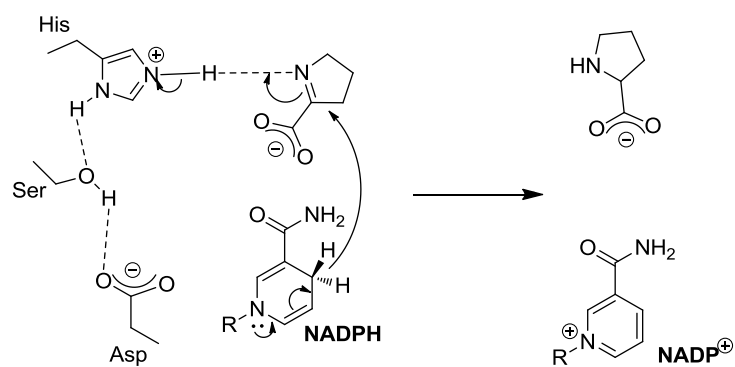
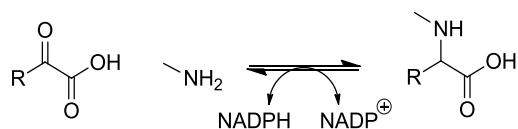


Figure 5. Proposed mechanism of action for NMAADH.

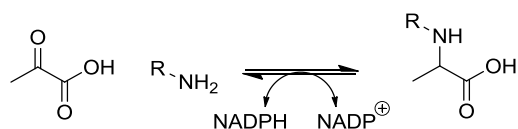
In the literature these enzymes have been used on a small number of pyruvates, however they have not been demonstrated on any ketones that were not keto acids.⁹² **Table 4** shows examples of pyruvates screened against the *P. putida* NMAADH and their activities relative to methyl pyruvate **57**. The enzyme displayed some activity for straight chain pyruvates (**119**, **120**) and phenylpyruvate **122**, but branched chains, such as **123**, were not tolerated and showed no conversion.⁹²



Scheme 30. General scheme of reactions shown in Table 4.

Keto acid	Activity relative to methyl pyruvate 57	Keto acid	Activity relative to methyl pyruvate 57
 58	100	 119	27
 120	52	 121	5
 122	30	 123	0

Table 4. Range of keto acids and their relative activities (relative to reaction of pyruvate **58** and methylamine **76**) when screened against *P. putida* NMAADH.⁹² **Table 5** shows a selection of amines and their activity in comparison to methylamine **76**, which was the most effective by a large margin. An increase of one carbon to ethylamine **124** gives a large decrease in activity. As the chain length increases the activity continues to decrease, and the enzyme does tolerate large amines (such as spermidine **129**) to a small degree. Interestingly, the enzyme is inactive with ammonia and therefore does not form primary amines.⁹²



Scheme 31. General scheme of reactions shown in Table 5.

Amine	Activity relative to methylamine 75	Amine	Activity relative to methylamine 75
$\text{H}_2\text{N}-\text{CH}_3$ 76	100	$\text{H}_2\text{N}-\text{CH}_2\text{CH}_3$ 124	4.4
$\text{H}_2\text{N}-\text{CH}_2\text{CH}_2\text{Cl}$ 125	0.74	$\text{H}_2\text{N}-\text{CH}_2\text{CH}_2\text{CH}_2\text{CH}_3$ 126	0.16
$\text{N}(\text{H})\text{CH}_3$ 127	0.12	$\text{H}_2\text{N}-\text{OH}$ 128	<0.06
NH_3 73	0	$\text{H}_2\text{N}-\text{CH}_2\text{CH}_2\text{CH}_2\text{N}(\text{H})\text{CH}_2\text{CH}_2\text{CH}_2\text{NH}_2$ 129	<0.06

Table 5. Variety of amines and their relative activities (relative to reaction of methyl pyruvate 58 and methylamine 76) when screened against *P. putida* NMAADH.

NMAADHs were identified as part of a new super family of NAD(P)H dependant oxidoreductases, which were sequentially and structurally different from the known eukaryotic enzymes that carry out the same reactions.⁹³ This family included enzymes that carried out a diverse set of reactions, such as ureidoglycolate dehydrogenases and sulfolactate dehydrogenases, while many have been putatively identified as malate or lactate dehydrogenases.^{94, 95} Interestingly all of the enzymes in this family apart from the NMAADHs act on α -oxo acids or α -hydroxy acids, so the reductive amination aptitude of NMAADHs is not entirely surprising.⁹³ Goto *et al.* have reported the crystal structure for *P. syringae* NMAADH.⁹⁶

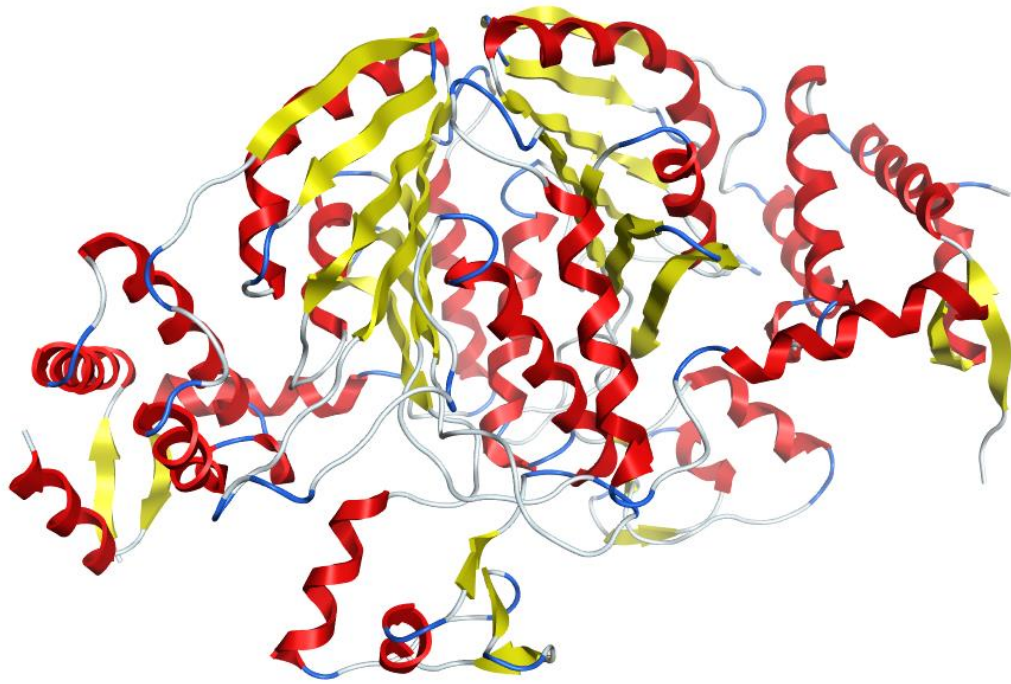


Figure 6. Crystal structure of *P. syringae* NMAADH. (PDB ID: 2CWH).

Malate and lactate dehydrogenases contain a Rossmann fold, which consists of a repeated $\beta\alpha\beta$ fold pattern that binds to the co-factor, (as do most NAD(P)H dependant enzymes).⁹⁶⁻⁹⁸ Whereas, NMAADHs have a seven-stranded sheet as their NADPH binding site, called seven-stranded anti-parallel β -sheet (SEASS). This fold results in a similar shaped binding domain to a Rossmann fold, but a different folding architecture.

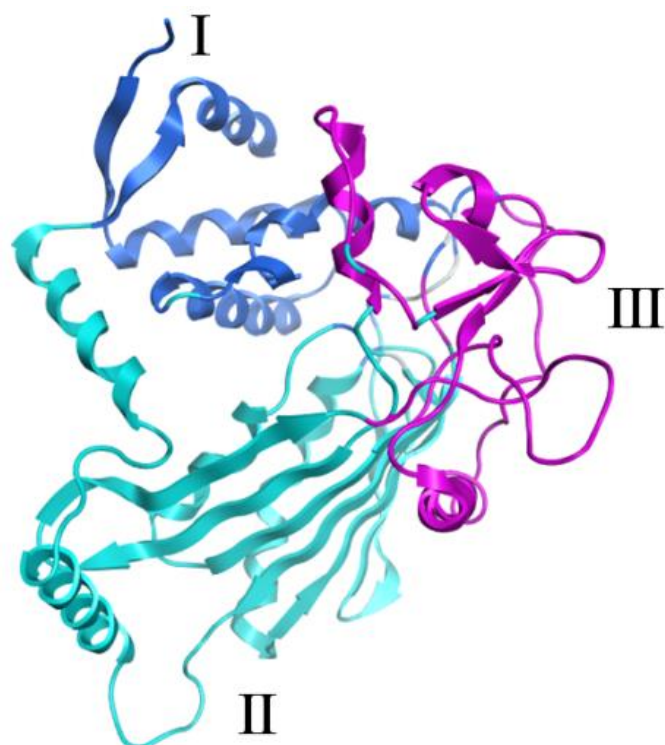


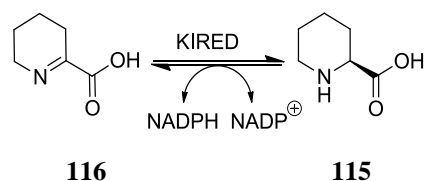
Figure 7. Three domains in NMAADH enzymes. (PDB ID: 2CWH).

NMAADHs (and the other bacterial NAD(P)H dependant oxidoreductases) are dimeric enzymes, with each subunit containing three domains (I, II and III) (**Figure 7**). Domain II is the site of NADPH binding, while I and III are more flexible regions involved in substrate binding. These domains show a far higher degree of movement between the substrate bound and free states, than other known enzymes. This is a common feature amongst NADPH-dependant oxidoreductases; they have distinct “open” and “closed” conformations.⁹⁶ The enzyme exists in the open conformation in its free state, and then closes in order to bind the substrate. This can complicate the interpretation of the crystal structure, as it will not be fully representative of the range of movement of the enzyme.⁹⁶

1.3.8. Ketimine reductases (KIREDs)

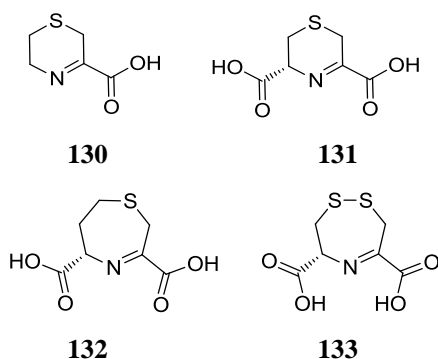
Mammalian ketimine reductases (KIREDs, EC 1.5.1.25) are another unrelated class of enzymes that carry out the same natural reaction as NMAADHs.⁹⁹⁻¹⁰² It has been demonstrated that eukaryotic lysine metabolism is part of a unique pathway that is not accessible to other naturally occurring amino acids.¹⁰³ The pipercolate pathway

incorporates ketimine reductases (also known as μ -crystallins or CRYMs), which carry out the reduction of cyclic imines (**Scheme 32**) in the same way as NMAADHs.⁹¹



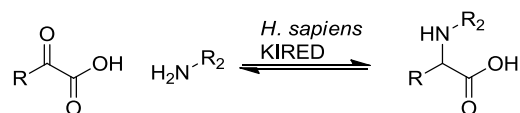
Scheme 32. Role of ketimine reductase in lysine metabolism.⁹¹

A variety of naturally occurring sulfur containing cyclic imino acids are also reduced by human ketimine reductase (**Scheme 33**).¹⁰⁴ These compounds are found in varying concentrations within the human brain, though Hallen *et al.* do not specify the relative activities for these sulfur containing compounds.⁵⁷



Scheme 33. Sulfur containing imino acids accepted by ketimine reductases.¹⁰⁴

In another paper, Hallen *et al.* reported four examples of *N*-functionalised amino acid preparation using *H. sapiens* KIREd. The relative rates quoted in **Table 6** are in comparison to piperidine-2-carboxylate, as can be seen the rates for the acyclic keto acids are far lower but still demonstrate significant activity. However, these are the only examples of keto acids being used with these enzymes. Therefore, these enzymes have a potential reductive amination ability that has yet to be explored.



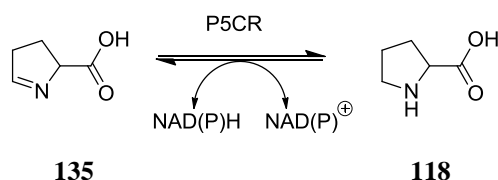
Scheme 34. General scheme for the reaction of substrates in Table 6.

Ketone substrate	Amine substrate	Relative rate
 58	 76	25
 58	 124	24
 134	 76	16
 122	 76	12

Table 6. *N*-functionalised amino acids synthesised using a KIREd. Reaction conditions: keto acid (5 mM), amine (30 mM), NADPH (0.008 mM), potassium phosphate buffer (200 mM, pH 7.2), *H. sapiens* KIREd (2.6 nM). Rates relative to piperidine-2-carboxylate.

1.3.9. Pyrroline-5-carboxylate reductases (P5CRs)

P5CRs are perhaps the least characterised of the enzyme classes described in this chapter. While several examples have been identified, these enzymes have not been used to catalyse enzymatic reactions. These enzymes have a similar natural reaction to NMAADHs and KIREdS, but are differentiated by the position of the imine (P5CRs operate on pyrroline-5-carboxylate **135** not pyrroline 2-carboxylate **117**, **Scheme 35**).¹⁰⁵ This enzyme is part of the biosynthesis of proline in nature.¹⁰⁶



Scheme 35. Reaction catalysed by P5CR enzymes.¹⁰⁵

However, as the natural reaction is so close to NMAADHs, which are known to have non-natural reductive amination activity, an example was selected to be screened for this type of activity. The P5CR from *N. crassa* was selected as one of the best known and characterised examples, the pH profile (**Figure 8**) had already been established.¹⁰⁵ The pH was determined using pyrroline-5-carboxylate **135**, and the relative rates were calculated for pHs between 5.5 and 8.0.

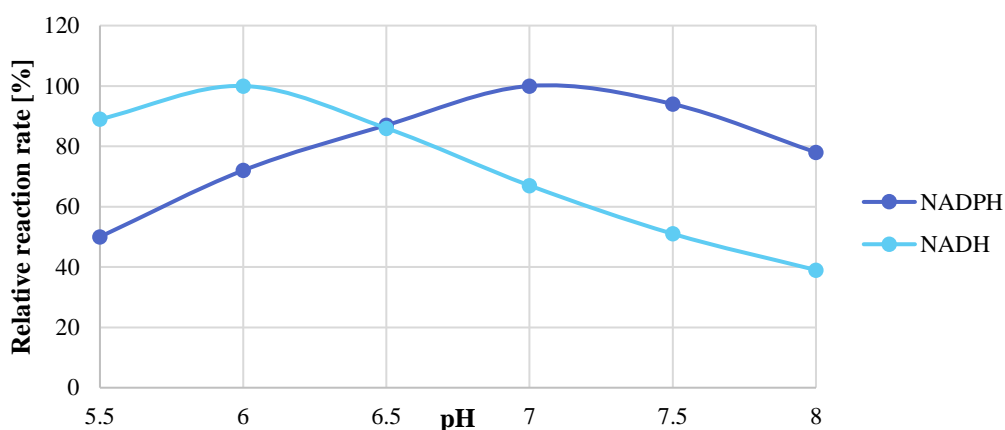


Figure 8. pH profile of *N. crassa* P5CR.¹⁰⁵ Relative reaction rates were calculated in phosphate buffer (100 mM), using the reaction shown in Scheme 35.

This pH profile shows that the optimum pH falls at 7.0, though it is interesting to note that the optimum pH is co-factor dependant. The NADH dependant process has an optimum pH at 6.0. This difference in pH could be due to the stability of the two co-factors, as NADH is more stable at lower pHs than NADPH.¹⁰⁷

Little is known about P5CRs and there is very little characterisation in the literature. While they potentially share the non-natural reductive amination activity of NMAADHs and KIREDS, this has not been demonstrated. They have therefore been included in the scope of this study, to determine if they have any reductive amination activity.

1.4. Conclusions

N-functionalised amino acids are an important class of building blocks for peptide drugs and fine chemicals. While there are a variety of chemical synthetic methods, including *N*-alkylation, reductive amination, palladium catalysis and the Mitsunobu reaction, these have some associated problems, which could be overcome by biocatalysis. These include the use of metal catalysts, toxic or highly flammable, use of environmentally unfriendly solvents and extensive use of protecting group approaches.

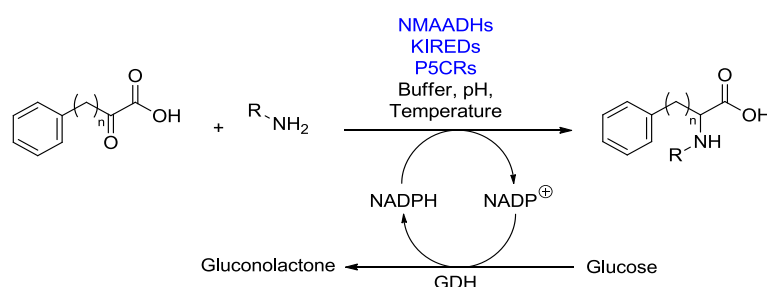
There are also a range of biocatalytic strategies that can be employed in amino acid synthesis, which avoid many of the problems listed in the case of chemical methods. These strategies are broadly based on different enzyme classes (many of which have similar activities, despite having diverse structures and sequences) that can participate in amino acid biosynthesis or metabolism. However, many of these clusters are not suited to making *N*-functionalised amino acids, as they cannot incorporate amines other than ammonia **73**.

This project set out to develop an enzyme catalysed reductive amination method for the synthesis of *N*-functionalised amino acids. This would provide a more environmentally friendly strategy than the existing methods. The NMAADHs, and to a lesser extent KIREDs, have been shown to have the desired reductive amination activity and ability to incorporate amines other than ammonia. The expansion of the substrate scope and the number of known active enzymes would fulfil the aims of the project. These enzyme classes were therefore selected for further study within this research, in addition to P5CRs (as they have similar natural substrates, as discussed in **1.3.9**). The objectives set out in the subsequent section will be carried out with these three selected enzyme classes.

2. Objectives

As has been demonstrated in the preceding section, the development of sustainable manufacturing routes to chiral *N*-alkylated amino acids poses a significant challenge in the pharmaceutical and fine chemical industries. Therefore, a panel of diverse enzymes, consisting of NMAADHs, KIREDs and P5CRs, was generated and evaluated for α -keto acid reductive amination. For this the model enzymatic reaction shown in **Scheme 36** was selected. Currently several factors are impacting the use of these enzymes in the synthesis of *N*-protected amino acids, including:

- the high excess of amine required,
- the very narrow amine scope and
- the high keto acid specificity.



Scheme 36. Model biocatalytic reaction to investigate reductive amination potential of NMAADHs, KIREDs and P5CRs

In order to investigate the reductive amination synthesis of *N*-functionalised amino acids from α -keto acids, the following objectives were set out:

- Select of enzymes from the three enzyme clusters of interest (NMAADHs, KIREDs and P5CR). These should have known sequences and characterisation data if possible. This will allow for vector preparation and possible correlation of sequence and structure to activity.
- Demonstrate cloning and expression of these enzymes in *E. coli*. This host organism is easy to use and widely applicable, optimised expression conditions will allow for large scale enzyme generation.
- Purify these proteins for accurate screening and establish protein stability and formulation. Protein purification will allow more accurate data collection, without influence from other enzymes present in lysate or lyophilised powder.

- Establish optimised reaction parameters, including:
 - pH
 - buffer concentration
 - catalyst loading
 - substrate loading
 - use of recycling system

The optimised conditions will give the best chance of identifying new substrates, by maximising the conversions observed.

- Investigate the substrate scope with respect to the keto acid and amine. This will include different aromatic and alkyl pyruvates as well as a range of amines of different sizes (**Figure 9**).

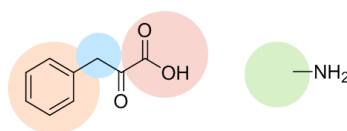


Figure 9. Areas of substrate scope exploration

New substrates would expand the range of amino acids that can be synthesised enzymatically. Also, the identification of accepted substrates would allow for relationships between sequence and activity to be better understood.

- Synthesis of racemic and enantiomerically pure product markers where relevant for analysis. This would allow conversion and ee to be established and confirm that the desired product was being produced in the enzymatic reaction.
- Demonstrate synthetic utility of these enzymes in large scale, industrially relevant reactions. This is important to demonstrate the industrial relevance of these enzymes.
- Establish the enantioselectivity of any active enzymes and rationalise this stereo-selectivity. The stereoselectivity is important to the pharmaceutical industry, as drugs need to be synthesised as a single enantiomer.

Chapter 2

Results and discussion: optimisation and use of NAD(P)H oxido-reductases to carry out the synthesis of amino acids

3. Results and Discussion

In order to investigate the α -keto acid reductive amination activity within the enzyme clusters shown in

Figure 2, seven enzymes were selected from this space with similar native activities. These were selected from three disparate clusters namely: (**En01-En03**) belonging to NMAADH space, (**En04-En06**) from KIREd cluster, and the fungal enzyme (**En07**) from the P5CR superfamily (**Table 7**). Selected enzymes are not only diverse in sequence space but also in their origin (mammalian, fungal and bacterial).

These enzyme clusters were selected for study as the aim of the project was to synthesise *N*-functionalised amino acids. The NMAADH class had previously been demonstrated to catalyse this type of reductive amination (as described in section **1.3.7**). The ketimine reductases were selected as they catalyse the same reaction in nature as the NMAADHs, and therefore might be applicable to reductive amination. The P5CR class was selected as their natural activity (reducing a pyrroline-5-carboxylate) is similar to the NMAADHs and KIREds (which reduce the pyrroline-2-carboxylate), but have a different active site. It was unknown if the P5CR class would be able to catalyse reductive amination. Having selected these classes for study, a practical examination of the enzymes was begun.

3.1. Enzymes selection

Three NMAADHs were selected from the literature for optimisation and screening, **En01-03**. All three enzymes were isolated from *Pseudomonas* strains, *putida*, *syringae* and *fluorescens* respectively (**Table 7, En01-03**). Apart from **En01** these enzymes had never previously been demonstrated to possess reductive amination activity. The *P. syringae* NMAADH was selected as a crystal structure had already been obtained.¹⁰⁸ The *P. fluorescens* enzyme had previously been classified as a lactate dehydrogenase, but it had a high sequence homology with the other NMAADHs selected, so it seemed likely that it has been misclassified.

Three ketimine reductases were also selected from the literature, namely **En04-06**. Each of these proteins originate from a mammalian species (rat, human and cow respectively) (**Table 7**). There was a crystal structure for **En05**, which was also well

characterised by Hallen *et al.*¹⁰⁴ The other two enzymes (**En04** and **En06**) were selected as they had a very high homology to **En05**, but they were less well characterised.

Finally, a pyrroline-5-carboxylate reductase (P5CR, **En07**), which has a different natural reaction to the other selected enzymes, has also been selected for comparison with the NMAADHs and KIREDS. It was unknown whether this class would share the reductive amination activity of the other enzyme classes. This enzyme was isolated from a fungus (*N. crassa*, **Table 7**) and is one of the best characterised P5CRs.

Enzyme	Host organism	Protein name	Gene name	Ref
En01	<i>P. putida</i>	Δ^1 -Piperidine/ pyrroline-2-carboxylate reductase	dpkA_P. putida	109
En02	<i>P. syringae</i>	Δ^1 -Piperidine-2-carboxylate reductase	dpkA_P.syringae	110
En03	<i>P. fluorescens</i>	Putative lactate dehydrogenase	PSF113_2799	111
En04	<i>R. novogicus</i>	Ketimine reductase mu-crystallin	Crym_rat	112
En05	<i>H. sapiens</i>	Ketimine reductase mu-crystallin	Crym_human	101
En06	<i>B. taurus</i>	Ketimine reductase mu-crystallin	Crym_bovin	113
En07	<i>N. crassa</i>	Pyrroline-5-carboxylate reductase	P5CR	114

Table 7. Enzymes selected for screening.

A similarity matrix for all seven enzymes was calculated using MOE v2015.1001. This revealed that the three NMAADHs (**En01-03**) had a moderately high sequence similarity, with a minimum similarity of 68% (**Table 8**), while the mammalian KIREDS had an extremely high sequence homology (all greater than 94%). The inter-cluster similarity for all three enzyme classes values all fell between 20% and 30%, with no significant sequential motifs in common.

	En01	En02	En03	En04	En05	En06	En07
En01		68	70	26	26	26	25
En02	68		80	26	25	25	26
En03	70	80		27	27	27	28
En04	22	22	23		95	94	27
En05	22	21	22	95		96	28
En06	22	21	22	95	96		28
En07	21	22	23	27	28	27	

Table 8. Percentage similarity of En01-07 calculated using MOE v2015 software.

Although these enzymes exhibit comparable substrate scope (all reducing pyrroline carboxylates in nature), a closer look at their structures highlights the diverse origins and lack of homology between clusters, as discussed in Section 1.3.^{115, 116} Each of the three clusters had at least one protein sequence with known 3D crystal structure. **Figure 10** shows a representative structure from each of the protein families. A comparison of the crystal structures demonstrates the high degree of variability an enzyme can have and still perform a similar transformation. The main commonality among these enzymes is that they function as dimers and utilize NADPH as a cofactor. Most of the enzymes utilize the Rossmann fold for binding NADPH, but this is not the case with the NMAADH family.

While all these enzyme structures exist as dimers and contain a NAD(P)H binding domain, they have diverse folding architectures. The dimer interface for KIREDs and NMAADHs consists of beta sheets (**Figure 10A** and **B**), while for IREDs it is alpha helical (**Figure 10D**). This reinforces the lack of relationship between IREDs and these less well known reductive amination enzyme classes.

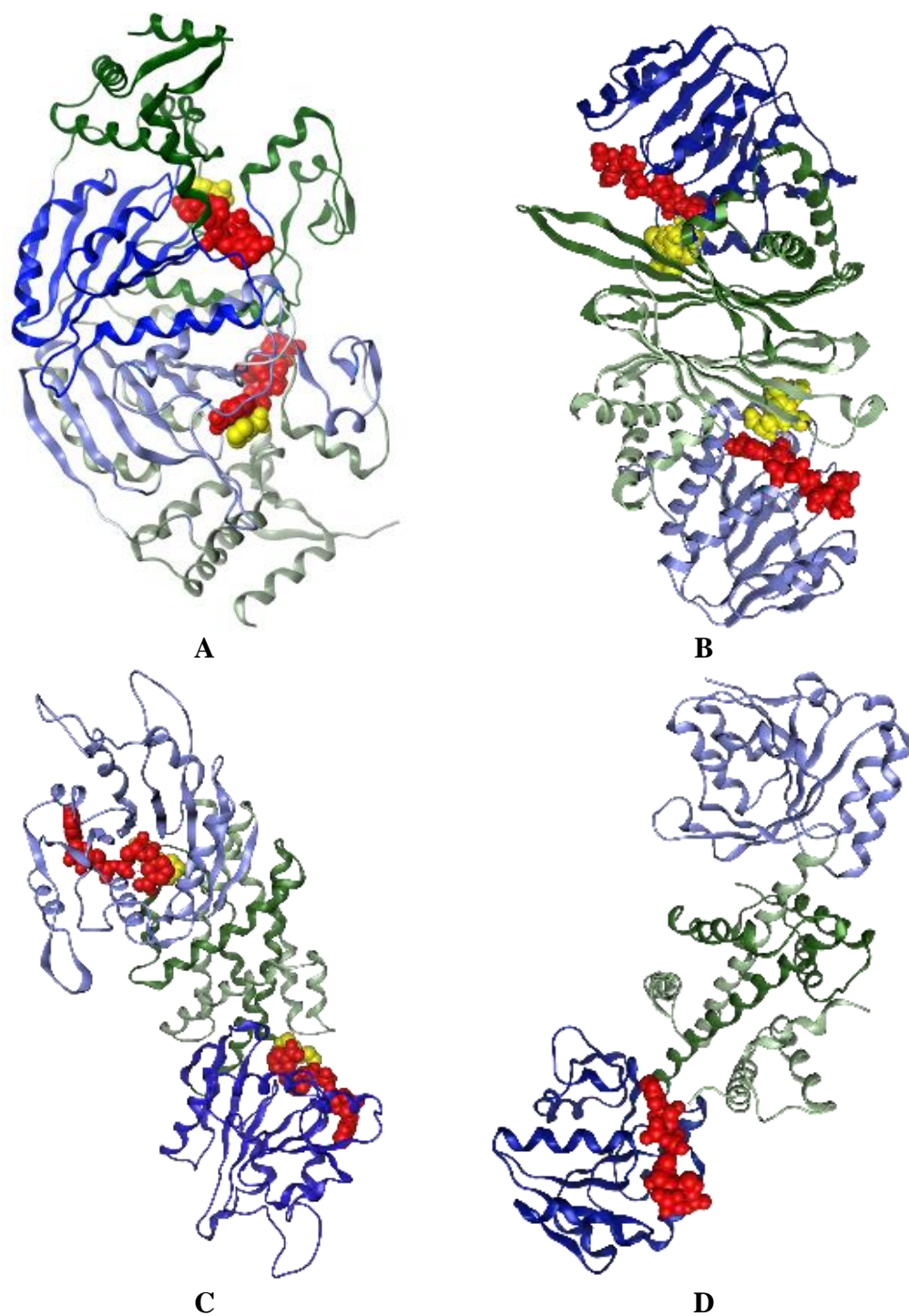


Figure 10. Structures of different enzyme classes. A: En02 (NMAADH), B: En06 (KIREd), C: En07 (P5CR), D: Aspergillus oryzae imine reductase (IREd). Models of the enzymes were generated using MOE program and PDB 2CWH (En01), 4BVA (for En04), 5BSF (for En07) and 5G6R (for IREd comparison) as templates with NADP⁺ (red) and the co-crystallized ligand (yellow) maintained during model building. In each structure, the dimer interface is coloured as dark green (first monomer) and light green (the second monomer), while the NADP⁺ binding domain is coloured as dark blue (first monomer) and light blue (second monomer).

KIREDs have a canonical Rossmann fold to bind NAD(P)⁺ (**Figure 10B**), however the dimer interface domain is at the *N*-terminus and Rossmann fold at the *C*-terminus. This is unlike IREDs (**Figure 10D**), which have these domains reversed. In contrast, NMAADHs (**Figure 10A**) have a completely different NAD(P)H binding domain to both KIREDs (**Figure 10B**) and IREDs (**Figure 10D**). While P5CR (**Figure 10C**) enzymes also have a Rossmann fold, they have these domains arranged as in IREDs (**Figure 10D**), despite their natural substrate being more similar to that of NMAADHs (A). The diversity in folding, co-factor binding domain and domain arrangements emphasises the lack of relationship between these enzyme classes. This also supports the hypothesis that these enzymes have evolved convergently from different ancestors to carry out the same function.

3.2. Enzymes expression and purification

In order to obtain enzymes for screening, initial efforts were focussed on enzyme expression and purification. Therefore, seven genes were synthesised and cloned into pET28a vector with codon optimisation for expression in *E. coli*. This vector was selected as it allowed for the incorporation of an *N*-terminal histidine tag, which allows the proteins to be easily purified. This vector also gives kanamycin resistance, allowing for standard antibiotic resistant *E. coli* growth protocols to be employed.

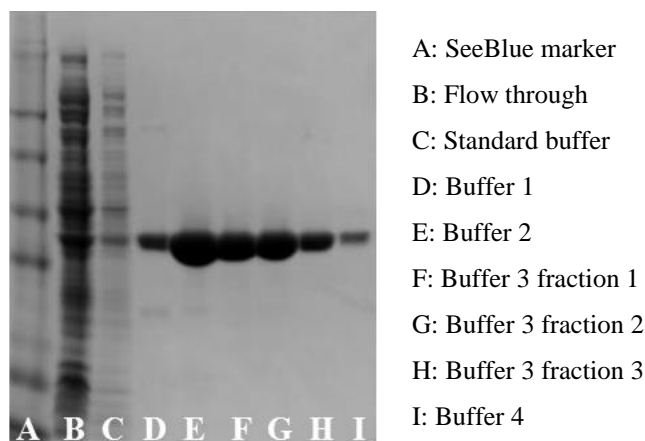


Figure 11. Purification of En02 shown on gel electrophoresis. Run according to standard gel protocol, for buffer composition see section 6.2.2.4.

The genes of interest were then transformed into competent *E. coli* BL21(DE3), which were grown in Luria-Bertani medium with kanamycin (0.5 µg/mL) and D-glucose (1%

v/v) on a 1 L scale in 2.5 L Ultraflasks. Cultures were induced with IPTG (0.5 mM) after an optical density of approximately 1.0 was achieved and expression was analysed by gel electrophoresis, for example **En02** shown in **Figure 11**.

Enzyme	Final concentration [mg/mL]
En01	9.7
En02	11.7
En03	5.2
En04	5.1
En05	1.6
En06	19.4
En07	19.5

Table 9. Concentration of purified proteins calculated using Bradford assay

Since all enzymes were expressed with a *N*-terminal 6His-tag they could be easily purified using nickel affinity chromatography. After purification, protein concentrations were determined using a Bradford assay with a bovine serum albumen (BSA) standard, the resultant concentration of the purified enzymes being in the range 1.6-19.5 mg/mL, **En05** showing the poorest expression (1.6 mg/L) (full data shown in **Table 9**).

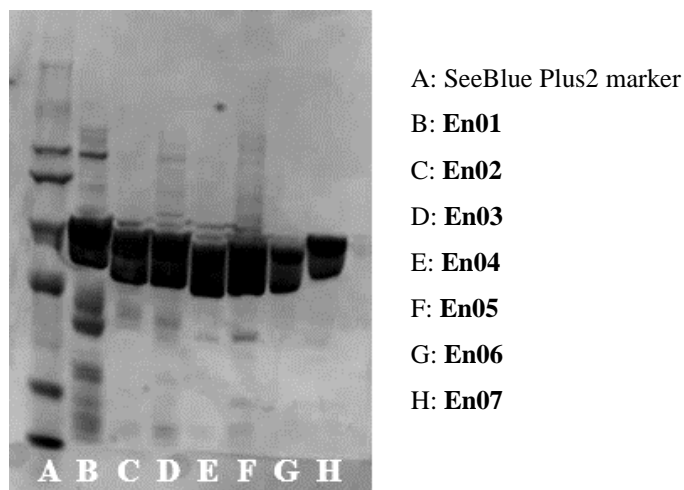


Figure 12. SDS-PAGE gel showing expression of NMAADHs in BL21(DE3). Gel electrophoresis analysis showing the profile of purified proteins (at a standardised concentration of 1.5 mg/mL) from *E. coli* expressing En01-07, with expression observed as bands of 20-40 kDa.

For use in reactions the proteins were diluted with buffer to a standard concentration so the enzymes activity could be directly compared. The SDS-PAGE gel shown in **Figure 12** shows all seven enzymes diluted to 1.5 mg/mL. The enzyme stock solutions in Tris HCl buffer (pH 8.5, 200 mM) were then stored in glycerol (50% v/v final concentration) at -80 °C for a period of maximum of 1 year. These storage conditions were selected as the absence of high glycerol concentrations, resulted in a large loss of activity upon freezing. However, enzyme activity tests showed that the activity declined over the storage time even with 50% glycerol, but the glycerol decreased the rate of decay.

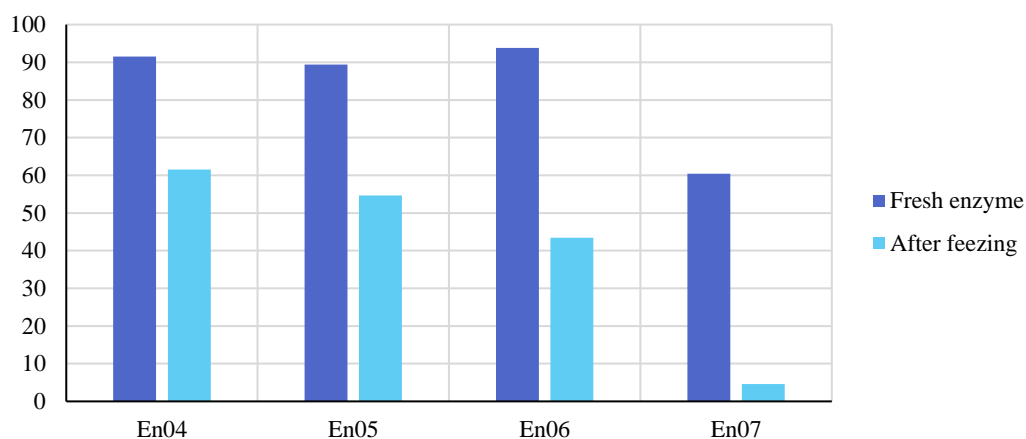
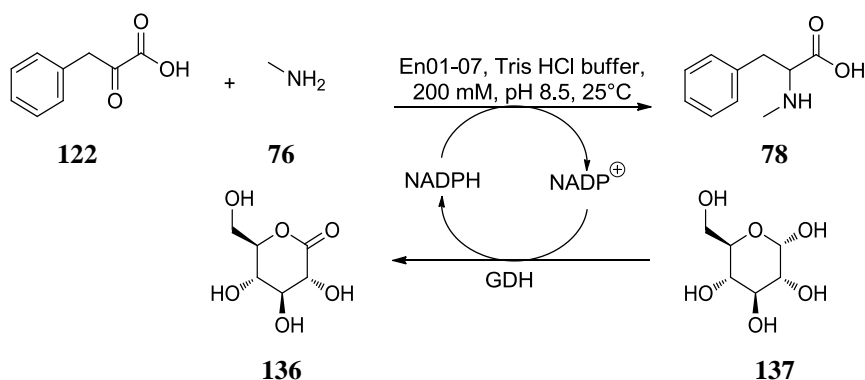


Figure 13. Comparison of activity levels in enzymes stored in buffer, without glycerol, before and after freezing. Reaction conditions: phenyl pyruvate 122a (10 mM), methylamine hydrochloride 76a (100 mM), NADPH (1 mM), En01 (1.2 $\mu\text{g}/\text{mL}$) Tris HCl (100 mM, pH 8.5).

3.3. Reaction optimisation

After successfully expressing **En01-07** in *E. coli* and purification under standard conditions, enzymes were tested against phenyl pyruvate **122** with methylamine hydrochloride **76** (**Scheme 37**). Since all seven enzymes are NADPH dependent, glucose dehydrogenase recycling system comprised of glucose dehydrogenase (GDH) and D-glucose was initially investigated in order to eliminate the addition of equimolar amounts NADPH which could result in enzyme inhibition and increase costs.¹¹⁷ The use of a recycling system also increases the potential use of these enzymes in industry since costs are minimised.



Scheme 37. Model reaction used for reaction optimisation.

Glucose dehydrogenase enzymes from two different sources were investigated initially (GDH-CDX-901 and GDH from *Pseudomonas sp.*) with loadings of 0.25 mg/mL for GDH and 1 mM NADPH, similar to values reported in literature.¹¹⁸ Results suggested that at these loadings the reactions are not stalling or being limited by the GDH and therefore these conditions were used in future experiments. D-glucose loading was also investigated, results showing that an excess of 3 equivalents is sufficient to keep the recycling system ongoing. It is possible that a lower concentration would also be suitable, however an excess is preferable as it limits the rate of reaction. Several experiments were then performed to improve parameters that are known to influence enzyme activity namely: pH, buffer, catalyst and substrate loading, with a focus on **En01-03**.

3.3.1. pH profile and buffer impact

Initial screening experiments, based on the previously reported example for **En01**, showed reaction stalling.¹⁰⁹ This showed rapid conversion within the first hour, followed by a decreasing reaction rate. Reaction conditions were therefore investigated to determine the source of the stalling, with the influence of pH being studied.

In the case of NMAADHs, the initial reaction rate was determined spectrophotometrically using phosphate and tris buffers at pHs between 6.5 and 9.5. Results pointed towards the use of Tris buffer, a pH optimum of 8.5 was determined for **En01** and **En02**, with no discernible maxima for **En03** (**Figure 14**). Therefore, Tris

HCl buffer was the first choice, although phosphate buffer seems to represent a viable buffer in instances when substrates or products are not stable at high pHs.

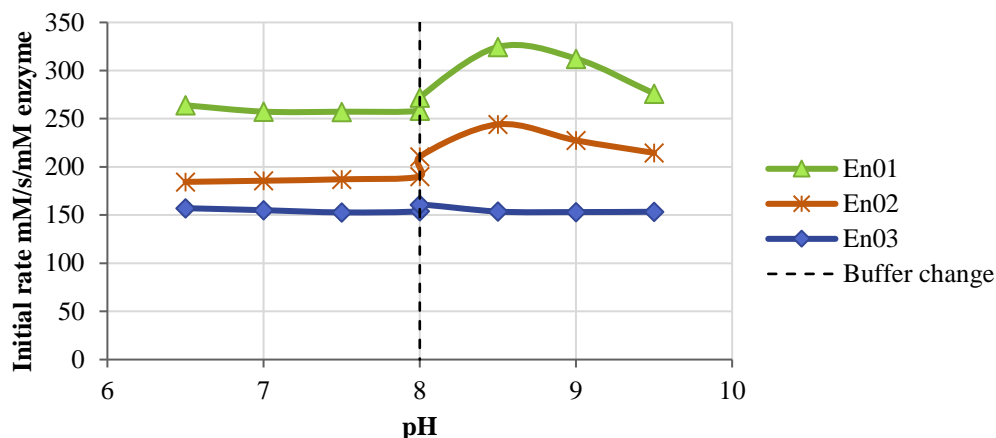


Figure 14. pH profile of three NMAADHs (En01-03) based on initial rate. Reaction conditions: phenyl pyruvate 122 (0.8 mM), methylamine hydrochloride 76 (700 mM), NADPH (0.8 mM), En01 (1.2 $\mu\text{g}/\text{mL}$) either phosphate buffer (100 mM, pHs 6.5-8.0) or Tris HCl (100 mM, pHs 8.0-9.5). Consumption of NADPH monitored at 340 nm. Rate calculated based on NADPH standard curve.

When reactions (with phenyl pyruvate and methylamine) were run using Tris buffer at pH 8.5, stalling was still observed after several hours. Constant pH monitoring showed that the pH decreases with the reaction progress (**Figure 15**). This change in pH is known for enzymes which use a glucose recycling system since the formation of the gluconic acid contributes to the lower pH. As can be seen, the rate of reaction decreased as the pH fell, and the reaction stopped below pH 5. Therefore, to get the reaction to go to completion, maintaining a constant pH was required. This could be achieved by constant pH monitoring and adjustment, or by increasing the buffer concentration to buffer the gluconic acid.

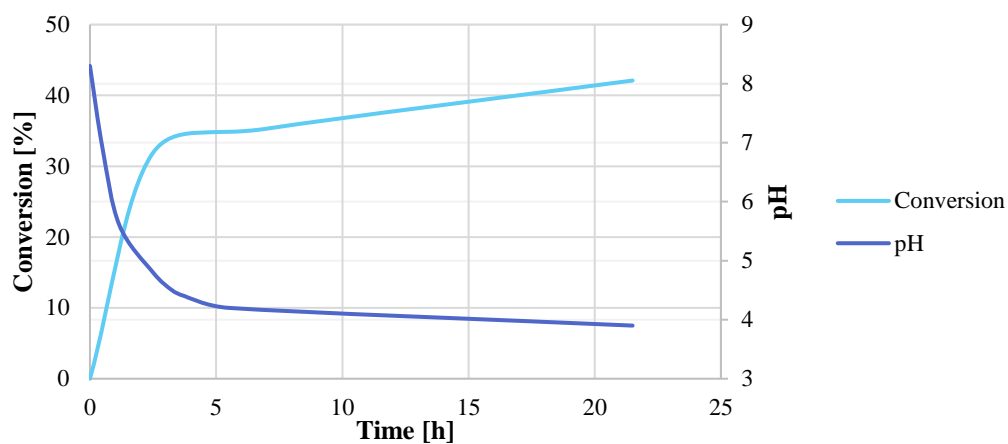


Figure 15. Conversion over time using En01, without pH adjustment. Reaction conditions: phenyl pyruvate 122 (100 mM), methylamine hydrochloride 76 (700 mM), NADPH (1 mM), D-glucose (300 mM), En01 (1.2 µg/mL), GDH (0.25 mg/mL) pH 8.5, 25 °C, enzyme lysed in Tris HCl buffer (50 mM) with sodium chloride (300 mM). Conversion calculated against benzonitrile internal standard, based on the production of 78

The optimum pH was also investigated for the KIREDS **En04-06**. The initial reaction rate was therefore determined spectrophotometrically in a similar fashion as NMAADHs at a range of pHs between 6.5 and 9.5, using phosphate and tris buffers. Interestingly the pH optima established for these enzymes was lower than those observed for NMAADHs, with a maximum activity at approximately pH 7.0 (**Figure 16**), but also far lower rates were observed in general. The rates observed for the NMAADHs showed values in excess of 200 mM/min/mM enzyme loading, suggesting that the KIREDS generally demonstrated a lower level of activity.

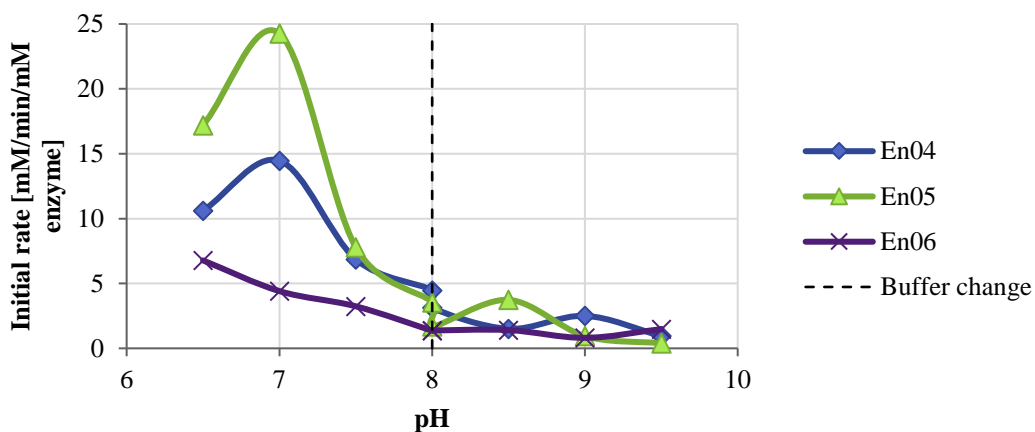


Figure 16. pH profile of En04-06 based on initial rate. Reaction conditions: phenyl pyruvate 122 (0.8 mM), methylamine hydrochloride 76 (700 mM), NADPH (0.8 mM), En04-06 (0.3 mg/mL). Consumption of NADPH monitored at 340 nm. Rate calculated based on NADPH standard curve.

When the optimum pH was investigated for P5CR **En-07**, again much lower initial rates were observed when compared to the NMAADHs or KIREDDs. Also, it appears that this enzyme has a lower pH optima than those previously observed for the other two enzyme classes, which is similar to the results found in the literature, where the maxima was seen at 7.0.¹⁰⁵

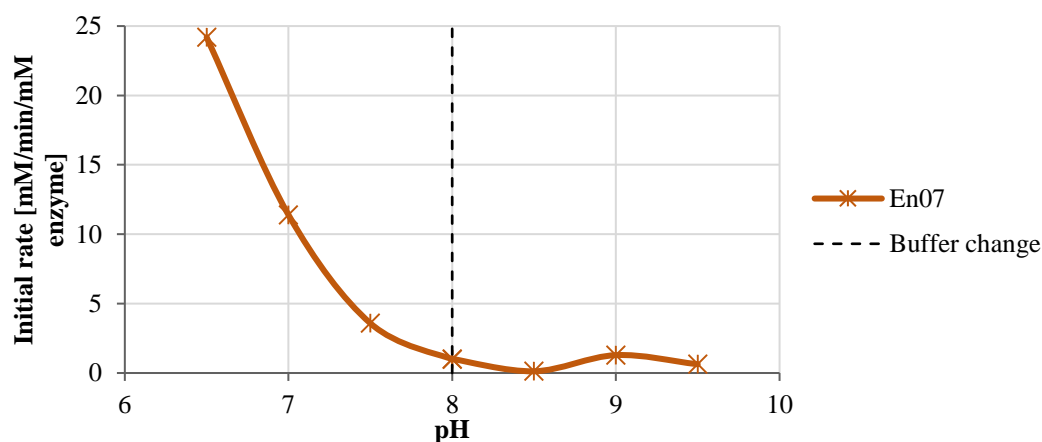


Figure 17. pH profile of En07 based on initial rate. Reaction conditions: phenyl pyruvate 122 (0.8 mM), methylamine hydrochloride 76 (700 mM), NADPH (0.8 mM), En07 (0.3 mg/mL). Consumption of NADPH monitored at 340 nm. Rate calculated based on NADPH standard curve.

Next the most desirable buffer concentration for the reaction was determined by carrying out reactions with **En01** in a variety of buffer concentrations all using Tris buffer at pH 8.5 (**Figure 18**). At this point reactions were performed using 100 mM keto acid substrate and 700 mM amine according to previously published protocols.¹⁰⁹

Data analysis showed that while a small (<5%) inhibition effect was observed in the initial rate, this was a surmountable obstacle given the large increase in overall conversion. This is particularly useful in the case of small scale reactions, where constant pH monitoring and adjusting is not practical. Therefore, all future reactions were carried out with 200 mM Tris HCl pH 8.5.

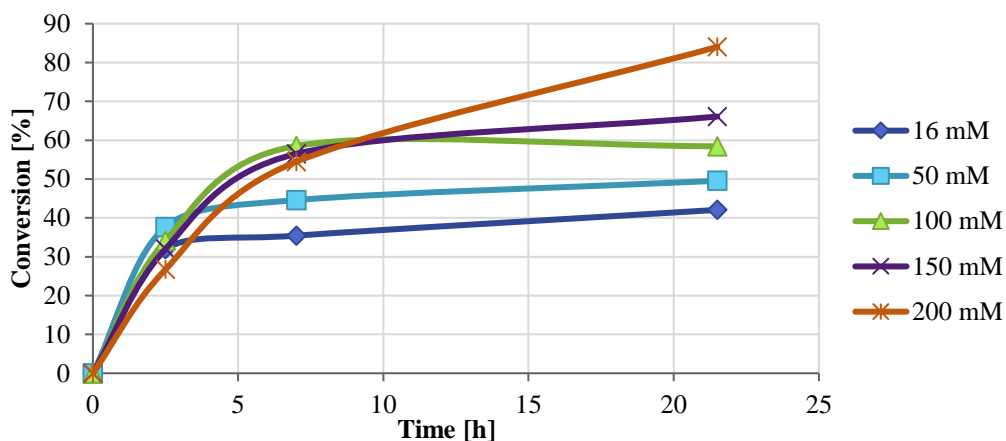


Figure 18. Effect of Tris HCl buffer (pH 8.5) concentration on conversion using En01. Reaction conditions: phenyl pyruvate 122 (100 mM), methylamine hydrochloride 76 (700 mM), NADPH (1 mM), D-glucose (300 mM), En01 (1.2 µg/mL), GDH (0.25 mg/mL), 25 °C, enzyme lysed in 50 mM Tris HCl buffer (50 mM, pH 8.5, 300 mM NaCl). Conversion calculated against benzonitrile internal standard, based on the production of 78.

Having optimised the initial reaction parameters a large-scale reaction was carried out using **En01** clarified lysate to demonstrate the utility of this biocatalytic system. The choice of the enzyme form was made after it was observed that reactions employing clarified lysate are cleaner when compared with unclarified lysate. A 3 g scale reaction at 100 mM substrate **122** loading was carried out in an EasyMax reactor (**Figure 19**) with in-line pH monitoring, which allowed the pH to be adjusted to 8.5 and maintain a high turnover (**Figure 20**). This gave a conversion value by HPLC monitoring of 87% with an isolated yield of 83% and excellent ee 99% (*S*), results that correlate with previous scale-up findings.¹⁰⁹



Figure 19. Reaction mixture and reactor used for large scale reaction (3 g scale).

This initial successful scale-up demonstrated the high biocatalytic potential of **En01** and in addition that the process can be scaled up effectively and **En01** is viable for further development as a biocatalyst.

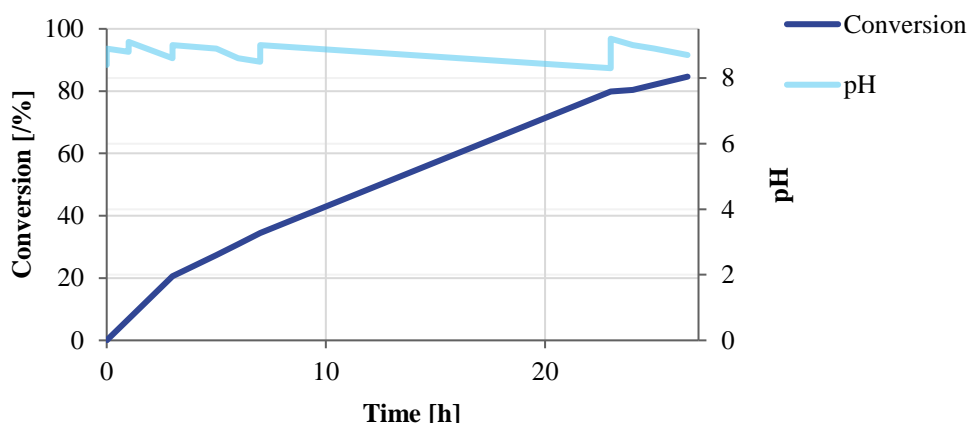


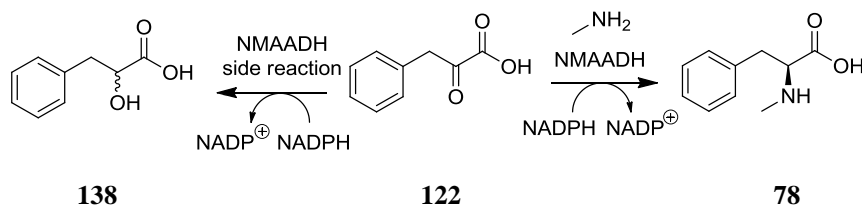
Figure 20. Reaction profile of large scale production of *N*-methyl phenylalanine 78 with En01. Reaction conditions: phenyl pyruvate 122 (100 mM), methylamine hydrochloride 76 (700 mM), D-glucose (300 mM), NADPH (1 mM), GDH (0.01 mg/mL Glucose dehydrogenase from *Pseudomonas sp.*, initial pH 8.3, 25 °C, enzyme lysate in Tris HCl buffer (200 mM). Total volume: 180 mL. Conversion calculated using benzonitrile as internal standard, based on production of 78.

3.3.2. Substrate and catalyst loading

One of the drawbacks of the known reductive amination enzymes (such as IREDs) is that they do not provide high conversions when a low amine stoichiometry is employed, which makes them industrially unattractive. This means that to achieve high conversions and maximum efficiency in manufacturing, high amine stoichiometry

needs to be employed. This reduces the environmental friendliness of the process, as this excess of amine needs to be removed from the final product and recycled or disposed. Therefore, reducing the amine stoichiometry is economically desirable, and enzymes that can use a stoichiometric amine loading would be beneficial.

Another aspect that merits mention is the side reactions that may result in ketone reduction to alcohol. These reactions are catalysed either by endogenous keto reductases and/or by reductive amination enzymes, such as IREDs as previously reported.¹¹⁹



Scheme 38. Side reaction of the NMAADHs.

Initial reactions showed that the NMAADH enzymes were also capable of reducing the ketone substrate to the corresponding alcohol (in the case of phenyl pyruvate **122** this is 3-phenyl lactic acid **138**), albeit at a much slower rate than the reductive amination. Phenyl pyruvate in the absence of enzyme does not produce any 3-phenyl lactic acid **138** (Scheme 38), which suggests that the NMAADHs are carrying out the reduction. Initial development work was performed using purified *P. putida* NMAADH (En01), phenyl pyruvate (**122**, 0.8 mM) and varying concentrations of methylamine hydrochloride **76**. The results show a decrease in absorbance in the samples containing methylamine hydrochloride **76** as NADPH is converted to NADP⁺. There is a significant difference when these are compared to the negative controls containing no amine or no ketone. The range of amine concentrations tested show different rates of reaction, (Figure 21). It was seen that 700 mM methylamine **76** resulted in rapid consumption of co-factor, while lower amine concentrations gave rise to correspondingly slower conversions. Additionally, the negative control with no amine present was carried out, showing a low level of co-factor consumption presumably from the background keto-reductase activity.

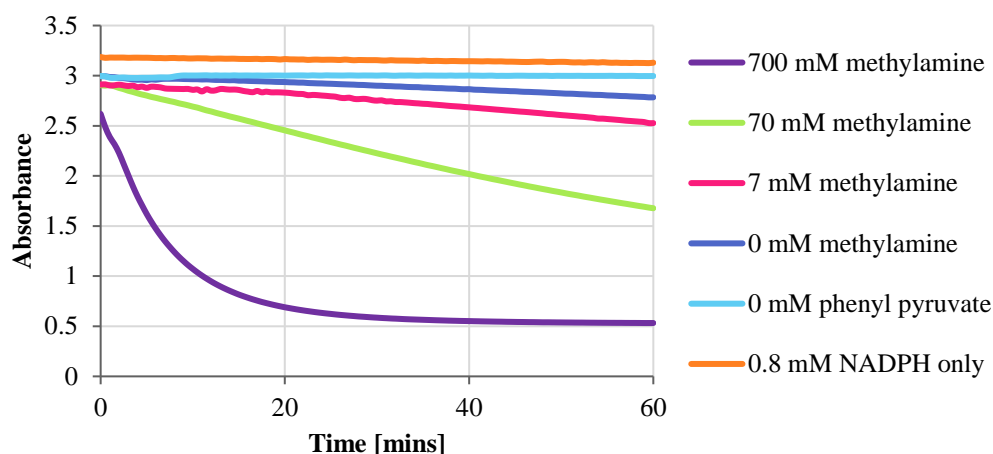


Figure 21. NADPH consumption assay demonstration with controls. Reaction conditions: phenyl pyruvate 122 (0.8 mM), methylamine HCl 76 (as shown in figure), NADPH (0.8 mM), purified *P. putida* NMAADH En01 (0.04 mg/mL), Tris HCl buffer (200 mM) pH 8.5.

Therefore, to minimise background reactions, it is important to maintain a high amine concentration, which conflicts with the goal of reducing the amine stoichiometry. To determine an effective amine loading (providing the best compromise between conversion and amine stoichiometry) a range of methylamine concentrations were tested simultaneously with a range of enzyme concentrations. These experiments were carried out at 10 mM concentration of phenyl pyruvate and a range of 0.1 to 100 amine equivalents were explored.

Amine loadings greater than 10 equivalents (100 mM) resulted in near quantitative conversion, except in the case of the lowest enzyme loadings where some inhibition was observed at high amine concentrations (**Figure 22A**). Higher enzyme loadings up to 0.005 mM (the highest tested) resulted in an increased level of conversion to 3-phenyl lactic acid, with near quantitative conversion at amine loadings less than 10 mM (**Figure 22B**). Using an excess of keto acid (less than 10 mM amine loading) resulted in conversions below 20% at all enzyme loadings. Optimum conversion was seen at 0.0005 mM enzyme loading, as at lower concentrations the conversion was diminished, but higher concentration saw increased loss of substrate to 3-phenyl lactic acid.

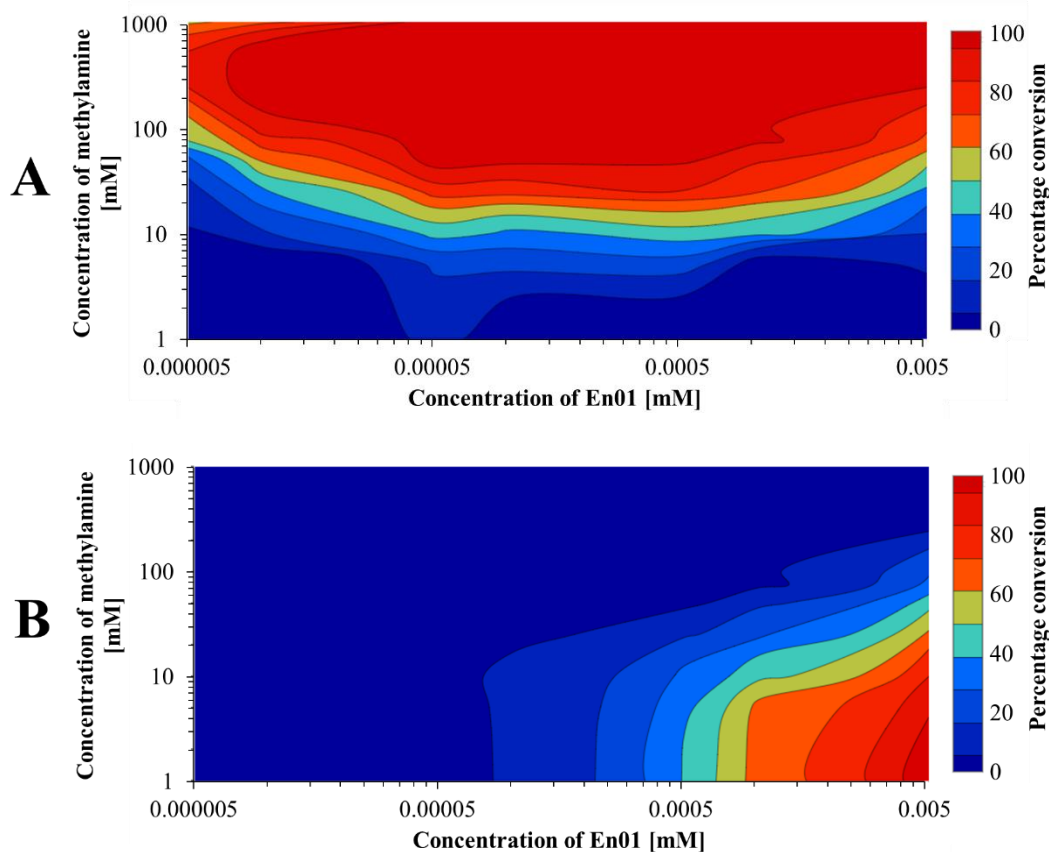


Figure 22. Conversion to **A** desired product *N*-methyl phenylalanine **78** and **B** undesired product 3-phenyl lactic acid **138**. Reaction conditions: phenyl pyruvate **122** (10 mM), methylamine hydrochloride **76** (0-1000 mM), NADPH (1 mM), D-glucose (30 mM), En01 (5.000-0.005 mM), GDH (0.25 mg/mL), 25 °C, Tris HCl buffer (200 mM, pH 8.5).

The optimal enzyme and amine loadings were also investigated for the KIREDD enzymes. The KIREDDs demonstrated a lower level of activity, with higher enzyme loadings being more favourable (**Figure 23A**). However, despite the lower activity these enzymes also showed a lower level of conversion to 3-phenyl lactic acid (**Figure 23B**).

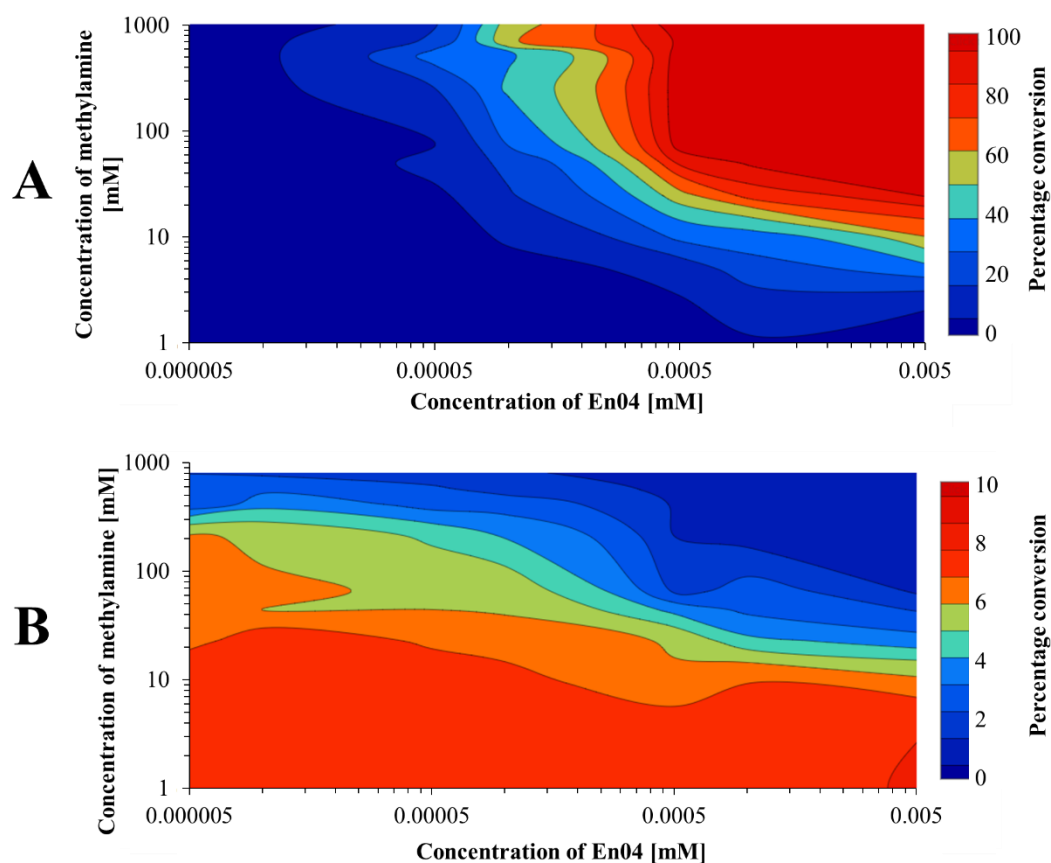


Figure 23. Conversion to **A** desired product *N*-methyl phenylalanine **78** and **B** undesired product 3-phenyl lactic acid **138**. Reaction conditions: Phenyl pyruvate **122** (10 mM), methylamine hydrochloride **76** (0 -1000 mM), NADPH (1 mM), D-glucose (30 mM), En04 (0.005-5.000 mM), GDH (0.25 mg/mL), 25 °C, Tris HCl buffer (200 mM, pH 8.5).

In the interests of generating consistent screening conditions, a lower enzyme loading (0.1 μ M) was chosen. While **En04** performed best at higher enzyme loadings, these resulted in high conversions to 3-phenyl lactic acid for **En01**. Minimising this background reaction would provide the clearest outlook on which substrates were best accepted by the enzymes.

3.3.3. Enzyme formulation

Preparation of purified proteins on scale is costly, and nickel resin is insufficiently environmentally friendly to be used on a large scale. Therefore, crude cell lysates were investigated as a cheaper alternative. Payton *et al.* stated that NMAADH lysates became inactive rapidly; therefore, the lysate stability over time was assessed.

Lysates were prepared from *E. coli* whole cells expressing NMAADH proteins by sonicating the cell pellet in buffer (50 mM Tris HCl, 300 mM NaCl, pH 8.5). The cell debris was cleared by centrifugation (4000 rpm, 20 minutes, 4 °C) and the clarified lysate was stored at 4 °C. A second lysate preparation was produced with the addition of stabilising reagents (1 mM EDTA and 1 mM DTT) to the lysis buffer in an attempt to improve the stability. Lysates were assayed for activity towards the reductive amination of phenylpyruvate **122** with methylamine **76** after storage for up to 4 days. Each reaction was allowed to proceed for 2 hours and the conversion was analysed by HPLC (results in **Figure 24**). The results show that both lysate preparations maintained some activity over 4 days and the stabilized lysate had higher activity prior to storage (time: 0 h) as well as throughout the experiment.

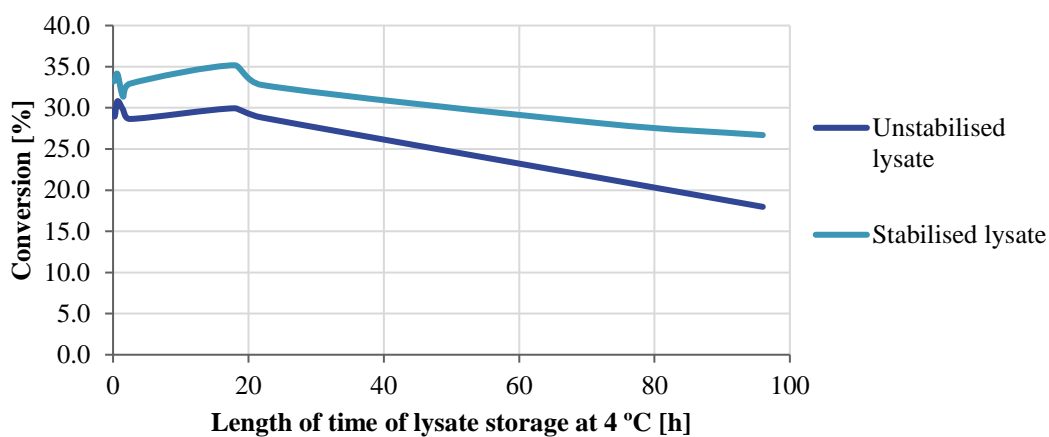


Figure 24. Activity of lysate over time when refrigerated. Reaction conditions: phenyl pyruvate **122** (100 mM), methylamine hydrochloride **76** (700 mM), D-glucose (300 mM), NADPH (1 mM), GDH (0.025 mg/mL GDH from *Pseudomonas sp.*), initial pH 8.3, 25 °C, Tris HCl buffer (50 mM), En01 enzyme lysate. Conversion calculated using benzonitrile internal standard.

In addition, the use of lysates (or other non-purified protein) was problematic as side reactions were observed. Phenyl pyruvate was seen to be converted to L-phenylalanine, likely due to the presence of endogenous transaminases in the *E. coli*. This reaction was observed at less than 5% conversion, so it was not thought to present an insurmountable problem.

In most cases, industrial enzymatic processes require the enzyme to be in a lyophilised form rather than as fresh lysate. It allows the enzyme to be stored for longer periods of time, retaining stability and allowing the enzyme to be transported. Enzyme can also be lyophilised and retains a near identical activity profile between lysate and

lyophilisation. This increases the utility of the enzyme as it removes the necessity of purification and allows the enzyme to be stored long term.

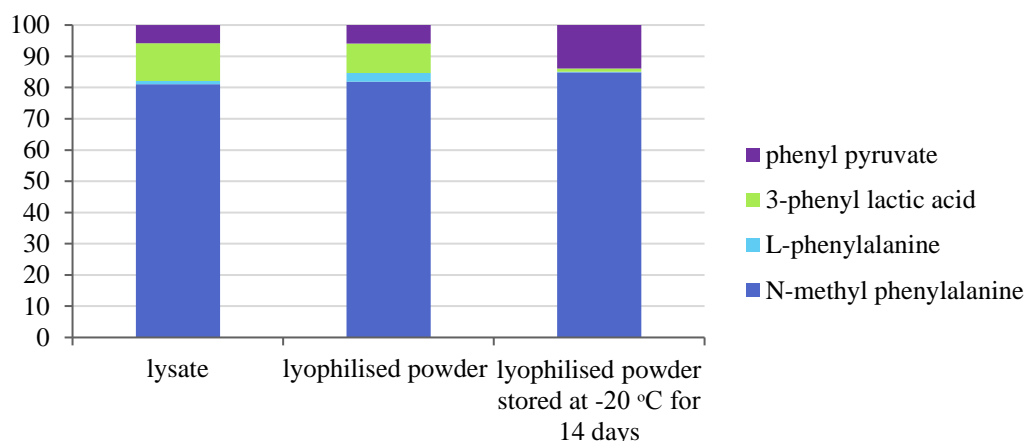


Figure 25. Product profile of En01 lysate versus lyophilised powder. Reaction conditions: phenyl pyruvate 122 (100 mM), methylamine hydrochloride 76 (700 mM), D-glucose (300 mM), NADPH (1 mM), GDH (0.025 mg/mL GDH from *Pseudomonas sp.*), initial pH 8.3, 25 °C, Tris HCl buffer (50 mM), En01 crude lysate (0.5 mL) or En01 lyophilised powder (11.2 mg).

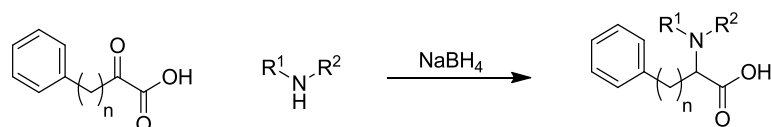
Lyophilised powder was prepared by lyophilising clarified enzyme **En01** lysate, and the enzymatic powder used to run a comparison experiment with lysate. As it can be seen in **Figure 25**, the conversion to *N*-methyl phenylalanine **78** remained consistent between the clarified lysate and the lyophilised powder (once corrected to give the same concentration). The lyophilised powder was also stored at -20 °C and this did not result in a significant loss in activity.

3.4. Enzyme screening

Having successfully produced purified protein and lyophilised powder, as well as optimising the reaction conditions, screening of other substrates was started. A variety of different amine and ketone substrates were selected for investigation. For many of these product standards also needed to be synthesised and appropriate analytical methods identified.

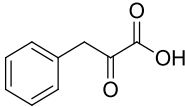
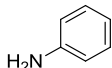
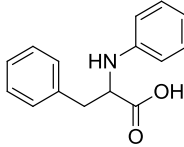
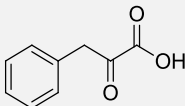
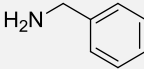
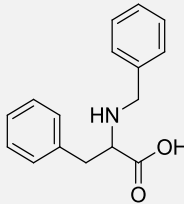
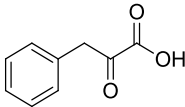
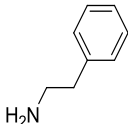
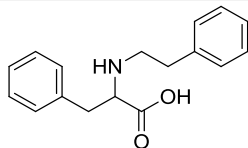
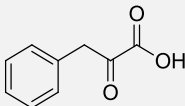
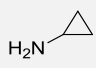
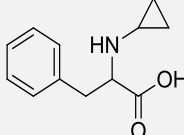
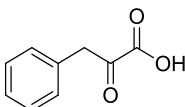
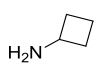
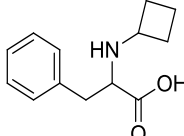
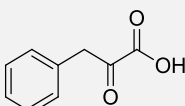
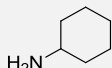
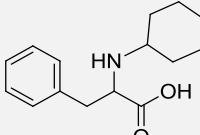
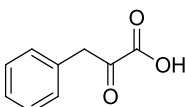
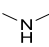
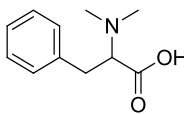
3.4.1. Synthesis of product standards

Most of the analytical standards for the amino acid products were commercially unavailable, however a number of products have been synthesised using chemical methods. Several *N*-functionalised amino acids were synthesised *via* sodium borohydride reductive amination for use as product standards (**Scheme 39**). Although the initial reaction yields were low to moderate (**Table 10**) no optimisation was carried out to improve the yield, as these compounds were to be used as markers.



Scheme 39. Synthesis of racemic product standards. Reaction conditions: i) keto acid (25 mM), amine 75 mM), in methanol, stirred for a minimum of 1 h. (ii) sodium borohydride (75 mM).

Keto acid	Amine	Product	Yield [%]
 122	 124	 139	80
 122	 140	 141	77
 122	 142	 143	77
 122	 144	 145	69
 122	 146	 147	17

 122	 148	 149	20
 122	 150	 151	52
 122	 152	 153	34
 122	 154	 155	73
 122	 156	 157	44
 122	 158	 159	73
 122	 127	 160	25

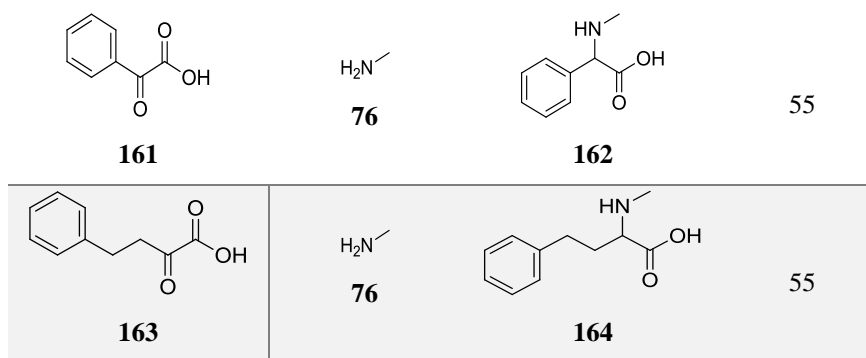
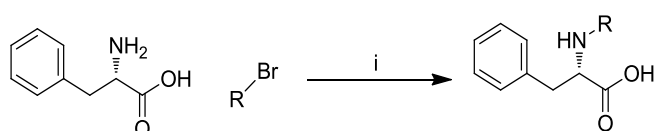


Table 10. Racemic standards preparation. Isolated yield after mass directed auto purification (MDAP). Reaction conditions: i) keto acid (25 mM), amine 75 mM), in methanol, stirred for a minimum of 1 h. (ii) sodium borohydride (75 mM). Amines were added as the free amine, except for 76, 142 and 146 which were added as the HCl salt.

The conversions observed under the metal hydride reductive amination can be compared to the enzymatic conversions. In many cases the trends are similar, possibly due to the efficacy of the imine formation. For example, aniline **148** gave a low conversion (20%) and did give conversion within the enzymatic reaction. However, some of the low conversions are due to difficulty in isolation and problems with stability, such as **147**.

Single enantiomer product standards were synthesised using authentic L-phenylalanine, by alkylation using the relevant alkyl bromides, as shown in **Scheme 40**.¹²⁰ Again the yields are low, and the reaction and optimisation conditions were not optimised as they were only required as product standards. The products were very pure, this was the priority, not achieving high yields.



Scheme 40. Synthesis of single enantiomer product standards. Reaction conditions: (i) L-phenylalanine (700 mM), alkyl bromide (833 mM), sodium hydroxide (850 mM) in 50:50 ethanol/water, reflux, 2h.

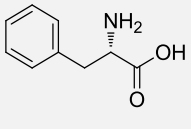
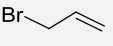
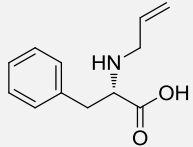
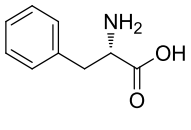
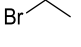
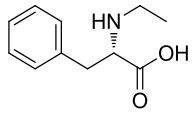
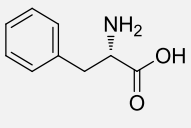
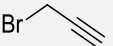
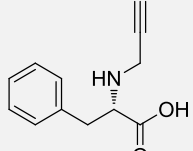
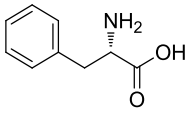
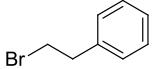
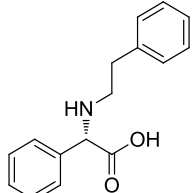
Amino acid	Alkyl halide	Product	Yield [%]	ee
 78	 165	 145a	2	>99%
 78	 166	 139a	6	>99%
 78	 167	 147a	5	>99%
 78	 168	 153a	37	>99%

Table 11. L-enantiomers synthesised as product standards. Reaction conditions: L-phenylalanine (700 mM), alkyl bromide (833 mM), sodium hydroxide (850 mM) in 50:50 ethanol/water, reflux, 2h.

3.4.2. Screening plates assay

The possibility of expressing the enzymes and preparing the lysate in 96 well plates was investigated in order to carry out high throughput screening experiments. In this context a glycerol stock plate was prepared in the desired layout, followed by enzyme expression, lysis and purification using a Kingfisher nickel affinity system. However the growth of these enzymes was not consistent, as shown by the expression SDS-PAGE in **Figure 26**.

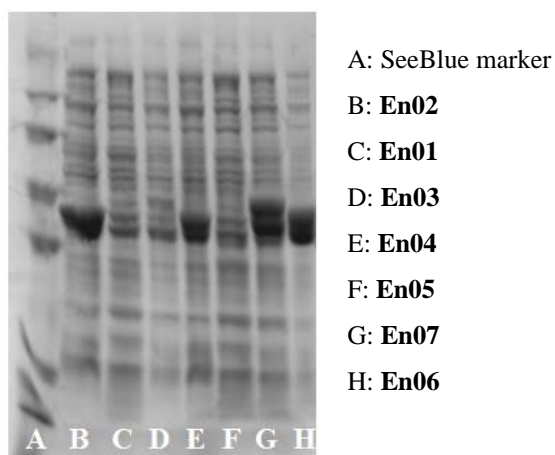
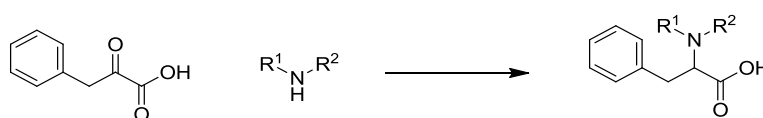
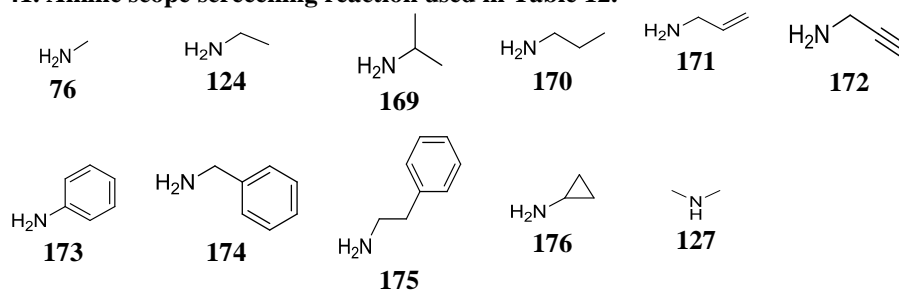


Figure 26. SDS-PAGE gel showing expression levels of En01-07 when grown in a 96 well plate.

Despite the differing expression levels these were screened against a variety of amines (Figure 26). This showed surprisingly high levels of conversion, including with some larger amines such as benzylamine and phenylethylamine. However, these values cannot be compared between enzymes as the expression levels were so variable.



Scheme 41. Amine scope screening reaction used in Table 12.



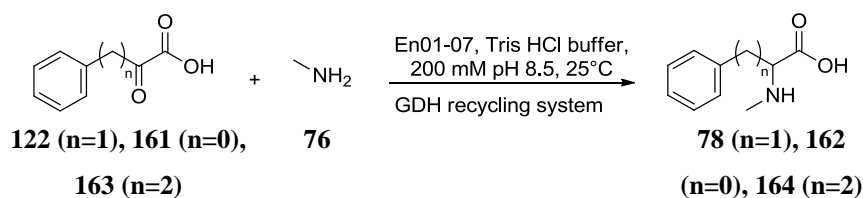
	76	124	140	142	144	146	148	150	152	154	127
En01	47	2	0	2	11	5	0	12	2	30	0
En02	73	36	0	38	66	52	0	73	14	72	0
En03	75	4	0	7	51	1	0	11	31	14	0
En04	93	26	0	0	62	1	0	99	5	72	0
En05	90	2	0	0	0	9	0	0	18	10	0
En06	89	18	0	1	34	0	0	30	14	68	0
En07	92	20	0	2	36	50	0	18	15	69	0
Negative control	0	0	0	0	3	0	0	1	0	11	0

Table 12. Results of amine screening against hit plate. Reaction conditions: phenyl pyruvate 122 (10 mM), amine (100 mM), D-glucose (30 mM), NADPH (1 mM), GDH (0.25 mg/mL), initial pH 8.5, 25 °C.

Future screening was carried out using purified protein at a standardised concentration of 0.1 μ M. The purified proteins were stored in 50% glycerol solution and diluted with buffer when used in reactions.

3.4.3. Keto acid scope screening

The α -keto acid substrate scope was initially tested, by altering the length of the chain connecting the keto acid and aromatic ring. The activity of compound **122** was compared to keto acids **161** and **163**, in reaction with methylamine **76** at 1 and 10 equivalents (**Table 13**). Results point towards a preference for aliphatic spacers as keto acid **161** showed very low conversions, with no conversion at stoichiometric amine loadings. Keto acid **163** delivered *N*-methyl amino acid **164** in good yield at 10 equivalents of amine, though lower activities were observed for **En04-07**. This was also reflected in the stoichiometric loading data, where the conversions to **164** were lower, but followed a similar trend.

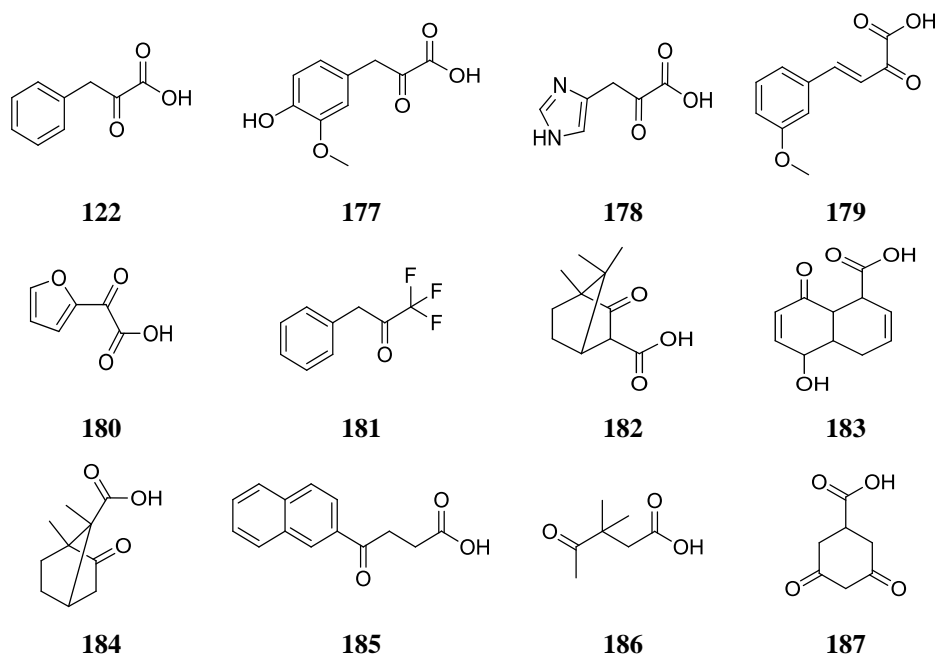


Scheme 42. Screening of alternative chain length keto acids.

Keto acid	Amine	Equivs of amine	Product	Yield [%]						
				Enzyme						
				01	02	03	04	05	06	07
		10		98	99	82	99	99	99	99
		10		7	2	3	4	2	4	4
		10		86	89	88	46	49	49	48
		1		69	65	72	33	37	11	26
		1		0	0	0	0	0	0	0
		1		64	65	71	33	18	26	24

Table 13. NMAADHs in reaction with several keto acids. Reaction conditions: keto acid (10 mM), amine 76 (10 mM or 100 mM), NADPH (0.1 equiv), GDH (1 mg/mL), D-glucose (3 equiv), 25 °C. Tris HCl buffer (200 mM, pH 8.5), 24 h.% Conversion (ketone area vs reductive amination product area vs carbonyl reduction side product area).

Having investigated adjusting the length of the linking carbon chain, a wider range of ketones was screened, to investigate whether a wider scope of ketones (**Scheme 43**) could be accepted. These included α -keto acids **177-180**, a ketone analogue of phenyl pyruvate **181**, a β -keto acid **182** and a variety of γ -keto acids **183-187**. These substrates were screened with 10 equivalents of methylamine, and the resulting reactions analysed by LCMS after 24 hours.



Scheme 43. Wider scope of ketones screened. Reaction conditions: keto acid (10 mM), methylamine **76** (100 mM), NADPH (0.1 equiv), GDH (1 mg/mL), D-glucose (3 equiv), 25 °C. Tris HCl buffer (200 mM, pH 8.5), 24 h. %

This screening showed no activity for any substrates apart from α -keto acids (no activity observed with **181-187**), which would support the theory that the α -keto acid functionality and geometry is important for binding the substrate in the correct orientation for enantioselective reduction. In addition, only **177** and **179** from the α -keto acids showed activity with any of the seven enzymes. These were also screened with propargylamine **146**, which also demonstrated conversions across the enzyme panel. **177** gave higher conversions than **179**, which was consistent with the results in **Table 13** as **179** has a longer linking chain between the keto acid and the phenyl ring. In addition, both substrates were accepted better by the NMAADHs (**En01-03**) than the other enzymes. Again, this is consistent with previously observed results.

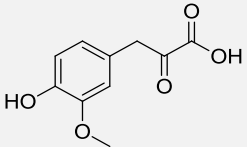
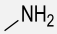
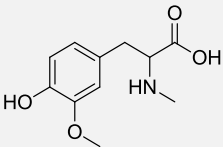
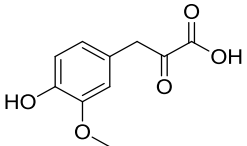
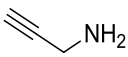
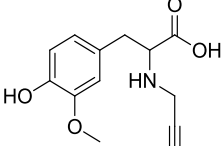
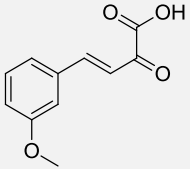
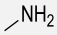
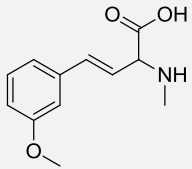
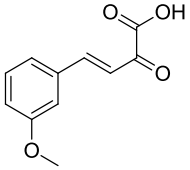
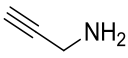
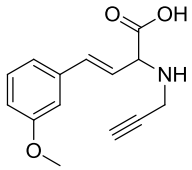
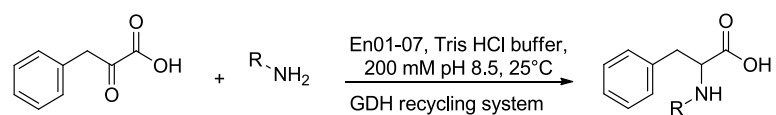
Keto acid	Amine	Product	Yield [%]						
			Enzyme						
			01	02	03	04	05	06	07
 177	 76	 188	72	44	75	23	6	2	2
 177	 146	 189	47	38	43	18	25	31	33
 179	 76	 190	11	14	23	8	11	8	5
 179	 146	 191	7	9	39	0	2	10	7

Table 14. Other accepted keto acid substrates. Reaction conditions: keto acid **177**, **179** (10 mM), amines **76**, **146**(100 mM), NADPH (0.1 equiv), GDH (1 mg/mL), glucose (3 equiv), Tris HCl buffer (200 mM, pH 8.5), 25°C, 24 h. ^cconversion to desired product determined by LC-MS.

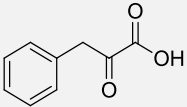
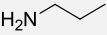
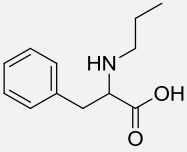
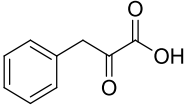
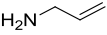
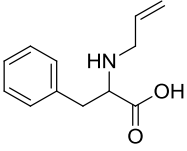
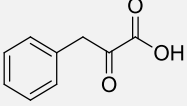
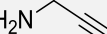
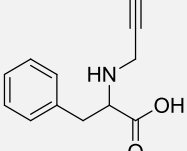
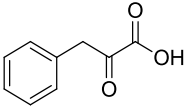
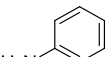
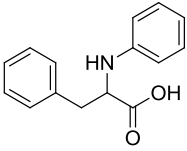
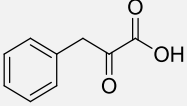
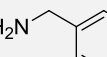
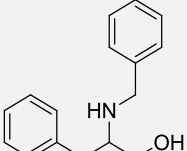
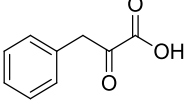
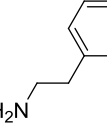
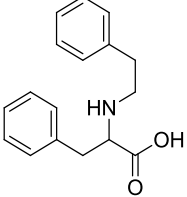
3.4.4. Amine scope screening

Subsequently, all seven enzymes were screened against the optimised reaction of phenyl pyruvate **122** and methylamine **76**. With 10 equivalents of amine all the biocatalysts yielded the product **78** in good conversions. **En01-03** gave higher conversions than the other enzymes. Having established that all seven enzymes could carry out this reaction the amine scope was expanded to cover a variety of amine types, including alkyl-, aryl- and secondary amines. The results shown in **Table 15** reveal some excellent conversions, with many of the other amines in combination with phenyl pyruvate gave excellent conversions.



Scheme 44. Reaction investigated in Table 15.

Keto acid	Amine	Product	Yield [%]						
			Enzymes						
			01	02	03	04	05	06	07
<p>122</p>	<p>76</p>	<p>78</p>	97	98	98	51	81	32	33
<p>122</p>	<p>124</p>	<p>139</p>	16	6	5	5	9	2	2
<p>122</p>	<p>140</p>	<p>141</p>	0	0	0	0	0	0	0

Keto acid	Amine	Product	Yield [%]						
			Enzymes						
			01	02	03	04	05	06	07
 122	 142	 143	1	0	0	0	1	0	0
 122	 144	 145	12	6	5	16	30	10	23
 122	 146	 147	92	52	58	19	24	26	82
 122	 148	 149	0	0	0	0	0	0	0
 122	 150	 151	0	0	0	18	17	7	0
 122	 152	 153	0	0	0	3	5	1	2

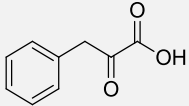
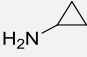
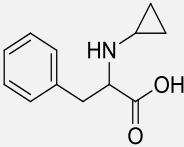
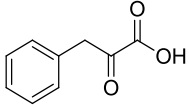
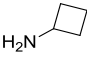
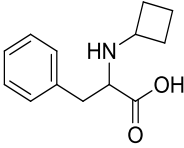
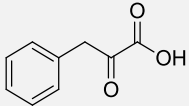
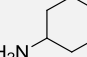
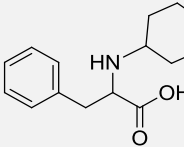
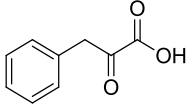
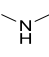
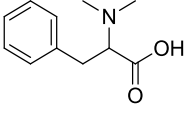
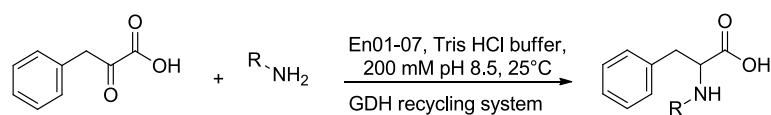
Keto acid	Amine	Product	Yield [%]						
			Enzymes						
			01	02	03	04	05	06	07
 122	 154	 155	59	27	29	43	79	29	2
 122	 156	 157	0	0	0	0	0	0	0
 122	 158	 159	0	0	0	0	0	0	0
 122	 127	 160	0	0	0	0	0	0	0

Table 15. Comparison of reductive amination activity between phenyl pyruvate **122** with different amines. Reaction parameters: keto acid **122** (10 mM), amine (100 mM), NADPH (1 mM), En01-07 (0.1 μ M), GDH (0.25 mg/mL), D-glucose (3 equiv), 25°C, Tris HCl buffer (200 mM, pH 8.5), 24 h. Conversion calculated from HPLC. Enantiomeric excess for all the compounds with conversion greater than 3% were >99% (*S*)

Reaction with ethylamine **124** gave low conversions to product **139** in accordance with previous findings for **En01**.⁹² Isopropylamine **140** gave no conversion to **141**, while *n*-propylamine **142** gave only trace conversions, in both cases this is probably due to the steric bulk. The unsaturated systems of **144** and **146**, gave higher conversions than **142**, which is likely due to a combination of reduced steric bulk and potential π - interactions. Results are in accordance with Höhnes's findings for similar π -systems in the case of IRED catalysed aminations.⁸⁸ Aniline **148** showed no conversion in our hands, however whether this is due to the electron rich character of the amine or the steric bulk remains unclear. By comparison benzylamine **150** showed excellent

conversions with **En04-06**, with no conversion for the other four enzymes. Phenyl ethyl amine **152** showed a similar pattern of activity, albeit with far lower conversions. Cyclopropylamine **154** was also accepted with high conversions, as it is much smaller than the majority of the other amines investigated this is not surprising, sterically constrained amines appear to be favoured.

Having demonstrated that the reactions work well at 10 equivalents of amine, the successful reactions were repeated with stoichiometric amine loading. These demonstrated lower conversions across the board, but with similar trends to the 10 equivalents of amine (**Table 16**). While *n*-propylamine **142** demonstrates no conversion, π -conjugated molecule **146** is accepted, though the maximum conversion was 5%. Amine **154** was well accepted across all enzymes, in particular NMAADHs. Benzylamine **150** gave very little conversion for NMAADHs, but shows higher conversions for KIREDs, especially **En05**.



Scheme 45. Reaction shown in **Table 16**.

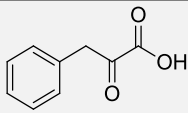
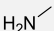
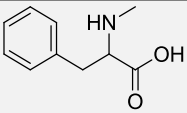
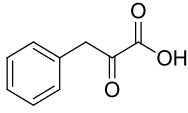
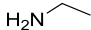
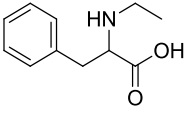
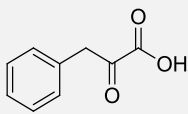
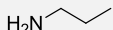
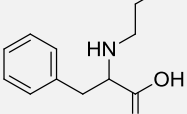
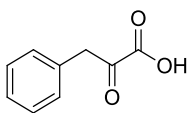
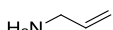
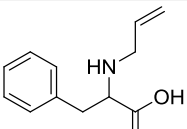
Keto acid	Amine	Product	Yield [%]						
			Enzymes						
			01	02	03	04	05	06	07
 122	 76	 78	55	47	50	14	23	10	8
 122	 124	 139	2	1	1	0	1	0	0
 122	 142	 143	0	0	0	0	0	0	0

Keto acid	Amine	Product	Yield [%]						
			Enzymes						
			01	02	03	04	05	06	07
			2	1	1	3	5	2	3
			20	9	10	0	3	2	21
			0	0	0	7	18	4	-
			0	0	0	3	3	2	1
			32	11	11	11	23	1	-

Table 16. Comparison of reductive amination activity between phenyl pyruvate **122** with different amines. Reaction parameters: keto acid **122** (10 mM), amines (10 mM), NADPH (1 mM), En01-07 (0.1 μ M), GDH (0.25 mg/mL), D-glucose (3 equiv), 25°C, Tris HCl buffer (200 mM, pH 8.5), 24 h.

These results represent an important extension of the amine scope since only methylamine **76** and, to a lower extent ethylamine **124**, have been previously reported as amines in the reductive amination of α -keto acids. Interestingly other amine substrates such as isopropylamine **140**, dimethylamine **127** or aniline **148** derivatives

did not work in our hands, suggesting that substrate scope needs to be further improved. Furthermore, background carbonyl reduction to the corresponding alcohol, was slower than the rate of reductive amination, but was observed at lower amine concentrations with poor substrates.

Keto acid	Amine	Product	Yield [%]						
			Enzymes						
			01	02	03	04	05	06	07
 122	 76	 78	>99	>99	>99	>99	>99	>99	>99
 122	 124	 139	>99	>99	>99	>99	>99	>99	>99
 122	 142	 143	>99	>99	>99	>99	>99	>99	>99
 122	 144	 145	>99	>99	>99	>99	>99	>99	>99

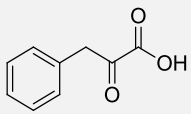
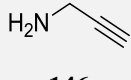
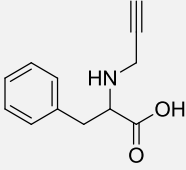
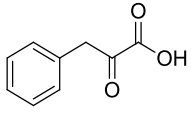
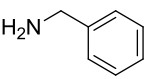
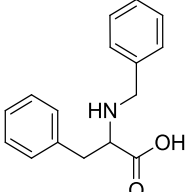
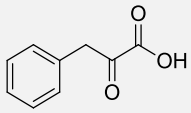
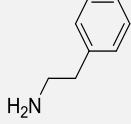
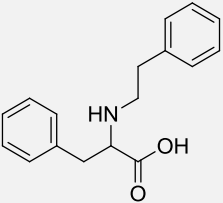
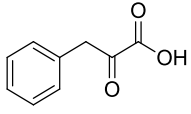
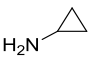
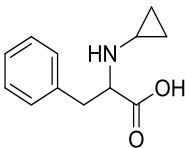
Keto acid	Amine	Product	Yield [%]						
			Enzymes						
			01	02	03	04	05	06	07
 122	 146	 147	>99	>99	>99	>99	>99	>99	>99
 122	 150	 151	>99	>99	>99	95	88	>99	97
 122	 152	 153	-	-	-	-	-	-	-
 122	 154	 155	>99	>99	>99	>99	>99	>99	>99

Table 17. Enantioselectivity of reactions between phenyl pyruvate 122 and different amines. Reaction parameters: keto acid 122 (10 mM), amines (10 mM), NADPH (1 mM), En01-07 (0.1 μ M), GDH (0.25 mg/mL), D-glucose (3 equiv), 25°C, Tris HCl buffer (200 mM, pH 8.5), 24 h. – indicates ee not determined.

It was also found that all these reactions were highly enantioselective, all the reactions shown in **Table 17** showed ee greater than 99% (*S*), with the exception of the reaction of benzylamine catalysed by KIREDDs. This may be due to the larger steric bulk of benzylamine **150** forcing a new conformation to take place. Unfortunately, the ee for phenylethylamine **152** could not be determined for comparison, due to low conversions, as this could be used to support this theory. Alternatively, epimerisation

could be taking place after product formation, which is an area requiring greater investigation.

The ee was determined using the chiral method detailed in **Table 26**, by comparison of chemically synthesised racemic product standards and L-enantiomer with reaction products. This supports the theory that α -keto acids are required as substrates to ensure a specific binding orientation, leading to a single enantiomer being formed.

This screening has determined that all seven of the enzymes selected have reductive amination activity, with a far wider range of amines than anticipated. In all cases the enzymes resulted in the *S* enantiomer, in most cases in greater than 99% ee. These enzymes are excellent enantioselective biocatalysts for the synthesis of *N*-functionalised amino acids.

3.4.5. Expanding the substrate scope

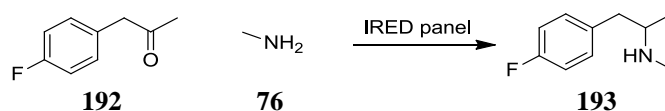
To establish the relevance of the seven enzyme panel previously selected, it was desirable to screen a wider range of enzymes. The reasons for this are two-fold, firstly to expand the range of reactions that can be enzyme catalysed, but also to compare the activity of the seven enzymes previously studied with IREDs. This could demonstrate the complementarity of the substrate scopes of the different enzyme classes.

A published panel of IREDs was screened against two model reactions. This panel consisted of 85 novel enzymes (**Figure 27**) from a variety of organisms set up in a 96 well plate with negative controls and replicates, designed by Roiban *et al* (see **section 8** for the complete paper).⁵⁵ **En04-07** were also inserted into the panel for comparison.

A1	A2	A3	A4	A5	A6	A7	A8	A9	A10	A11	A12
B1	B2	B3	B4	B5	B6	B7	B8	B9	B10	B11	B12
C1	C2	C3	C4	C5	C6	C7	C8	C9	C10	C11	C12
D1	D2	D3	D4	D5	D6	En04	D8	D9	D10	D11	D12
E1	E2	E3	E4	E5	E6	En05	C1	E9	E10	E11	E12
F1	F2	F3	F4	F5	F6	F7	A1	F9	F10	F11	F12
G1	G2	G3	G4	G5	C11	En07	G1	G9	G10	G11	G12
H1	H2	H3	H4	H5	H6	En06	H8	A3	H10	H11	H12

Figure 27. Plate map of IRED panel. Green cells: IRED containing wells, Black border: Enzyme replicates, Yellow cells: negative controls, Blue cells En04-07.

The first screening consisted of an amphetamine-like molecule (1-(4-fluorophenyl)propan-2-one **191**), a desirable substrate class to access (**Scheme 46**). The literature suggested running this plate at a pH of 7.0, so potassium phosphate buffer (pH 7.0, 100 mM) was used and the results are shown in



Scheme 46. Model reaction using 1-(4-fluorophenyl)propan-2-one **192** and methylamine **76** to synthesise amphetamine-like compound **193**.

	1	2	3	4	5	6	7	8	9	10	11	12		
A	66	2	0	0	0	0	5	0	0	5	0	0	Scale	
B	25	2	0	0	0	12	0	0	0	0	0	0		20
C	5	0	0	0	4	11	0	0	0	0	0	0		40
D	0	0	0	7	9	0	0	0	0	0	0	0		60
E	9	0	3	0	3	0	0	7	0	0	4	0		80
F	0	0	0	0	5	0	0	64	2	0	0	0		100
G	3	0	17	0	0	0	0	0	3	0	0	0		
H	0	4	9	0	3	0	0	0	0	3	0	0		

Figure 28. Heat map representing conversion of 1-(4-fluorophenyl)propan-2-one **192** and methylamine **76** (10 equiv) at pH 7.0 after 24 h. General procedure in 6.5.5. Reactions analysed by GC

The conversions achieved are moderate, with conversion observed in approximately 25% of wells. The highest conversions were observed in wells A1 and F8 (containing the same enzyme), which coincides with Roiban *et al.*'s most active enzyme.⁵⁵ However, as the earlier optimisation experiments with the seven enzyme panel had

shown an optimum pH of 8.5, the plate was also run at a higher pH with Tris HCl buffer (pH 9.0, 100 mM) (**Figure 29**).

	1	2	3	4	5	6	7	8	9	10	11	12	
A	97	5	0	4	0	0	9	0	2	27	0	0	0
B	38	2	0	0	0	0	0	0	0	0	0	0	20
C	58	0	0	0	7	3	5	0	4	0	0	0	40
D	0	0	0	3	13	0	0	0	0	0	0	0	60
E	65	2	0	0	0	0	0	81	0	0	64	0	80
F	0	3	0	0	4	0	0	97	19	0	0	3	100
G	17	0	16	0	0	0	0	8	3	0	0	0	
H	5	15	11	0	0	0	0	0	0	15	0	0	

Figure 29. Heat map representing conversion of 1-(4-fluorophenyl)propan-2-one **192** and methylamine **76** (10 equiv) at pH 9.0. General procedure in 6.5.5. Reactions analysed by GC.

Far higher conversions were achieved across the plate at pH 9.0, again with wells A1 and F8 again performing the best, giving nearly complete conversion after 24 hours.⁵⁵ The higher pH also gave a wider range of hits, some of which did not show reaction at pH 7.0. In light of the high conversions observed when 10 equivalents of amine was used (at pH 9.0), the plate was rescreened with only 1.1 equivalents of methylamine at pH 9.0 (**Figure 30**).

	1	2	3	4	5	6	7	8	9	10	11	12	
A	49	0	0	0	0	0	0	0	0	10	0	0	0
B	31	0	0	0	0	0	0	0	0	0	0	0	20
C	15	0	0	0	7	5	0	0	0	0	0	0	40
D	0	0	0	7	10	0	0	0	0	0	0	0	60
E	22	0	0	0	0	0	0	26	0	0	25	0	80
F	0	0	0	0	7	0	0	47	0	0	0	0	100
G	7	0	20	0	0	0	0	5	0	0	0	0	
H	0	0	10	0	0	0	0	0	0	0	0	0	

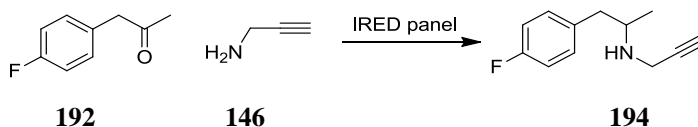
Figure 30. Heat map representing conversion of 1-(4-fluorophenyl)propan-2-one **192** and methylamine **76** (1.1 equiv) at pH 9.0. General procedure in 6.5.5. Reactions analysed by GC.

Several enzymes showed up to 50% conversion with 1.1 equivalents of amine. While this compound has been synthesised enzymatically previously, such a low stoichiometry of amine had never been achieved.¹²¹ In addition, the ee was determined for the hits that had conversion of greater than 5% (**Figure 31**). Generally, the ee's were high (greater than 80%), but a few examples showed lower enantioselectivity. IREDs are not as enantioselective as the seven enzymes previously screened.

	1	2	3	4	5	6	7	8	9	10	11	12	
A	90	-	-	-	-	-	-	-	-	37	-	-	100
B	61	-	-	-	-	-	-	-	-	-	-	-	50
C	88	-	-	-	-87	-93	-	-	-	-	-	-	0
D	-	-	-	-93	-90	-	-	-	-	-	-	-	-50
E	83	-	-	-	-	-	-	91	-	-	77	-	-100
F	-	-	-	-	-82	-	-	88	-	-	-	-	
G	-78	-	-83	-	-	-	-	-51	-	-	-	-	
H	-	-	-89	-	-	-	-	-	-	-	-	-	

Figure 31. Heat map representing enantioselectivity of 1-(4-fluorophenyl)propan-2-one **192** and methylamine **76** (1.1 equiv) at pH 9.0. General procedure in 6.5.5. Reactions analysed using Method 4.

Given the number of successful hits when using 1.1 equivalents of methylamine, other amines were also screened under this set of conditions, using Tris buffer at pH 9.0. Propargylamine **146** and *n*-propylamine **142** were selected to demonstrate whether the large number of enzymatic hits is replicated for larger amines. Propargylamine is known to be a good substrate for many IREDs and previously showed high activity with the seven enzyme panel investigated in this project.



Scheme 47. Extension of the amine scope screened to include propargylamine **146**.

	1	2	3	4	5	6	7	8	9	10	11	12	
A	59	7	0	3	0	0	0	0	0	15	0	0	0
B	27	3	0	0	0	0	0	0	0	0	0	0	20
C	2	0	0	0	5	3	6	0	2	0	0	0	40
D	0	0	0	8	5	0	0	0	0	0	0	0	60
E	9	0	0	0	0	0	0	5	0	0	62	0	80
F	0	0	0	0	5	0	0	61	47	0	0	35	100
G	5	0	16	0	0	0	0	3	3	0	0	0	
H	4	6	6	0	0	0	0	0	0	10	0	0	

Figure 32. Heat map representing conversion of 1-(4-fluorophenyl)propan-2-one **192** at pH 9.0 with 1.1 equivalent of amine **146**. General procedure in 6.5.5. Reactions analysed by GC.

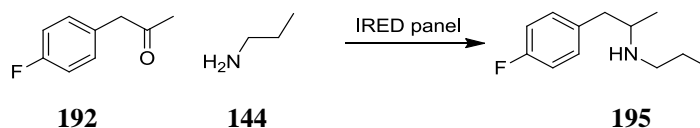
Propargylamine **146** also gave good results with maximum conversions of approximately 60% after 24 hours (**Figure 32**). These conversions were generally higher than those observed with methylamine (**Figure 30**). This is consistent with

findings with other IREDs (as discussed in 1.3.6) where propargylamine is an excellent substrate. This also coincides with the findings screening the seven enzyme panel, that propargylamine is a well-accepted amine. The enantioselectivity for this plate was also determined (Figure 33).

	1	2	3	4	5	6	7	8	9	10	11	12	
A	77	-	-	-	-	-	-	-	-	-10	-	-	100
B	42	-	-	-	-	-	-	-	-	-	-	-	50
C	36	-	-	-	-42	-100	-	-	-	-	-	-	0
D	-	-	-	-56	-100	-	-	-	-	-	-	-	-50
E	46	-	-	-	-	-	-	54	-	-	30	-	-100
F	-	-	-	-	-36	-	-	80	-	-	-	-	-
G	-100	-	-100	-	-	-	-	-100	-	-	-	-	-
H	-	-	-100	-	-	-	-	-	-	-	-	-	-

Figure 33. Heat map representing conversion of 1-(4-fluorophenyl)propan-2-one **192** at pH 9.0 with 1.1 equivalent of amine **146**. General procedure in 6.5.5. Reactions analysed by GC, as shown in 6.4.2.

The enantioselectivities were consistent with those observed in the case of methylamine (Figure 31). There were several examples of the ee being greater than 99%, but again the IREDs did not show as high enantioselectivity as the NMAADHs and KIREDS.



Scheme 48. Extension of the amine scope screened to include amine **146**.

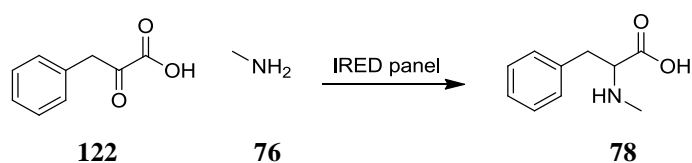
	1	2	3	4	5	6	7	8	9	10	11	12	
A	20	0	0	0	0	0	0	0	0	4	0	0	0
B	6	0	0	0	0	0	0	0	0	0	0	0	20
C	0	0	0	0	0	0	0	0	0	0	0	0	40
D	0	0	0	0	0	0	0	0	0	0	0	0	60
E	3	0	0	0	0	0	0	0	0	0	2	0	80
F	0	0	0	0	0	0	0	23	3	0	0	0	100
G	0	0	4	0	0	0	0	0	0	0	0	0	-
H	0	0	0	0	0	0	0	0	0	0	0	0	-

Figure 34. Heat map representing conversion of 1-(4-fluorophenyl)propan-2-one **192** at pH 9.0 with 1.1 equivalent of amine **142**. General procedure in 6.5.5. Reactions analysed by GC.

Substrate *n*-propylamine **142** did not yield high conversions when screened across this plate of IREDs. The maximum conversion observed was 23% (Figure 34), again from

the enzyme in wells A1 and F8. This was similar to the results seen for the NMAADHs and KIREds, where *n*-propylamine **142** was a poor substrate and did not achieve high conversions.

It should be noted that under none of these conditions or combinations of substrates did **En04-07** show any conversion to product (wells D7, E7, G7 and H7). Having demonstrated excellent activity levels with 1-(4-fluorophenyl)propan-2-one **192** as the substrate, the other model reaction screened utilised phenyl pyruvate **122** and methylamine **76** (**Scheme 49**). This was once again screened using both pH 7.0 and pH 9.0 with 10 equivalents of methylamine; the results are shown in **Figure 35** and **Figure 36** below.



Scheme 49. Examination of utility of IRED panel to synthesize *N*-methyl amino acids.

	1	2	3	4	5	6	7	8	9	10	11	12	
A	0	0	0	1	2	3	1	0	0	1	0	0	0
B	1	1	0	1	0	2	1	0	1	2	0	0	20
C	0	0	0	0	0	1	1	3	1	1	2	1	40
D	1	0	0	0	0	0	81	1	0	1	3	0	60
E	1	0	1	0	0	0	65	1	0	2	0	4	80
F	0	0	0	0	2	0	0	2	3	2	1	0	100
G	0	0	0	0	0	0	10	1	1	0	0	4	
H	0	0	0	0	0	1	75	0	0	0	2	2	

Figure 35. Heat map representing conversion of phenyl pyruvate **122** at pH 7.0 with 10 equivalent of methylamine **76**. General procedure in 6.5.5. Reactions analysed by GC.

When screening was carried out at pH 7.0 good conversions were observed, but only for the included KIREds and P5CR (**En04-07**). Maximum conversion observed was 81% for **En04**. However, when the plate was screened again at pH 9.0 the conversions were increased, as might be expected based on the previous success at higher pHs. Reactions catalysed by both **En04** and **En06** went to completion.

In addition, the reactions were performed using lysates, which resulted in some background activity in the phenyl pyruvate reactions. The low level of conversion observed across **Figure 36** was a result of conversion of phenyl pyruvate to L-

phenylalanine, which could not be distinguished from product formation. This meant that the concentration of biocatalyst in each well was not exactly equal as it will depend on the efficiency of expression and cell growth.

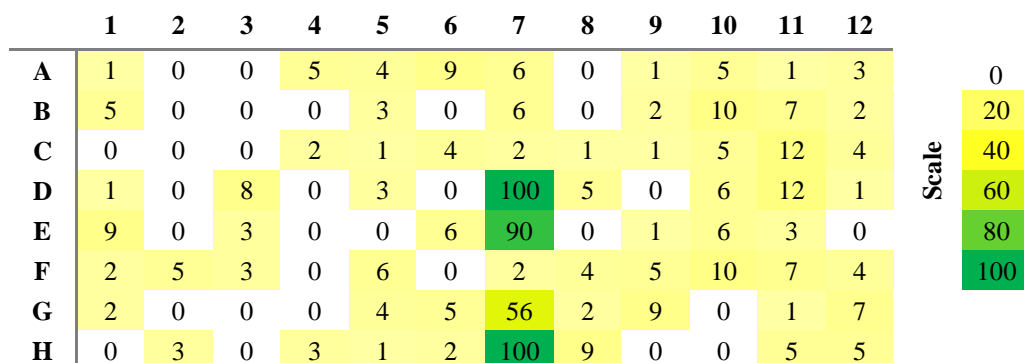


Figure 36. Heat map representing conversion of phenyl pyruvate **122** at pH 9.0 with 10 equivalent of methylamine **76**. General procedure in 6.5.5. Reactions analysed by GC.

This shows excellent complementarity between the IREDs and enzymes used to synthesise *N*-methyl amino acids. There does not appear to be an overlap in the types of ketones accepted by these enzyme clusters. While many IREDs showed excellent conversions with 1-(4-fluorophenyl)propan-2-one **192**, they did not show an analogous activity with phenyl pyruvate **122**. The α -keto acid is not accepted by the IREDs and the converse is true, the KIREDS and P5CR did not accept 1-(4-fluorophenyl)propan-2-one **192**, but gave good conversion with phenyl pyruvate **122**. These two sets of enzymes appear to have complementary substrate scopes. This suggests that the previously selected enzyme panel allows enzymatic access to a set of products not otherwise available.

3.5. Scale-up enzymatic reactions

To demonstrate their synthetic utility, selected enzymes from each class (**En02**, **En04** and **En07**) were tested in preparative scale reactions, making use of lysates (**Table 18**). Results showed moderate to excellent conversions. In the case of **En02** conversion reached 68%, however the majority of the starting material was reduced to 3-phenyl lactic acid **138**, with only 17% being converted to the desired product **3** (**Table 18**). **En04** and **En07** gave quantitative conversions, in the former case the reductive amination product was 98% with only 2% 3-phenyl lactic acid **138**, whereas in the

case of **En07** 32% reductive amination product was observed (**Table 18**). The product distribution is in accordance with small scale experiments.

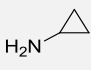
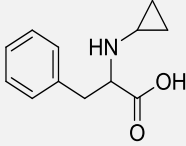
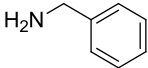
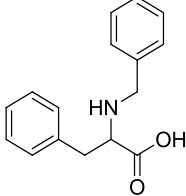
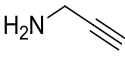
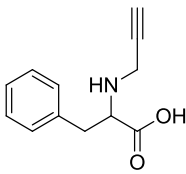
Enzyme	Amine	Product	Product [%]	3-phenyl lactic acid 138 [%]
En01	 154	 155	17	51
En04	 150	 151	98	2
En07	 146	 147	32	67

Table 18. Demonstration of NMAADH, KIREd and P5CR enzymes on a 200 mg scale. Reaction parameters: keto acid **122** (10 mM), amines **146**, **150** and **154** (100 mM), NADPH (0.1 equiv), GDH (1 mg/mL), D-glucose (30 mM), 25°C. Tris HCl buffer (200 mM, pH 8.5), 24 h. ^[b] % Conversion, calculated from HPLC peak area (ketone area vs reductive amination product area, carbonyl reduction side product and ketone area). Products were purified by MDAP.

While the conversions for these products were low, as a great deal of 3-phenyl lactic acid **138** was produced, these do represent conditions and enzymes not optimised to be carried out on scale. The use of lysates can also promote the formation of this reduction by-product (3-phenyl lactic acid **138**) as other enzymes in the lysate are also likely to cause this reaction. However, despite these short-comings it has been demonstrated that these enzymes can be used to synthesise *N*-functionalised amino acids on scale.

3.6. Molecular Docking

3.6.1. Characterisation and crystal structure

When phenyl pyruvate **122** was docked into the active site of the existing crystal structure of **En02**, the phenyl group appeared to extend outside of the channel of the active site (**Figure 37**). However, as this reaction yields high conversions, this is likely not to be representative of the true binding configuration. These enzymes are known to be highly flexible, so it is more likely that the active site can encompass the keto acid substrates.⁹⁶ Therefore, it was desirable to obtain a crystal structure of an NMAADH with a keto acid or amino acid bound. There are no previously published structures of **En01**, but it has high sequence homology to the **En02** that has been previously crystallised.

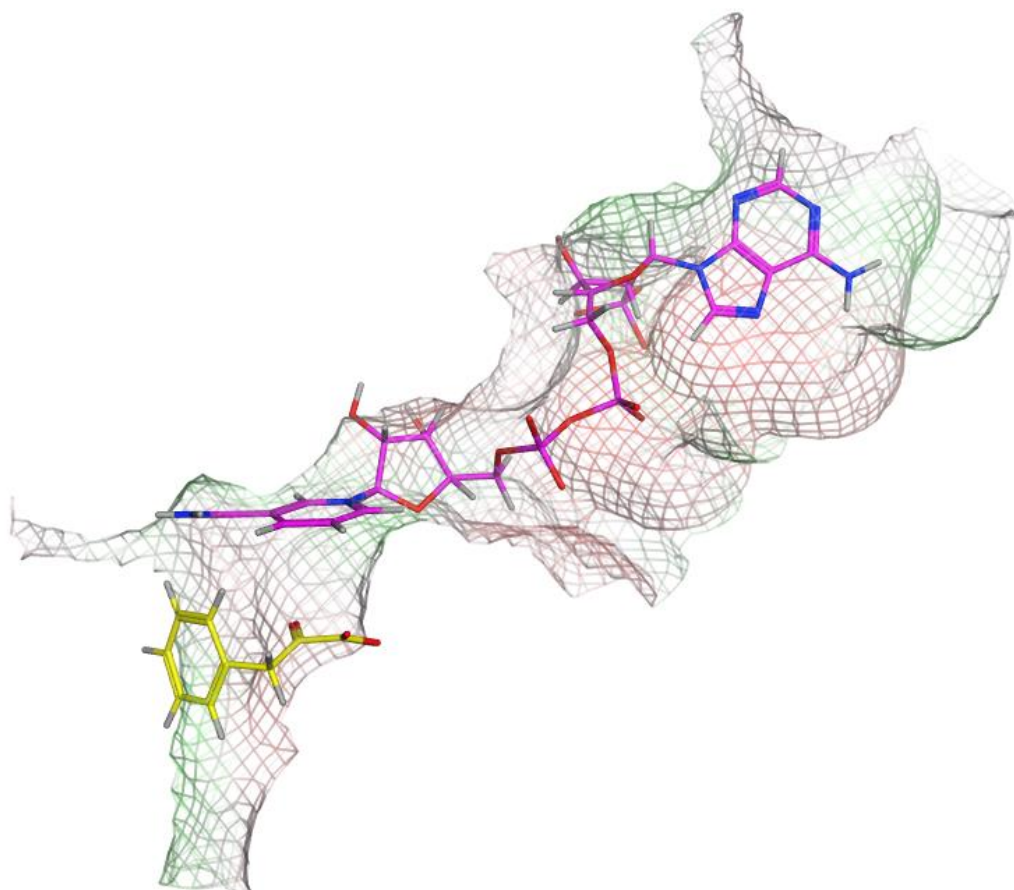


Figure 37. Model of the crystal structure of NMAADH from *P. syringae* with the substrate phenyl pyruvate 122 docked. This was achieved by overlaying phenyl pyruvate (yellow) with the natural substrate analogue and searching for the lowest energy conformation. The surface shown represents the active site, coloured based on lipophilicity, green representing lipophilic residues and pink polar residues.

Initial attempts to crystallise the protein were made using commercial screening kits and several sets of conditions were identified which resulted in good crystals. The best conditions identified gave a resolution of 2.84 Å, from which the enzyme structure was solved and refined.

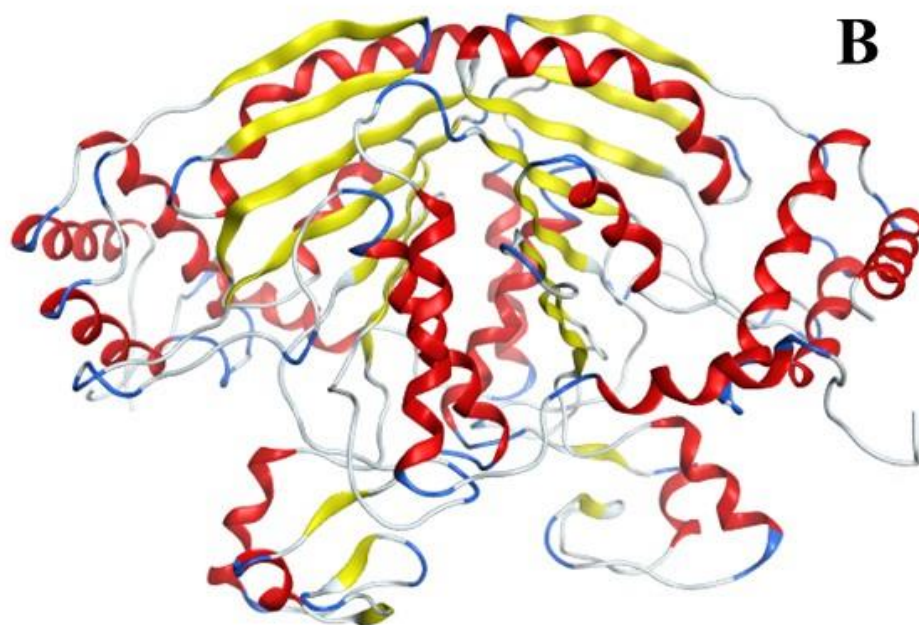
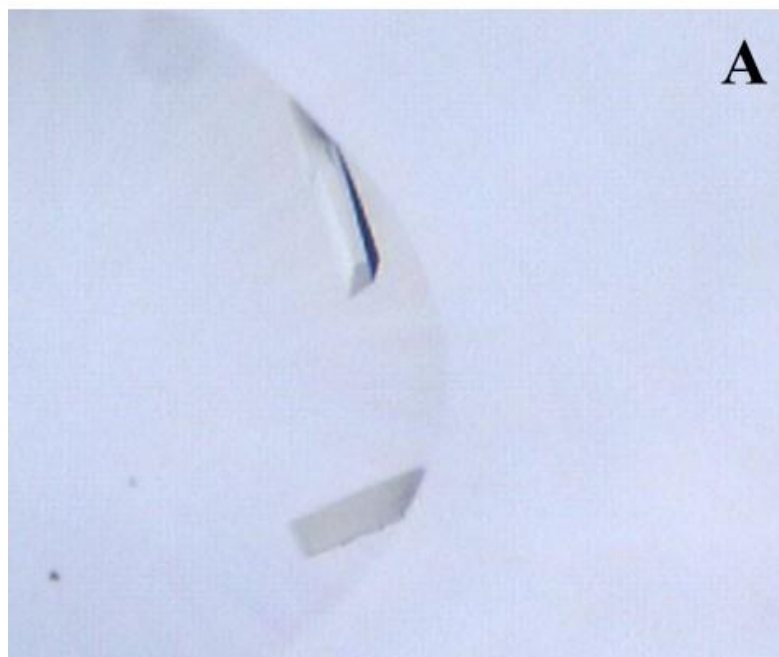


Figure 38. A. *P. putida* NMAADH crystal giving the best resolution. B. Newly acquired crystal structure of *P. putida* NMAADH.

Although the resolution was not sufficient to resolve the protein termini, most of the structure including the active site was resolved. This structure of **En01** shows a very high structural similarity to the existing crystal structure of **En02 (Figure 39)** with the super structure of the enzymes being very similar and variation only in the more flexible regions.³⁷



Figure 39. Comparison of new crystal structure of En01 (green) with existing structure of En02 (pink, 2CWH).

Further optimisation of the best conditions was carried out by investigating the concentration of precipitant (PEG 3350) and different pHs. However, this did not yield any improved crystals. The structure solved is the apo structure and does not contain co-factor (or substrate). Co-crystallisation of the enzyme with co-factor was attempted using the initial sets of screening conditions, however none of the conditions gave crystals. Co-crystallisation using both NADPH and phenyl pyruvate substrate was also attempted and unsuccessful. A crystal structure with a substrate or product bound was not achieved in our hands.

3.6.2. Rationalisation of the stereoselectivity

In an attempt to rationalise the high stereoselectivity demonstrated by these enzymes (in section 3.4.4), docking models of selected enzymes with various imine substrates were examined. A closer look at the crystal structures of the three enzyme classes revealed that NMAADHs (here **En01**) have an arginine that interacts with the carboxyl group of the substrate and a serine residue that is within distance to be a possible proton donor, this can be seen in **Figure 40**.

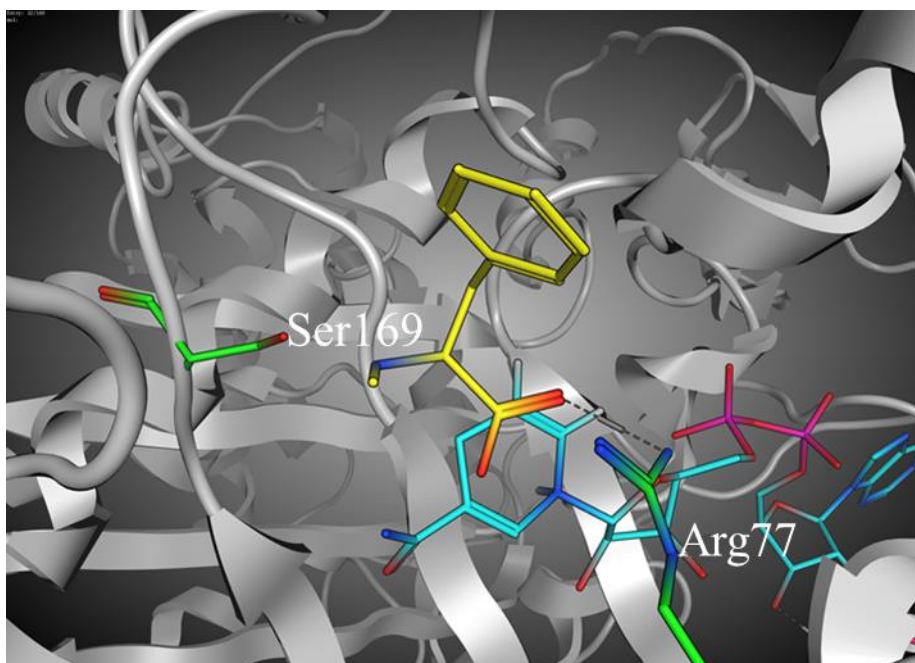


Figure 40. Model of En01 active site with product *N*-methyl phenylalanine 78 (yellow). Model was generated using MOE program and PDB 2CWH as a template with NADP⁺ (cyan) and the co-crystallized ligand (not shown) maintained during model building. 78 coordinates were generated using MOE program and subsequently manually fitted in the active site based on superposition to co-crystallized ligand followed by tethered minimization.

This is consistent with the KIREDD example examined (**En05, Figure 41**) an arginine is also implicated in the carboxylate binding, making this arginine highly-conserved. This arginine is thought to be responsible for the excellent enantioselectivity observed in section 3.4.4. The orientation observed in these docking exercises corresponds to the *S* enantiomer consistently observed in the experiments carried out.

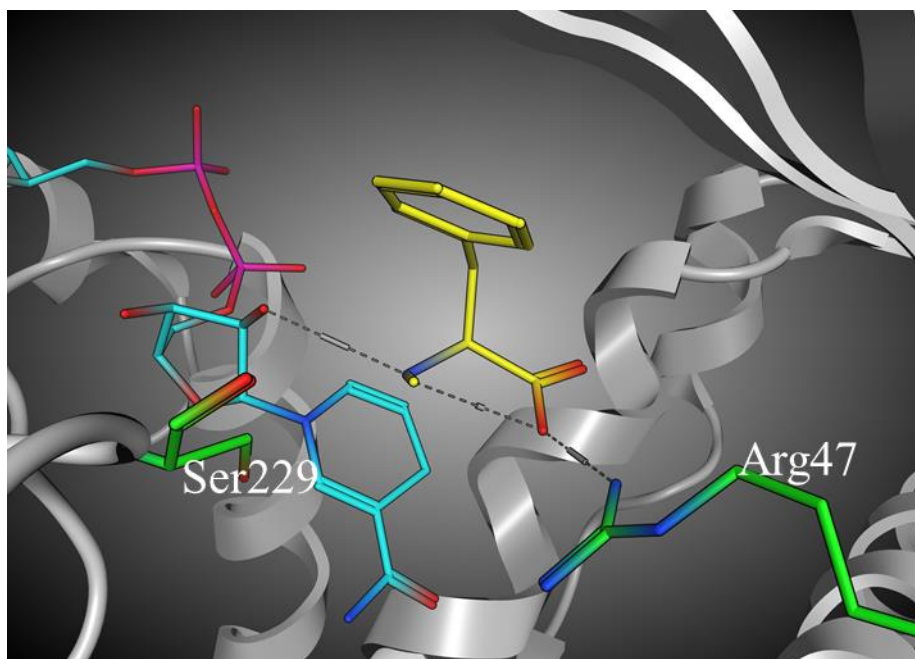


Figure 41. Model of En05 active site with compound *N*-methyl phenylalanine 78 (yellow). Model was generated using MOE program and PDB 4BVA as a template with NADP⁺ (cyan) and the co-crystallized ligand (not shown) maintained during model building. 78 coordinates were generated using MOE program and subsequently manually fitted in the active site based on superposition to co-crystallized ligand followed by tethered minimization.

The P5CR enzyme family (including **En07**) does not have this conserved arginine (**Figure 42**). It is postulated that the carboxylate group is interacting with Threonine 209 and the backbone NH of Threonine 154 and these are responsible for achieving the correct geometry. This is consistent with the *S* enantiomer observed in the experiments seen in section 3.4.4. It also seems likely that Serine 207 is a possible proton donor, given its proximity to the docked product.

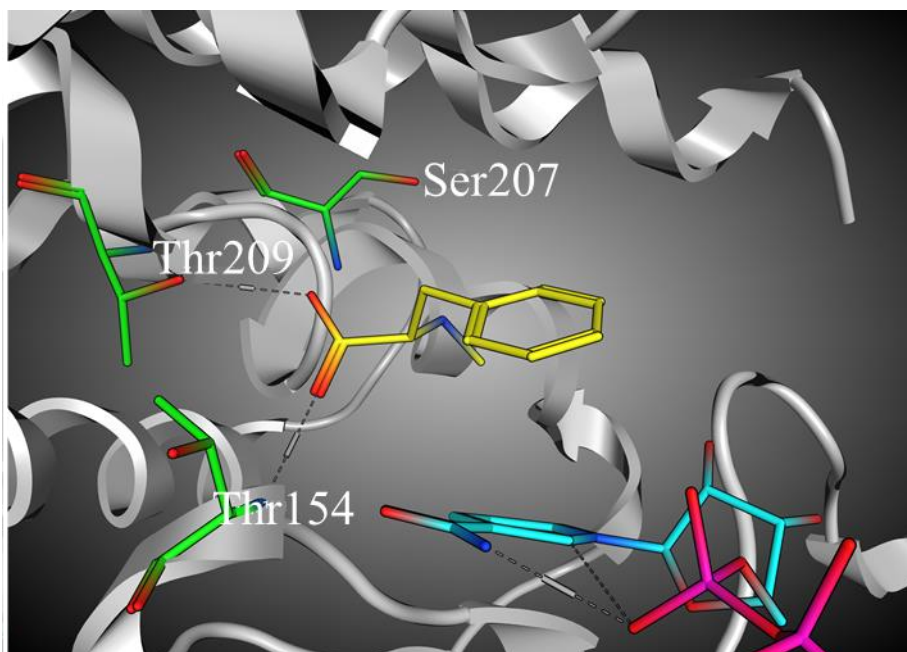


Figure 42. Model of En07 active site with compound *N*-methyl phenylalanine 78 (yellow). Model was generated using MOE program and PDB 5BSF as a template with NADP⁺ (cyan) and the co-crystallized ligand (not shown) maintained during model building. 78 coordinates were generated using MOE program and subsequently manually fitted in the active site based on superposition to co-crystallized ligand followed by tethered minimization.

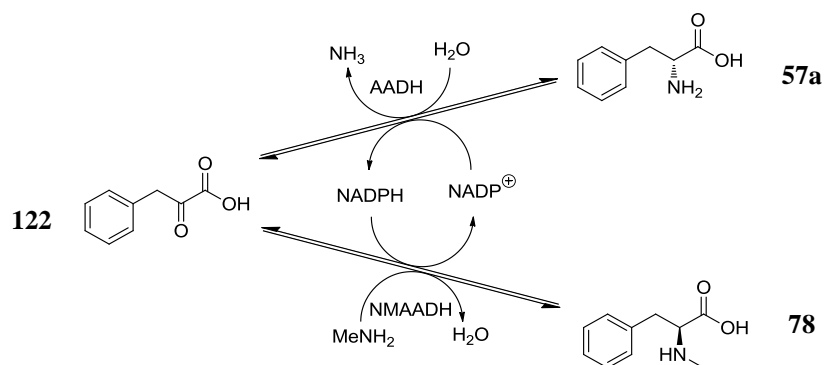
Selectivity in KIREDS and NMAADH families is most likely driven by the presence of the arginine that interacts with the carboxylate. It may be possible to switch the enantioselectivity, if the arginine was mutated to a small non-basic residue, and a charge stabilizing residue added on the opposite side of pocket, and if any other residues that are needed to fit substrate within active site are mutated. This could potentially be done with as little as 2 or 3 modifications to the active site.

3.7. Enzymatic cascades using NMAADHs for *N*-alkylation

N-Alkylation is a frequently employed reaction in organic synthesis, which commonly proceeds via a nucleophilic substitution reaction using an alkyl halide. However, controlling mono-alkylation is a challenge as the reaction product is often more nucleophilic than the starting amine. Thus, protecting group chemistry is often required, leading to poor atom economy and an increased number of reaction steps (this is not in keeping with green chemistry principles). Furthermore, alkylating reagents are highly reactive and toxic. Biocatalytic *N*-alkylation offers an

environmentally benign alternative to traditional chemical methods of *N*-alkylation. *N*-alkylation has the advantage of using amino acid starting materials which are more readily available than the keto acids used in reductive amination reactions.

Therefore, the application of an amino acid dehydrogenase (AADH)/NMAADH one-pot two enzyme *N*-alkylation reaction would allow access to expensive *N*-methyl amino acids from unprotected amino acids. This cascade reaction is redox neutral as AADHs use a NADP⁺ cofactor which is oxidised to NADPH, which then serves as the cofactor for the NMAADHs (**Scheme 50**). This coupled reaction minimises the requirement for expensive co-factors and recycling systems.



Scheme 50. Postulated *N*-methylation cascade.

This cascade would first use an AADH to oxidise the amino acid to a keto acid, then reduce this to an *N*-functionalised amino acid. This would allow a more stable and accessible starting material to be used. α -Keto acids are difficult to obtain and often unstable, this cascade will avoid this problem and allow a wider range of functionality to be incorporated into the *N*-functionalised amino acids.

Two NADPH dependent D-amino acid dehydrogenases (DAADHs) were selected from a review of the literature. The first DAADH (**En08**) is a variant of a *Corynebacterium glutamicum* DAADH which was engineered by Vedha-Peters *et al.* for increased substrate promiscuity.¹²² The second DAADH (**En09**) is an evolved variant of DAADH from *Ureibacillus thermosparicus* engineered by Akita *et al.* for increased thermostability.¹²³ DAADHs were selected as they have a broad substrate specificity and are easily expressed in *E. coli*. Ideally an LAADH will be used which would allow cheaper L-amino acids to be used as substrates, however there are few

examples of promiscuous NADPH dependent proteins which can be easily expressed in bacteria.

3.7.1. DAADH expression and purification

The DAADH gene sequences were ordered from Genscript, codon optimised for *E. coli* expression and cloned into pET28a. *E. coli* BL21(DE3) was transformed with the constructs and the protein was expressed using IPTG induction (0.5 mM) at 18 °C. Protein expression was evaluated by SDS-PAGE (**Figure 43**).

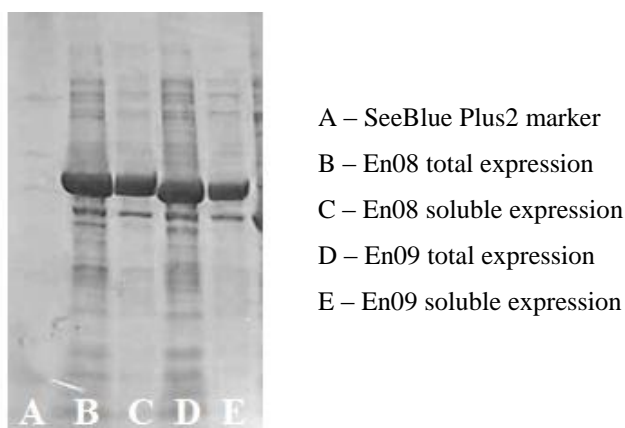


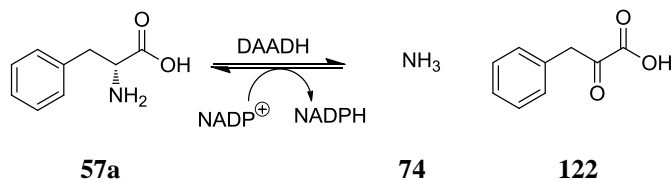
Figure 43. SDS Page gel showing the total and soluble expression of the two DAADH selected.

As with **En01-07** the enzymes have been expressed with a 6His tag, which allowed them to be purified with nickel affinity chromatography.

3.7.2. DAADH activity assay

The DAADHs were screened for activity towards D-phenylalanine in the oxidative direction, using clarified enzyme lysate. Cell pellets transformed with DAADHs were lysed by sonication, and the cell debris was cleared by centrifugation. DAADH from *Ureibacillus thermosphaericus* **En09** did not demonstrate any activity towards D-phenylalanine **57a** (25 mM) and the keto acid product **122** could not be detected by HPLC. However, the *Corynebacterium glutamicum* enzyme **En08** did show activity towards D-phenylalanine and 26% conversion to the expected product was detected by HPLC after 3 days.

Corynebacterium glutamicum DAADH was also screened for reductive amination activity using phenylpyruvate **122** (25 mM) and ammonia **74** (200 mM) according to a previously published method (**Scheme 51**).¹²² The reaction went to full conversion within 1 hour at 25 °C, and the D-phenylalanine product **57a** was detected by HPLC.



Scheme 51. DAADH catalysed reaction in the reductive direction.

En08 gave higher conversion in the reductive direction than the oxidative reaction. This is not unexpected as the enzyme has been modified with a view to improving the activity in the reductive direction. Given that **En09** did not demonstrate activity towards phenylalanine, only **En08** was tested in subsequent reactions.

The activity of **En08** was screened for methylamine tolerance, as excess amine is used for the *N*-alkylation step. The DAADH catalysed oxidation of D-phenylalanine was screened in the presence of varying methylamine concentrations and the conversion to phenylpyruvate was detected by HPLC. The results show that high concentrations of methylamine inhibit the enzyme (**Figure 44**). However, as conversion was still observed at 750 mM methylamine, so high concentrations of amine are tolerated.

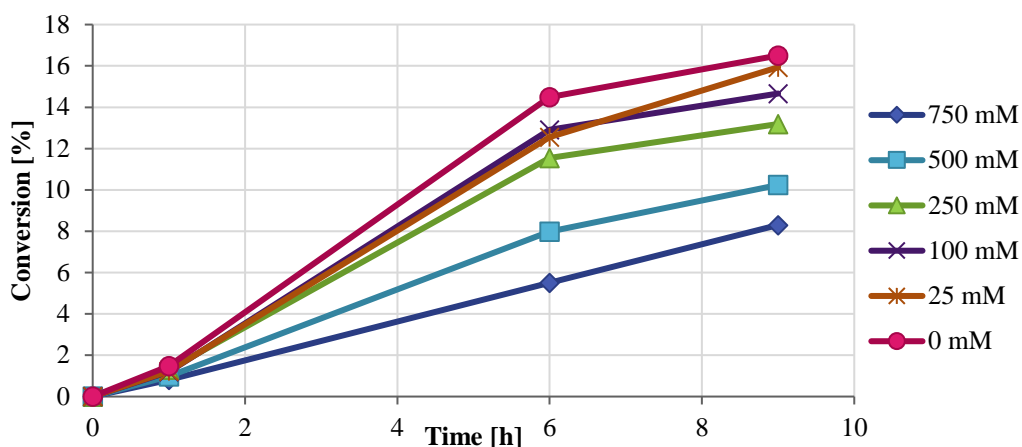


Figure 44. Reaction profile at different concentrations of methylamine. Reaction conditions: D-phenylalanine **57a** (25 mM), NADP⁺ (25 mM), methylamine hydrochloride **76** (0-750 mM), 25 °C, enzyme lysate in Tris HCl buffer (pH 9.0, 50 mM, NaCl (50 mM)). Conversion calculated using benzonitrile internal standard.

3.7.1. DAADH formulation

The different steps of the cascade were screened separately in both the oxidative and reductive directions, with ammonia and methylamine for the reductive reactions (**Table 19**). However, it was quickly observed that a by-product was formed, which overlapped with the *N*-methylphenylalanine **78**. A chiral HPLC method was utilised to separate the product and by-product peaks. The by-product was shown to be L-phenylalanine through the use of LCMS. This could be produced by an endogenous enzyme (**Table 19**), possibly a transaminase. There is no mention of this activity being observed by other groups working with these enzymes, but the majority of this work was carried out using purified protein.

Enzyme	Substrate	Amine	N-methyl-L-phenylalanine 78 [% conv]	L-phenylalanine 57b [% conv]	D-phenylalanine 57a [% conv]	Phenyl pyruvate 122 [% conv]	3-phenyl lactic acid 138 [% conv]
En08	57a	-	0	20	24	37	18
En08	78	-	100	0	0	0	0
En08	122	74	0	99	1	0	0
En08	122	76	0	66	0	33	0
En01	122	74	0	6	0	94	0
En01	122	76	83	6	0	11	0
En01	57a	-	0	5	95	0	0
En01	78	-	98	0	0	2	0
En01	57b	-	0	83	0	0	17

Table 19. DAADH and NMAADH catalysed reactions. Reaction conditions: substrate (25 mM), methylamine HCl **76** or ammonia HCl **74** (700 mM), NADPH or NADP⁺ (25 mM), 25 °C, clarified enzyme lysate in Tris HCl buffer (pH 9.0, 50 mM, NaCl (50 mM)). Conversion calculated from percentage peak area after 12 h shaking.

The data obtained in **Table 19** was sufficient to give us confidence that the DAADH and NMAADH enzymes was compatible, but the data was complex. **En08** lysate in conjunction with D-phenylalanine **57a** showed conversion to desired phenyl pyruvate (37%), but also conversion to L-phenylalanine (20%) and 3-phenyl lactic acid (18%). These results showed that the reaction profile had the potential to become very complex, the proposed sequence of steps is shown in **Scheme 52**. However, the DAADH **En08** showed no reaction with N-methylphenylalanine **78**, therefore the final cascade product would not be consumed by the DAADH. Additionally, both in the presence and absence of excess ammonia the **En08** lysate was reducing phenyl pyruvate **122** to L-phenylalanine **57b**, further suggesting an endogenous enzyme using ammonia from the cell lysate.

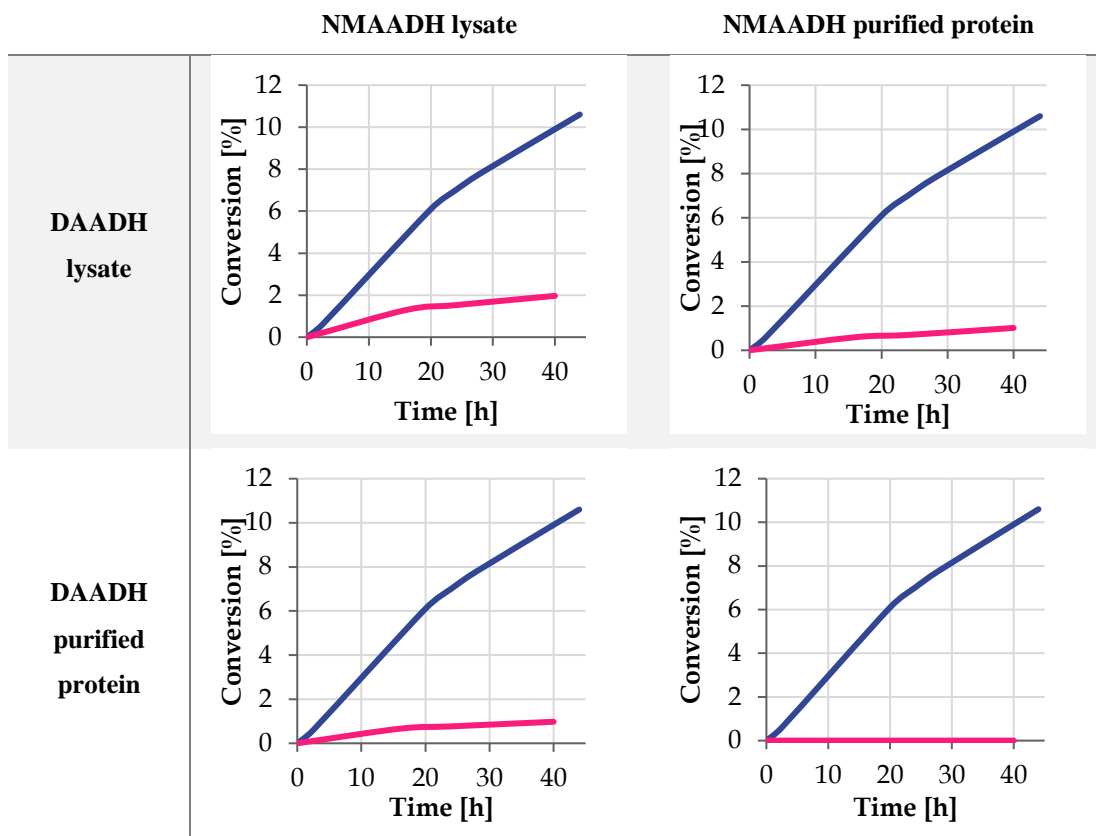


Figure 45. Cascade reaction using purified enzyme and crude lysate combinations. Showing production of *N*-methyl phenylalanine 78 (blue) and L-phenylalanine 57b (pink). Reaction conditions: D-phenylalanine 57a (25 mM), methylamine HCl 76 (700 mM), NADP⁺ (1 mM), 25 °C, enzyme lysate in Tris HCl buffer (pH 9.0, 50 mM NaCl (50 mM)), purified protein (2.5 μM).

3.7.2. Enzymatic cascade optimisation

A one-pot two enzyme *N*-alkylation reaction was performed using purified **En01** and **En08**. The conversion with excess methylamine (700 mM) was detected by HPLC.

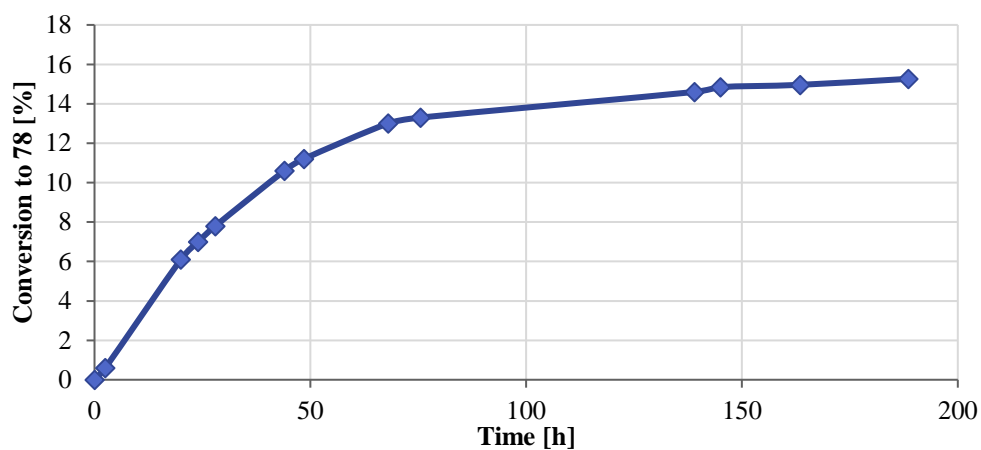


Figure 46. Cascade reaction profile using purified protein and catalytic co-factor, showing conversion to *N*-methylphenylalanine **78**. Reaction conditions: *D*-phenylalanine **57a** (25 mM), methylamine HCl **76** (700 mM), NADP⁺ (1 mM), 25 °C, purified protein (2.5 μM).

The reaction produced 15% *N*-methylphenylalanine after 4 days and no phenylpyruvate intermediate was detected, suggesting that possibly DAADH is the limiting enzyme. In order to investigate this further, the reaction mixture was subdivided after 215 hours, to which were added additional **En08**, **En01** and NADP⁺ respectively. The reactions with added NMAADH and NADPH showed no further conversion, but the reaction with additional **En08** showed an increased conversion (**Figure 47**) a clear indication that DAADH was the limiting factor. Despite the low conversion this proof of concept shows that this cascade is a practical and redox neutral method for alkylating amino acids.

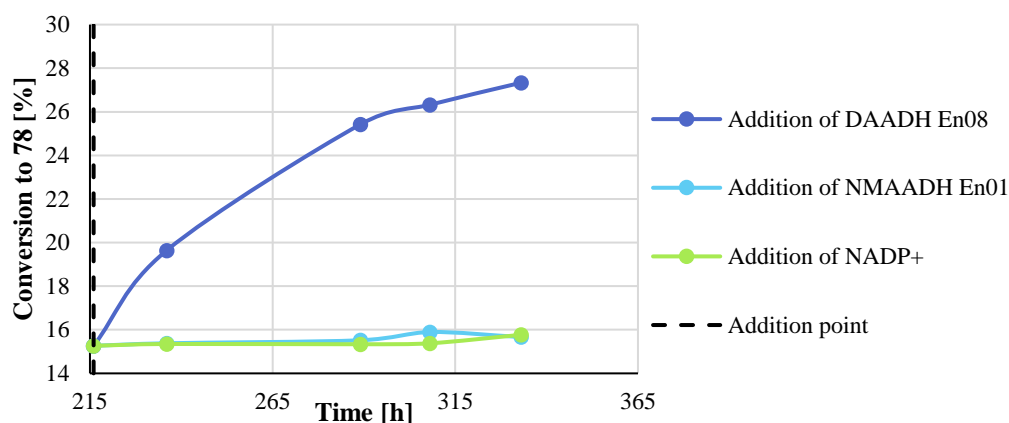
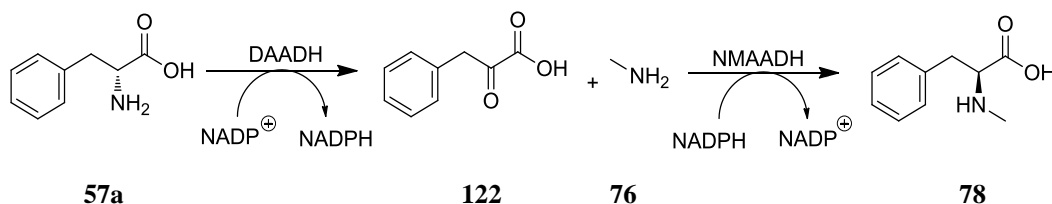


Figure 47. Cascade reaction profile, showing conversion to *N*-methylphenylalanine **78**, with the addition of further DAADH, or both enzymes and co-factor at 210 h. Reaction conditions: *D*-phenylalanine **57a** (25 mM), methylamine HCl **76** (700 mM), NADP⁺ (1 mM), Tris HCl buffer (pH 9.0, 200 mM), 25 °C, purified protein in 50 mM Tris and 50% glycerol (2.5 μM). Further enzyme (final concentration 5 μM) and NADP⁺ (final concentration 2 mM) added after 210 h.

Additionally, the ratio of the different proteins was investigated, which showed that the DAADH was acting as the limiting factor. If the concentration of DAADH was increased the conversion increased (**Figure 48**) however increasing the NMAADH concentration had little to no effect.



Scheme 53. Reaction being investigated in Figure 48.

The DAADH seems to be unstable, as the turnover slows over time. Additionally, the oxidative direction is not the preferred direction for these enzymes, which decreases the productivity of this cascade. The rate of reaction is being limited by the initial oxidation step.

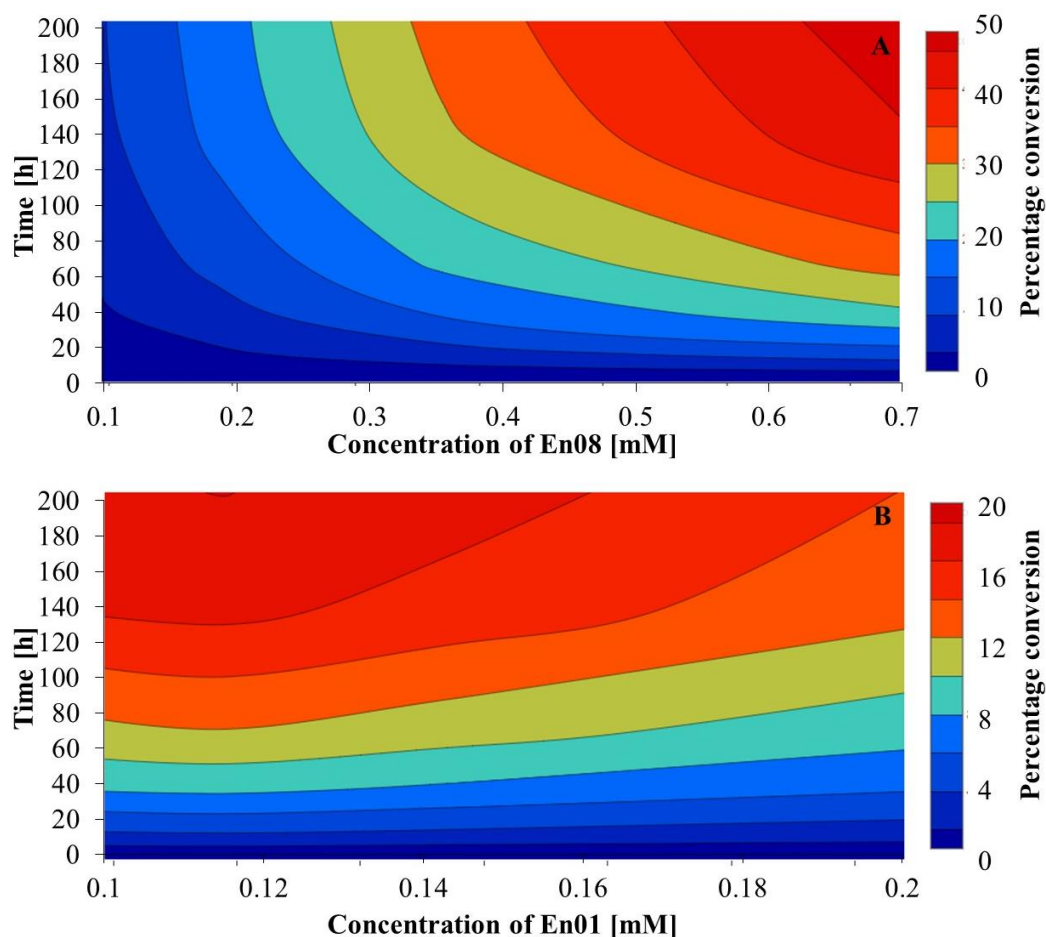


Figure 48. Heat maps showing the differences in conversion over time for different loadings of En08 (A) and En01 (B). Reaction conditions: D-phenylalanine 57a (25 mM), methylamine HCl 76 (700 mM), NADP⁺ (1 mM), pH 9.0, 25 °C, En08 A (0.009-0.074 mM), B (0.05 mM) En01 A (0.05 mM), B A (0.009-0.074 mM).

To conclude, it has been demonstrated that the DAADH/NMAADH cascade is a viable option for *N*-methylation reactions. The lysate reaction demonstrated some of the desired reaction, but with a substantial by-product formation. However, on transferring the process to purified protein a clean reaction with reasonable conversion was achieved. The by-product formation will require further investigation to determine how much the effects can be mitigated, and further optimisation will be required to improve the process.

4. Conclusions

The problem posed by sustainable manufacturing routes to chiral *N*-alkylated amino acids is a relevant challenge to the pharmaceutical industry. In this project an enzyme panel consisting of NMAADHs, KIREds and P5CRs, was generated and evaluated for α -keto acid reductive amination. These enzymes classes were selected as they were poorly characterised as biocatalysts and they could offer access to a reaction space not previously accessible biocatalytically. Five of the seven enzymes examined in this project had never been demonstrated as reductive amination biocatalysts, but they have now been shown to demonstrate reductive amination activity for the synthesis of *N*-functionalised amino acids.

These enzymes have been expressed and purified and optimised reaction conditions have been identified. This included optimising pH, buffer concentration, amine stoichiometry and catalyst loading. A 96-well plate screening approach was then employed to explore the substrate scope. The range of ketones that could be accepted was explored, with only α -keto acids being accepted by any of the enzymes.

New substrate scope has been demonstrated for all seven of the enzymes tested, with a much wider variety of amines being accepted than previously known. Particularly successful amines included propargylamine **146**, cyclopropylamine **154** and benzylamine **150**. A variety of phenylalanine derivatives have been successfully synthesised using this new enzymatic route. Additionally, this method was found to have excellent enantioselectivity, with greater than 99% ee for all the demonstrated examples.

In the case of NMAADHs and KIREds this has expanded the known substrate scope for both ketones and amines. In addition, the first example of a P5CR catalysed reductive amination is demonstrated here. The enzyme isolated from *N. crassa* is able to perform reductive aminations in a similar fashion to NMAADHs and KIREds on a wide range of amines, despite low sequence similarity. Overall P5CR **En07** provided low to moderate conversions suggesting the potential of this enzyme cluster, suggesting that other useful enzymes could be identified.

In summary, three distantly related enzyme classes have been shown to have reductive amination utility. The synthetic utility of these seven enzymes was demonstrated on a larger scale, with reactions being successfully carried out at low amine loading. These

enzymes have the potential to provide an environmentally friendly, atom efficient alternative synthesis for *N*-functionalised amino acids.

In addition, a crystal structure was obtained for **En01**, which did not have a published crystal structure. This showed a high folding pattern similarity between the NMAADHs. This enzyme could not be crystallised with either the product or substrate analogue in the active site, which would have provided useful mechanistic information. However, this crystal structure has increased the known NMAADH crystal structures, as only one previously existed. A rationalisation of the stereoselectivity was established, by docking the *N*-methyl phenylalanine product into the active site. In the case of NMAADHs and KIREDS the presence of an arginine and serine was conserved across both classes. These residues provide the correct binding architecture to achieve the *S* selective reactions observed. This provides further understanding of the mechanism of these enzymes, about which little is known.

In addition, for the P5CR enzyme class no reductive amination activity has ever been observed, and the active site appears to be distinct from the NMAADHs and KIREDS. This is clearly an area for future exploration, but provides some insight into the mechanism of this newly discovered activity.

Another area that was investigated was the use of NMAADHs in a redox neutral amino acid alkylation cascade. To this end amino acid dehydrogenases were investigated and paired with the NMAADH (**En01**). It was established that these two enzymes could be paired to allow this *N*-alkylation to occur. While the DAADH needs further optimisation, as it is the slower step, but it has been demonstrated that this cascade is a viable method for carrying out *N*-alkylation.

5. Future work

The progress made in this project could be continued in a number of directions, including the identification of other biocatalysts, further optimisation, mutagenesis to improve the process or further investigation of the enzymes' mechanisms.

5.1. Identification of other reductive amination biocatalysts

- Use of the CLANS approach to identify other enzymes in the three clusters. As the CLANS approach can be used to identify other enzymes that fall into the NMAADH, KIREA and P5CR categories. Other members of these classes could be identified and screened. This has the potential to identify enzymes that are more robust or have a wider substrate scope. In particular, P5CRs have never been used for reductive amination, so it would be useful for a greater understanding of this class to find other active examples.

5.2. Make improvements to the enzyme via mutagenesis

- Use of mutagenesis to improve the stability of the enzymes, which would allow for improved storage times. Currently the enzymes used in this project can be stored at -80°C, but loss of activity is observed after extended periods. This could be carried out using a random mutagenesis approach, then testing for improved stability.
- Use of mutagenesis to achieve a wider substrate scope, with a view to expanding the utility to other keto acids or even ketones. A targeted mutagenesis approach could be used to design a wider active site to accommodate larger substrates. Some large residues (phenylalanine and tryptophan) that impact on the active site are highlighted in **Figure 49**.

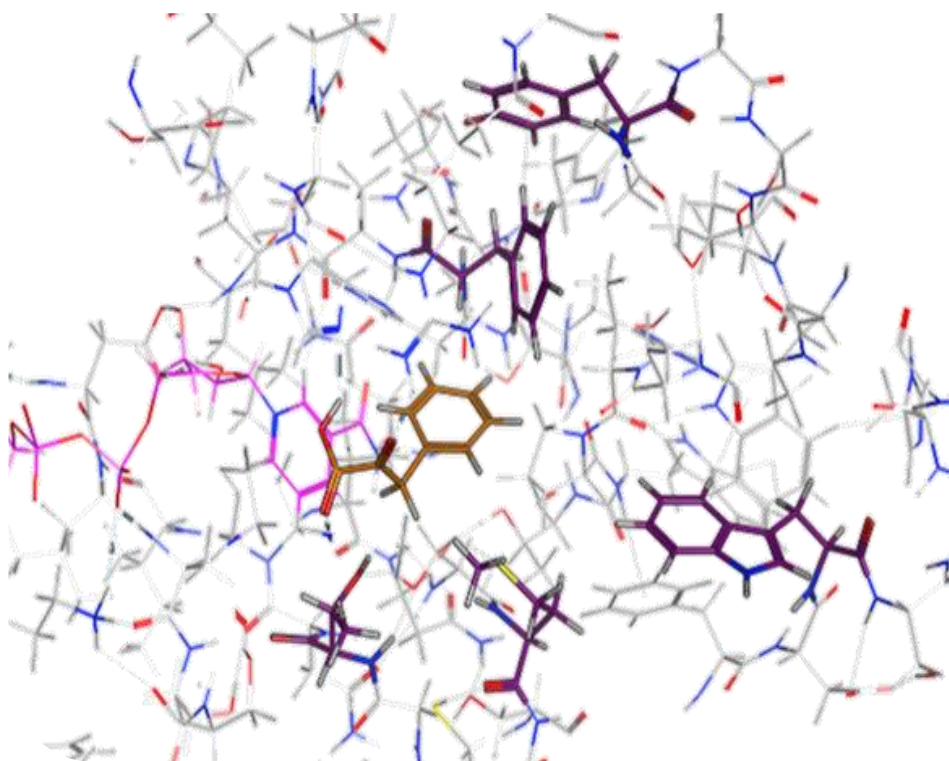


Figure 49. Active site of En01, with large residues that could be mutated to expand the active site highlighted in purple.

- Additionally, mutagenesis may provide a route to decreasing the conversion to reduction by-product. This would allow these enzymes to be used as lysates or lyophilised powder with greater efficiency. As the mechanism of this is not well understood, a random mutagenesis approach with screening for conversion to product and by-product would be the simplest approach.
- Reversal of the stereoselectivity of these enzymes. It has been proposed in this work that the high stereoselectivity of the NMAADHs and KIREDs could be reversed to obtain the non-natural D-enantiomer product. If the conserved arginine residue in these enzyme classes was mutated to an alanine and an arginine placed on the opposite side of the active side, this may allow this reversal to take place. However, other mutations will likely be required and a range of mutants would need to be screened.

5.3. Investigation of enzyme mechanism

- The enzyme mechanism for the NMAADHs has been proposed in the literature previously.⁹⁶ However, for the KIREd and P5CR enzyme classes there is no published enzyme mechanism. Building on the docking calculations, discussed in section 3.6, would allow the mechanism to be better understood.
- Obtain a crystal structure with substrate or product bound, to improve the understanding of the mechanism of imine formation. Perhaps a wider range of co-crystallisation condition screening could be attempted, to find suitable conditions. If this crystal structure could be obtained this would provide a more accurate understanding of the conformation of the active site during reaction. This would improve on the current docking that makes use of previous crystal structures. These will have other substrates docked and have a different conformation to the reductive amination reaction.
- Understanding of the impact of imine formation on the enzyme mechanism. At present, there is a lack of understanding of how the imine formation occurs in the active site. If this could be understood through crystallisation of a substrate analogue in the active site, it would improve understanding of how this non-natural reductive amination occurs. In addition, the geometry of the imine is unknown and this could also be determined by crystallising enzymes with substrate or imine analogues. This would again help to establish a deeper understanding of the mechanism.

5.4. Correlation of conversions and imine formation

- There is a lack of understanding as to the relationship between the ease of the imine formation step and the overall success of the reductive amination. If a deeper understanding of this relationship could be established, it would provide useful background to understanding the enzyme mechanisms. This could be done by using in-line IR monitoring to determine the rate of imine formation for different substrates, then correlating this with the conversions achieved.

6. Experimental

6.1. Equipment

- All chemicals were obtained from Sigma Aldrich® unless otherwise stated.
- All biological buffers and kits were obtained from Invitrogen® unless otherwise stated.
- All NMR data was taken using a Bruker B-ACS 60 at 400MHz. All coupling constants are reported in Hertz (Hz), and multiplets are recorded using the abbreviations: singlet (s), doublet (d), triplet (t) and multiplet (m) and combinations of these. The techniques used are proton NMR (¹H-NMR), carbon NMR (¹³C-NMR), Homonuclear Correlation Spectroscopy (COSY), Heteronuclear Single Quantum Coherence (HSQC) and Heteronuclear Multiple Bond Correlation (HMBC). The data were processed using ACD Labs v12.5 software.
- All LCMS data were collected using a Hewlett Packard P1100 HPLC system, with Waters Micromass ZQ mass detector. The data was analysed using FractionLynx software.
- Nanodrop 3300 fluorospectrometer was used to measure DNA concentrations.
- Qiagen QIAprep® Spin Mini-prep kit was used for DNA preparations.
- All computer modelling was carried out using MOE 2012 v10 or MOE 2015.
- Mass directed auto prep was carried out using a Waters 2996 Photodiode detector a Waters 2767 sample manager with Waters Micromass ZQ mass detector.

6.2. Enzymes

6.2.1. Enzyme selection

Gene sequences, codon optimised for expression in *E. coli*, were synthesised at GenScript and cloned into pET28a.¹²⁴ The protein sequences have an *N*-terminal 6His tag and are as follows:

6.2.1.1. Δ^1 -Piperideine-2-carboxylate reductase *P. putida* (En01)

MGSSHHHHHHSSGLVPRGSHMSAPSTSTVVRVPFTELQSLQAIQFQRHGCSE
AVARVLAHNCASAQRDGAHSHGVFRMPGYVSTLASGWVDGQATPQVSDV
AAGYVRVDAAGGFAQPALAAARELLVAKARSAGIAVLAIHNSHHFAALWP
DVEPFAEEGLVALSVNSMTCVVPHGARKPLFGTNPIAFAAPCAEHDPIVFD
MATSAMAHGDVQIAARAGQQLPEGMGVDADGQPTTDPKAILEGGALLPFG
GHKGSALSMMVELLAAALTGGHFSWEFDWSGHPGAKTPWTGQLIIVINPGK
AEGERFAQRSRELVEHMQAVGLTRMPGERRYREREVAEEEGVAVTEQELQ
GLKELG

6.2.1.2. Δ^1 -Pyrroline/ Piperideine-2-carboxylate reductase *P. syringae* (En02)

MGSSHHHHHHSSGLVPRGSHMSASHADQPTQTVSYPQLIDLRRIFVVHGTS
PEVADVLAENCASAQRDGSHTSHGIFRIPGYLSSLASGWVDGKAVPVVEDVG
AAFVRVDACNGFAQPALAAARSLLIDKARSAGVAILAIRGSHHFAALWPDV
EPFAEQGLVALSMVNSMTCVVPHGARQPLFGTNPIAFGAPRAGGEPVFDLA
TSAIAHGDVQIAAREGRLLPAGMGVDRDGLPTQEPRAILDGGALLPFGGHKG
SALSMMVELLAAGLTGGNFSFEFDWSKHPGAQTPWTGQLLIVIDPKGAGQ
HFAQRSEELVRQLHGVGQERLPGDRRYLERARSMAGIVIAQADLERLQEL
AGH

6.2.1.3. Putative lactate dehydrogenase *P. fluorescens* 113 (En03)

MGSSHHHHHHSSGLVPRGSHMSAPSDHAASCTLSFDALVNLEKIFLRHGTS
TEVARCLAENCAGAERDGAHSHGVFRIPGYVSTLDSGWVNGKAVPVVEDV
ASGFVAVDAGNGFAQPALAAARPLLAKARSAGIAILAIRNSHHFAALWPD

VEPFAYEGLVALSVVNSMTCVPHGADRPLFGTNPIAFAAPRADGEPVFDL
ATSAIAHGDVQIAARKGELLPPGMGVDSLQPTRDPKAILEGGALLPFGGHK
GSALSMMVELLAAALTGGNFSFEFDWHNHPGAKTPWTGQLLIVIDPSKTAG
QNFAERSQELVRQMhGVGLRRLPGDRRHRERSKSNEHGISLNEQTLAQLRE
LAGI

6.2.1.4. Ketimine reductase mu-crystallin *R. norvegicus* (En04)

MGSSHHHHHHSSGLVPRGSHMRRAPAFLSADEVQDHLRSSSLLIPPLEAALA
NFSKGPDDGGVMQPVRTVVPVAKHRGFLGVMPAYSAAEDALTTKLVTFYEG
HSNNAVPSHQASVLLFDPSNGSLLAVMDGNVITAKRTAAVSAIATKFLKPPG
SDVLCILGAGVQAYSHYEIFTEQFSFKEVRMWNRTRENAEKFASSVQGDVR
VCSSVQEAVTGADVITVTMATEPILFGEWVKPGAHINAVGASRPDWRELDD
ELMKQAVLYVDSREAALKESGDVLLSGADIFAELGEVVSGAKPAYCEKTTV
FKSLGMAVEDLVAAKLVYDSWSSGK

6.2.1.5. Ketimine reductase mu-crystallin *H. sapiens* (En05)

MGSSHHHHHHSSGLVPRGSHMSRVPAFLSAAEVEEHLRSSSLLIPPLETALAN
FSSGPEGGVMQPVRTVVPVTKHRGYLGVMPAYSAEADALTTKLVTFYEDR
GITSVVP SHQATVLLFEP SNGTLLAVMDGNVITAKRTAAVSAIATKFLKPPSS
EVL CILGAGVQAYSHYEIFTEQFSFKEVRIWNRTKENAEKFADTVQGEV RVC
SSVQEAVAGADVITVTLATEPILFGEWVKPGAHINAVGASRPDWRELDDEL
MKEAVLYVDSQEAALKESGDVLLSGAEIFAELGEVIKGVKPAHCEKTTVFKS
LGMAVEDTVAAKLIYDSWSSGK

6.2.1.6. Ketimine reductase mu-crystallin *B. taurus* (En06)

MGSSHHHHHHSSGLVPRGSHMSSRPVFLSAADVQDHLRSSSLLIAPLETALA
NFSSGPDGGVVQPVRTVVPVAKHRGFLGVMPAYSAAEDALTTKLVTFYEDH
SATSTVPSHQATVLLFQPSNGSLLAVMDGNVITAKRTAAVSAIATKFLKPPNS
EVL CILGAGVQAYSHYEVFTEQFFFKEVRIWNRTKENAEKFVNTVPGEV RIC
SSVQEAVTGADVITVTMATEPILFGEWVKPGAHINAIGASRPDWRELDDEL
MKQAVLYVDSQEAALKESGDVLLSGAEIFAELGEVVKGVKPAHCEKTTVFK
SLGMAVEDMVAAKLVYDSWSSGK

6.2.1.7. Pyrroline-5-carboxylate reductase *Neurospora crassa* OR74A (En07)

MGSSHHHHHSSGLVPRGSHMGISILSGILSSLSSIAQDPSPPPTNPPALPRHFI
ATVRSPSSVAKVESALSPLVKPSVSTLRVLQSTSNVSAAAEADIILLGCKPYM
VSGLLSASGMKDALTVKHTEGHARSQKIIISICAGVTVPDLERVLREDVGLSA
DNLPIVVRAMPNTASKIRESMTVINTVDPPLPDTVTELLTWIFERIGEYVYLPP
HLMDACTSLCASGTAFFALMMEAADGGVAMGLPRAEANRMAAQTMRG
AAGLVLEGEHPAILREKVSTPGGCTIGLLVLEEGVRAAVARAVREATVV
ASLLGGGGAKNVNGTRH

6.2.1.8. Similarity matrix

The similarity matrix was calculated using MOE v2015.1001. All sequences were downloaded from the Protein Databank and aligned using sequence only alignment. The similarity was calculated as follows using the Pairwise Similarity Matrix: the table value at row *i*, column *j* equals the number of positive matches between sequences *i* and *j*, divided by the length of sequence *j*. A residue substitution is positive if the BLOSUM62 substitution score is greater than zero.

6.2.2. Enzyme Expression

6.2.2.1. General procedure for *E. coli* transformation

Plasmid containing the gene of interest (3 μ L, 100 ng/ μ L) was added to chemically competent cells (50 μ L, either BL21(DE3) or TOP10) that were incubated on ice for 30 mins. Cells were heat shocked at 42 °C for 1 min, then incubated on ice for a further 10 minutes. SOC solution (250 μ L) was added and cells were the incubated at 37 °C for 1 h, with shaking at 200 rpm. The transformed cells were plated onto LB agar plates containing kanamycin (50 μ g/mL) and incubated at 37 °C overnight.

6.2.2.2. General procedure for DNA preparation

A single *E. coli* TOP10 colony (transformed with a plasmid of interest) was used to inoculate 10 mL LB media containing kanamycin (50 μ g/mL) and glycerol (1%). The culture was incubated in a thermomixer at 37 °C, with shaking (200 rpm) overnight.

Cells were pelleted by centrifugation (3000 x g, 10 min, 4 °C) and the supernatant was removed. The DNA was isolated using Qiagen QIAprep® Spin Mini-prep kit, per the manufacturer's instructions. The concentration of DNA and the A260:280 ratio was measured using a Nanodrop.

6.2.2.3. General procedure for protein expression

LB media (15 mL) supplemented with D-glucose (1% v/v) and kanamycin (50 µg/mL), was inoculated with a single colony of *E. coli* BL21(DE3) transformed with the gene of interest. The culture was incubated overnight at 37 °C with shaking (200 rpm). The overnight culture (15 mL) was used to inoculate 1L LB broth containing kanamycin (50 µg/mL) and D-glucose (1% v/v) in a 5 L Ultraflask. The flasks were incubated in a Kühner shaker at 37 °C for 2 h, 180 rpm until the optical density reached approximately $OD_{600} = 1.0$. The expression was induced with the addition of 1 M IPTG (500 µL, to a final concentration of 0.5 mM) and the cultures were incubated at 20 °C, overnight at 180 rpm. The final optical density (OD_{600}) was measured using a 10x dilution with LB broth. The cells were pelleted by centrifugation (4 °C, 20 min, 1700 x g). The supernatant was poured off and the pellets weighed, cells were either used immediately or stored at -80 °C until required.

6.2.2.4. General procedure for SDS-PAGE analysis

For expression cultures, a 1 mL sample was taken from each expression culture, the cells were pelleted by centrifugation (1 min at 16000 x g) and the supernatant discarded. The pellets were resuspended in Bugbuster at a dilution of 1/10 of the optical density and allowed to stand for 5 mins. Gel samples of the total lysate were prepared using 4x SDS Page buffer (10 µL), water (20 µL) and lysate (10 µL). Samples were boiled for 5 min, loaded onto a 4-20% Tris-glycine precast gel and run for 1 h at 200 V with SeeBlue Plus2® marker. The gel was stained using InstantBlue® stain and imaged.

6.2.2.5. General procedure for cell lysis

Pelleted cells were resuspended in lysis buffer (8 mL/g cell pellet, 200 mM Tris, 50 mM NaCl, pH 8.5). The lysate was sonicated, on ice, using a 6 mm probe for a total of 6 min (9 s on, 9 s off) at 40% amplitude. The lysate was cleared by centrifugation

at 4 °C for 1 h, 19000 x g. The cell lysate was collected and used directly in reactions or the protein was subsequently purified.

6.2.3. Enzyme Purification

6.2.3.1. General procedure for purification of His-tagged enzymes

Buffer Solutions:

Lysis buffer: Tris base (50 mM), NaCl (50 mM), pH 8.5.

Buffer 1: Tris base (200 mM) and imidazole (20 mM), pH 8.5.

Buffer 2: Tris base (200 mM) and imidazole (100 mM), pH 8.5.

Buffer 3: Tris base (200 mM) and imidazole (300 mM), pH 8.5.

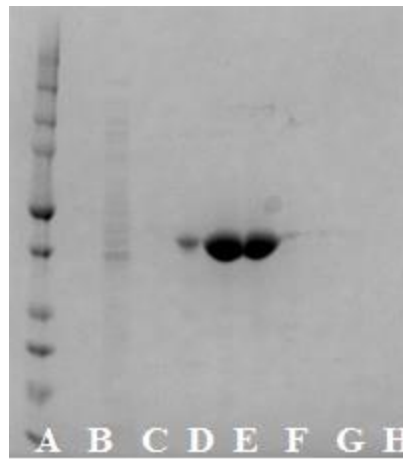
Ni-NTA resin solution (15 mL) was washed as follows: The resin was resuspended in lysis buffer (35 mL) in a 50 mL centrifuge tube and then centrifuged for 5 min at 1000 rpm. The supernatant was poured off and the wash step was repeated. Finally, the resin was resuspended in lysis buffer to a total volume of 15 mL.

Ni-NTA solution was added to the clarified lysate (1 mL Ni resin/ 20 mL lysate) and left to bind overnight under gentle agitation at 4 °C.

The matrix was packed into a 10 ml polypropylene column and the flow through was collected. The column was washed with lysis buffer (10 mL), Buffer 1 (10 mL), Buffer 2 (10 mL) and Buffer 3 (3 x 2 mL). All fractions were collected separately.

Samples from each fraction were analysed by SDS-PAGE. Fractions containing purified protein were combined, desalted using a PD10 desalting column (GE Healthcare) and concentrated using a centrifugal concentrator (Vivaspin, with a 10,000 Da molecular weight cut off), according to the manufacturer's protocol.

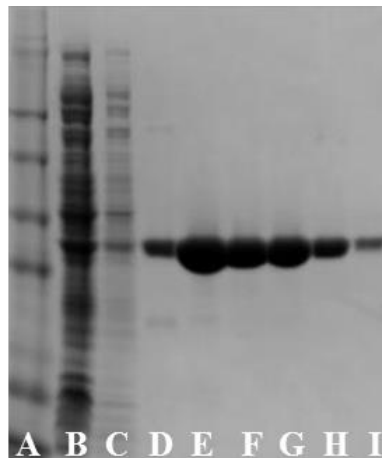
Purified protein was stored at -80 °C in 50% v/v solution.



- A: SeeBlue marker
- B: Flow through
- C: Standard buffer
- D: Buffer 1
- E: Buffer 2
- F: Buffer 3 fraction 1
- G: Buffer 3 fraction 2
- H: Buffer 3 fraction 3

En01

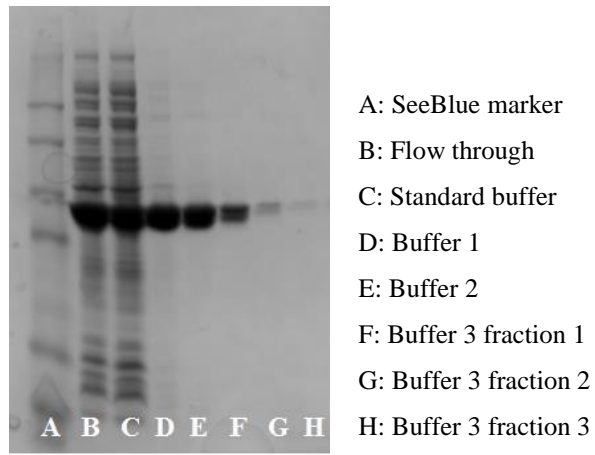
Figure 50. En01 purification SDS-PAGE.



- A: SeeBlue marker
- B: Flow through
- C: Standard buffer
- D: Buffer 1
- E: Buffer 2
- F: Buffer 3 fraction 1
- G: Buffer 3 fraction 2
- H: Buffer 3 fraction 3
- I: Buffer 4

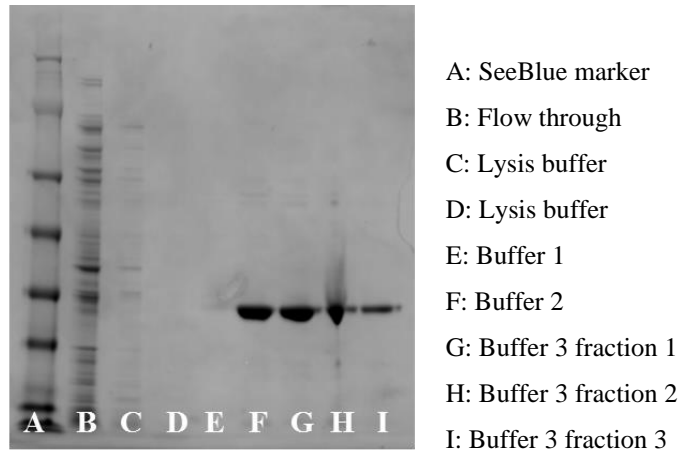
En02

Figure 51. En02 purification SDS-PAGE.



En03

Figure 52. En03 purification SDS-PAGE.



En04

Figure 53. En04 purification SDS-PAGE.

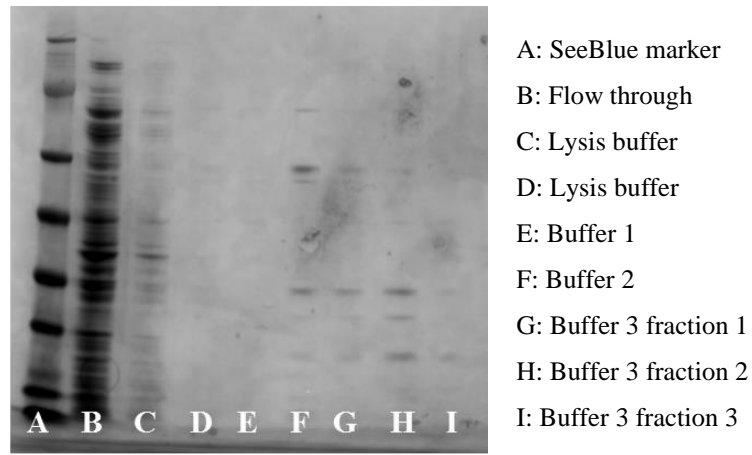


Figure 54. En05 purification SDS-PAGE.

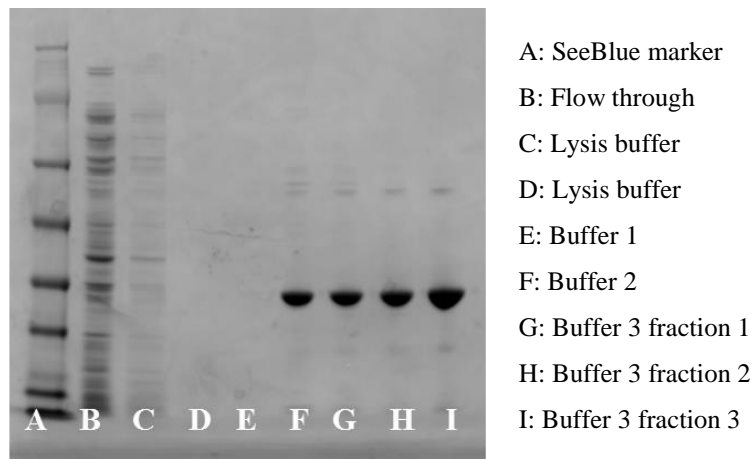


Figure 55. En06 purification SDS-PAGE.

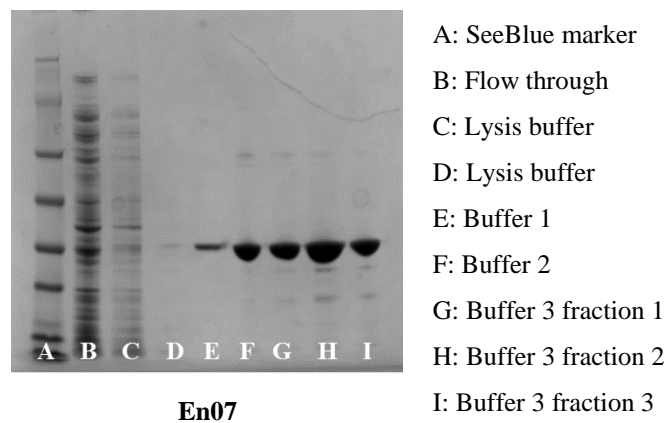


Figure 56. En07 purification SDS-PAGE.

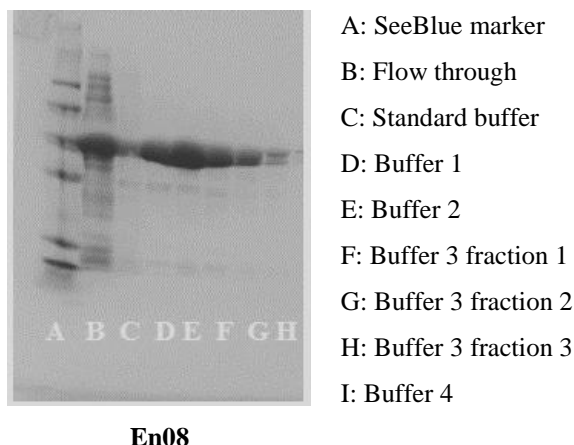


Figure 57. En08 purification SDS-PAGE.

6.2.3.2. General procedure for Bradford microplate assay

A Quick Start ® Bradford assay kit was used. Bovine serum albumen (BSA) standards were prepared as shown in **Table 20**. Each standard (5 µL) was added to Coomassie dye (250 µL) in a clear bottomed 96 shallow well plate. All wells were carried out in triplicate. The absorbance was measured spectrophotometrically at 595 nm and a standard curve plotted (**Figure 58**).

Stock number	Concentration BSA [mg/mL]
1	2.000
2	1.000
3	0.750
4	0.250
5	0.125
6	0.000

Table 20. Preparation of BSA stock solutions.

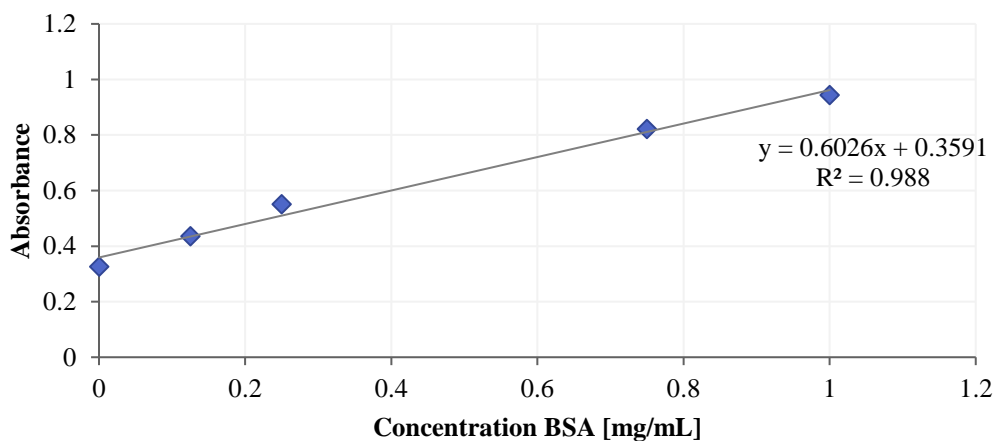


Figure 58. BSA calibration curve.

For proteins of unknown concentrations samples were made up at a variety of dilutions and 5 μ L added to 250 μ L of Coomassie dye. The absorbance was determined at 595 nm and this was used to calculate the protein concentration relative to the standard curve shown.

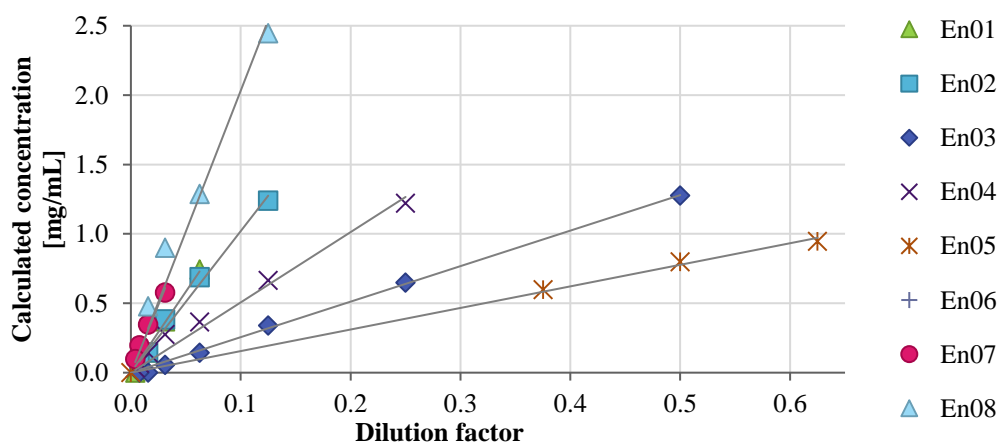


Figure 59. Calculated concentration of purified protein En01-08.

The concentration of the protein was then calculated by adjusting the concentration to the final volume once sterile glycerol had been added, to a final concentration of 50% (v/v) glycerol.

	Volume purified protein [mL]	Concentration calculated from Bradford assay [mg/mL]	Total mass of protein [mg]	Final volume after processing [mL]	Final concentration [mg/mL]
En01	3.5	10.2	35.7	3.7	9.7
En02	6.5	11.7	75.9	6.5	11.7
En03	6.5	2.6	16.6	3.2	5.2
En04	7.4	5.1	37.5	7.4	5.1
En05	6.6	1.6	10.3	6.6	1.6
En06	7.2	19.4	139.8	7.2	19.4
En07	5.2	19.5	101.5	5.2	19.5
En08	14.0	20.3	284.6	25.6	11.1

Table 21. Final concentrations calculated from Bradford assay.

6.3. Reaction optimisation

6.3.1. Determination of pH optima

The following buffers were prepared; potassium phosphate buffer at pHs 6.5, 7.0, 7.5 and 8.0 and Tris HCl buffer at pHs 8.0, 8.5, 9.0 and 9.5.

Stock solutions were made up as follows: phenyl pyruvate **122** (1.3 mg, 0.8 mM) in each buffer (2 mL), methylamine hydrochloride **76** (472 mg, 700 mM) in each buffer (2 mL) and NADPH (6.7 mg, 0.8 mM) in each buffer (2 mL). Each enzyme was diluted in buffer of the appropriate pH to a final concentration of 0.05 mg/mL (final concentration ~ 0.0001 mM). The reactions were set up in triplicate in a clear bottom 96 shallow well plate as shown below (**Figure 60**). 50 μ L of phenyl pyruvate **122** stock, 50 μ L of methylamine **76** stock, 50 μ L NADPH stock, 98 μ L of buffer and 2 μ L of enzyme stock.

Buffer	Ph	En01		
Phosphate	6.5	A1	A2	A3
	7.0	B1	B2	B3
	7.5	C1	C2	C3
	8.0	D1	D2	D3
Tris	8.0	E1	E2	E3
	8.5	F1	F2	F3
	9.0	G1	G2	G3
	9.5	H1	H2	H3

Figure 60. Plate layout for NMAADH pH optima determination.

The reaction was monitored spectrophotometrically at 595 nm every 30 s for 1 h. The results were plotted and a linear fit made with $R^2 > 0.99$. From this the rate of change in absorbance/second was calculated the rate in mM/min/mM enzyme was established.

6.3.2. Buffer concentration

A buffer solution of Tris HCl (pH 8.5, 300 mM) was made up.

Clarified lysate was made using **En01** cell pellet (2.5 g) in 50 mL of 50 mM Tris HCl buffer (50 mL, pH 8.5, 50 mM, NaCl (300 mM), EDTA (1 mM), DTT (1 mM)). The pellet was resuspended and then sonicated for 10 mins at 40 % amplitude, using pulses of 10 s on and 3 s off. Internal standard was made up in a volumetric flask using benzonitrile (0.026 mL, 0.252 mmol) in water (25 mL).

To each of 5 Falcon tubes was added 2-oxo-3-phenylpropanoic acid **122** (246 mg, 1.499 mmol), methylamine hydrochloride **76** (708 mg, 10.49 mmol) and D-glucose (810 mg, 4.50 mmol), each of these was dissolved in a different ratio of buffer and water to give final concentrations of buffer (16 mM, 50 mM, 100 mM, 150 mM and 200 mM), then adjusted to pH 8.5. A solution of NADPH (55 mg, 0.074 mmol) in water (0.1 mL) was made up and 0.02mL was added to each falcon tube. The pH and conversion were monitored at intervals using HPLC Method 1.

6.3.3. D-Glucose loading

Solutions were made up as follows:

A: Phenyl pyruvate **122** (6.6 mg, 0.04 mmol) in Tris HCl buffer (1 mL, pH 8.5, 200 mM).

B: Methylamine HCl **76** (27.0 mg, 0.4 mmol) in Tris HCl buffer (1 mL, pH 8.5, 200 mM).

C: NADPH (3.3 mg, 0.004 mmol) in Tris HCl buffer (1 mL, pH 8.5, 200 mM).

D: D-glucose (216.2 mg, 1.2 mmol) in Tris HCl buffer (1 mL, pH 8.5, 200 mM).

The reaction was then set up according to **Table 22**. The reaction was the monitored using HPLC method 1.

Volume A [ml]	Volume B [ml]	Volume C [ml]	Volume D [ml]	Volume Tris HCl buffer [ml]
0.250	0.250	0.250	0.250	0.000
0.250	0.250	0.250	0.025	0.225

Table 22. Reaction set up for D-glucose concentration reaction.

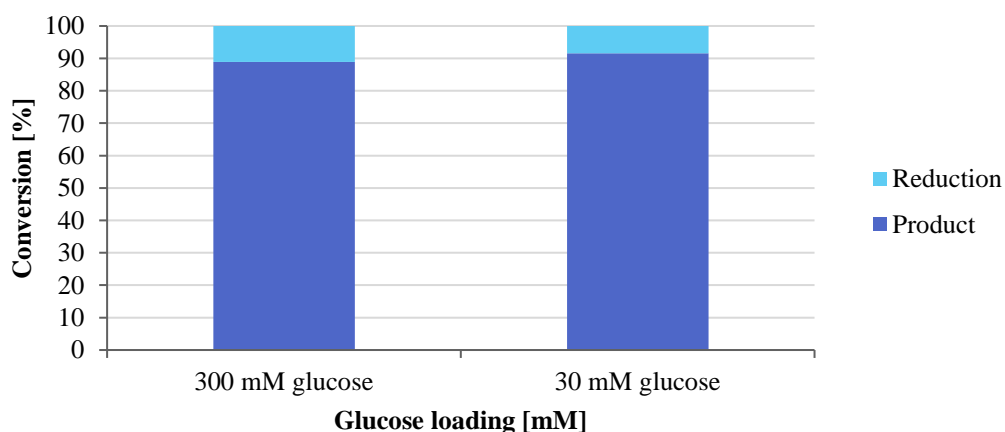


Figure 61. Results of lowering glucose loading.

6.3.4. Amine and enzyme loading

Stock solutions were made up using:

Phenyl pyruvate **122** (99 mg, 0.6 mmol) in Tris HCl Buffer (15 mL, pH 8.5, 200 mM).

Methylamine hydrochloride **76** (5400 mg, 80 mM) in Tris HCl Buffer (20 mL, pH 8.5, 200 mM). NADPH (67 mg, 0.08 mmol), D-glucose (433 mg, 2.4 mmol) and GDH-CDX-901 (20 mg) in Tris HCl Buffer (20 mL, pH 8.5, 200 mM). The plate was then set up according to **Figure 62**.

		Concentration of methylamine [mM]											
		1000	700	500	250	100	75	50	25	10	5	1	0
Concentration of enzyme [μ M]	5.000												
	1.000												
	0.500												
	0.100												
	0.050												
	0.010												
	0.005												
	0.000												

Figure 62. Plate layout for amine and enzyme loading screening. Reaction conditions: phenyl pyruvate 122 (10 mM), methylamine hydrochloride 76 (0-1000 mM), NADPH (1 mM), D-glucose (30 mM), GDH (0.25 mg/mL), En01 (0.005-5 μ M) 25 °C, Tris HCl (pH 8.5, 200 mM).

6.3.5. Enzyme formulation

En01 lysate was prepared from cell pellet (44.5 g) resuspended in Tris HCl buffer (300 mL, pH 8.5, 200 mM). This was then lysed via sonication for 10 mins with pulses of 9 s on and 9 s off. The lysate was then clarified by centrifugation (19000 x g, 45 mins) and lyophilised according to the recipe shown in **Figure 63**.

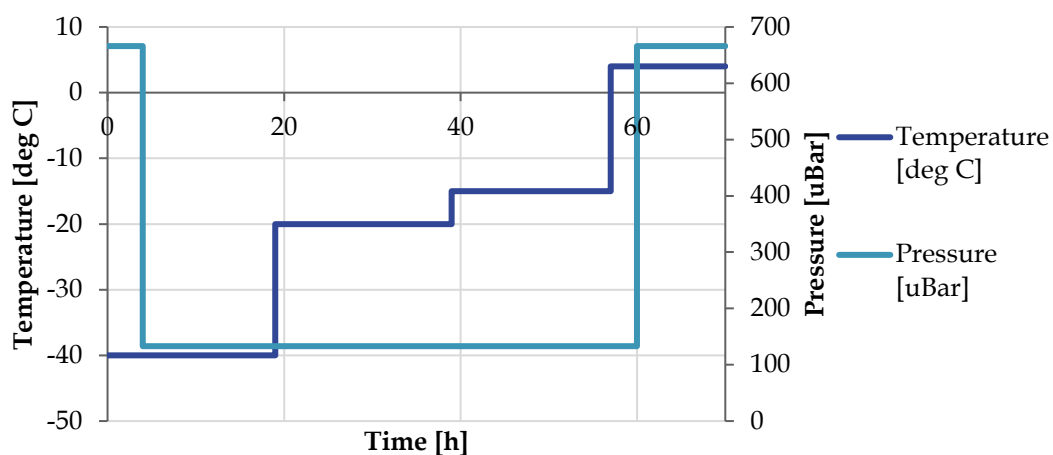


Figure 63. Freeze dry recipe for lyophilisation of En01.

The concentration of lyophilised powder was scaled to the concentration of lysate as shown in **Table 23**.

Mass cell pellet [g]	44.5
Volume lysate [ml]	300
Mass lyophilised powder [g]	6.7
Concentration [mg/ml]	148
Volume of lysate [ml]	0.5
Reaction concentration [mg/ml]	49.4
To achieve and analogous concentration between lysate and powder	
Conversion factor	6.64
Reaction concentration [mg/ml]	7.44
Mass of lyophilised powder needed in reaction [mg]	11.2

Table 23. Sample calculation for the conversion of lysate volume to lyophilised powder mass.

The reactions were set up with phenyl pyruvate **122** (10 mM), methylamine HCl **76** (100 mM), NADPH (1 mM), D-glucose (300 mM), GDH CDX-901 (0.25 mg/mL) in Tris HCl buffer (pH 8.5, 200 mM). They were sampled at reaction time of 2 hours.

6.4. Method development

6.4.1. Liquid chromatography

To monitor reactions effective high performance liquid chromatography (HPLC) and liquid chromatography mass spectrometry (LCMS) methods were required. These needed to be capable of separating the *N*-methyl amino acid products from the keto acid substrates. The methods developed are shown below.

6.4.1.1. Method 1: Achiral HPLC 8 minute method

Run time:	8 min
UV detection:	215 nm
Column:	Luna C18
Temperature:	40 °C
Flow rate:	1.0 ml/min,
Solvent A:	Water with 0.05% TFA
Solvent B:	Acetonitrile with 0.05% TFA
Gradient	0-95% B
Injection volume:	10 µL

Table 24. HPLC method 1.

6.4.1.2. Method 2: Chiral HPLC method

For the chiral analysis of *N*-methyl phenylalanine **78**

Run time:	30 min
UV detection:	215 nm
Column:	Chirobiotic T, 25 cm x 10 mm, 5 µm
Temperature:	Room temperature
Flow rate:	1.0 mL/min,
Solvent A:	Ethanol
Solvent B:	Water
Gradient	25% B
Injection volume:	5 µL

Table 25. HPLC method 2.

6.4.1.3. Method 3: Chiral HPLC method

For the chiral analysis of *N*-functionalised amino acids

Run time:	20 min
UV detection:	215, 258 nm
Column:	Zwix (+), 15 cm x 3 mm, 3 µm
Temperature:	30 °C
Flow rate:	0.4 mL/min,
Solvent:	Acetonitrile/methanol/water (49:49:2), formic acid (50 mM), diethylamine (25 mM)
Gradient	Isocratic
Injection volume:	5 µL

Table 26. HPLC method 3.

6.4.1.4. Method 4: Chiral HPLC method

For the analysis of 1-(4-fluorophenyl)-*N*-methylpropan-2-amine **193**

Run time:	20 min
UV detection:	265 nm
Column:	AD-RH, 15 cm x 4.6 mm, 5µm
Temperature:	Room temperature
Flow rate:	0.6 mL/min,
Solvent A:	Sodium borate buffer (10 mM, pH 9.0)
Solvent B:	Methanol
Gradient	55% B
Injection volume:	1 µL

Table 27. HPLC method 4.

6.4.1.5. Method 5: LCMS method

Run time:	2 min
UV detection:	210-350 nm (summed)
Column:	Acquity UPLC CSH C18 column, 50mm x 2.1mm, 1.7µm
Temperature:	40 °C
Flow rate:	1 mL/min,
Solvent A:	Water, ammonium bicarbonate (10 mM, pH 10.0)
Solvent B:	Acetonitrile
Gradient	3-95% B
Injection volume:	0.3 µL
Ionisation mode:	Alternate-scan Positive and Negative Electrospray
Scan range:	100-1000 AMU

Table 28. LCMS Method 5.

6.4.1.6. Method 6: LCMS method

Run time:	10 min
UV detection:	215 nm
Column:	Hypersil Gold
Temperature:	60 °C
Flow rate:	0.5 mL/min,
Solvent A:	Water with 0.1% FA
Solvent B:	Acetonitrile with 0.1% FA
Gradient	2% B (isocratic)
Injection volume:	10 µL

Table 29. LCMS Method 6.

6.4.1.7. Mass directed auto-purification (MDAP)

Additionally, mass directed auto-preparation methods were used for final purification of desired compounds. The methods used are summarised below.

Instruments:	Waters 2996 photodiode detector Waters 2767 sample manager Waters micromass ZQ mass detector
Run time:	25 min
UV detection:	210-350 nm
Column:	XSelect CSH Prep Select C18 30 mm x 150 mm, Particle size: 5 µm
Temperature:	40 °C
Flow rate:	1 mL/min
Solvent A:	10 mM ammonium bicarbonate solution in water
Solvent B:	Acetonitrile
Gradient	0-25%B

Table 30. Mass directed auto preparation methods.

6.4.2. Gas chromatography

For the analysis of *N*-(1-(4-fluorophenyl)propan-2-yl)prop-2-yn-1-amine

Column:	CHIRASIL DEX-CB, 25 M X 0.25 MM, 1µm
Pressure:	1.2 bar
Carrier gas:	Helium
Injector temperature:	200 °C
Oven temperature gradient	2 °C/min (50-154 °C), 20 °C/min (154-200 °C)
FID-detector temperature:	300 °C

Table 31. GC Chiral Method 7.

6.4.3. Spectrophotometric assay

An NADPH consumption assay was also developed. NADPH absorbs strongly at 340 nm, which is not the case for the reduced form. Therefore, the consumption of NADPH can be used to monitor the reaction progress. This assay has the advantage of allowing a high frequency of readings (up to 1 single wavelength reading per 30 s).

6.4.3.1. Initial development

Solutions of NADPH (1 mM) and NADP⁺ (1 mM) were prepared in Tris HCl buffer (pH 8.5, 200 mM) and pipetted in triplicate into a 96-well shallow clear bottomed plate. Absorbance readings were taken from 200-800 nm (**Figure 64**).

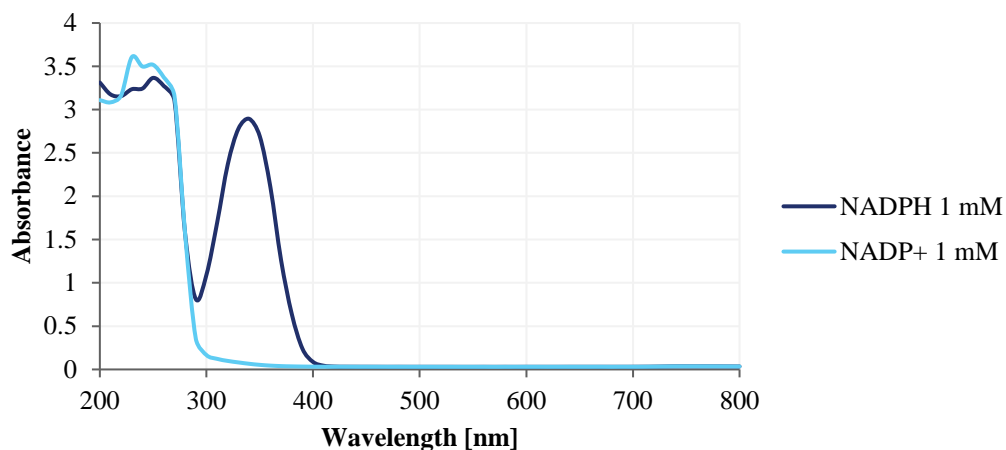


Figure 64. NADPH and NADP⁺ absorbance between 200 and 800 nm.

Solutions of phenyl pyruvate **122** (1 mM), methylamine x (1 mM) and *N*-methyl phenylalanine **78** were prepared in Tris HCl buffer (pH 8.5, 200 mM). These were pipetted into a 96 well shallow clear bottom plate and the absorbance measured at wavelengths from 200-800 nm (**Figure 65**). This showed that only NADPH absorbed at 340 nm.

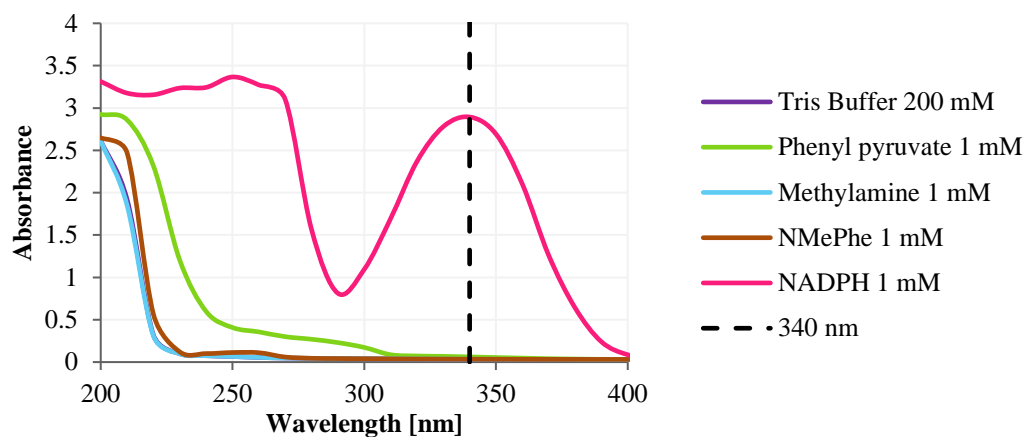


Figure 65. Absorbance of reaction components (1 mM) between 200 and 800 nm.

6.4.3.2. Calibration

To quantify the functional range of this assay, the range of co-factor concentrations that gave a linear response was determined. A solution of NADPH (8.62 mg, 10.34 mM) was made up in Tris HCl buffer (1 mL, pH 8.5, 200 mM). This was diluted according to **Table 32** and the absorbance at 340 nm recorded.

Volume of 10 mM NADPH stock / μ L	Concentration of NADPH /mM	Average absorbance reading
125.0	5.2	3.320
62.5	2.6	3.315
31.3	1.3	3.287
15.6	0.6	2.592
7.8	0.3	1.398
3.9	0.2	0.725
2.0	0.1	0.338
1.0	0.0	0.229
0.5	0.0	0.143
0.2	0.0	0.103
0.1	0.0	0.079
0.0	0.0	0.072

Table 32. Molarity and absorbance of NADPH solutions.

This data was plotted and a linear relationship between molarity and absorbance determined up to 0.8 mM NADPH (**Figure 66**).

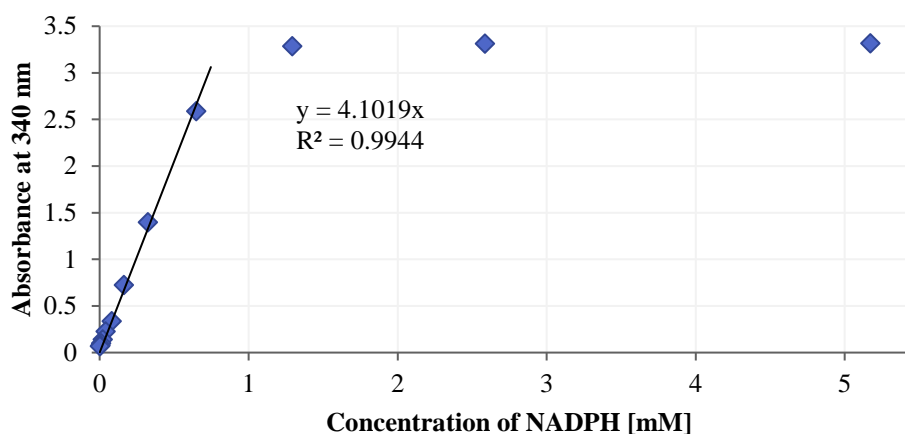


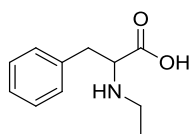
Figure 66. Calibration of concentration of co-factor with absorbance.

6.5. Screening

6.5.1. General procedure for preparation of racemic *N*-alkylated amino acid standards

Ketone (25 mM) was dissolved in methanol, to which was added amine (175 mM, 7 eq). This was stirred for 16 h, after which sodium borohydride (75 mM, 3 equiv) was added portionwise over 0.5 h. The reaction was stirred for a further 1 h, and monitored by HPLC Method 1. The reaction was dried under reduced pressure and the residue was dissolved in methanol/water (1:1, 1 mL) and purified using MDAP method 7.

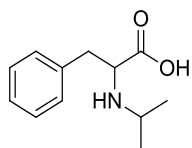
6.5.1.1.1. 2-(Ethylamino)-3-phenylpropanoic acid **139**



Compound **139** was prepared according to the general procedure. Appearance: white amorphous powder. Yield: 80%. ¹H-NMR (400 MHz, D₂O) δ ppm 7.30 (2 H, dd, *J*=7.4, 7.0 Hz), 7.23 (1 H, t, *J*=7.0 Hz), 7.20 (2 H, d, *J*=7.4 Hz), 3.26 (1 H, dd, *J*=8.0, 5.8 Hz), 2.87 (1 H, dd, *J*=13.3, 5.8 Hz), 2.77 (1 H, dd, *J*=13.4, 8.1 Hz), 2.49 (1 H, q, *J*=7.2 Hz), 2.40 (1 H, q, *J*=7.2 Hz), 0.98 (3 H, t, *J*=7.2 Hz). ¹³C-NMR (101 MHz, D₂O) δ ppm 181.6 (1 C), 138.1 (1 C), 129.3 (2 C), 128.5 (2 C), 126.6 (1 C), 65.0 (1 C), 41.4 (1 C), 39.1 (1 C), 13.7 (1 C). Melting point: 242 °C. HPLC Method 1 rt = 2.2 min.

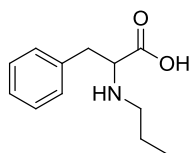
Chiral HPLC method 3 rt = 6.2 min (D), 7.0 min (L). HRMS: (C₁₁H₁₇NO₂) [MH]⁺ required 194.1103, found [MH]⁺ = 194.1184

6.5.1.1.2. 2-(Isopropylamino)-3-phenylpropanoic acid **141**.¹²⁵



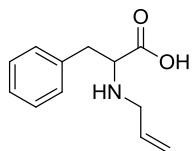
Compound **141** was prepared according to the general procedure. Appearance: white amorphous solid. Yield: 77%. ¹H-NMR (400 MHz, D₂O) δ ppm 7.30 - 7.40 (3 H, m), 7.25 - 7.30 (2 H, m), 3.89 (1 H, dd, *J*=7.3, 6.5 Hz), 3.36 (1 H, spt, *J*=6.6 Hz), 3.15 (1 H, dd, *J*=14.2, 6.5 Hz), 3.10 (1 H, dd, *J*=14.2, 7.3 Hz), 1.25 (3 H, d, *J*=6.5 Hz), 1.22 (3 H, d, *J*=6.5 Hz). ¹³C-NMR (101 MHz, D₂O) δ ppm 173.3 (1 C), 135.0 (1 C), 129.3 (2 C), 129.0 (2 C), 127.6 (1 C), 61.2 (1 C), 50.5 (1 C), 36.3 (1 C), 19.0 (1 C), 17.8 (1 C). Melting point: 267 °C. HPLC Method 1 rt = 2.6 min. LCMS Method 5 rt = 0.46 min [MH]⁺ = 208.07, [M-H]⁻ = 206.23.

6.5.1.1.3. 3-Phenyl-2-(propylamino)propanoic acid **143**.¹²⁵



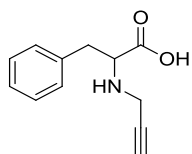
Compound **143** was prepared according to the general procedure. Appearance: white amorphous solid. Yield: 77%. ¹H-NMR (400 MHz, D₂O) δ ppm 7.16 - 7.37 (5 H, m), 3.25 (1 H, dd, *J*=7.9, 5.4 Hz), 2.88 (1 H, dd, *J*=13.0, 5.4 Hz), 2.78 (1 H, dd, *J*=13.0, 7.9 Hz), 2.30 - 2.46 (2 H, m), 1.28 - 1.50 (2 H, m), 0.81 (3 H, t, *J*=7.3 Hz). ¹³C-NMR (101 MHz, D₂O) δ ppm 181.6 (1 C), 138.1 (1 C), 129.3 (2 C), 128.5 (2 C), 126.6 (1 C), 65.3 (1 C), 49.0 (1 C), 39.1 (1 C), 22.0 (1 C), 11.0 (1 C). Melting point: 266 °C. HPLC Method 1 rt = 2.7 min. LCMS Method 5 rt = 0.49 min [MH]⁺ = 208.08 [M-H]⁻ = 206.32. HRMS: (C₁₂H₁₈NO₂) [MH]⁺ required 208.1259, found [MH]⁺ = 208.1342

6.5.1.1.4. 2-(Allylamino)-3-phenylpropanoic acid **145**.¹²⁰



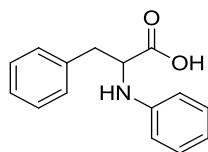
Compound **145** was prepared according to the general procedure. Appearance: white amorphous solid. Yield: 69%. ¹H-NMR (400 MHz, D₂O) δ ppm 7.29 - 7.40 (3 H, m), 7.23 - 7.29 (2 H, m), 5.80 (1 H, ddt, *J*=17.1, 10.5, 6.8 Hz), 5.43 (1 H, dd, *J*=10.5, 2.6 Hz), 5.40 (1 H, dd, *J*=17.1, 2.6 Hz), 3.84 (1 H, dd, *J*=6.6, 6.2 Hz), 3.62 (1 H, dd, *J*=13.5, 6.8 Hz), 3.55 (1 H, dd, *J*=13.5, 6.8 Hz), 3.18 (1 H, dd, *J*=14.4, 6.2 Hz), 3.14 (1 H, dd, *J*=14.4, 6.6 Hz). ¹³C-NMR (101 MHz, D₂O) δ ppm 173.3 (1 C), 134.8 (1 C), 129.4 (2 C), 129.0 (2 C), 127.7 (1 C), 127.4 (1 C), 124.0 (1 C), 62.4 (1 C), 48.9 (1 C), 36.0 (1 C). Melting point 230 °C (decomposition). HPLC Method 1 rt = 2.6 min. Chiral HPLC Method 3 rt = 6.3 min (D), 7.5 min (L). LCMS Method 5 rt = 0.46 min [MH]⁺ = 206.05 [M-H]⁻ = 204.22. HRMS: (C₁₂H₁₆NO₂) [MH]⁺ required 206.1103, found [MH]⁺ = 206.1188

6.5.1.1.5. 3-Phenyl-2-(prop-2-yn-1-ylamino)propanoic acid **147**.¹²⁰



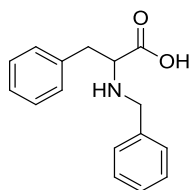
Compound **147** was prepared according to the general procedure. Appearance: beige amorphous powder. Yield: 17%, ¹H-NMR (400 MHz, D₂O) δ ppm 7.28 - 7.34 (2 H, m), 7.19 - 7.27 (3 H, m), 3.46 (1 H, s), 3.47 (1 H, t, *J*=6.8 Hz), 3.33 (1 H, d, *J*=16.6 Hz), 3.20 (1 H, d, *J*=16.6 Hz), 2.86 (2 H, d, *J*=6.8 Hz). ¹³C-NMR (101 MHz, D₂O) δ ppm 180.7 (1 C), 137.9 (1 C), 129.3 (2 C), 128.6 (2 C), 126.7 (1 C), 63.8 (1 C), 63.1 (1 C), 39.0 (1 C), 35.7 (1 C). Melting point: 202 °C. HPLC Method 1 rt = 2.3 min. LCMS Method 5 rt = 0.44 min [MH]⁺ = 204.04 [M-H]⁻ = 202.24.

6.5.1.1.6. 3-Phenyl-2-(phenylamino)propanoic acid **149**



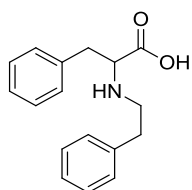
Compound **149** was prepared according to the general procedure. Appearance: white amorphous solid. Yield: 20%, $^1\text{H-NMR}$ (400 MHz, D_2O) δ ppm 7.22 - 7.36 (5 H, m), 7.18 (2 H, td, $J=7.5$, 0.8 Hz), 6.76 (1 H, tt, $J=7.5$, 0.8 Hz), 6.68 (2 H, dd, $J=7.5$, 0.8 Hz), 4.08 (1 H, dd, $J=7.6$, 5.9 Hz), 3.09 (1 H, dd, $J=13.7$, 5.9 Hz), 2.96 (1 H, dd, $J=13.7$, 7.6 Hz). $^{13}\text{C-NMR}$ (101 MHz, D_2O) δ ppm 178.7 (1 C), 147.4 (1 C), 138.0 (1 C), 129.5 (2 C), 129.3 (2 C), 128.6 (2 C), 126.8 (1 C), 118.8 (1 C), 114.6 (2 C), 61.1 (1 C), 38.5 (1 C). Melting point: 180 °C (decomposition). HPLC Method 1 r_t = 5.1 min LCMS Method 5 r_t = 0.65 min $[\text{MH}]^+ = 242.10$ $[\text{M-H}]^- = 240.29$.

6.5.1.1.7. 2-(Benzylamino)-3-phenylpropanoic acid **151**



Compound **151** was prepared according to the general procedure. Appearance: white amorphous solid. Yield: 52%. $^1\text{H-NMR}$ (400 MHz, D_2O) δ ppm 7.15 - 7.40 (14 H, m), 3.70 (1 H, d, $J=12.7$ Hz), 3.52 (1 H, d, $J=12.7$ Hz), 3.30 (1 H, dd, $J=7.6$, 6.3 Hz), 2.88 (1 H, dd, $J=13.5$, 6.3 Hz), 2.82 (1 H, dd, $J=13.5$, 7.6 Hz). $^{13}\text{C-NMR}$ (101 MHz, D_2O) δ ppm 181.2 (1 C), 138.9 (1 C), 138.1 (1 C), 129.3 (2 C), 128.7 (4 C), 128.5 (2 C), 127.4 (1 C), 126.6 (1 C), 64.5 (1 C), 51.0 (1 C), 39.1 (1 C). Melting point: 226 °C. HPLC Method 1 r_t = 3.6 min. Chiral HPLC Method 3 r_t = 6.9 min (D), 11.5 min (L). LCMS Method 5 r_t = 0.62 min $[\text{MH}]^+ = 256.09$ $[\text{M-H}]^- = 254.29$. HRMS: ($\text{C}_{16}\text{H}_{19}\text{NO}_2$) $[\text{MH}]^+$ required 256.1338, found $[\text{MH}]^+ = 256.1335$

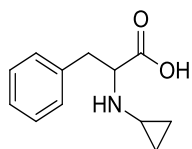
6.5.1.1.8. 2-(Phenethylamino)-3-phenylpropanoic acid **153**



Compound **153** was prepared according to the general procedure. Appearance: white amorphous powder. Yield: 34%. $^1\text{H-NMR}$ (400 MHz, D_2O) δ ppm 7.25 - 7.34 (4 H, m), 7.19 - 7.25 (4 H, m), 7.16 (2 H, dd, $J=7.0$, 1.6 Hz), 3.28 (1 H, dd, $J=7.6$, 6.2 Hz), 2.82 (1 H, dd, $J=13.4$, 6.2 Hz), 2.60 - 2.79 (5 H, m). $^{13}\text{C-NMR}$ (101 MHz, D_2O) δ ppm

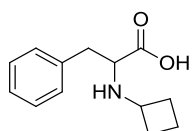
181.2 (1 C), 140.0 (1 C), 138.0 (1 C), 129.3 (1 C), 128.8 (1 C), 128.7 (1 C), 128.5 (1 C), 126.6 (1 C), 126.4 (1 C), 65.1 (1 C), 48.3 (1 C), 38.9 (1 C), 34.9 (1 C). Melting point: 261 °C. HPLC Method 1 rt = 3.7 min. LCMS Method 5 rt = 0.68 min $[MH]^+ = 270.11$ $[M-H]^- = 268.27$. HRMS: $(C_{17}H_{20}NO_2)$ $[MH]^+$ required 270.1416, found $[MH]^+ = 270.1501$

6.5.1.1.9. 2-(Cyclopropylamino)-3-phenylpropanoic acid **155**



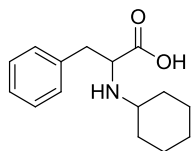
Compound **155** was prepared according to the general procedure. Appearance: white amorphous solid. Yield: 73%. 1H -NMR (400 MHz, D_2O) δ ppm 7.33 (2 H, t, $J=7.5$ Hz), 7.20 - 7.29 (3 H, m), 3.41 (1 H, dd, $J=8.5, 5.5$ Hz), 2.89 (1 H, dd, $J=13.3, 5.5$ Hz), 2.77 (1 H, dd, $J=13.3, 8.5$ Hz), 2.06 (1 H, quin, $J=3.8$ Hz), 0.36 - 0.50 (3 H, m), 0.23 - 0.33 (1 H, m). ^{13}C -NMR (101 MHz, D_2O) δ ppm 181.7 (1 C), 138.1 (1 C), 129.3 (2 C), 128.5 (2 C), 126.6 (1 C), 65.4 (1 C), 38.9 (1 C), 28.3 (1 C), 5.1 (1 C), 4.2 (1 C). Melting point: 206 °C. HPLC Method 1 rt = 2.5 min. Chiral HPLC Method 3 rt = 6.3 min (D), 7.1 min (L). LC-MS Method 2 rt = 0.46 min $[MH]^+ = 206.04$ $[M-H]^- = 204.24$. HRMS: $(C_{12}H_{17}NO_2)$ $[MH]^+$ required 206.1181, found $[MH]^+ = 206.1180$

6.5.1.1.10. 2-(Cyclobutylamino)-3-phenylpropanoic acid **157**



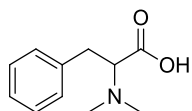
Compound **157** was prepared according to the general procedure. Appearance: white amorphous solid. Yield: 44%. 1H -NMR (400 MHz, D_2O) δ ppm 7.29 (2 H, t, $J=7.8$ Hz), 7.17 - 7.25 (3 H, m), 3.20 (1 H, dd, $J=8.6, 5.8$ Hz), 3.14 (1 H, quin, $J=7.8$ Hz), 2.82 (1 H, dd, $J=13.3, 5.8$ Hz), 2.73 (1 H, dd, $J=13.3, 8.6$ Hz), 1.98 - 2.08 (2 H, m), 1.48 - 1.74 (4 H, m). ^{13}C -NMR (101 MHz, D_2O) δ ppm 181.9 (1 C), 138.2 (1 C), 129.25 (2 C), 128.5 (2 C), 126.5 (1 C), 63.4 (1 C), 52.2 (1 C), 39.4 (1 C), 29.8 (1 C), 29.4 (1 C), 14.4 (1 C). LCMS Method 5 rt = 0.47 min $[MH]^+ = 220.06$ $[M-H]^- = 218.26$.

6.5.1.1.11. 2-(Cyclohexylamino)-3-phenylpropanoic acid **159**



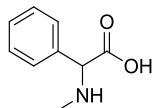
Compound **159** was prepared according to the general procedure. Appearance: white amorphous solid. Yield: 73%. ¹H-NMR (400 MHz, CD₃OD) δ ppm 7.19 - 7.30 (4 H, m), 7.14 (1 H, tt, *J*=7.0, 1.8 Hz), 3.50 (1 H, dd, *J*=7.5, 6.3 Hz), 2.92 (1 H, dd, *J*=13.4, 7.5 Hz), 2.84 (1 H, dd, *J*=13.4, 6.3 Hz), 2.46 (1 H, tt, *J*=10.3, 3.3 Hz), 1.95 (1 H, d, *J*=12.3 Hz), 1.78 (1 H, d, *J*=12.3 Hz), 1.65 - 1.74 (2 H, m), 1.60 (1 H, d, *J*=11.2 Hz), 1.06 - 1.31 (4 H, m), 0.92 - 1.05 (1 H, m). ¹³C-NMR (101 MHz, CD₃OD) δ ppm 180.9 (1 C), 140.0 (1 C), 130.4 (2 C), 129.2 (2 C), 127.2 (1 C), 63.8 (1 C), 56.5 (1 C), 41.2 (1 C), 34.5 (1 C), 32.7 (1 C), 27.1 (1 C), 26.3 (1 C), 26.0 (1 C). LCMS Method 5 rt = 0.49 min [MH]⁺ = 248.11 [M-H]⁻ = 246.29.

6.5.1.1.12. 2-(Dimethylamino)-3-phenylpropanoic acid **160**



Compound **160** was prepared according to the general procedure. Appearance: white amorphous solid. Yield: 44%. ¹H-NMR (400 MHz, D₂O) δ ppm 7.24 - 7.40 (5 H, m), 3.78 (1 H, dd, *J*=9.1, 5.8 Hz), 3.29 (1 H, dd, *J*=13.7, 5.8 Hz), 3.07 (1 H, dd, *J*=13.7, 9.2 Hz), 2.88 (6 H, s). ¹³C-NMR (101 MHz, D₂O) δ ppm 172.4 (1 C), 135.3 (1 C), 129.2 (2 C), 128.9 (2 C), 127.4 (1 C), 72.2 (1 C), 41.8 (2 C), 34.1 (1 C). Melting point: 225 °C

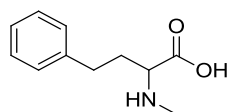
6.5.1.1.13. 2-(Methylamino)-2-phenylacetic acid **162**



Compound **162** was prepared according to the general procedure. Appearance: white amorphous solid. Yield 55%. ¹H-NMR (400 MHz, D₂O) δ ppm 7.34 - 7.46 (5 H, m), 4.43 (1 H, s), 2.49 (3 H, s). ¹³C-NMR (101 MHz, D₂O) δ ppm 174.2 (1 C), 133.8 (1 C), 129.4 (1 C), 129.4 (2 C), 128.2 (2 C), 67.3 (1 C), 31.5 (1 C). Melting point: 264 °C.

HPLC Method 1 rt = 0.6 min. Chiral HPLC Method 3 rt = 7.2 min, 7.9 min. LCMS Method 2 rt = 0.99 min $[MH]^+ = 166.1$ $[M-H]^- = 164.2$.

6.5.1.1.14. 2-(Methylamino)-4-phenylbutanoic acid **164**



Compound **164** was prepared according to the general procedure. Appearance: white amorphous solid. Yield: 55%. 1H -NMR (400 MHz, D_2O) δ ppm 7.15 - 7.36 (5 H, m), 2.89 (1 H, t, $J=6.7$ Hz), 2.57 (2 H, t, $J=8.1$ Hz), 2.18 (3 H, s), 1.68 - 1.86 (2 H, m). ^{13}C -NMR (101 MHz, D_2O) δ ppm 182.4 (1 C), 142.4 (1 C), 128.6 (2 C), 128.5 (2 C), 126.1 (1 C), 65.2 (1 C), 34.9 (1 C), 33.2 (1 C), 31.7 (1 C). Melting point: 205 °C. HPLC Method 1 rt = 2.8 min. LCMS Method 2 rt = 0.99 min $[MH]^+ = 166.1$ $[M-H]^- = 164.2$. Chiral HPLC Method 3 rt = 7.0 min, 7.6 min.

6.5.2. General procedure for the synthesis of L-amino acid standards

L-phenylalanine (470 mg, 570 mM), alkyl bromide (825 mM) and sodium hydroxide (171 mg, 857 mM) were dissolved in a mixture of ethanol (2.5 mL) and water (2.5 mL), which was refluxed for 2 h. The reaction was then dried under reduced pressure, dissolved in a 1:1 mixture of methanol and water (1 mL) and purified by MDAP.

6.5.3. Small scale amine substrate scope screening

Stock solutions (4x) of assay components was prepared as follows

Stock A: Keto acid (40 mM), Stock B: amine (400 mM), Stock C: D-glucose (120 mM), NADPH (1 mM) and GDH-CDX-901 (1 mg/mL) in Tris HCl buffer (pH 8.5, 200 mM). Reactions were set up to the plate map shown (**Figure 67**), this gave final concentrations of phenyl pyruvate x (100 mM), methylamine hydrochloride x (700 mM), D-glucose (30 mM) and NADPH (1 mM). Reactions were shaken at 800 rpm at 25 °C.

	Different substrates tested in each column											
En01												
En02												
En03												
En04												
En05												
En06												
En07												
NC												

Figure 67. Plate map for substrate scope screening. Reaction conditions: keto acid (10 mM), amine (100 mM), NADPH (1 mM), D-glucose (30 mM), GDH-CDX-901 (0.25 mg/mL), En01-07 (0.0001 μ M) 25 °C, Tris HCl (pH 8.5, 200 mM). NC = negative control.

6.5.4. Analysis of expressed recombinant protein for IRED plate screening

A 5 μ L aliquot of the clarified lysates was removed to enable quantitative analysis of IRED expression by capillary electrophoresis using a Protein Express 100 Assay set up with a LabChip (Perkin Elmer/760499) and LabChip GXII Touch HT instrument (Perkin Elmer) (**Figure 68**). Chip and gel dye preparation were carried out according to the instructions provided by the manufacturer. Concentration and molecular weight of the IREDS were estimated using the LabChip GX software version 4.2.1745.0 (Perkin Elmer).

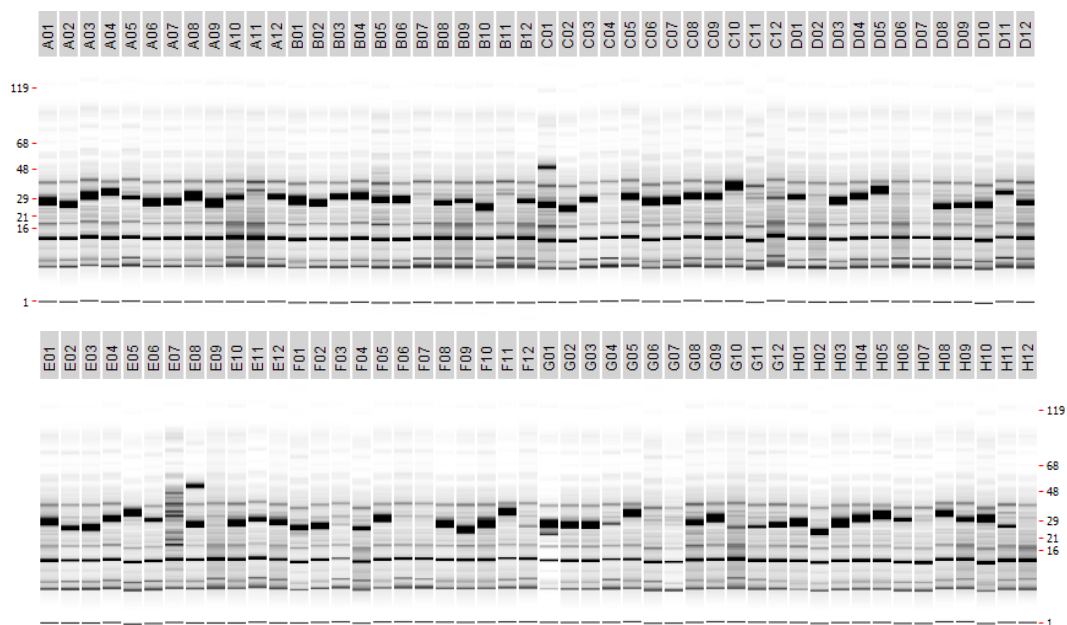


Figure 68. Capillary electrophoresis analysis showing the profile of soluble protein extracts from *E. coli* expressing recombinant IREDs from the panel. IRED expression was observed as bands of ~25-40 kDa, grown in Terrific Broth. Letters across the top of the wells represent the well position of each tested IRED.. Molecular weights are shown on the side of the gels in kDa.

6.5.5. General procedure for screening of IRED plate⁵⁵

All reactions were carried out in a deep-well 96-well plate at a final volume of 400 μ L per well. Enzymatic reactions were conducted at a final concentration of 100 mM buffer (either potassium phosphate (pH 7.0) or tris HCl (pH 9.0)), containing 15 mM glucose, 0.3 mM NADP⁺, and 0.04 mg/mL glucose dehydrogenase (Codexis, CDX-901) and DMSO (10% v/v). Ketone substrates were added to the reaction mixtures to a final concentration of 6 mM. Amine substrates were added to the reaction mixtures to a final concentration of either 60 mM (10 equivs) or 6.6 mM (1.1 equivs).

To lyse the 96-well panel plate of enzyme catalysts, 400 μ L of lysis buffer (either potassium phosphate (pH 7.0) or tris HCl (pH 9.0)) containing 1 mg/mL lysozyme, 1 mg/mL polymixin B sulfate, and 0.5 units/mL of benzonase, was added to each well containing pelleted *E. coli* cells. The plate was sealed with a breathable seal and shaken at 800 rpm for 2 h at room temperature on a bench-top shaker.

The cell debris was pelleted by centrifugation at 4000 rpm for 10 min at 4 $^{\circ}$ C. 200 μ L of clarified lysate was then pipetted from this plate and added to the reaction mixture to initiate the enzymatic reaction. The plate was sealed with a peelable aluminium seal

and then shaken at 500 rpm at 30 °C. Reaction aliquots of 100 uL were removed from each well after 4 h and 24 h..

For HPLC analysis, an 300 uL of acetonitrile was added and the mixture shaken at 850 rpm for 10 min. Debris was pelleted by centrifugation at 4000 rpm for 10 min, and the supernatant was removed for HPLC analysis. For GC analysis, 300 uL of EtOAc was added per well and the plate was sealed and then shaken at 850 rpm for 20 min at room temperature to extract the product into the organic layer. The plate was centrifuged at 4000 rpm for 5 min at 4 °C, and 200 uL of supernatant was removed for GC analysis.

6.6. Biocatalytic large scale reactions

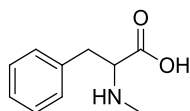
6.6.1. Scale-up procedure for 2-(methylamino)-3-phenylpropanoic acid **78** based on literature conditions

Phenyl pyruvate **122** (2.95 g, 17.97 mmol, final concentration 100 mM), methylamine HCl **76** (8.49 g, 126 mmol, final concentration 700 mM) and D-glucose (9.71 g, 53.9 mmol, final concentration 300 mM) were dissolved in 120 mL of Tris HCl buffer (50 mM, pH 9.5). NADPH (0.134 g, 0.118 mmol, final concentration 1 mM) was added and the solution was transferred to an EasyMax 402 reactor. **En01** lysate (60 mL) and glucose dehydrogenase solution (100 µL of 2000 U/mL) were added, initial reaction pH was measured at 8.2. The reaction was stirred at 750 rpm impeller speed at 30 °C for 27 hours, a bright yellow colour being observed. The pH was monitored over time and adjusted using NaOH (5 M) to maintain the pH between 7.0 and 9.5. The reaction was sampled by diluting 20 µL of the homogeneous reaction mixture with 100 µL aqueous acetic acid (2% v/v) and the sample was analysed by HPLC. The conversion was calculated based on the peak areas of *N*-methylphenylalanine **x** and the benzonitrile internal standard.

After 27 hours, HPLC showed that the reaction had reached 85% conversion and the product was isolated. The reaction was acidified to pH 2 using 1 M aqueous HCl, and the precipitated proteins from the cell lysate were removed by centrifugation for 20 mins at 4 °C at 3500 x g. The supernatant containing product was poured off and dried under reduced pressure.

Dowex 50wx8 ion exchange resin was used to extract the product. A slurry of 20 g of Dowex resin in water was loaded into a glass column. The resin was then washed with 2 column volumes (CV) of water, 2 CV methanol then 2 CV water. The resin was washed with 1 M HCl until it reached pH 5, then with water until it returned to neutral. The resin was then washed with 1 M ammonium hydroxide until it reached pH 9, then with water until it returned to neutral. Finally, the resin was washed with 1 M hydrochloric acid until it reached pH 5, then with water until it returned to neutral. The product residue was dissolved in a minimal volume of water and acidified to pH 3, this was loaded onto the column and allowed to flow through the resin. The residue was washed with water until the flow through reached pH 7, with fractions being collected. Elution was then carried out with 1 M ammonium hydroxide, again collecting fractions. These were analysed by spotting on a glass TLC plate, dried using a heatgun and stained using ninhydrin.

1 M ammonium hydroxide was added until samples did not show the presence of amine. Then the resin was stripped using 5 M ammonium hydroxide. The fractions containing product were dried under reduced pressure, then dried further in a vacuum oven.



Compound **78** was isolated as an off white powder, 2.65 g. Yield 81%. ee >99%. ¹H-NMR (400 MHz, D₂O) δ ppm 7.16 - 7.32 (5 H, m), 3.44 (1 H, s), 3.14 (1 H, t, *J*=6.8 Hz), 2.80 (2 H, dd, *J*=6.8, 4.3 Hz), 2.16 (3 H, s) ¹³C-NMR (101 MHz, D₂O) δ ppm 181.47 (1 C), 138.20 (1 C), 129.31 (2 C), 128.52 (2 C), 126.58 (1 C), 66.91 (1 C), 63.58 (1 C), 56.26 (1 C), 39.06 (1 C), 33.21 (1 C). HPLC Method 1 rt = 1.6 min. Chiral HPLC method 2 rt = 9.9 min (L), 12.9 min (D).

6.6.2. Scale-up procedure

The clarified lysate (50 mL) was transferred to a Schott bottle (1000 mL) containing Tris HCl buffer (pH 8.5, 50 mL, 200 mM), D-glucose (0.81 g, 4.5 mmol, 3 equiv, 30 mM final), glucose dehydrogenase CDX-901 (40 mg, 0.25 mg/mL final) and NADP⁺ (125 mg, 0.15 mmol, 1.0 mM final). Further Tris HCl buffer (pH 8.5, 50 mL, 200 mM)

containing phenyl pyruvate (240 mg, 1.5 mmol, 10 mM final) was added. Reaction was started by the addition of amine (15 mmol, 10 equiv, 100 mM final) in Tris HCl buffer (pH 8.5, 50 mL, 200 mM). The reaction was carried out at 25 °C at 200 rpm (Kuhner shaker). During the reaction time, several aliquots (250 µL) were withdrawn quenched with acetonitrile (750 µL) to evaluate conversion by HPLC. After reaction 24 h the reaction mixture was quenched with methanol and spun at 4000 rpm for 10 mins to remove solids. The supernatant was dried under reduced pressure and the residue was subjected to mass directed auto purification (MDAP) to give the corresponding reductive amination products.

6.7. Molecular docking and crystal structure

6.7.1. Screening of commercial crystallisation kits

Purified **En01** (13 mg/mL) that had been flash frozen and stored at -80 °C was thawed on ice. The protein was centrifuged at 4°C for 5 min at 13000 rpm using a bench top centrifuge. A variety of commercially available screening kits were used to assess a wide range of conditions. The screens used were: Index HR2-144 (Hampton Research), Morpheus HT-96 (Molecular Dimensions), PACT premier HT-96 (Molecular Dimensions), PEGs II suite (Qiagen) and JCSG+ suite (Qiagen). These were carried out according to the manufacturer's protocols.

Conditions selected were: Index G9, well volume: 75 µL, 25% w/v PEG 3350, 0.1 M Tris, pH 8.5, 0.2 M ammonium acetate, 20 °C.

6.7.2. Optimisation of crystallisation conditions

Two screens were set up to optimise the crystallisation conditions.

		PEG 3350 concentration (% w/v)											
		15	16	17	18	19	20	21	22	23	24	25	26
pH	8.1												
	8.2												
	8.3												
	8.4												
	8.5												
	8.6												
	8.7												
	8.8												

Figure 69. Plate map of first optimisation screen.

Screen 1 was set up using the conditions shown in **Figure 69**, with well volume: 75 μ L, 0.1 M Tris, 0.2 M sodium chloride, 20 $^{\circ}$ C.

		PEG 3350 concentration (% w/v)											
		20	21	22	23	24	25	26	27	28	29	30	31
pH	8.1												
	8.2												
	8.3												
	8.4												
	8.5												
	8.6												
	8.7												
	8.8												

Figure 70. Plate map of second optimisation screen.

Screen 2 – This screen was set up using the conditions shown in **Figure 70**, with well volume: 75 μ L, 0.1 M Tris, 0.2 M ammonium acetate, 20 $^{\circ}$ C.

6.7.3. Co-crystallisation protocols

This was carried out using the best conditions from the previous screening: well volume: 75 μ L, 25% w/v PEG 3350, 0.1 M Tris, pH 8.5, 0.2 M ammonium acetate, 20 $^{\circ}$ C. However, prior to the screen 50 mM NADPH and 50 mM phenyl pyruvate were

added to the defrosted enzyme solution and incubated on ice for 10 mins. This was then centrifuged at 4°C for 10 minutes at 13000 rpm on a bench top centrifuge.

6.8. Enzymatic cascade

6.8.1. DAADH expression

All of the expression and formulation was carried out according to the general procedure set out in 6.2.

6.8.1.1. D-amino acid dehydrogenase *C. Glutamicum* En08

MGSSHHHHHMTNIRVAIVGYGNLGRSVEKLIKQPDMDLVGIFSRRATLD
TKTPVFDVADVDKHADDVDVLFVLCMGSATDIPEQAPKFAQFACTVDTYDN
HRDIPRHRQVMNEAATAAGNVALVSTGWDPGMFSINRVYAAAVLAEHQQH
TFWGPGLSQGHSDALRRIPGVQKAVQYTLPSDALEKARRGEAGDLTGKQT
HKRQCFVVADAADHERIENDIRTMPDYFVGYEVEVNFIDEATFDSEHTGMP
HGGHVITTGDTGGFNHVEYILKLDNPDFTASSQIAFGRAAHRMKQQGQSG
AFTVLEVAPYLLSPENLDDLIARDV

6.8.1.2. D-amino acid dehydrogenase *U. Thermophilus* En09

MGSSHHHHHMSKIRIGIVGYGNLGRGVEAAIQQNPDMELVAVFTRRDPKT
VAVKSNVVLHVDDAQSYPKDEIDVMILCGGSATDLPEQGPYFAQYFNTIDSF
DTHARIPDYFDAVNAAEQSGKVAIISVGWDPGLFSLNRLLEGEVLPVGNTYT
FWGGVSLGHSGAIRRIQGVKNAVQYIIPIDEAVNRVRSNGENPELSTREKHAM
ECFVVLEEGADPAKVEHEIKTMPNYFDEYDTTVHFISEEELKQNHSGMPNGG
FVIRSGKSDEGHKQIIEFSLNLESNPMFTSSALVAYARAYRLSQNGDKGAKT
VFDIPFGLLSPKSPEDLRKELL

6.8.2. DAADH screening reaction

A reaction stock solution was prepared containing D-phenylalanine (0.04 g, 0.24 mmol) dissolved in Tris buffer (3.5 mL), and adjusted to pH 9.5 using 1 M NaOH, then NADP⁺ (0.162 g, 0.217 mmol) was added. Reactions were prepared using 0.6 mL of stock solution and either 0.5 mL enzyme lysate or 10 µL of purified protein (21 mg/ml) and buffer (490 µL) to give a final concentration of phenylalanine (25 mM) and NADP⁺ (1 mM). Reactions were incubated at 25 °C with shaking at 750 rpm.

6.8.3. Cascade protocol

D-phenylalanine (25 mM) was dissolved in 1mL of Tris buffer, then adjusted to pH 9.5 using 1 M NaOH. Just prior to reaction set up NADP⁺ (1 mM) was added.

10 µL **En01** (20 mg/mL final concentration ~ 4.5 mM) and 10 µL **En08**(18 mg/mL, final concentration ~ 4.5 mM) were added (purified protein). Reactions were incubated at 25 °C with shaking at 750 rpm. Samples (20 µL) were taken from the reaction and diluted with 20 µL aqueous acetic acid (2% v/v).

7. References

1. U. T. Bornscheuer, G. W. Huisman, R. J. Kazlauskas, S. Lutz, J. C. Moore, *et al.*, *Nature*, 2012, **485**, 185-194.
2. R. N. Patel, *Biomol.*, 2013, **3**, 741-777.
3. R. Finking and M. A. Marahiel, *Annu. Rev. Microbiol.*, 2004, **58**, 453-488.
4. M. A. Martínez-Núñez and V. E. L. y. López, *Sustain. Chem. Process.*, 2016, **4**, 1-8.
5. D. P. Fairlee, G. Abbenante and D. R. March, *Curr. Med. Chem.*, 1995, **2**, 654-686.
6. L. Aurelio, R. T. Brownlee and A. B. Hughes, *Chem. Rev.*, 2004, **104**, 5823-5846.
7. D. P. Levine, *Clin. Infect. Dis.*, 2006, **42**, S5-S12.
8. R. Kannan, C. M. Harris, T. M. Harris, J. P. Waltho, N. J. Skelton, *et al.*, *J. Am. Chem. Soc.*, 1988, **110**, 2946-2953.
9. S. A. Survase, L. D. Kagliwal, U. S. Annapure and R. S. Singhal, *Biotechnol. Adv.*, 2011, **29**, 418-435.
10. G. R. Pettit, Y. Kamano, C. L. Herald, Y. Fujii, H. Kizu, *et al.*, *Tetrahedron*, 1993, **49**, 9151-9170.
11. D. Wang, C. Wang, P. Gui, H. Liu, S. M. H. Khalaf, *et al.*, *Front. Microbiol.*, 2017, **8**, 1147.
12. D. S. Pereira, C. I. Guevara, L. Jin, N. Mbong, A. Verlinsky, *et al.*, *Mol. Cancer Ther.*, 2015, **14**, 1650-1660.
13. F. Haviv, T. D. Fitzpatrick, R. E. Swenson, C. J. Nichols, N. A. Mort, *et al.*, *J. Med. Chem.*, 1993, **36**, 363-369.
14. R. Schmidt, A. Kalman, N. N. Chung, C. Lemieux, C. Horvath, *et al.*, *Int. J. Pept. Protein Res.*, 2009, **46**, 47-55.
15. F. E. Ali, D. B. Bennett, R. R. Calvo, J. D. Elliott, S.-M. Hwang, *et al.*, *J. Med. Chem.*, 1994, **37**, 769-780.
16. C. A. Lipinski, F. Lombardo, B. W. Dominy and P. J. Feeney, *Adv. Drug Delivery Rev.*, 2012, **64**, 4-17.
17. D. J. Gordon, R. Tappe and S. C. Meredith, *J. Pept. Res.*, 2008, **60**, 37-55.
18. E. Arceo and P. Melchiorre, *ChemCatChem*, 2012, **4**, 459-461.

19. S. M. So, H. Kim, L. Mui and J. Chin, *Eur. J. Org. Chem.*, 2012, **2012**, 229-241.
20. H. Kuang and M. D. Distefano, *J. Am. Chem. Soc.*, 1998, **120**, 1072-1073.
21. C.-X. Chen, B. Jiang, C. Branford-White and L.-M. Zhu, *Biochem. (Mosc)*, 2009, **74**, 36-40.
22. F. G. Healy, M. Wach, S. B. Krasnoff, D. M. Gibson and R. Loria, *Mol. Microbiol.*, 2000, **38**, 794-804.
23. R. R. King and L. A. Calhoun, *Phytochem.*, 2009, **70**, 833-841.
24. T. Wang, *J. Org. Chem.*, 1974, **39**, 3591-3594.
25. K. A. Trujillo and H. Akil, *Drug Alcohol Depend.*, 1995, **38**, 139-154.
26. L. Aurelio and A. B. Hughes, in *Amino Acids, Peptides and Proteins in Organic Chemistry*, Wiley-VCH, 2009, pp. 245-289.
27. J. J. Chruma, D. Sames and R. Polt, *Tetrahedron Lett.*, 1997, **38**, 5085-5086.
28. E. W. Baxter and A. B. Reitz, in *Organic Reactions*, 2004, vol. 59, ch. 1, pp. 1-714.
29. A. Kumar, S. Sharma and R. A. Maurya, *Adv. Synth. Catal.*, 2010, **352**, 2227-2232.
30. V. A. Soloshonok, H. T. Catt and T. Ono, *J. Fluor. Chem.*, 2010, **131**, 261-265.
31. E. Rothstein, *J. Chem. Soc.*, 1949, **1**, 1968-1972.
32. F. Effenberger and U. Burkard, *Liebigs Ann. Chem.*, 1986, **1986**, 334-358.
33. F. Degerbeck, B. Fransson, L. Grehn and U. Ragnarsson, *J. Chem. Soc., Perkin Trans. 1*, 1992, 245-253.
34. T. W. Greene and P. G. M. Wuts, in *Greene's Protective Groups in Organic Synthesis*, Wiley, Fourth edn., 2006, ch. Protection for the Amino Group, pp. 696-926.
35. S. C. Miller and T. S. Scanlan, *J. Am. Chem. Soc.*, 1997, **119**, 2301-2302.
36. S. C. Miller and T. S. Scanlan, *J. Am. Chem. Soc.*, 1998, **120**, 2690-2691.
37. A. Isidro-Llobet, M. Alvarez and F. Albericio, *Chem. Rev.*, 2009, **109**, 2455-2504.
38. M. Prashad, D. Har, B. Hu, H. Y. Kim, O. Repic, *et al.*, *Org. Lett.*, 2003, **5**, 125-128.
39. M. Stodulski and J. Mlynarski, *Tetrahedron: Asymmetry*, 2008, **19**, 970-975.
40. T. Tsunoda, Y. Yamamiya and S. Ito, *Tetrahedron Lett.*, 1993, **34**, 1639-1642.

41. R. A. Turner, N. E. Hauksson, J. H. Gipe and R. S. Lokey, *Org. Lett.*, 2013, **15**, 5012-5015.
42. J. F. Reichwein and R. M. J. Liskamp, *Tetrahedron Lett.*, 1998, **39**, 1243-1246.
43. D. Papaioannou, C. Athanassopoulos, V. Magafa, N. Karamanos, G. Stavropoulos, *et al.*, *Acta Chem. Scand.*, 1994, **48**, 324-333.
44. F. I. McGonagle, D. S. MacMillan, J. Murray, H. F. Sneddon, C. Jamieson, *et al.*, *Green Chem.*, 2013, **15**.
45. M. Ebata, Y. Takahashi and H. Otsuka, *Bull. Chem. Soc. Jpn.*, 1966, **39**, 2535-2538.
46. P. Quitt, J. Hellerbach and K. Vogler, *Helv. Chim. Acta*, 1963, **46**, 327-333.
47. K. N. White and J. P. Konopelski, *Org. Lett.*, 2005, **7**, 4111-4112.
48. D. Pajtas, K. Konya, A. Kiss-Szikszai, P. Dzubak, Z. Petho, *et al.*, *J. Org. Chem.*, 2017, **82**, 4578-4587.
49. K. Kónya, D. Pajtás, A. Kiss-Szikszai and T. Patonay, *Eur. J. Org. Chem.*, 2015, **2015**, 828-839.
50. Y. M. Ahn, L. Vogeti, C. J. Liu, H. K. Santhapuram, J. M. White, *et al.*, *Bioorg. Med. Chem.*, 2007, **15**, 702-713.
51. T. Frickey and G. Weiller, *Bioinformatics*, 2007, **23**, 1170-1171.
52. V. Kunin and C. A. Ouzounis, *BMC Bioinformatics*, 2005, **6**, 24.
53. WO 2013/170050 A1, 2013.
54. G. A. Aleku, S. P. France, H. Man, J. Mangas-Sanchez, S. L. Montgomery, *et al.*, *Nat. Chem.*, 2017, **9**, 961-969.
55. G.-D. Roiban, M. Kern, Z. Liu, J. Hyslop, P. Lyn Tey, *et al.*, *ChemCatChem*, **9**, 4475-4479.
56. H. Muramatsu, H. Mihara, R. Kakutani, M. Yasuda, M. Ueda, *et al.*, *J. Biol. Chem.*, 2005, **280**, 5329-5335.
57. A. Hallen, A. J. Cooper, J. R. Smith, J. F. Jamie and P. Karuso, *Amino Acids*, 2015, **47**, 2457-2461.
58. M. Sato, M. Takeuchi, N. Kanno, E. Nagahisa and Y. Sato, *Comp. Biochem. Physiol. B Biochem. Mol. Biol.*, 1993, **106**, 955-960.
59. S. H. Smits, A. Mueller, L. Schmitt and M. K. Grieshaber, *J. Mol. Biol.*, 2008, **381**, 200-211.

60. Y. Kato, H. Yamada and Y. Asano, *J. Mol. Catal. B: Enzym.*, 1996, **1**, 151-160.
61. N. Van Thoai, C. Huc, D. B. Pho and A. Olomucki, *Biochim. Biophys. Acta, Enzymol.*, 1969, **191**, 46-57.
62. S. Vazquez-Dorado, A. Sanjuan, A. S. Comesana and A. de Carlos, *Comp. Biochem. Physiol. Biochem. Mol. Biol.*, 2011, **160**, 94-103.
63. K. B. Storey, *J. Exp. Zool.*, 1983, **225**, 369-378.
64. N. Kan-no, M. Sato, T. Yokoyama and E. Nagahisa, *Comp. Biochem. Physiol. Biochem. Mol. Biol.*, 1999, **123**, 125-136.
65. *United States of America Pat.*, 2013.
66. S. L. Lovelock and N. J. Turner, *Bioorg. Med. Chem.*, 2014, **22**, 5555-5557.
67. F. Parmeggiani, N. J. Weise, S. T. Ahmed and N. J. Turner, *Chem. Rev.*, 2018, **118**, 73-118.
68. S. L. Lovelock, R. C. Lloyd and N. J. Turner, *Angew. Chem. Int. Ed.*, 2014, **53**, 4652-4656.
69. F. Parmeggiani, S. L. Lovelock, N. J. Weise, S. T. Ahmed and N. J. Turner, *Angew. Chem. Int. Ed.*, 2015, **54**, 4608-4611.
70. S. Viergutz, L. Poppe, A. Tomin and J. Retey, *Helv. Chim. Acta*, 2003, **86**, 3601-3612.
71. W. Hummel, N. Weiss and M.-R. Kula, *Arch. Microbiol.*, 1984, **137**, 47-52.
72. A. Menzel, H. Werner, J. Altenbuchner and H. Gröger, *Eng. Life Sci.*, 2004, **4**, 573-576.
73. N. Itoh, C. Yachi and T. Kudome, *J. Mol. Catal. B: Enzym.*, 2000, **10**, 281-290.
74. T. Matsumoto, B. Y. Hiraoka and J. Tobarí, *Biochim. Biophys. Acta, Enzymol.*, 1978, **522**, 303-310.
75. M. Iwaki, T. Yagi, K. Horiike, Y. Saeki, T. Ushijima, *et al.*, *Arch. Biochem. Biophys.*, 1983, **220**, 253-262.
76. M. J. Abrahamson, E. Vazquez-Figueroa, N. B. Woodall, J. C. Moore and A. S. Bommarius, *Angew. Chem. Int. Ed.*, 2012, **51**, 3969-3972.
77. T. Knaus, W. Bohmer and F. G. Mutti, *Green Chem.*, 2017, **19**, 453-463.

78. J. Chatterjee, F. Rechenmacher and H. Kessler, *Angew. Chem. Int. Ed.*, 2013, **52**, 254-269.
79. S-(5'-Adenosyl)-L-homocysteine,
<https://www.sigmaaldrich.com/catalog/product/sigma/a9384?lang=en®ion=GB>,
2018).
80. C. Dalhoff, G. Lukinavicius, S. Klimasauskas and E. Weinhold, *Nat. Protoc.*, 2006, **1**, 1879-1886.
81. G. L. Canton and P. J. Vignos, *J. Biol. Chem.*, 1954, **209**, 647-659.
82. D. D. Brown, R. Tomchick and J. Axelrod, *J. Biol. Chem.*, 1959, **234**, 2948-2950.
83. K. Mitsukura, M. Suzuki, S. Shinoda, T. Kuramoto, T. Yoshida, *et al.*, *Biosci. Biotechnol., Biochem.*, 2011, **75**, 1778-1782.
84. K. Mitsukura, M. Suzuki, K. Tada, T. Yoshida and T. Nagasawa, *Org. Biomol. Chem.*, 2010, **8**, 4533-4535.
85. F. Leipold, S. Hussain, D. Ghislieri and N. J. Turner, *ChemCatChem*, 2013, **5**, 3505-3508.
86. D. Ghislieri and N. J. Turner, *Top. Catal.*, 2013, **57**, 284-300.
87. P. N. Scheller, M. Lenz, S. C. Hammer, B. Hauer and B. M. Nestl, *ChemCatChem*, 2015, **7**, 3239-3242.
88. P. Matzel, M. Gand and M. Höhne, *Green Chem.*, 2017, **19**, 385-389.
89. M. Yasuda, M. Ueda, H. Muramatsu, H. Mihara and N. Esaki, *Tetrahedron: Asymmetry*, 2006, **17**, 1775-1779.
90. M. C. Lin and C. Wagner, *J. Biol. Chem.*, 1975, **250**, 3746-3751.
91. A. Hallen, J. F. Jamie and A. J. Cooper, *Amino Acids*, 2013, **45**, 1249-1272.
92. H. Mihara, H. Muramatsu, R. Kakutani, M. Yasuda, M. Ueda, *et al.*, *FEBS J.*, 2005, **272**, 1117-1123.
93. H. Muramatsu, H. Mihara, M. Goto, I. Miyahara, K. Hirotsu, *et al.*, *J. Biosci. Bioeng.*, 2005, **99**, 541-547.
94. A. Irimia, D. Madern, G. Zaccari and F. M. Vellieux, *EMBO J.*, 2004, **23**, 1234-1244.
95. E. Cusa, N. Obradors, L. Baldomà, J. Badía and J. Aguilar, *J. Bacteriol.*, 1999, **181**, 7479-7489.

96. M. Goto, H. Muramatsu, H. Mihara, T. Kurihara, N. Esaki, *et al.*, *J. Biol. Chem.*, 2005, **280**, 40875-40884.
97. T. Huber, L. Schneider, A. Präg, S. Gerhardt, O. Einsle, *et al.*, *ChemCatChem*, 2014, **6**, 2248-2252.
98. M. G. Rossmann, D. Moras and K. W. Olsen, *Nature*, 1974, **250**, 194-199.
99. M. Nardini, G. Ricci, A. M. Caccuri, S. P. Solinas, L. Vesci, *et al.*, *Eur. J. Biochem.*, 1988, **173**, 689-694.
100. A. Hallen, A. J. L. Cooper, J. R. Smith, J. F. Jamie and P. Karuso, *Amino Acids*, 2015, **47**, 2457-2461.
101. A. Hallen, A. J. L. Cooper, J. F. Jamie, P. A. Haynes and R. D. Willows, *J. Neurochem.*, 2011, **118**, 379-387.
102. M. Nardini, G. Ricci, L. Vesci, L. Pecci and D. Cavallini, *Biochim. Biophys. Acta, Biophys. Incl. Photosynth.*, 1988, **957**, 286-292.
103. N. Weissman and R. Schoenheimer, *J. Biol. Chem.*, 1941, **140**, 779-795.
104. A. Hallen, J. F. Jamie and A. J. Cooper, *Neurochem. Res.*, 2014, **39**, 527-541.
105. T. Yura and H. J. Vogel, *J. Biol. Chem.*, 1959, **234**, 335-338.
106. P. Singh, A. Tiwari, S. P. Singh and R. K. Asthana, *Physiol. Mol. Biol. Plants*, 2013, **19**, 521-528.
107. J. T. Wu, L. H. Wu and J. A. Knight, *Clin. Chem.*, 1986, **32**, 314-319.
108. I. Alfonso and V. Gotor, *Chem. Soc. Rev.*, 2004, **33**, 201-209.
109. H. Muramatsu, H. Mihara, R. Kakutani, M. Yasuda, M. Ueda, *et al.*, *Tetrahedron: Asymmetry*, 2004, **15**, 2841-2843.
110. M. Goto, H. Muramatsu, H. Mihara, T. Kurihara, N. Esaki, *et al.*, *J. Biol. Chem.*, 2005, **280**, 40875-40884.
111. M. Redondo-Nieto, M. Barret, J. P. Morrissey, K. Germaine, F. Martinez-Granero, *et al.*, *J. Bacteriol.*, 2012, **194**, 1273-1274.
112. D. S. Gerhard, L. Wagner, E. A. Feingold, C. M. Shenmen, L. H. Grouse, *et al.*, *Genome Res.*, 2004, **14**, 2121-2127.
113. A. V. Zimin, A. L. Delcher, L. Florea, D. R. Kelley, M. C. Schatz, *et al.*, *Genome Biol.*, 2009, **10**, R42.
114. C. R. Davis, M. A. McPeck and C. R. McClung, *Mol. Gen. Genet.*, 1995, **248**, 341-350.

115. F. Leipold, S. Hussain, S. P. France and N. J. Turner, in *Science of Synthesis: Biocatalysis in Organic Synthesis*, eds. K. Faber, W.-D. Fessner and N. J. Turner, Thieme, Stuttgart, 2015, vol. 2, pp. 359-382.
116. J. H. Schrittwieser, S. Velikogne and W. Kroutil, *Adv. Synth. Catal.*, 2015, **357**, 1655-1685.
117. W. Zhang, K. O'Connor, D. I. Wang and Z. Li, *Appl. Environ. Microbiol.*, 2009, **75**, 687-694.
118. A. Weckbecker and W. Hummel, in *Microbial Enzymes and Biotransformations: Methods in Biotechnology*, ed. J. L. Barredo, Humana Press, 2005, vol. 17, pp. 225-237.
119. S. Fademrecht, P. N. Scheller, B. M. Nestl, B. Hauer and J. Pleiss, *Proteins*, 2016, **84**, 600-610.
120. S. Kanao and Y. Sakayori, *Yakugaku Zasshi*, 1966, **86**, 1105-1108.
121. P. Matzel, M. Gand and M. Hohne, *Green Chem.*, 2017, **19**, 385-389.
122. K. Vedha-Peters, M. Gunawardana, J. D. Rozzell and S. J. Novick, *J. Am. Chem. Soc.*, 2006, **128**, 10923-10929.
123. H. Akita, K. Doi, Y. Kawarabayasi and T. Ohshima, *Biotechnol. Lett.*, 2012, **34**, 1693-1699.
124. J. D. Cui, S. Zhang and L. M. Sun, *Appl. Biochem. Biotechnol.*, 2012, **167**, 835-844.
125. S. T. Takemura, Hiromi; Kowata, Keiko; Nakano, Keiko; Okumura, Yuichi; Li, Keikan; Inamori, Yoshihiko, *Yakugaku Zasshi*, 1978, **98**, 869-879.

8. Appendix

8.1. Buffer and solution ingredients

- Luria Bertani (LB) medium: 1% Tryptone, 1% NaCl, 0.5% yeast extract adjusted to pH 7.0 and sterilised.
- Super optimal catabolite (SOC) solution: 0.5% Yeast Extract, 2% Tryptone, 10 mM NaCl, 2.5 mM KCl, 10 mM MgCl₂, 10 mM MgSO₄, 20 mM D-Glucose.
- Qiagen QIAprep® Spin Mini-prep kit was used for DNA preparations containing:

Buffer P1: Resuspension buffer contains Tris HCl (50 mM, pH 8.0), EDTA (10 mM), RNase A (100 µg/mL).

Buffer P2: Lysis buffer contains NaOH (200 mM), SDS (1% (w/v)).

Buffer N3: Neutralisation buffer contains potassium acetate (3 M, pH 5).

Buffer PE: Wash buffer contains NaCl (1 M), MOPS (50 mM, pH 7), IPA (15% (v/v)).

Buffer EB: Elution buffer contains NaCl (1.25 M), Tris-Cl (50 mM, pH 8.5), IPA (15% (v/v)).

Efficient Biocatalytic Reductive Aminations by Extending the Imine Reductase Toolbox

Gheorghe-Doru Roiban,^{*[a]} Marcelo Kern,^[a] Zhi Liu,^[b] Julia Hyslop,^[a, c] Pei Lyn Tey,^[a] Matthew S. Levine,^[b] Lydia S. Jordan,^[b] Kristin K. Brown,^[d] Timin Hadi,^[b] Leigh Anne F. Ihnken,^[b] and Murray J. B. Brown^[a]

Chiral secondary and tertiary amines are ubiquitous in pharmaceutical, fine, and specialty chemicals, but their synthesis typically suffers from significant sustainability and selectivity challenges. Biocatalytic alternatives, such as enzyme-catalyzed reductive amination, offer several advantages over traditional chemistry, but industrial applicability has not yet been demonstrated. Herein, we report the use of cell lysates expressing imine reductases operating at 1:1 stoichiometry for a variety of amines and carbonyls. A collection of biocatalysts with diversity in coverage of small molecules and direct industrial applicability is presented.

The majority of marketed drugs either contain amine functional groups or are derived from amine intermediates, and up to 40% of active pharmaceutical ingredients (APIs) contain a chiral amine moiety.^[1] Hence, the large-scale production of secondary and tertiary amines as structural motifs that are commonly found in APIs is of great interest to the pharmaceutical industry.^[2] There are many established chemical methods for the preparation of amines, including nucleophilic alkylation; hydrogenation of imines, enamines, and enamides; enantioselective hydroamination; nucleophilic carbanion or radical addition to imino compounds; and classical Mannich and Strecker reactions. These methods tend to use precious or heavy-metal catalysts, high pressures and/or temperatures, organic solvents, stoichiometric hydride reductants, or potentially genotoxic

alkyl halides.^[2,3] Recently, biocatalytic approaches have emerged as an attractive alternative, offering more sustainable processes under ambient aqueous conditions with high chemo-, regio-, and stereoselectivity with minimal hazardous waste. Biocatalysis also offers more flexibility, as the adoption of directed evolution allows for rapid optimization of an enzyme to meet the requirements of process chemistry.^[4]

Established biocatalytic processes for the preparation of amines have focused on chiral primary amines, notably hydrolytic resolution of racemic amides, desymmetrization with amine oxidases and chemical reductants, and direct installation through transaminases.^[1] There are also emerging opportunities with amine dehydrogenases, ammonia lyases, and aminomutases, and all give access to primary amines.^[5] Direct biocatalytic routes to secondary and tertiary amines have been reported by using imine reductases (IREDs).^[6] Initially, cyclic imine reduction was reported,^[7] followed by subsequent formal intermolecular reductive amination.^[8] These activities were restricted to small primary aliphatic amines and required a large excess amount of an amine nucleophile and a high biocatalyst loading, all of which made them less attractive for industrial applications. Recently, Aleku et al. reported an IRED homologue from *Aspergillus oryzae* (AspRedAm) capable of reductive amination at 1:1 stoichiometry for a subset of amines and carbonyls by using purified protein preparations.^[9] The purified protein approach allows for activity enrichment and reduction in background carbonyl reduction from endogenous host enzymes, but it is an undesirable manufacturing strategy owing to the extra cost and complexity associated with the purification process. Maugeri and Rother reported successful reductive amination with lyophilized whole cells expressing IREDS,^[10] a good first step toward industrial application but with limited demonstrated substrate scope. Herein, we report a collection of enzymes catalyzing reductive amination at 1:1 stoichiometry, as cell lysates, with diverse coverage of small-molecule space. We view the members of this IRED panel as potential evolution starting points on the path to deliver manufacturing-relevant enzymes for industrial biocatalytic reductive amination. The panel of 85 enzymes we tested includes AspRedAm,^[9] several other known IRED sequences from the literature^[7c,e,9,11] and IRED database,^[12] and novel putative IREDS chosen on the basis of homology to known, active sequences (see Supporting Information, Table S1, Figures S1 and S2). The proteins were expressed in 96-well plate format (see Table S2 and Figure S3) and were used in screening reactions as clarified cell lysates. Initial screening instead selected IREDS with arylamines indicat-

[a] Dr. G.-D. Roiban, Dr. M. Kern, J. Hyslop, P. L. Tey, Dr. M. J. B. Brown
Advanced Manufacturing Technologies
GlaxoSmithKline
Medicines Research Centre, Gunnels Wood Road, Stevenage SG1 2NY
(United Kingdom)
E-mail: gheorghe.d.roiban@gsk.com

[b] Z. Liu, M. S. Levine, L. S. Jordan, Dr. T. Hadi, Dr. L. A. F. Ihnken
Advanced Manufacturing Technologies
GlaxoSmithKline
709 Swedeland Road, King of Prussia, Pennsylvania 19406 (USA)

[c] J. Hyslop
Department of Pure and Applied Chemistry
University of Strathclyde
Glasgow, G1 1XL (United Kingdom)

[d] Dr. K. K. Brown
Molecular Design, Computational and Modeling Sciences
GlaxoSmithKline
1250 S. Collegeville Road, Collegeville, Pennsylvania 19426 (USA)

Supporting Information and the ORCID identification number(s) for the author(s) of this article can be found under <https://doi.org/10.1002/cctc.201701379>.

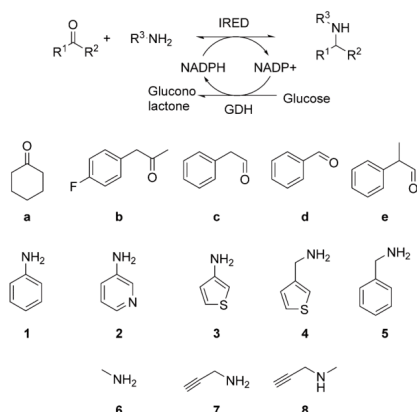
ed a pH optimum of 6–7 and a slight preference for potassium phosphate buffer (see Figure S3), in contrast to previously reported pH optima of 9–9.5 for enzymatic reductive amination with aliphatic amines.^[8b–d] Subsequent reactions were performed in 100 mM potassium phosphate pH 7 unless otherwise stated.

The reductive amination activity of each enzyme was tested across a number of carbonyl and amine pairs at 1:1 stoichiometry (Scheme 1). Results for selected enzymes are shown in Table 1 (see Supporting Information for the full data set, Table S3). High conversions (>60%) were seen for several en-

zymes for arylamines **1** and **3** with cyclohexanone (**a**) and aniline (**1**) with phenylacetaldehyde (**c**) or benzaldehyde (**d**). This represents an important extension of the substrate scope of IREDs, as arylamines have not previously been reported as good enzymatic reductive amination substrates. The compounds in Scheme 1 were chosen as model substrates, as they are representative of pharmacologically active moieties. *N*-Benzylaniline is used in the manufacture of antazoline, bepridil, and efonidipine^[13] and substituted *N*-phenethylamines have been reported as potent thrombin inhibitors.^[14]

Moderate (10–60%) to high conversions were also observed with aliphatic amines, including the formation of *N*-(thiophen-3-ylmethyl)cyclohexanamine (**4a**), the core of a potent melanin-concentrating hormone receptor antagonist^[15] and the chemical synthesis of which was reported as tedious and low yielding.^[16] Moderate conversions into amphetamine analogues **6b** and **7b** were observed after reductive amination of *p*-fluorophenylacetone (**b**) with methylamine (**6**) and propargylamine (**7**). Both IR-01 and IR-13 showed moderate conversion with *N*-methylpropargylamine (**8**) and cyclohexanone (**a**), the first report of IRED-catalyzed tertiary amine formation using equimolar reactants. No conversion was observed from any of the top-seven enzymes tested for the reaction of cyclohexanone (**a**) with an equimolar amount of isopropylamine, cyclohexylamine, *n*-propylamine, or *N*-methylpropan-1-amine.

Such levels of reductive amination upon using aqueous cell lysate, at neutral pH, and with low amine equivalents are unprecedented. Furthermore, there was <2% background carbonyl reduction to the corresponding alcohol, which indicated high IRED activity relative to endogenous host-cell ketoreductase activity, in contrast to previous reports.^[8b,10,17] Given the challenges of performing reductive aminations without a large excess amount of the amine,^[8] we were pleased to find a high



Scheme 1. Biocatalytic reductive amination. GDH = glucose dehydrogenase.

Table 1. Conversions and selectivities for chosen enzymatic reductive amination reactions.

IRED	1a ^[a]	1c ^[a]	1d ^[a,d]	1e ^[a]	2a ^[a]	3a ^[b]	4a ^[a]	5a ^[a]	6b ^[c]	7a ^[a]	7b ^[c]	8a ^[a]			
	Conv	Conv	Conv	Conv	Conv	Conv	Conv	Conv	Conv	Conv	Conv	Conv			
IR-01	93	>99	99	54	26 (-)	19	62	97	74	26	90 (+)	68	60	83 (R)	17
IR-10	99	>99	96	32	62 (+)	12	53	19	20	4	37 (+)	28	15	22 (R)	4
IR-13	96	>99	99	46	41 (-)	10	61	85	59	14	61 (+)	55	27	34 (S)	14
IR-22	56	95	89	30	56 (-)	1	60	43	12	0	(nd) ^[g]	63	0	(nd) ^[g]	7
IR-24	78	91	81	18	>99 (-)	11	48	81	54	0	(nd) ^[g]	15	0	(nd) ^[g]	<2
IR-49	64	94	88	3	(nd) ^[g]	0	36	15	<2	12	83 (+)	39	9	97 (R)	<2
IR-59	0	6	3	0	(nd) ^[g]	0	3	11	-	12	91 (+)	-	62	98 (R)	-
IR-69	0	0	2	7	(nd) ^[g]	0	13	30	-	0	(nd) ^[g]	-	47	95 (R)	-
IR-72	0	0	2	0	(nd) ^[g]	0	6	13	-	0	(nd) ^[g]	-	40	99 (R)	-
IR-75	3	0	2	0	(nd) ^[g]	0	15	82	-	4	83 (-)	-	15	99 (S)	-

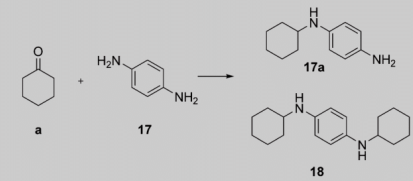
[a] % Conversion (Conv) at 4 h or [b] 1 h in 100 mM potassium phosphate pH 7 or [c] 24 h in 100 mM Tris pH 9; reaction conditions: **a–d** (32 mM), **1–8** (35 mM, 1.1 equiv.), GDH (0.31 mg mL⁻¹), glucose (63 mM), NADP⁺ (1.5 mM), 30 °C, final volume 0.4 mL; dash (-) indicates not tested. [d] Approximately 2% conversion was seen in background reaction. [e] Enantiomeric excess (ee) of first-eluting enantiomer, as determined by chiral-phase HPLC. [f] The ee reported with optical rotation sign. [g] Not determined (nd) owing to low or no conversion.

number of active enzymes (69 out of 86, 80%) giving at least 5% conversion for at least one carbonyl plus amine combination using stoichiometric reactants with unoptimized conditions (see Table S3). Further, in most cases, at least one enzyme gave >50% conversion, often with several >90%. This is indicative of the high quality of this panel of enzymes relative to that of other reported IRED collections.^[18] For the reactions presented here, IR-01 proved to be the most active enzyme in many cases. However, other screening efforts found IR-01 to be inactive, whereas other IREDs showed excellent activity, which demonstrates that a diverse collection of biocatalysts is beneficial. Furthermore, excellent and complementary enantioselectivity was demonstrated for **6b** and **7b**, providing access to both enantiomers. Reported chemical approaches to these compounds have been limited to wasteful resolutions,^[19] and recently reported IRED-catalyzed conversions required large excess amounts of amines and only provided a single enantiomer with good^[9] or moderate^[8d] enantiomeric excess (*ee*). Additionally, this panel demonstrates resolution of prochiral **e** with access to both enantiomers with moderate to excellent *ee* values.

The substrate scope of the seven best-performing enzymes producing **1a** was further investigated at lower biocatalyst loading with a series of substituted anilines and cyclohexanone (**a**) (Table 2). Both steric and electronic effects seemed to have an impact on enzyme activity. Generally, the tested IREDs were more active with *m*- and *p*-substituted anilines than with *o*-substituted anilines, and bulky *o*-substituents such as ethyl and isopropyl were not tolerated at all. Anilines with electron-donating substituents were preferred over those with electron-withdrawing groups. Though the mechanism was not explicitly investigated here, this suggests amine nucleophilicity and, therefore, imine formation at least partially contributes to the rate-determining step of the overall transformation.

The synthetic utility of these IREDs was further demonstrated by exploration of their regioselectivity. Selective monoalkylation of a symmetric diamine is chemically challenging, frequently requires the use of route-extending protecting groups, and employs catalytic nitro reduction in the case of aromatic amines.^[20] We incubated the top-seven IREDs with benzene-1,4-diamine (**17**) and either 1 or 2 equivalent(s) of cyclohexanone (**a**) and determined the monoalkylated/dialkylated product ratio (Table 3). Remarkably, IR-01 and IR-10 provided almost complete selectivity for monoalkylated product **17a**, even in the presence of 2 equivalents of cyclohexanone (**a**). Complementary preference for disubstituted product **18** was observed

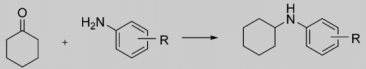
Table 3. Regioselective reductive amination.^[a]



IRED	Conversion [%] of a ^[b]	Product ratio 17a/18
IR-01	88 (97)	100:0 (99:1)
IR-10	78 (88)	99:1 (97:3)
IR-13	81 (98)	27:73 (6:94)
IR-22	32 (43)	88:12 (84:16)
IR-24	76 (89)	21:79 (10:90)
IR-49	71 (96)	94:6 (69:31)

[a] Reaction conditions were the same as those listed for Table 1, 4 h.
[b] Values shown in parentheses are for reactions run with 2 equivalents of cyclohexanone (**a**).

Table 2. Aryl amine substrate scope for enzymatic reductive amination.^[a]



1, R=H
9, R=2-OH
10, R=2-OMe
11, R=3-OMe
12, R=3-Me
13, R=4-OH
14, R=4-OMe
15, R=4-Cl
16, R=4-NO₂

1a, R=H
9a, R=2-OH
10a, R=2-OMe
11a, R=3-OMe
12a, R=3-Me
13a, R=4-OH
14a, R=4-OMe
15a, R=4-Cl
16a, R=4-NO₂

	Conversion [%]								
	1a	9a	10a	11a	12a	13a	14a	15a	16a
IR-01	36	9	4	60	65	52	70	42	<2
IR-10	20	<2	<2	49	53	59	16	<2	<2
IR-13	25	8	<2	46	52	57	68	32	<2
IR-22	4	18	<2	3	4	16	6	<2	<2
IR-24	12	<2	9	53	55	71	69	34	<2
IR-49	3	<2	<2	4	<2	39	13	<2	<2

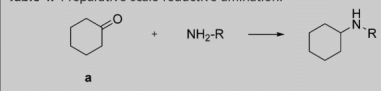
[a] Percent conversions under same reaction conditions as those listed for Table 1, 4 h.

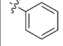
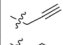
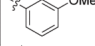
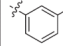
for IR-13 and IR-24, even in the presence of 1 equivalent of cyclohexanone (a).

Industrial applicability was examined with a subset of enzymes in 400 mg preparative reactions with cyclohexanone (a) plus a selection of amines (Table 4 and Chart S1). Reaction at

chemistry. With selectivity, high activity, crude preparation, low loadings, and low substrate stoichiometry demonstrated, members of this collection of enzymes exhibit all the characteristics of a potential industrial biocatalyst. These enzymes are actively in use at GlaxoSmithKline for project-direct applications.

Table 4. Preparative scale reductive amination.^[a]



R	IREd	Product	Yield ^[b] [%]
	IR-49	1 a	37
	IR-22	7 a	23
	IR-10	11 a	46
	IR-13	12 a	51

[a] Reaction conditions: ketone/aldehyde (11 mM), amine (11 mM), GDH (0.08 mg mL⁻¹ w/w), glucose (22 mM), NADP⁺ (0.5 mM), 100 mM potassium phosphate buffer pH 7, 30 °C, final volume 400 mL, 4 h. [b] Yield of product isolated after mass-directed auto purification (MDAP).

neutral pH with 1 equivalent of amine gave yields in the range of 20 to 50% from unoptimized reaction and isolation conditions, with automated purification emphasizing purity over yield. We also demonstrated successful preparative-scale reactions by using stoichiometric reactants for several other carbonyl and amine combinations (Supporting Information, Chart S1).

These results demonstrate that IREd-catalyzed reductive amination at low stoichiometric excess is far more common than previously reported. Aleku et al.^[9] described six key residues related to reductive aminase activity, and they were fully conserved in only three of the 85 IREds reported in this work. This includes the previously reported fungal enzymes AspRedAm^[9] (IR-72) and AdRedAm^[9] (IR-59) and bacterially derived IR-69 from *Streptomyces* sp. PRh5. None of these were in the top-seven performing enzymes, but they did give activity for at least one carbonyl–amine combination.

We have shown extended imine reductase (IREd) amine substrate scope to include a range of anilines and heteroaromatic amines, which were previously reported as incompatible with biocatalytic reductive amination.^[9] Importantly, these results were obtained with cell lysates without significant side reactions, which allowed for economical scale-up. Recently reported work with whole cells expressing IREds also has large-scale potential, but the biocatalyst loading was approximately 10–30 times higher than that in this study and appreciable ketone reduction was observed.^[10] Finally, we demonstrated that this panel of enzymes could perform regio- and stereoselective transformations in an efficient manner, even at low amine stoi-

Acknowledgements

This research was supported by the Innovative Medicines Initiative (IMI) joint undertaking project CHEM21 under grant agreement no. 115360, resources of which are composed of financial contributions from the European Union's Seventh Framework Programme (FP7/2007–2013) and EFPIA companies in kind contribution.

Conflict of interest

The authors declare no conflict of interest.

Keywords: amination · amines · asymmetric synthesis · biocatalysis · enzymes

- [1] D. Ghislieri, N. J. Turner, *Top. Catal.* **2014**, *57*, 284–300.
- [2] *Chiral Amine Synthesis: Methods, Developments and Applications* (Ed. T. C. Nugent), Wiley-VCH, Weinheim, **2010**.
- [3] a) *Amines: synthesis, properties and applications*, (S. A. Lawrence), Cambridge University Press, Cambridge, **2004**; b) *Stereoselective Formation of Amines, Vol. 343*, (Eds.: W. Li, X. Zhang) Springer, Berlin, **2014**.
- [4] a) J.-M. Choi, S.-S. Han, H.-S. Kim, *Biotechnol. Adv.* **2015**, *33*, 1443–1454; b) G. W. Huisman, S. J. Collier, *Curr. Opin. Chem. Biol.* **2013**, *17*, 284–292; c) R. Martinez, U. Schwaneberg, *Biol. Res.* **2013**, *46*, 395–405; d) N. J. Turner, *Catal. Sci. Technol.* **2012**, *2*, 1523.
- [5] a) M. J. Abrahamson, E. Vázquez-Figueroa, N. B. Woodall, J. C. Moore, A. S. Bommaris, *Angew. Chem. Int. Ed.* **2012**, *51*, 3969–3972; *Angew. Chem.* **2012**, *124*, 4036–4040; b) M. M. Heberling, B. Wu, S. Bartsch, D. B. Janssen, *Curr. Opin. Chem. Biol.* **2013**, *17*, 250–260.
- [6] a) J. H. Schrittwieser, S. Vellikogge, W. Krouitl, *Adv. Synth. Catal.* **2015**, *357*, 1655–1685; b) G. Grogan, N. J. Turner, *Chem. Eur. J.* **2016**, *22*, 1900–1907.
- [7] a) K. Mitsukura, M. Suzuki, K. Tada, T. Yoshida, T. Nagasawa, *Org. Biomol. Chem.* **2010**, *8*, 4533–4535; b) K. Mitsukura, M. Suzuki, S. Shinoda, T. Kuramoto, T. Yoshida, T. Nagasawa, *Biosci. Biotechnol. Biochem.* **2011**, *75*, 1778–1782; c) M. Rodríguez-Mata, A. Frank, E. Wells, F. Leipold, N. J. Turner, S. Hart, J. P. Turkenburg, G. Grogan, *ChemBioChem* **2013**, *14*, 1372–1379; d) M. Gand, H. Müller, R. Wardenga, M. Höhne, *J. Mol. Catal. B* **2014**, *110*, 126–132; e) P. N. Scheller, S. Fademrecht, S. Hofelzer, J. Pleiss, F. Leipold, N. J. Turner, B. M. Nestl, B. Hauer, *ChemBioChem* **2014**, *15*, 2201–2204.
- [8] a) T. Huber, L. Schneider, A. Präg, S. Gerhardt, O. Einsle, M. Müller, *ChemCatChem* **2014**, *6*, 2248–2252; b) P. N. Scheller, M. Lenz, S. C. Hammer, B. Hauer, B. M. Nestl, *ChemCatChem* **2015**, *7*, 3239–3242; c) D. Wetzl, M. Gand, A. Ross, H. Müller, P. Matzel, S. P. Hanlon, M. Müller, B. Wirz, M. Höhne, H. Iding, *ChemCatChem* **2016**, *8*, 2023–2026; d) P. Matzel, M. Gand, M. Höhne, *Green Chem.* **2017**, *19*, 385–389.
- [9] G. A. Aleku, S. P. France, H. Man, J. Mangas-Sanchez, S. L. Montgomery, M. Sharma, F. Leipold, S. Hussain, G. Grogan, N. J. Turner, *Nat. Chem.* **2017**, *9*, 961–969.
- [10] Z. Maugeri, D. Rother, *J. Biotechnol.* **2017**, *258*, 167–170.
- [11] a) S. Hussain, F. Leipold, H. Man, E. Wells, S. P. France, K. R. Mulholland, G. Grogan, N. J. Turner, *ChemCatChem* **2015**, *7*, 579–583; b) G. A. Aleku, H. Man, S. P. France, F. Leipold, S. Hussain, L. Toca-Gonzalez, R. Marchington, S. Hart, J. P. Turkenburg, G. Grogan, N. J. Turner, *ACS Catal.* **2016**, *6*, 3880–3889.

- [12] S. Fademrecht, P. N. Scheller, B. M. Nestl, B. Hauer, J. Pleiss, *Proteins Struct. Funct. Bioinf.* **2016**, *84*, 600–610.
- [13] a) M. Sittig, *Pharmaceutical Manufacturing Encyclopedia*, William Andrew Pub., **2015**; b) I. Agranat, *Synthesis* **2009**, 2116.
- [14] K. D. Kreutter, T. Lu, L. Lee, E. C. Giardino, S. Patel, H. Huang, G. Xu, M. Fitzgerald, B. J. Haertlein, V. Mohan, *Bioorg. Med. Chem. Lett.* **2008**, *18*, 2865–2870.
- [15] F. Giordanetto, O. Karlsson, J. Lindberg, L.-O. Larsson, A. Linusson, E. Evertsson, D. G. Morgan, T. Inghardt, *Bioorg. Med. Chem. Lett.* **2007**, *17*, 4232–4241.
- [16] N. Fleury-Brégeot, J. Rauschel, D. L. Sandrock, S. D. Dreher, G. A. Molander, *Chem. Eur. J.* **2012**, *18*, 9564–9570.
- [17] P. N. Scheller, B. M. Nestl, *Appl. Microbiol. Biotechnol.* **2016**, *100*, 10509–10520.
- [18] a) D. Wetzl, M. Berrera, N. Sandon, D. Fishlock, M. Ebeling, M. Muller, S. Hanlon, B. Wirz, H. Iding, *ChemBioChem* **2015**, *16*, 1749–1756; b) H. Li, Z.-J. Luan, G.-W. Zheng, J.-H. Xu, *Adv. Synth. Catal.* **2015**, *357*, 1692–1696.
- [19] a) Z. Nad, T. Kallay, M. Sziladi, T. Montay, (Chinoin Gyogyszer- Es Vegyeszeti Termek Gyara Rt., Hungary), US Patent 5449828A, **1995**; b) A. Plenevaux, S. L. Dewey, J. S. Fowler, M. Guillaume, A. P. Wolf, *J. Med. Chem.* **1990**, *33*, 2015–2019.
- [20] P. G. Wuts, T. W. Greene, *Greene's protective groups in organic synthesis*, Wiley, Hoboken, New Jersey, **2006**.

Manuscript received: August 24, 2017

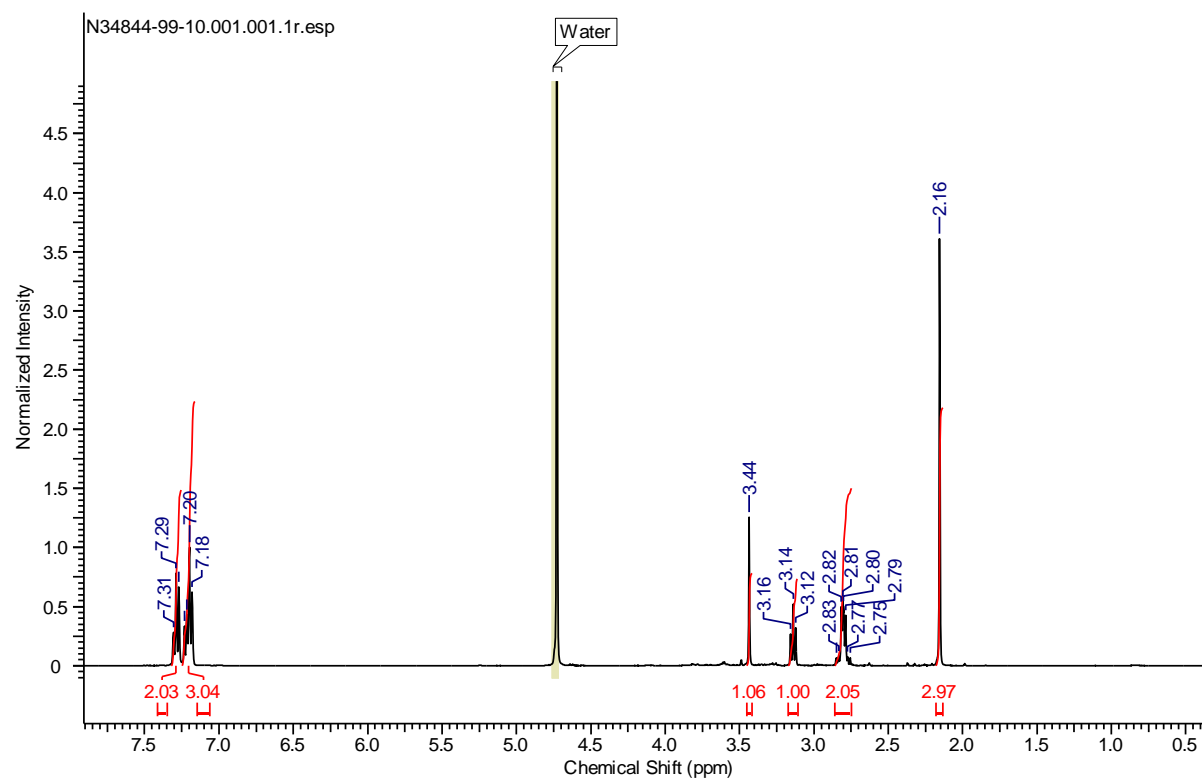
Accepted manuscript online: August 28, 2017

Version of record online: November 30, 2017

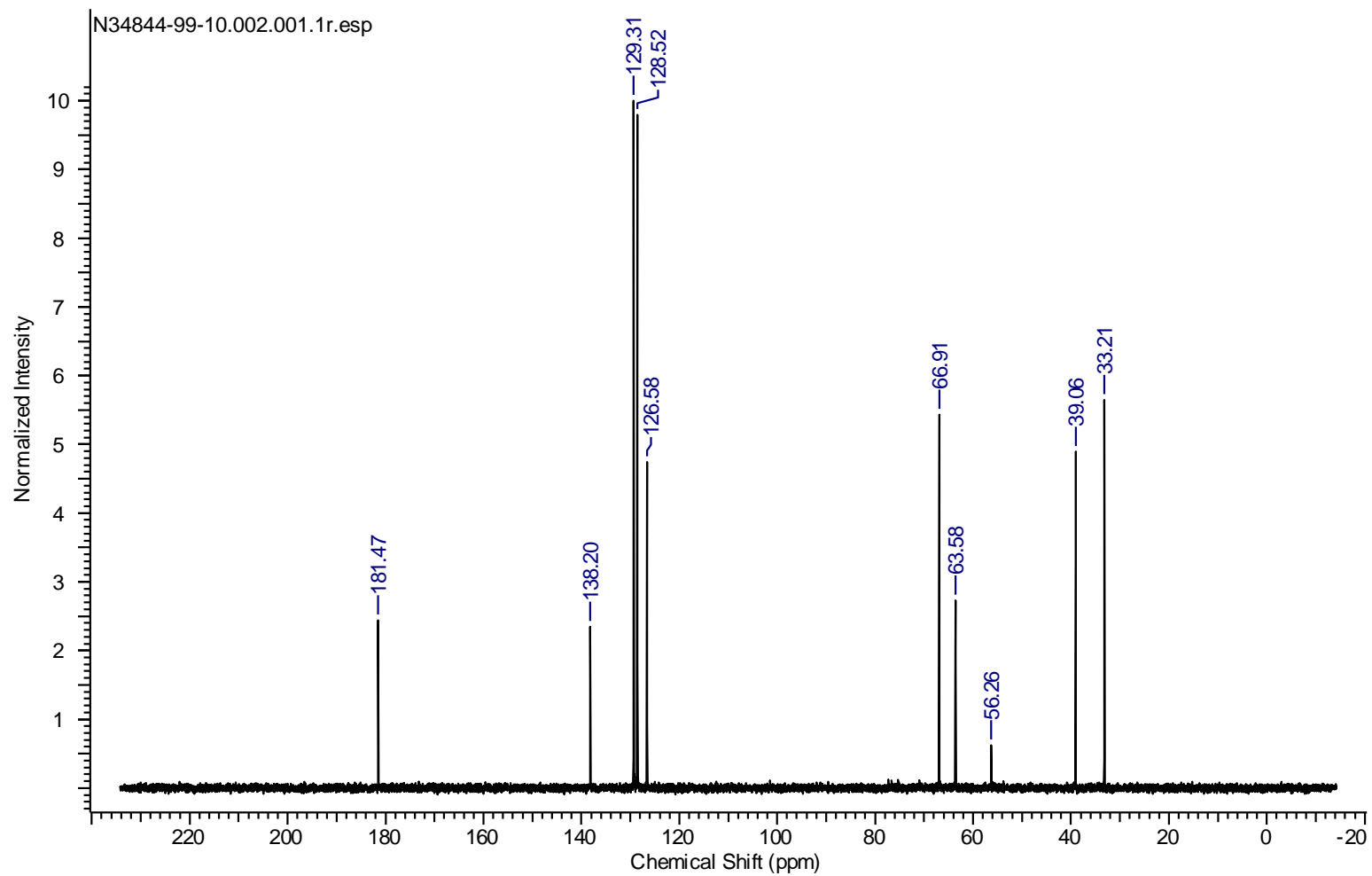
8.2. Experimental data

2-(Methylamino)-3-phenylpropanoic acid (**78**)

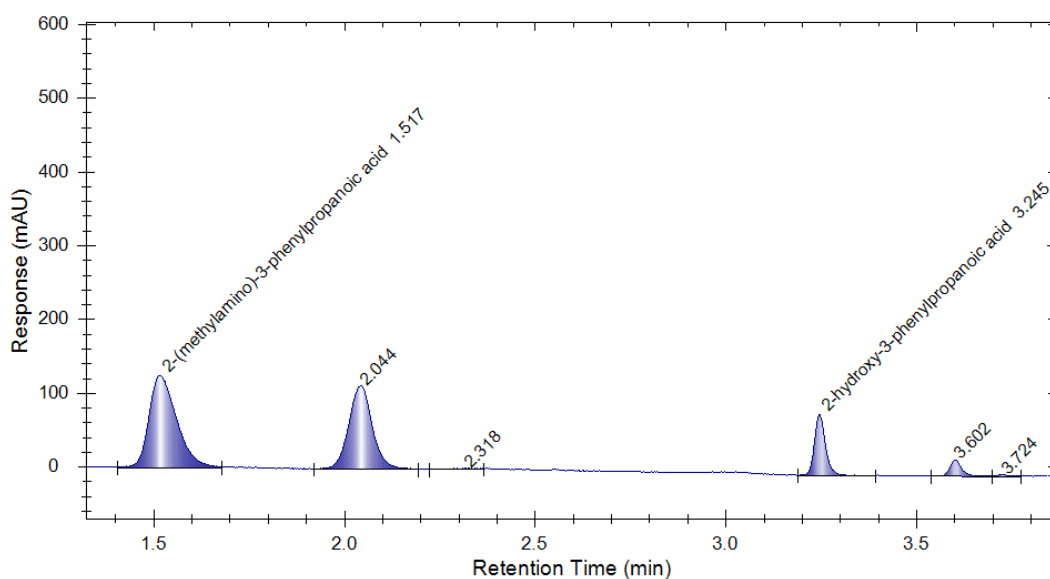
¹H-NMR spectrum of **78** generated from scale-up of reaction of keto acid **122** with amine **76** catalysed by En01.



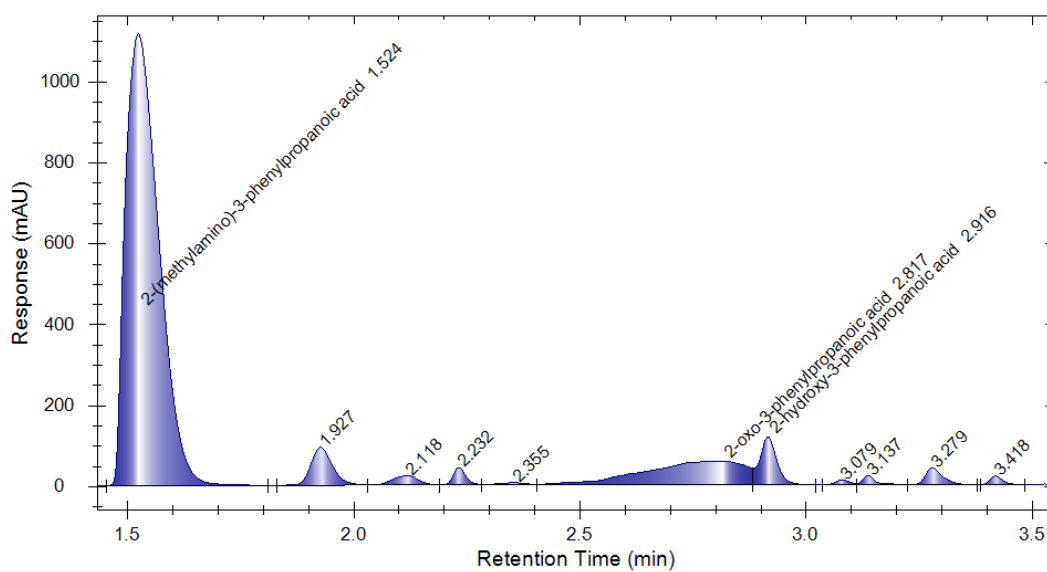
¹³C-NMR spectrum of 78 generated from scale-up of reaction of keto acid 122 with amine 76 catalysed by En01.



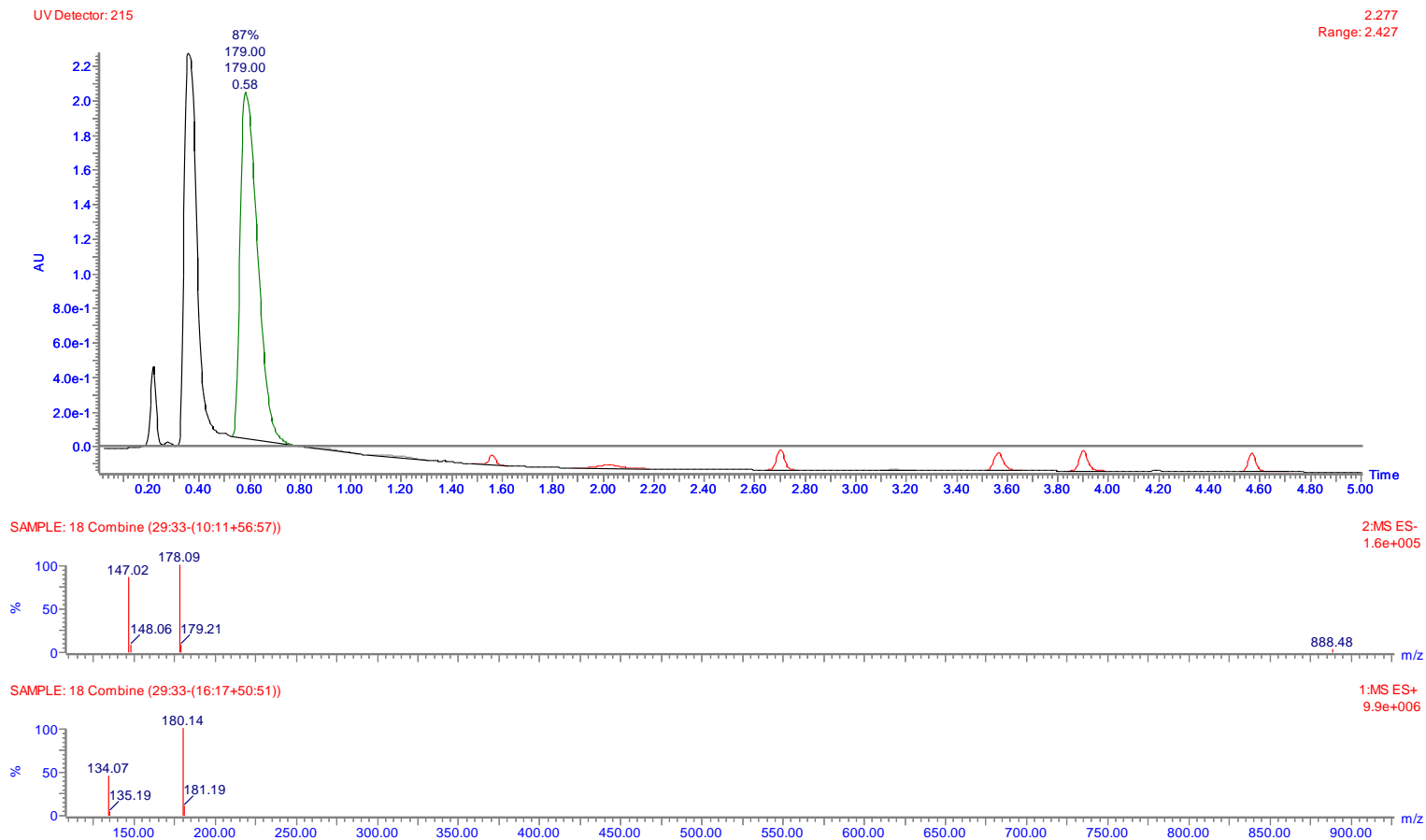
Achiral HPLC chromatogram of 78 generated from small scale reaction of keto acid 122 with amine 76 catalysed by En01 using Method 1.



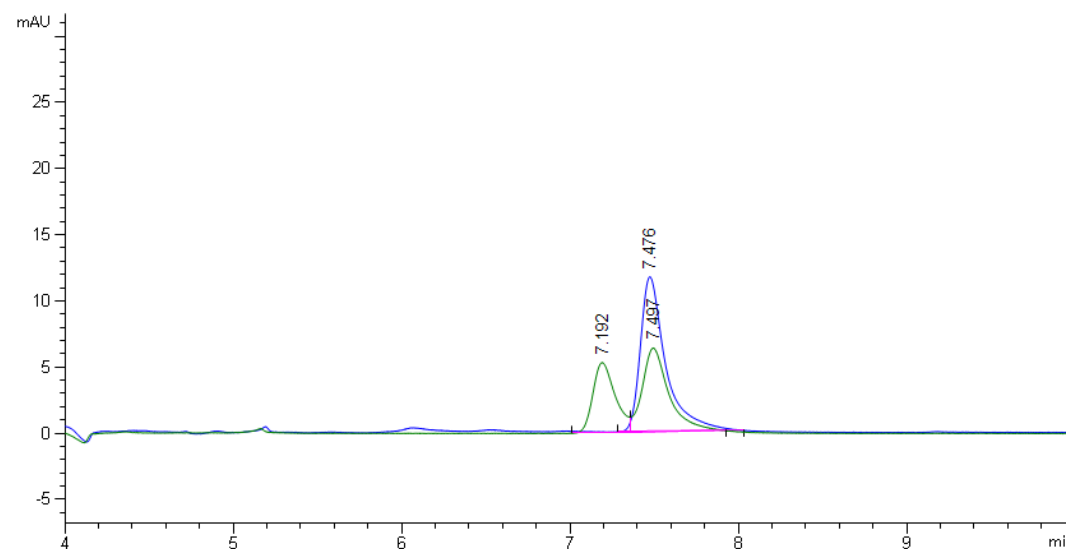
Achiral HPLC chromatogram of 78 generated from scale-up of reaction of keto acid 122 with amine 76 catalysed by En01 using Method 1.



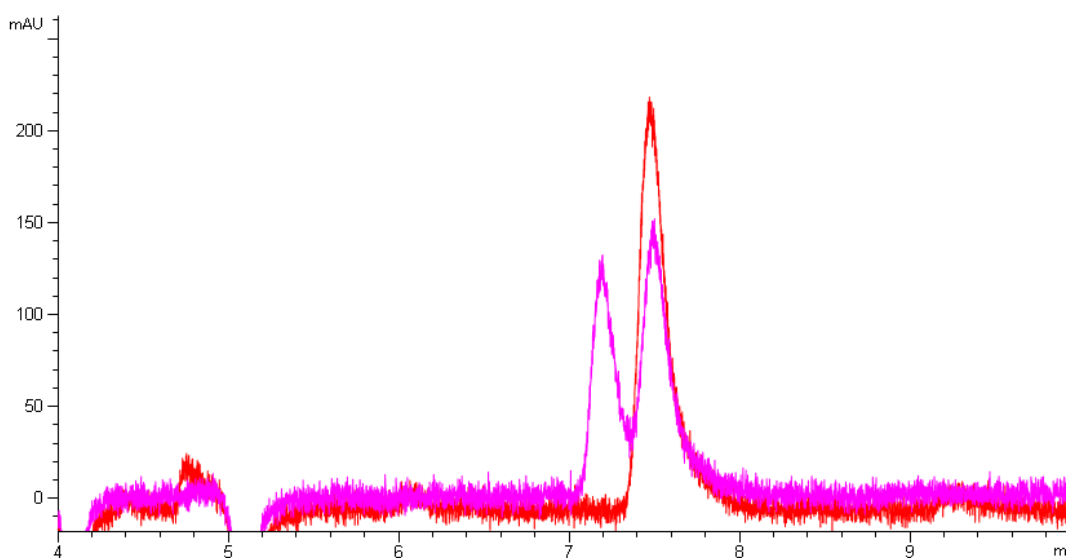
Achiral LCMS of 78 generated from scale-up of reaction of keto acid 122 with amine 76 catalysed by En01 using Method 4.



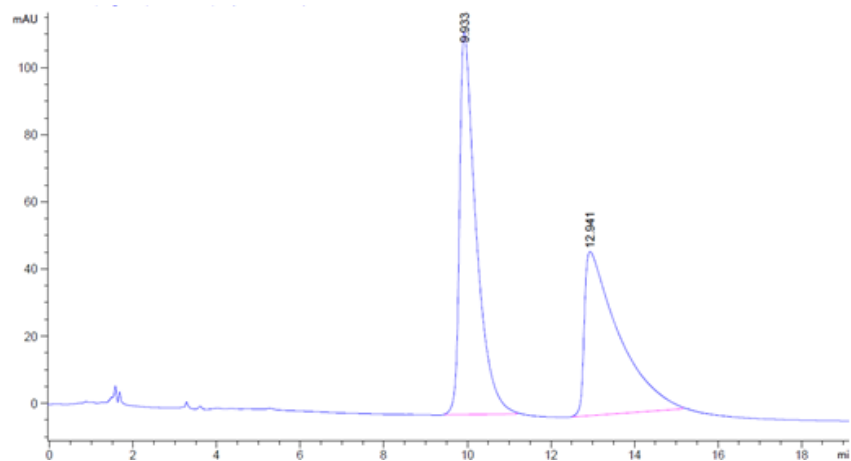
Chiral UPLC of 78 from the reaction of 122 and 76 catalysed by En02, overlaid with racemic 78 using Method 3-258 nm



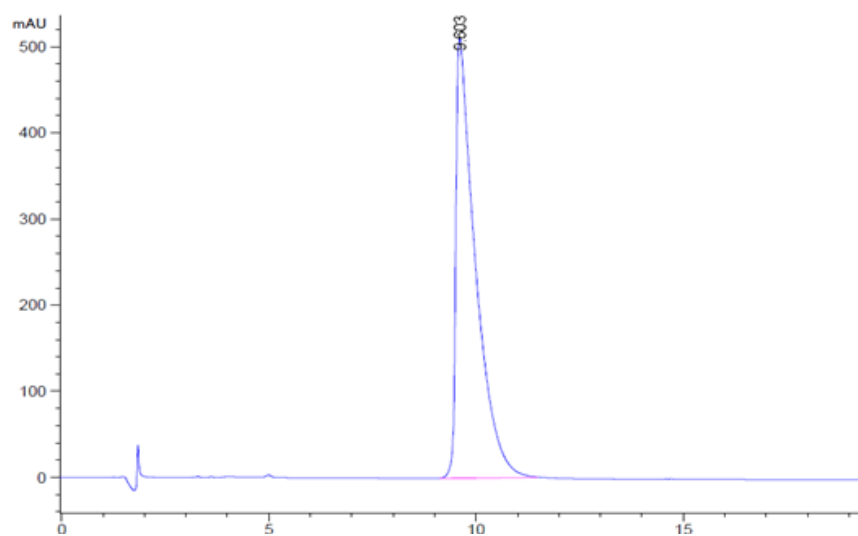
Chiral UPLC of 78 from the reaction of 122 and 76 catalysed by En02, overlaid with racemic 78 using Method 3-210 nm



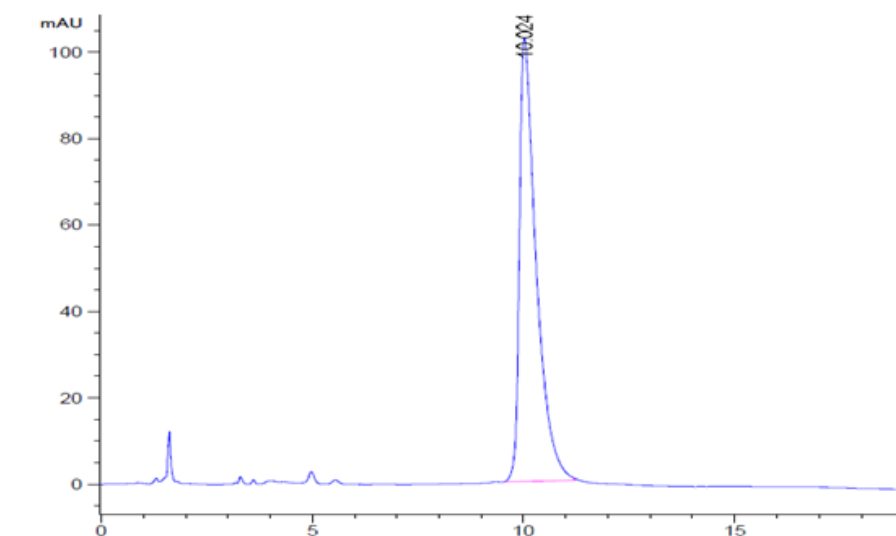
Chiral UPLC of racemic 78 using Method 2



Chiral UPLC of authentic L-enantiomer 78 using Method 2

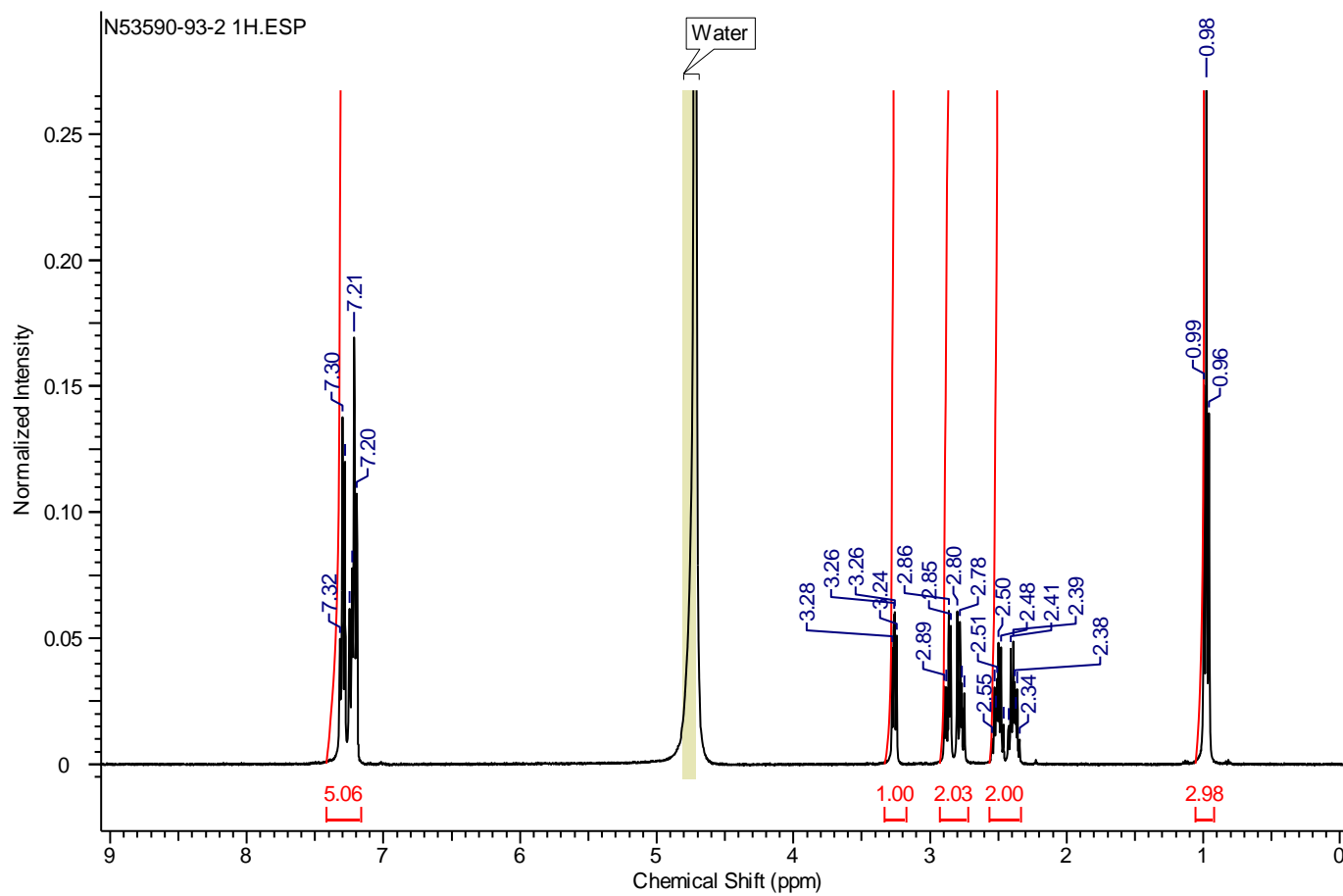


Chiral UPLC of 78 resulting from a biocatalytic reaction between keto acid 122 and amine 76 catalysed by En01 using Method 2.

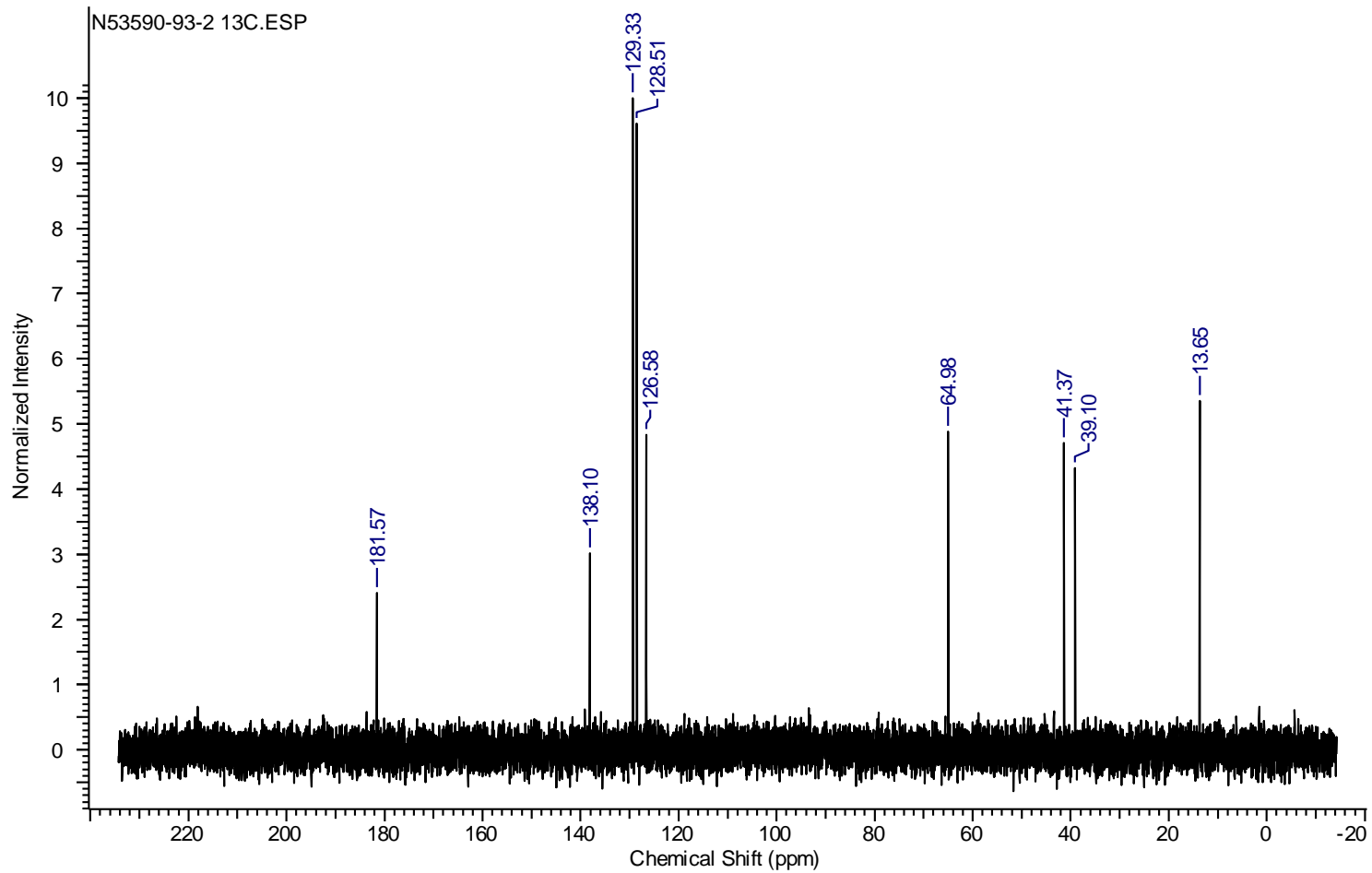


2-(Ethylamino)-3-phenylpropanoic acid 139

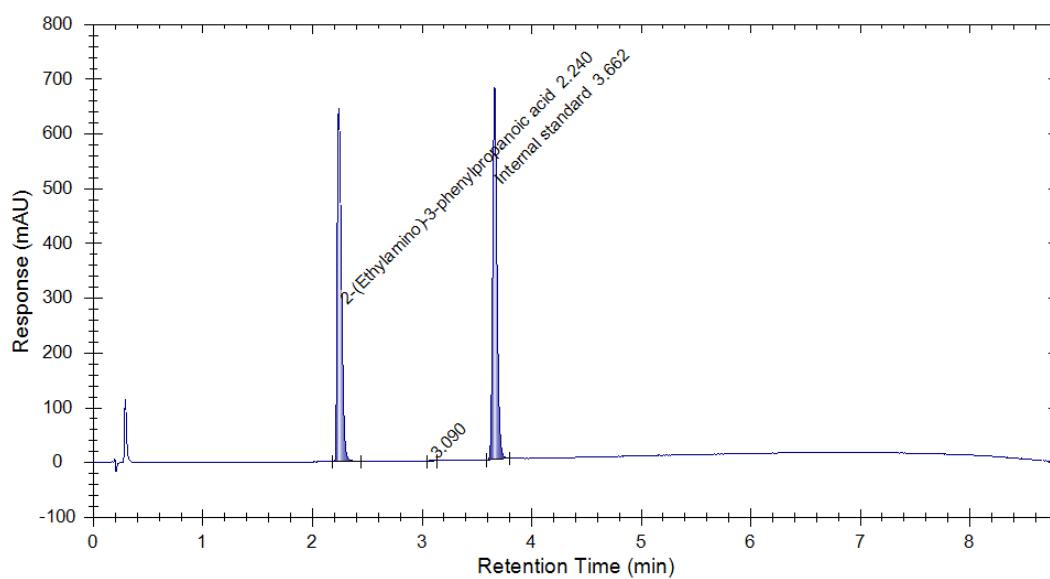
¹H-NMR spectrum of 139 from reductive amination of 122 with 124 and sodium borohydride



¹³C-NMR spectrum of 139 from reductive amination of 122 with 124 and sodium borohydride



Achiral HPLC chromatogram of racemic 139 from reductive amination of 122 with 124 and sodium borohydride using Method 1



Achiral LCMS of 139 from reductive amination of 122 with 124 and sodium borohydride using Method 4

SAMPLE: 1:19 Combine (949)

3:UV Detector
1.861 AU



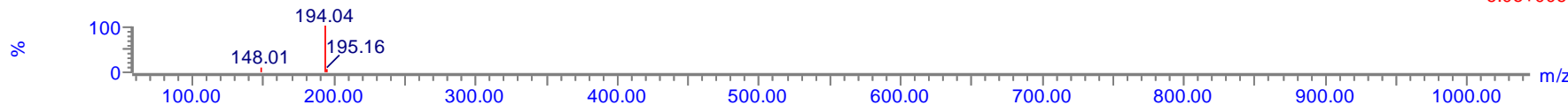
SAMPLE: 1:19 Combine (101:114-(74:77+139:141))

2:MS ES-
2.3e+004



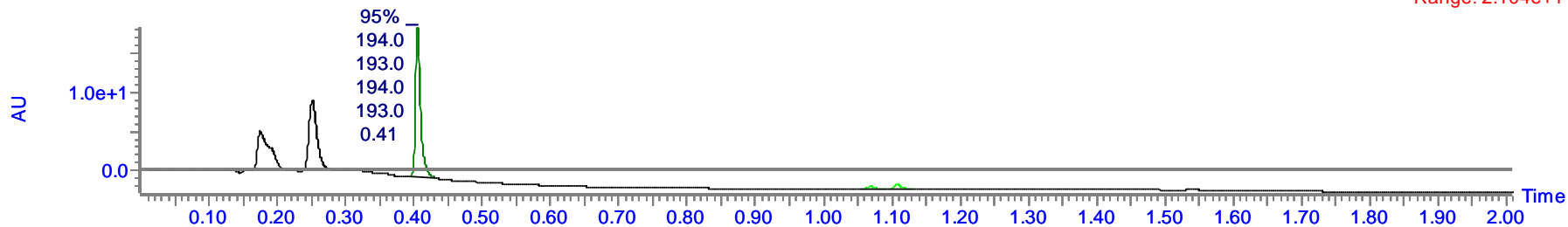
SAMPLE: 1:19 Combine (102:115-(72:75+149:152))

1:MS ES+
6.0e+006

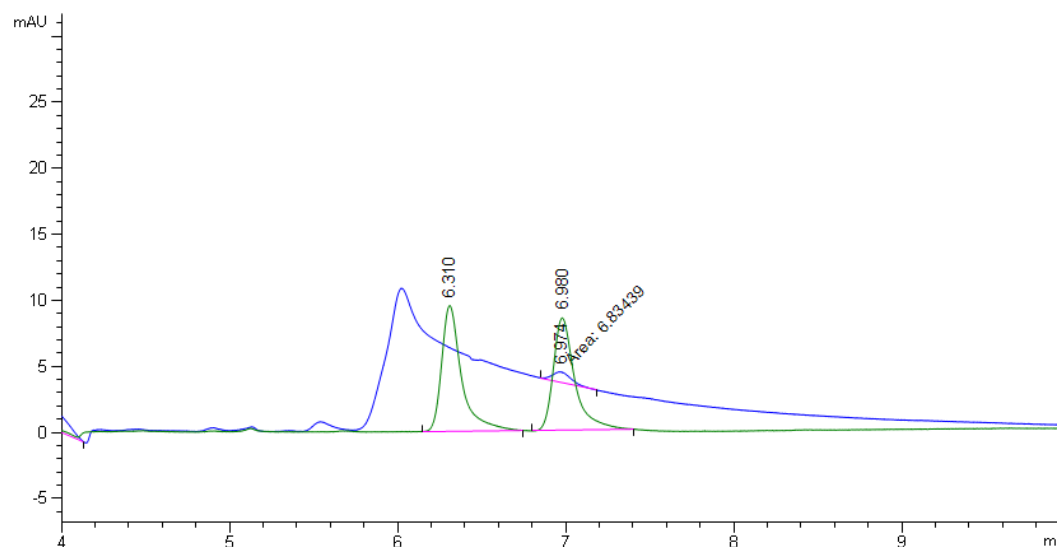


UV Detector: TIC

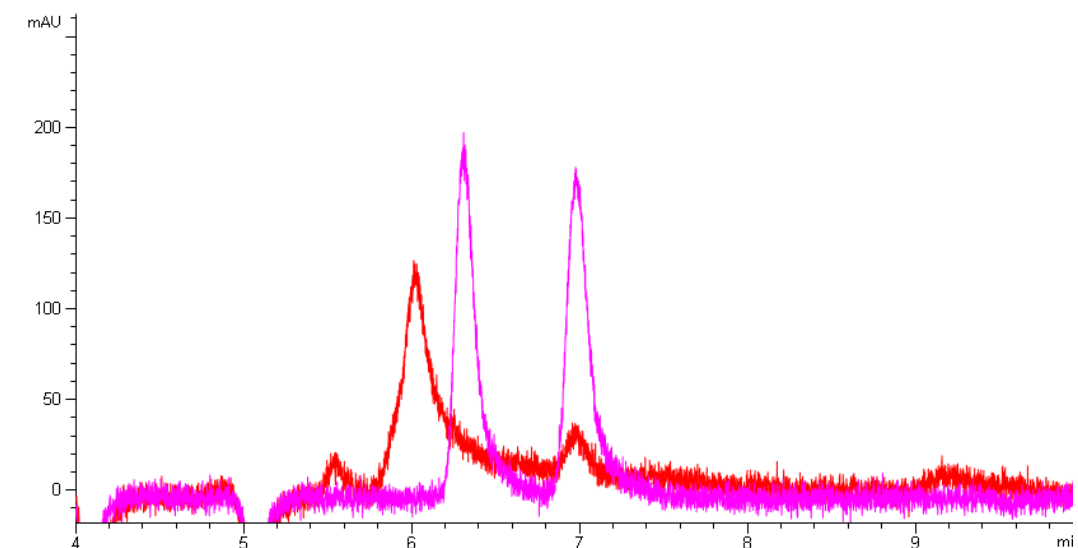
1.827e+1
Range: 2.104e+1



Chiral UPLC of 139 from the reaction of 122 and 124 catalysed by En01, overlaid with racemic 139 using Method 3-258 nm

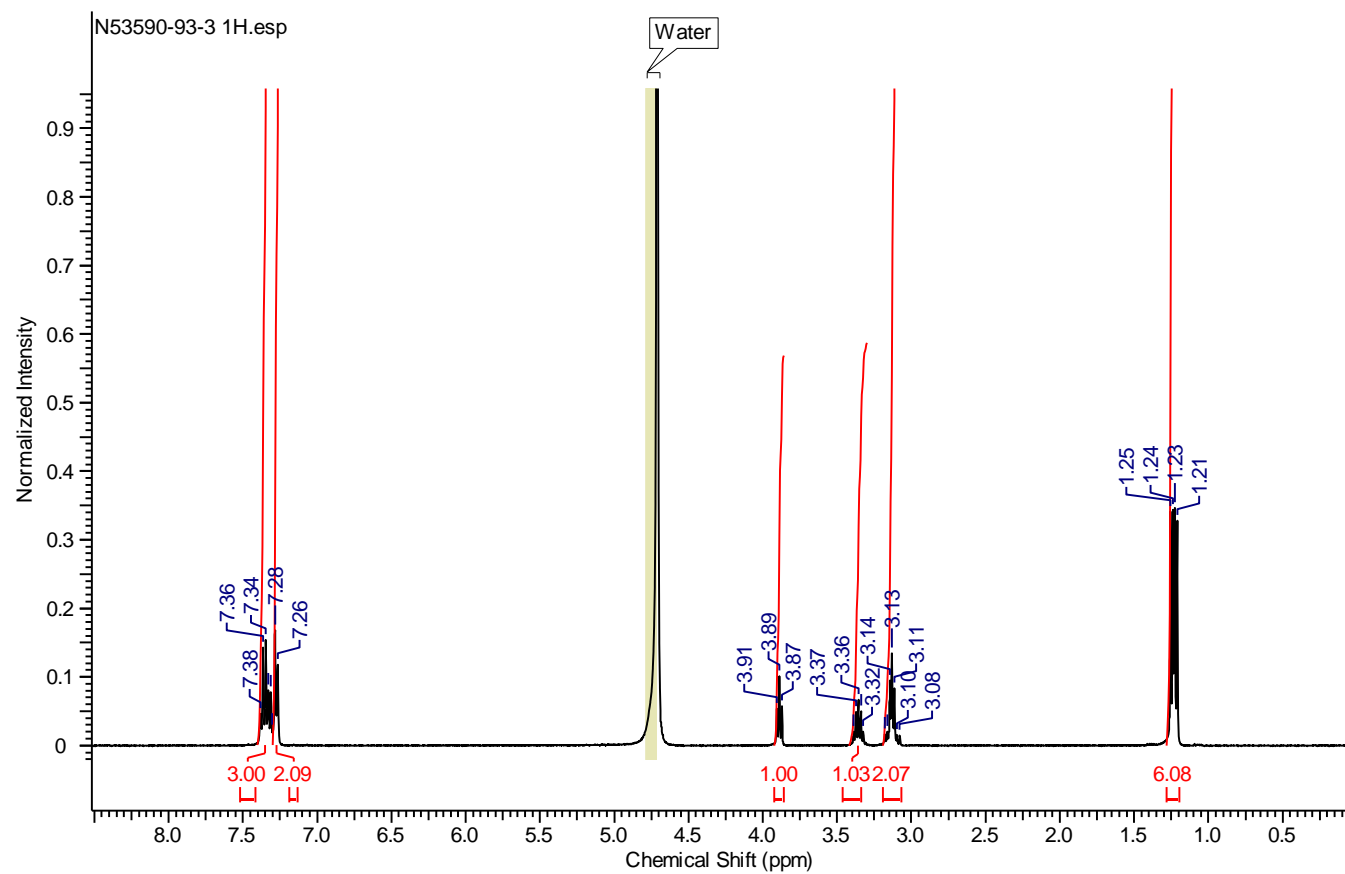


Chiral UPLC of 139 from the reaction of 122 and 124 catalysed by En01, overlaid with racemic 139 using Method 3-210 nm

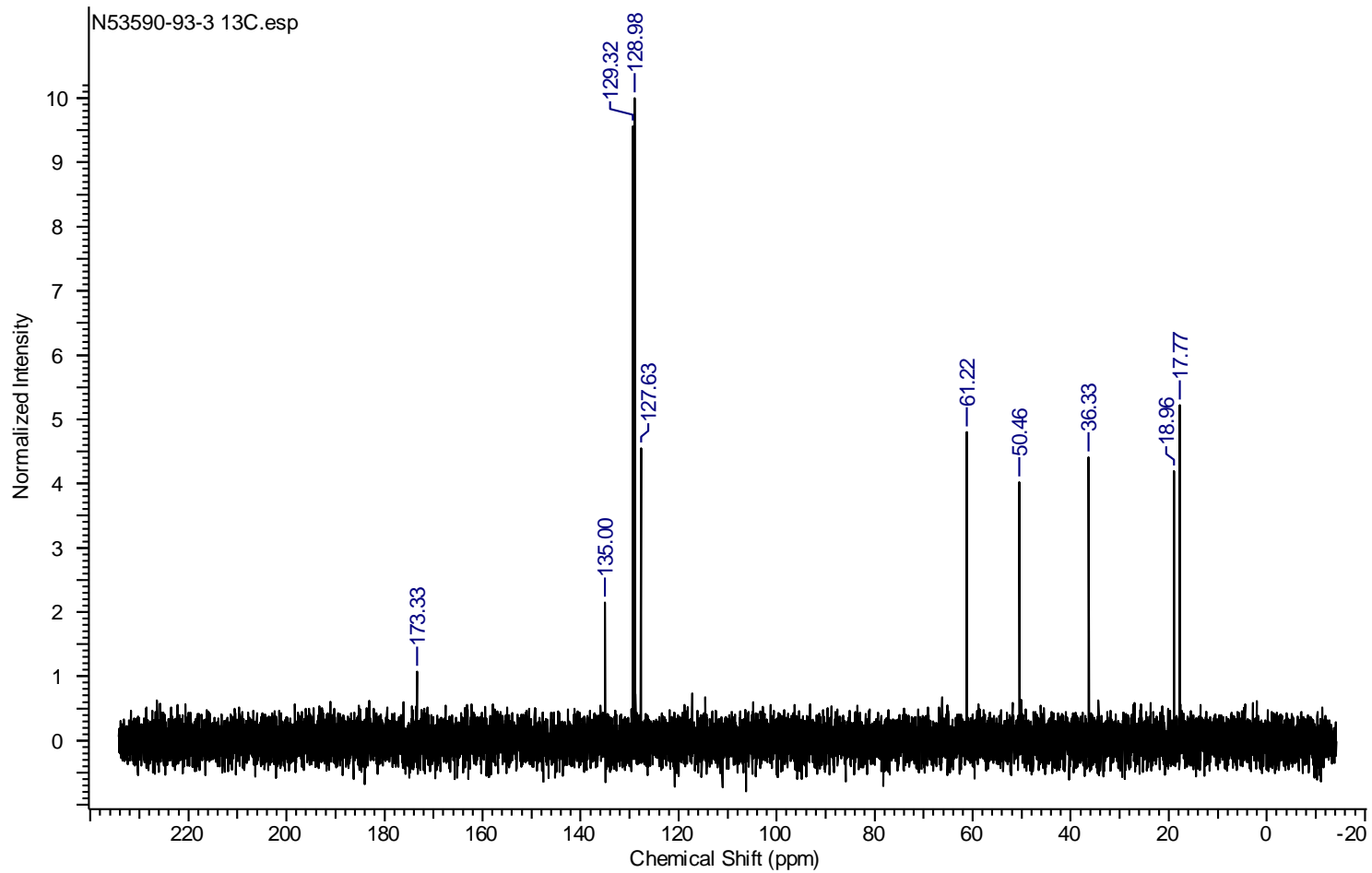


2-(Isopropylamino)-3-phenylpropanoic acid 141

¹H-NMR spectrum of 141 from reductive amination of 122 with 140 and sodium borohydride

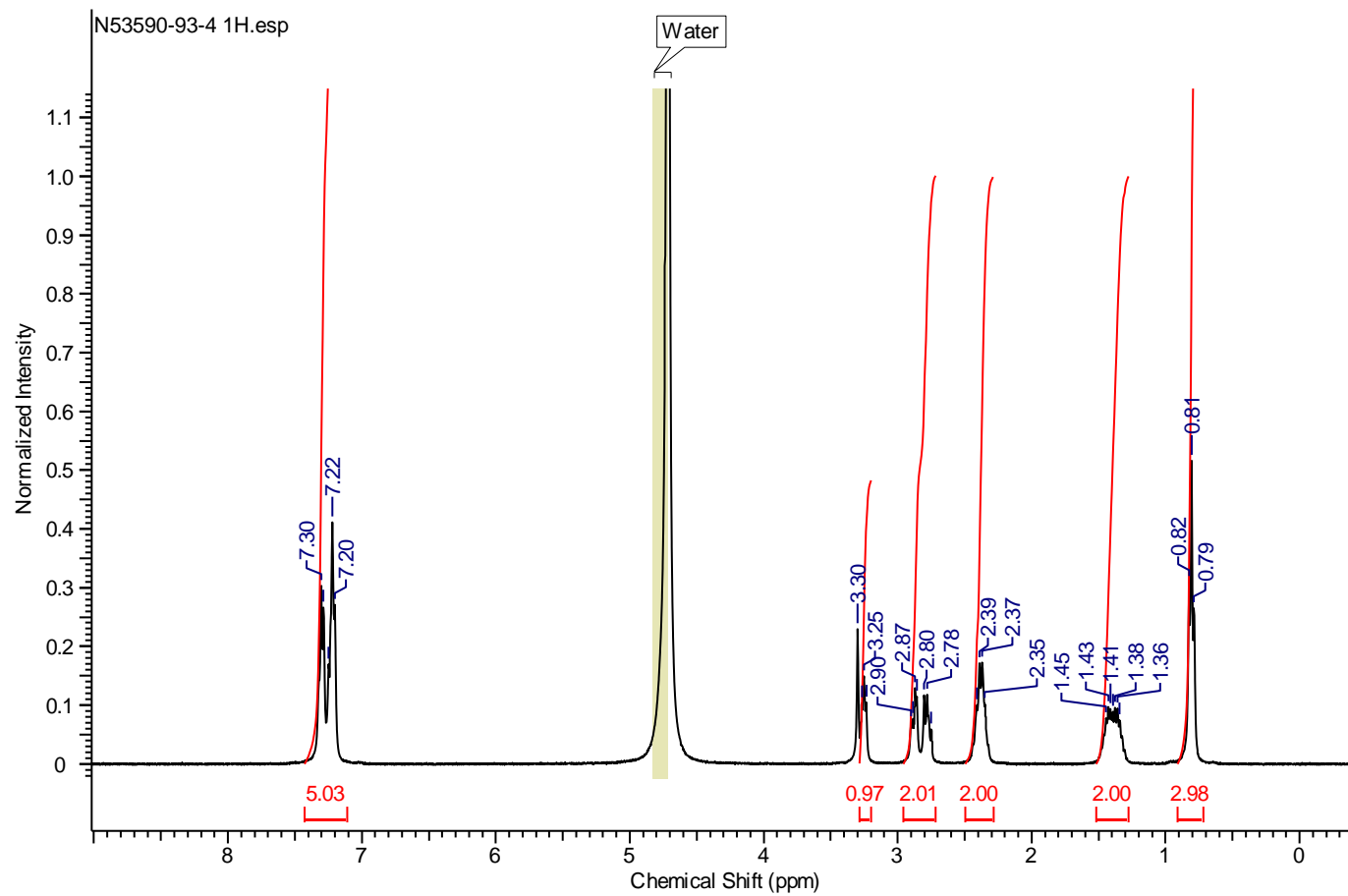


¹³C-NMR spectrum of 141 from reductive amination of 122 with 140 and sodium borohydride

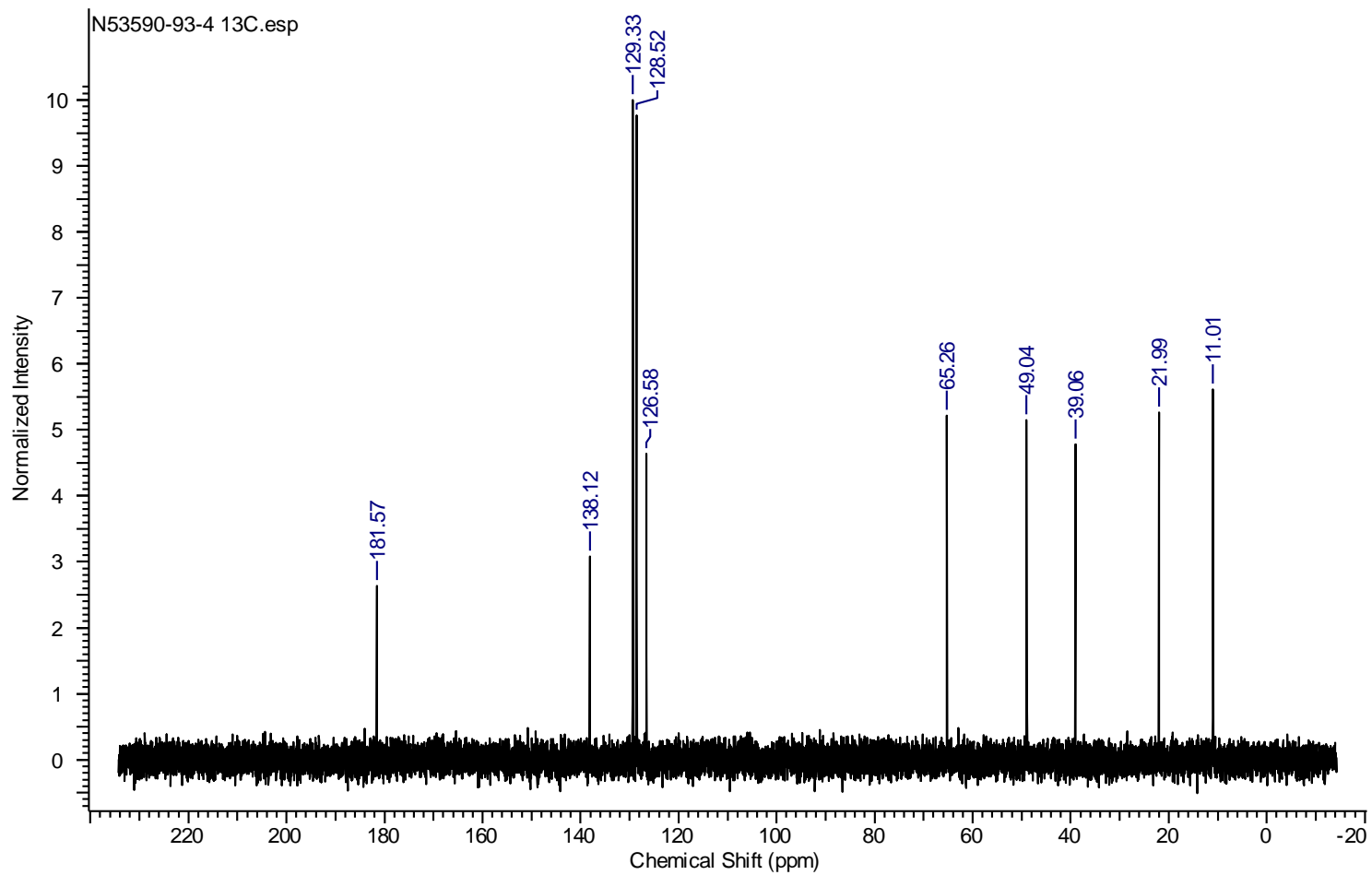


3-Phenyl-2-(propylamino)propanoic acid 143

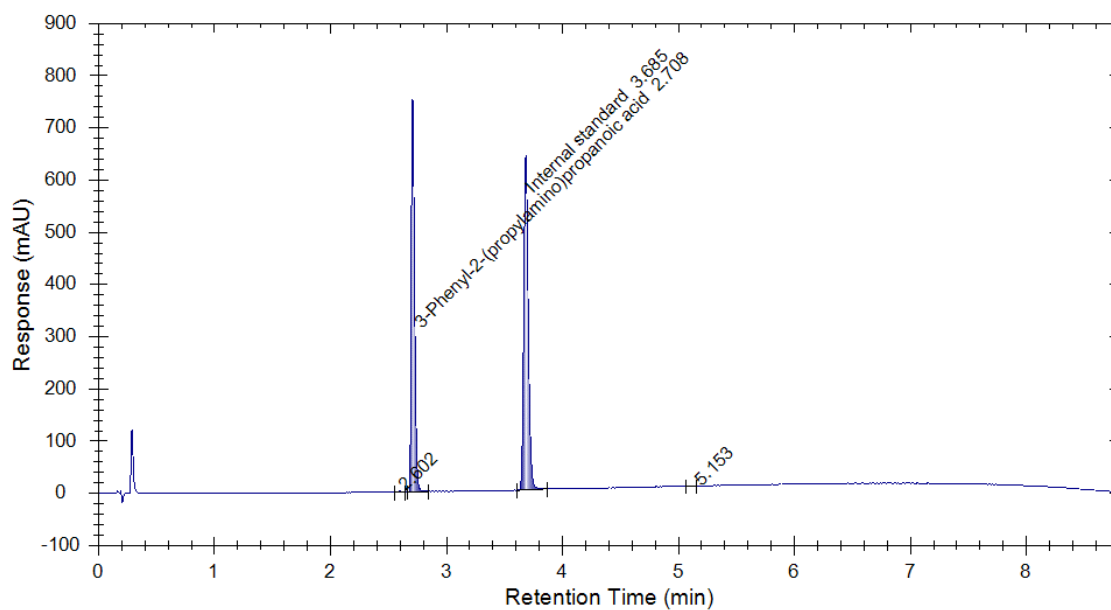
¹H-NMR spectrum of 143 from reductive amination of 122 with 142 and sodium borohydride



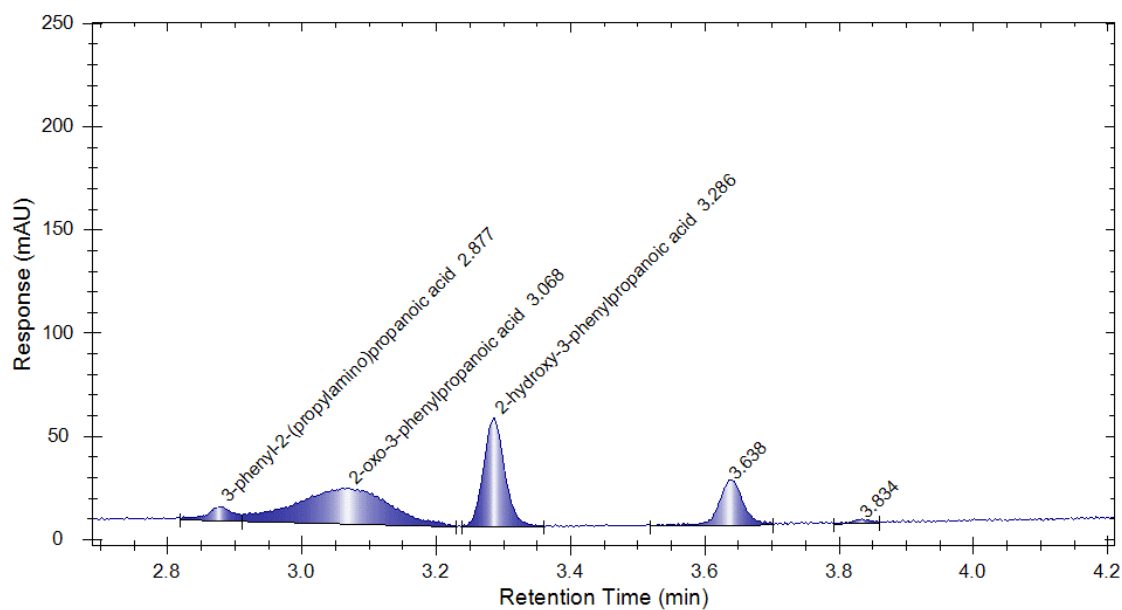
¹³C-NMR spectrum of 143 from reductive amination of 122 with 142 and sodium borohydride



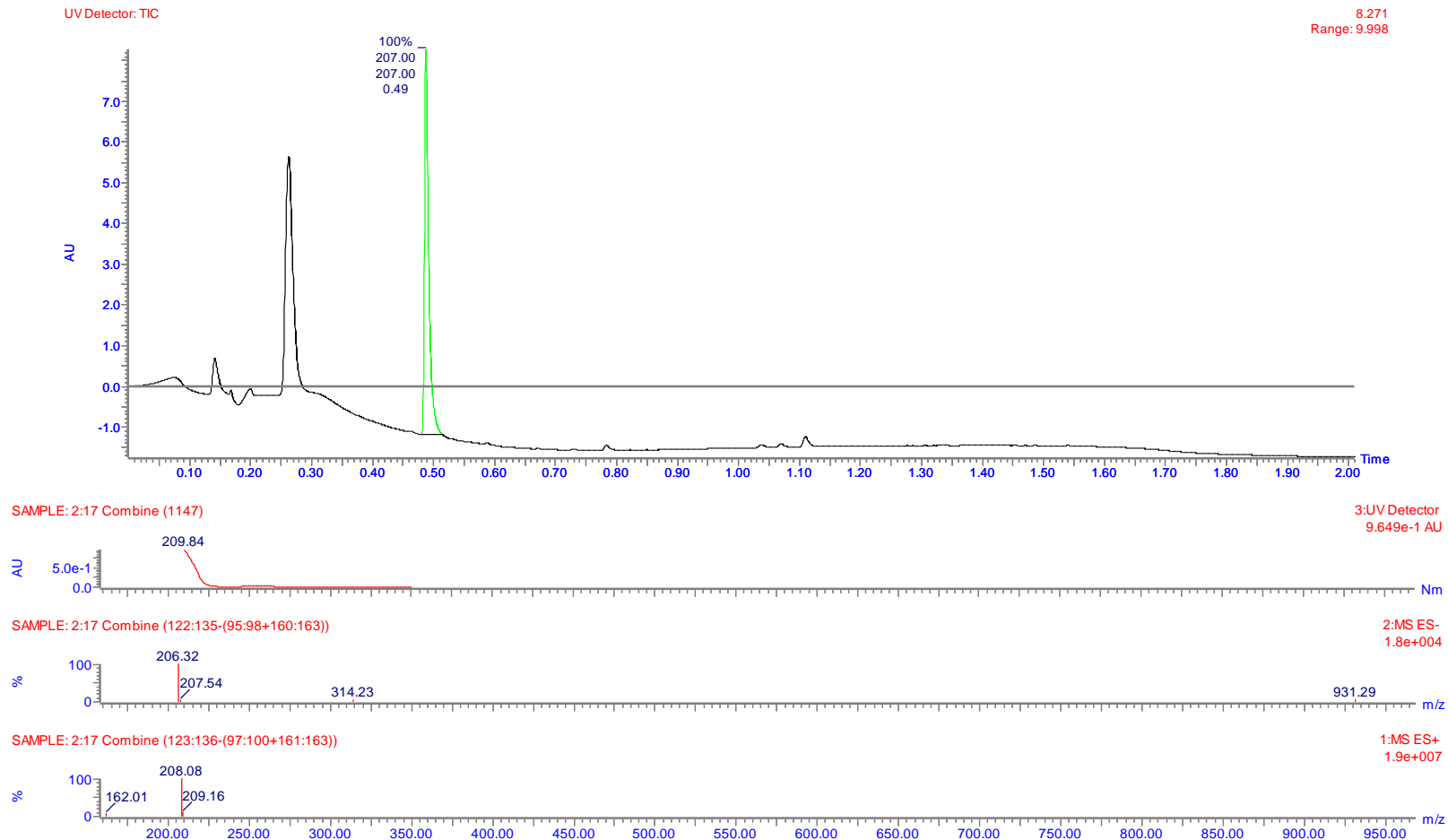
Achiral HPLC chromatogram of 143 from reductive amination of 122 with 142 and sodium borohydride using Method 1



Achiral HPLC of 143 resulting from a biocatalytic reaction between keto acid 122 and amine 142 catalysed by En05 using Method 1.

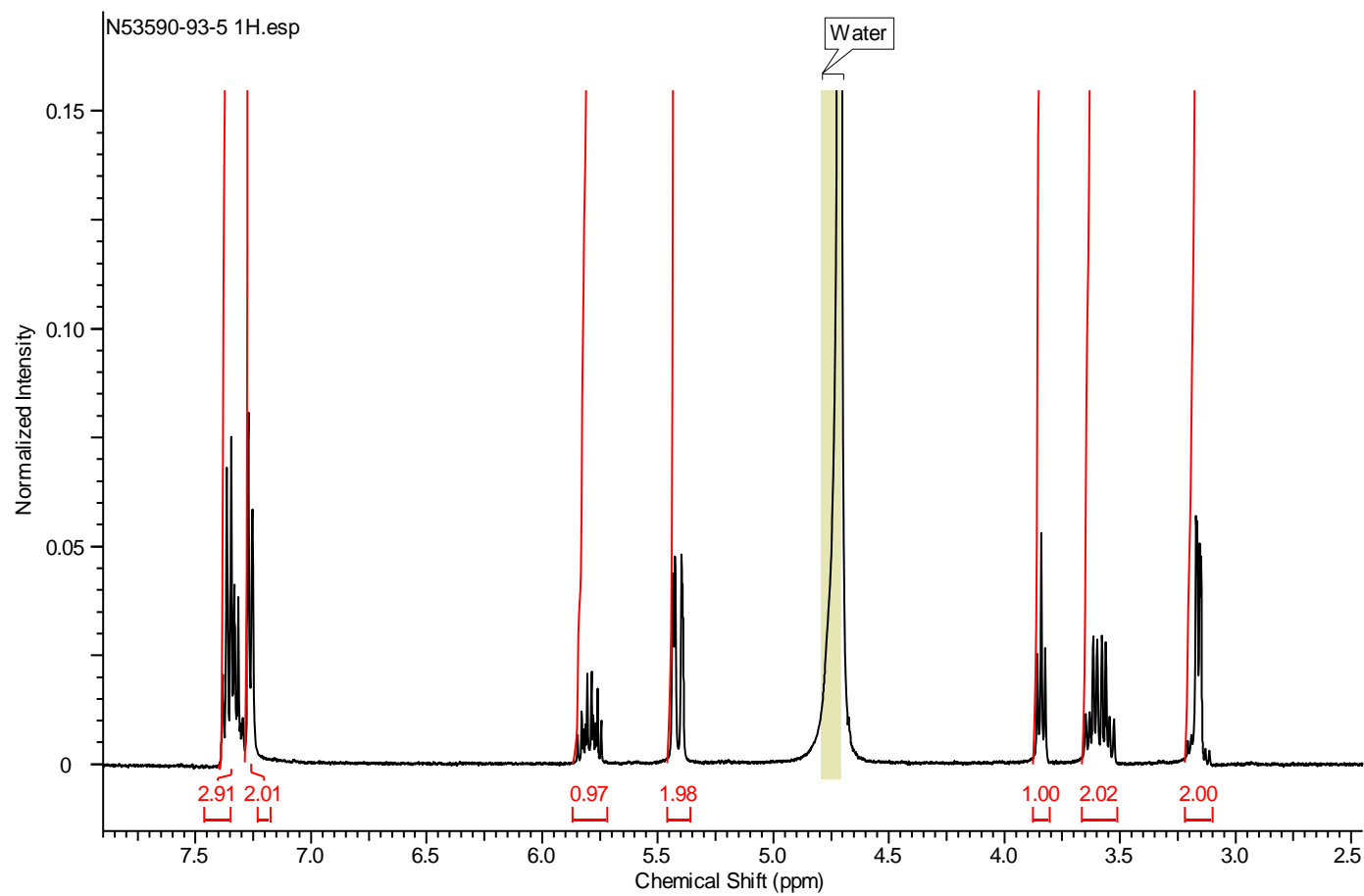


Achiral LCMS of 143 from reductive amination of 122 with 142 and sodium borohydride using Method 5

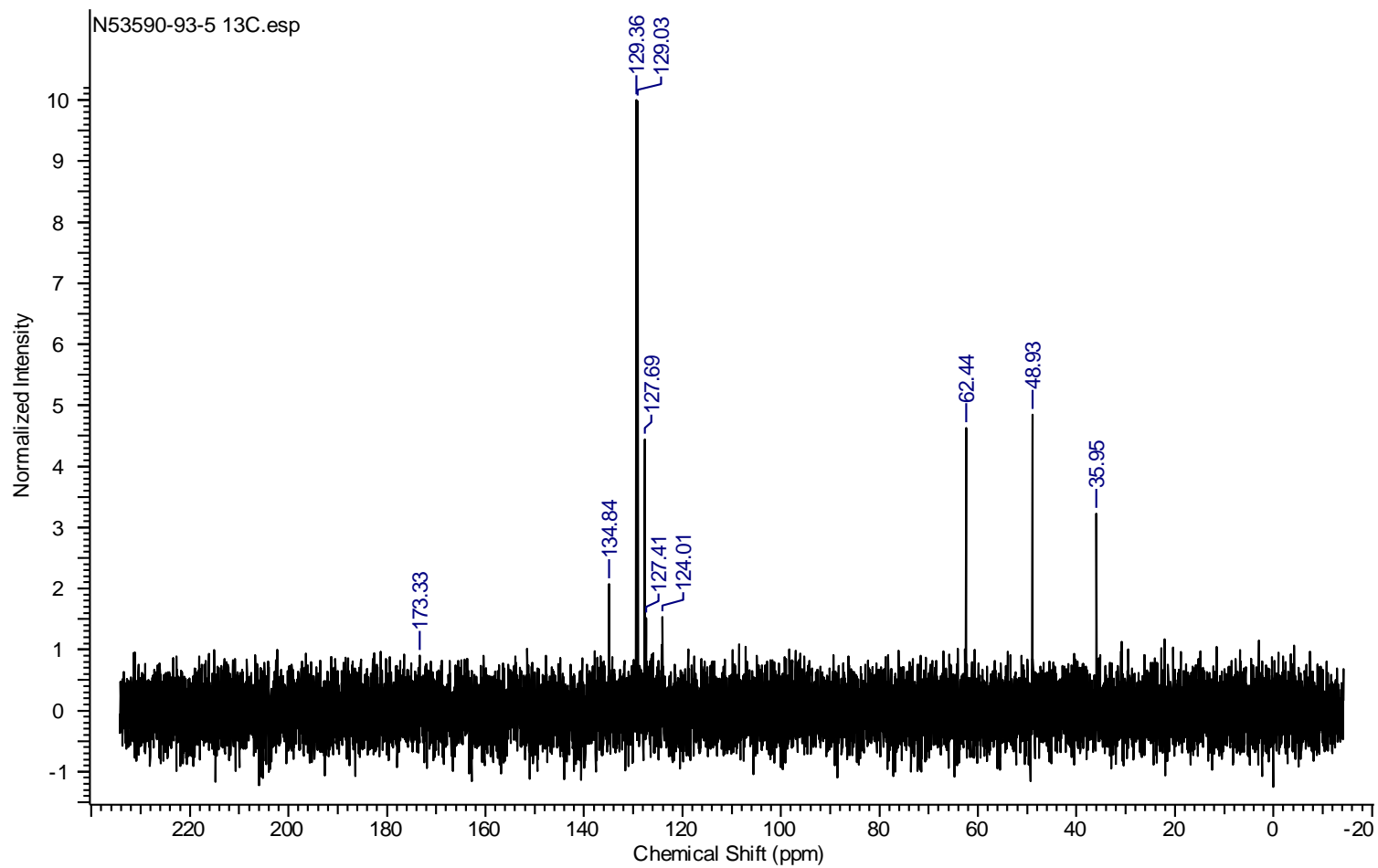


2-(Allylamino)-3-phenylpropanoic acid 145

¹H-NMR spectrum of 145 from reductive amination of 122 with 144 and sodium borohydride

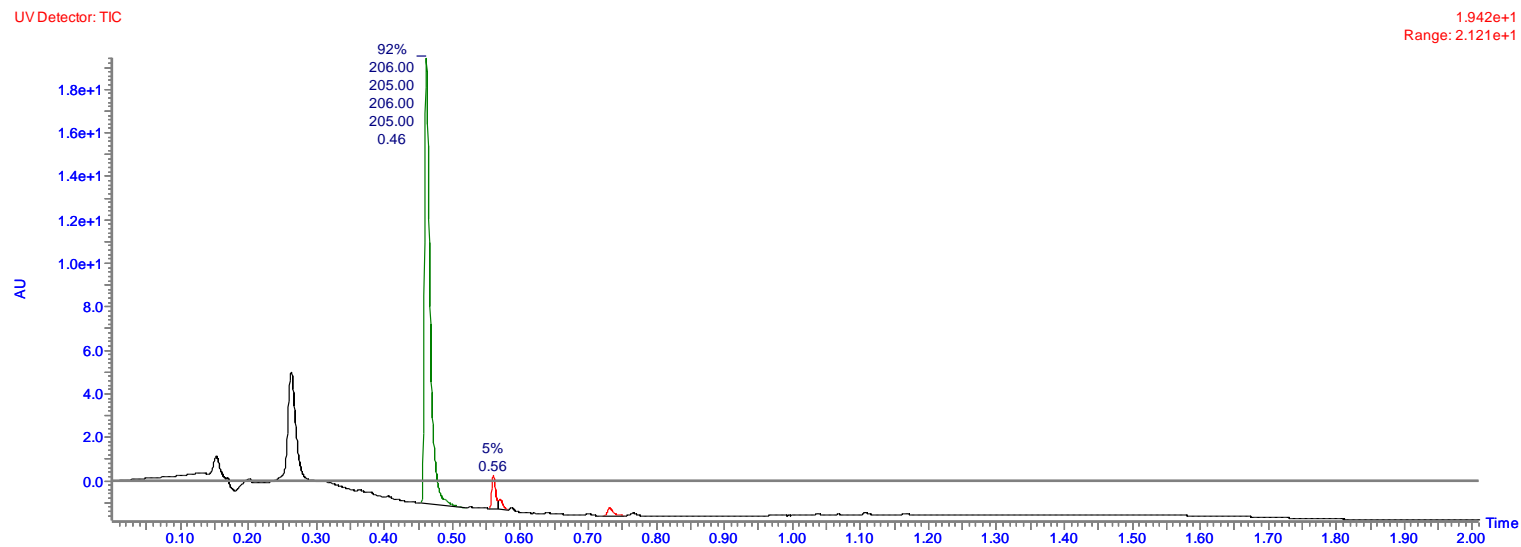


¹³C-NMR spectrum of 145 from reductive amination of 122 with 144 and sodium borohydride



Achiral LCMS of 145 from reductive amination of 122 with 144 and sodium borohydride using Method 5

UV Detector: TIC



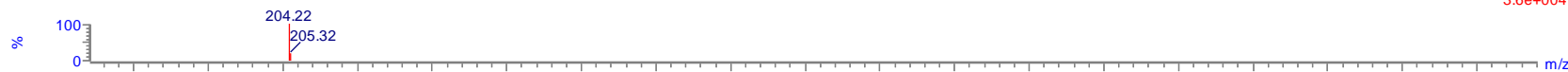
SAMPLE: 1:10 Combine (1085)

3:UV Detector
1.896 AU



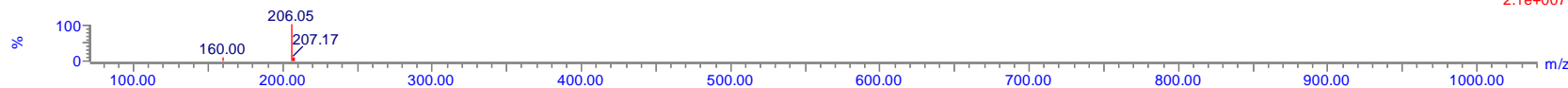
SAMPLE: 1:10 Combine (116:129-(88:91+152:155))

2:MS ES-
3.6e+004

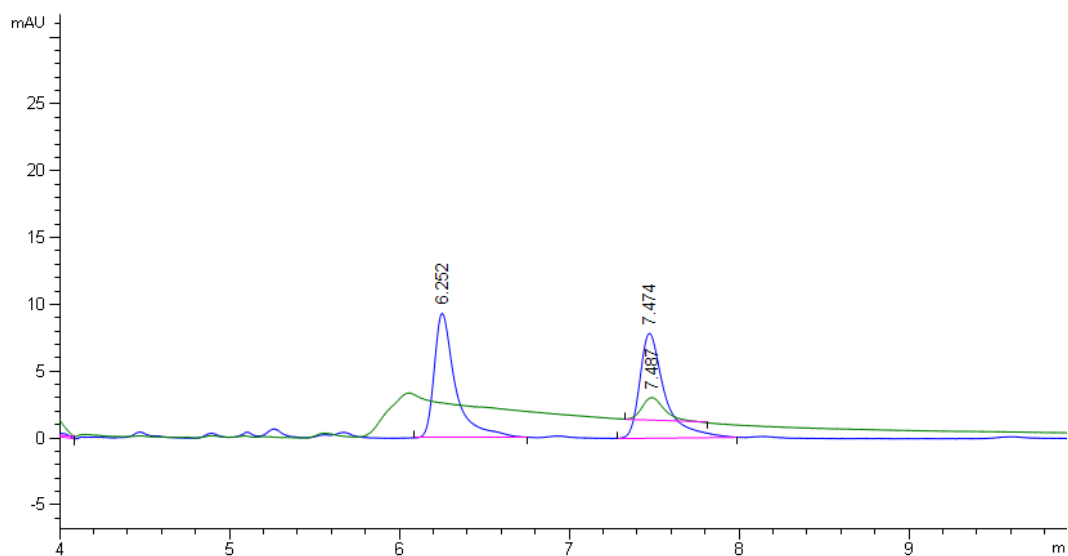


SAMPLE: 1:10 Combine (116:129-(88:91+165:168))

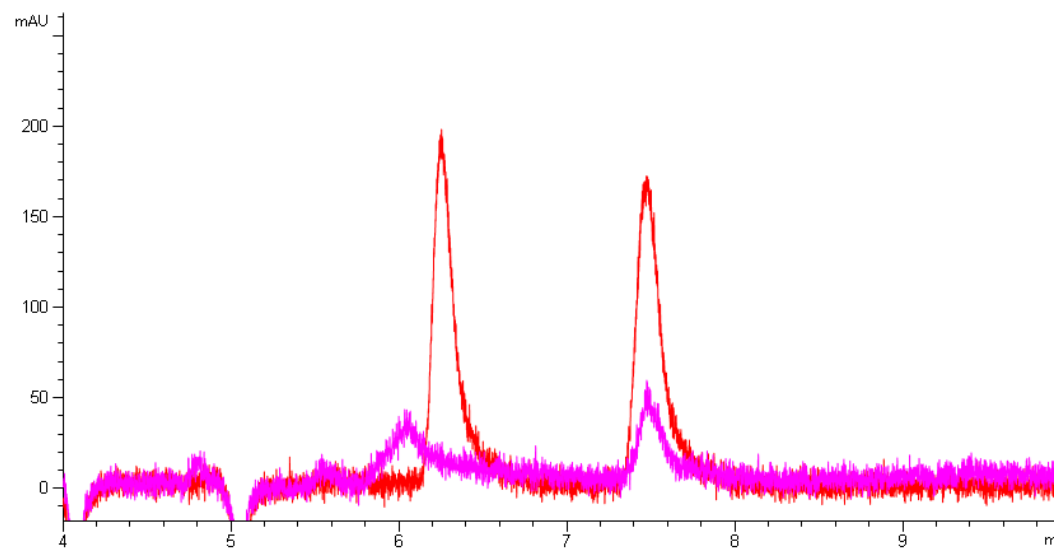
1:MS ES+
2.1e+007



Chiral UPLC of 145 from the reaction of 122 and 144 catalysed by En01, overlaid with racemic 145 using Method 3-258 nm

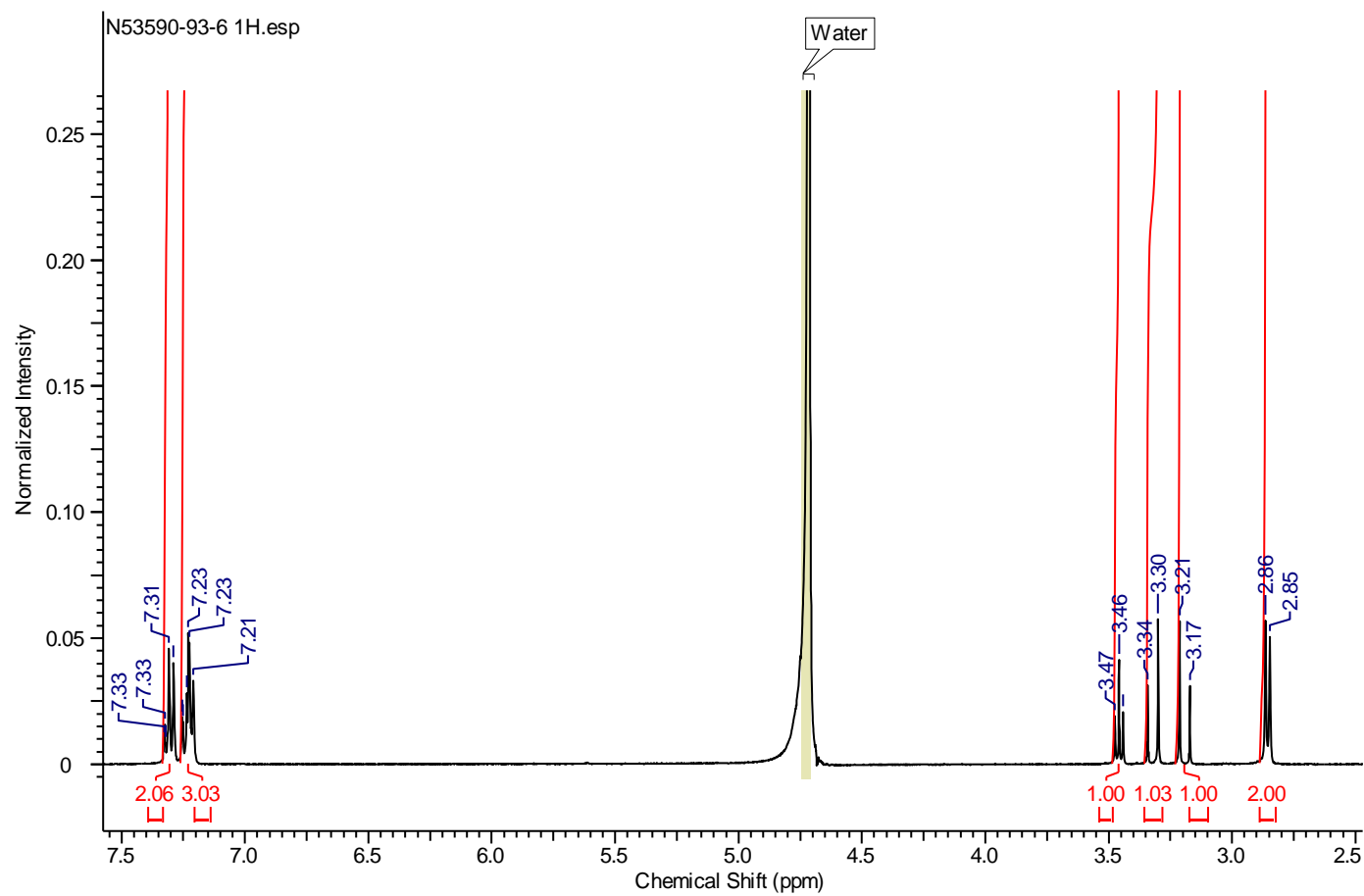


Chiral UPLC of 145 from the reaction of 122 and 144 catalysed by En01, overlaid with racemic 145 using Method 3-210 nm

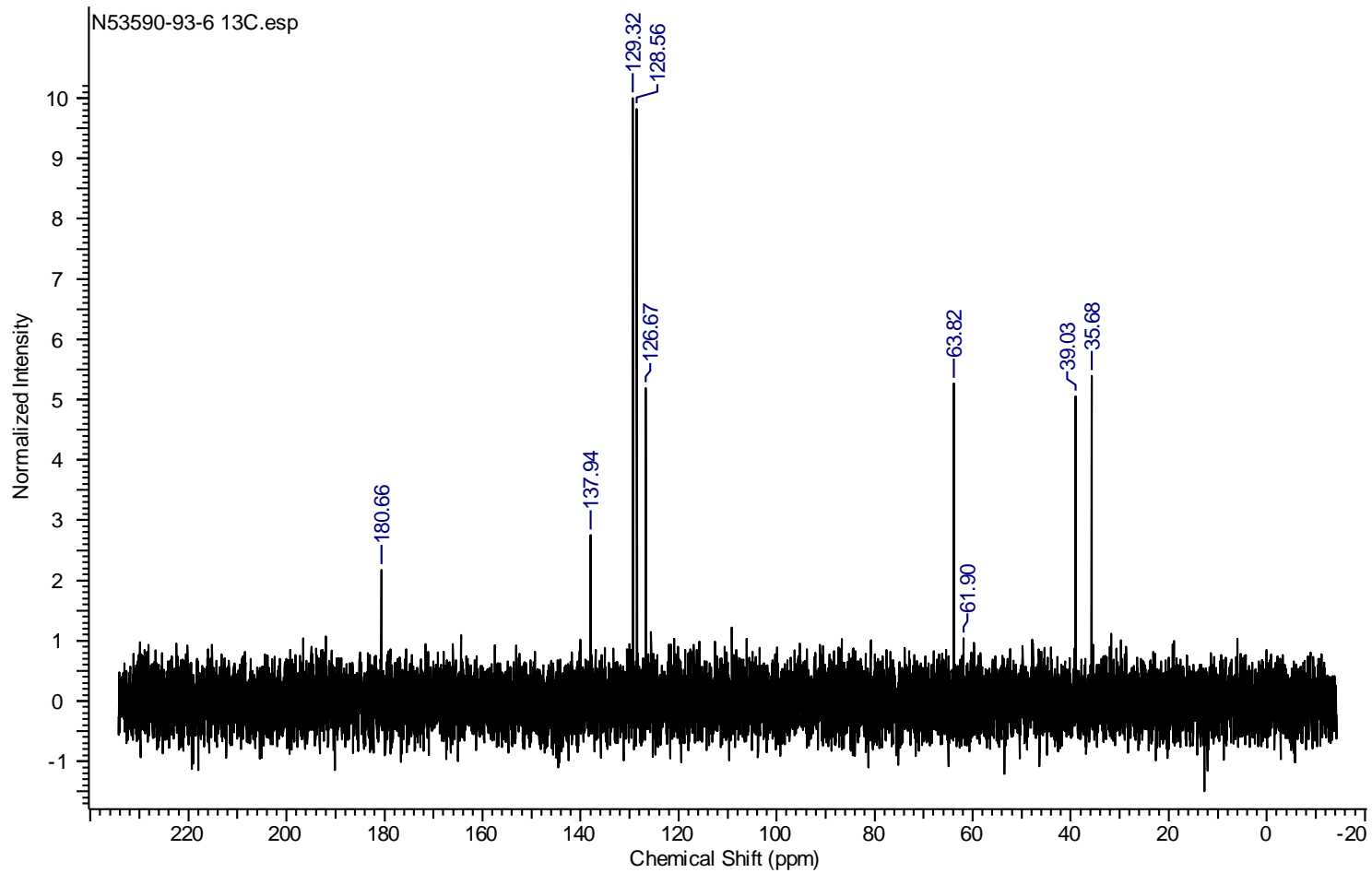


3-Phenyl-2-(prop-2-yn-1-ylamino)propanoic acid 147

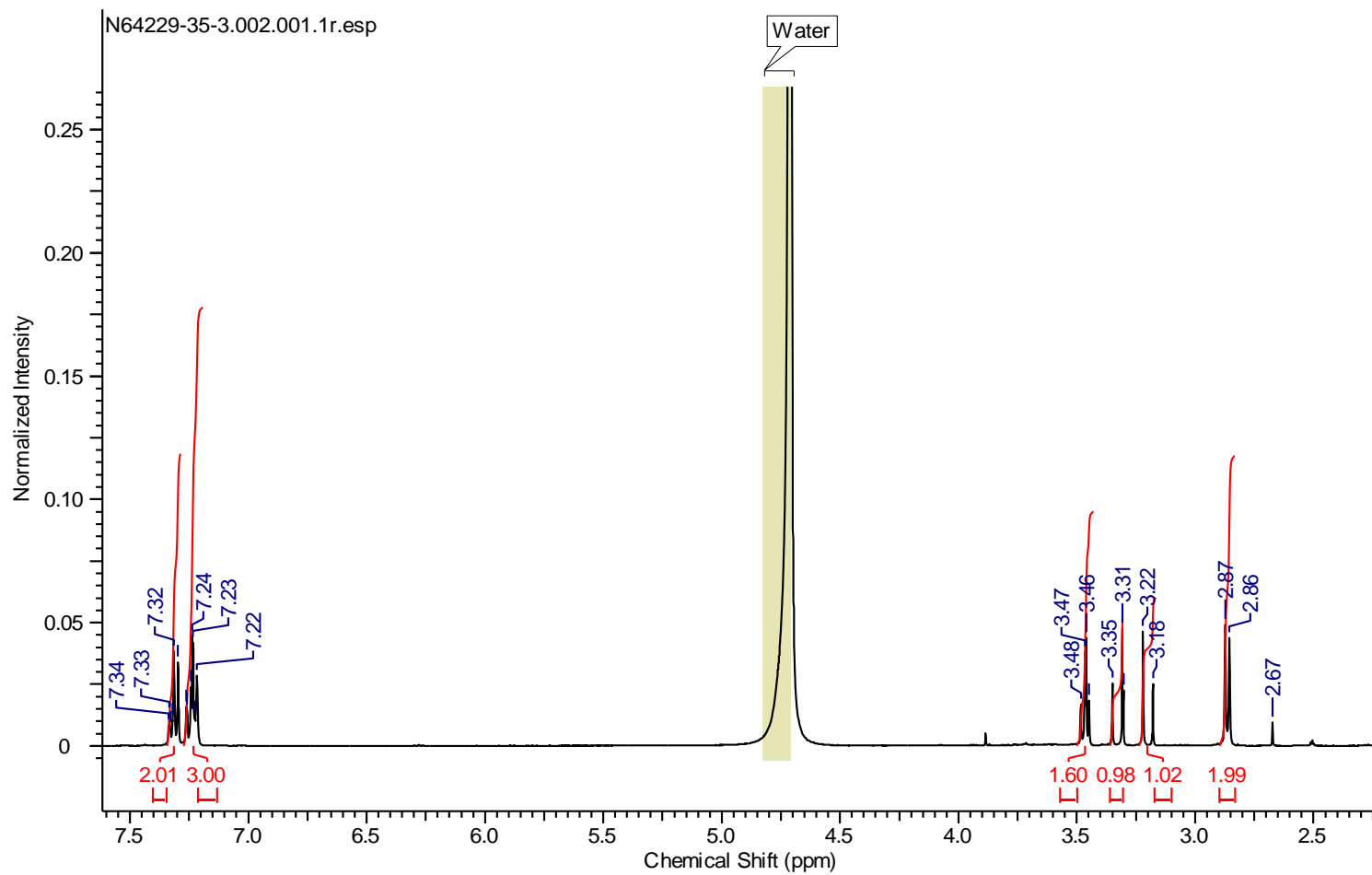
¹H-NMR spectrum of 147 from reductive amination of 122 with 146 and sodium borohydride



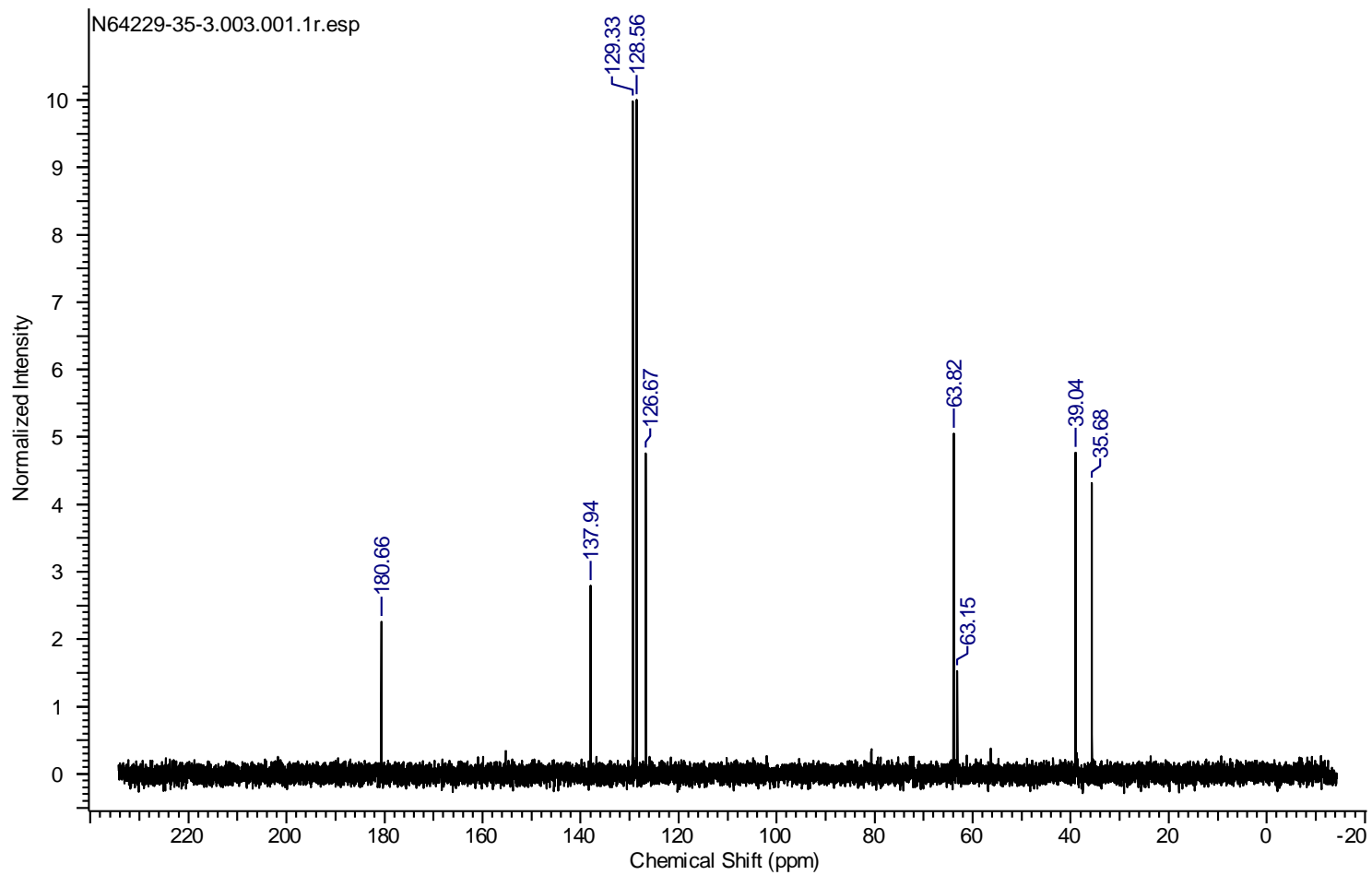
¹³C-NMR spectrum of 147 from reductive amination of 122 with 146 and sodium borohydride



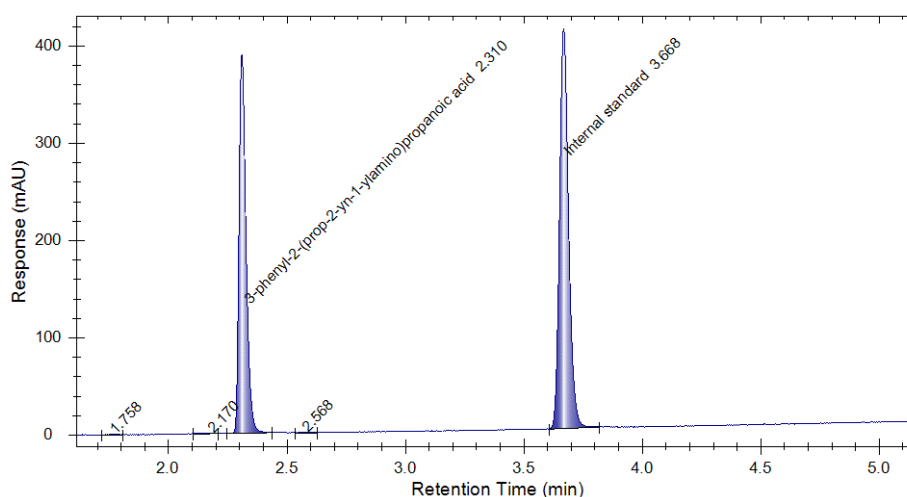
¹H-NMR of 147 generated from scale-up of reaction of keto acid 122 with amine 150 catalysed by En07.



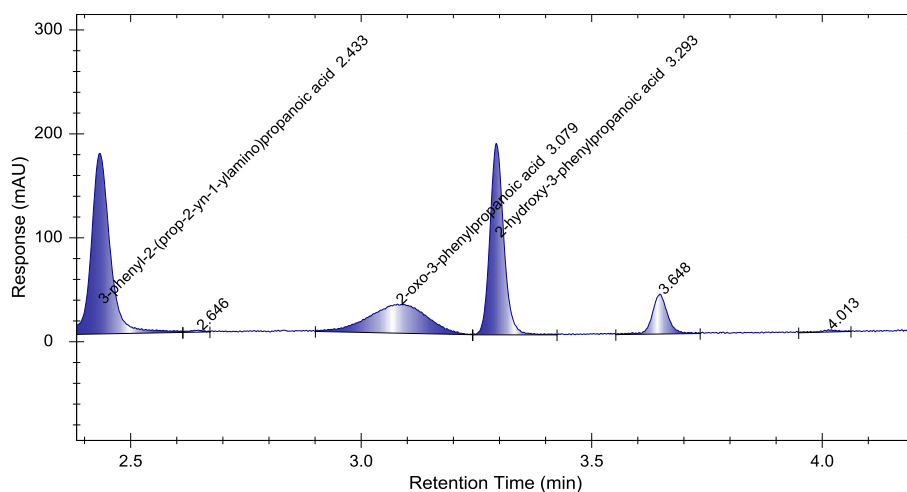
¹³C-NMR of 147 generated from scale-up of reaction of keto acid 122 with amine 150 catalysed by En07.



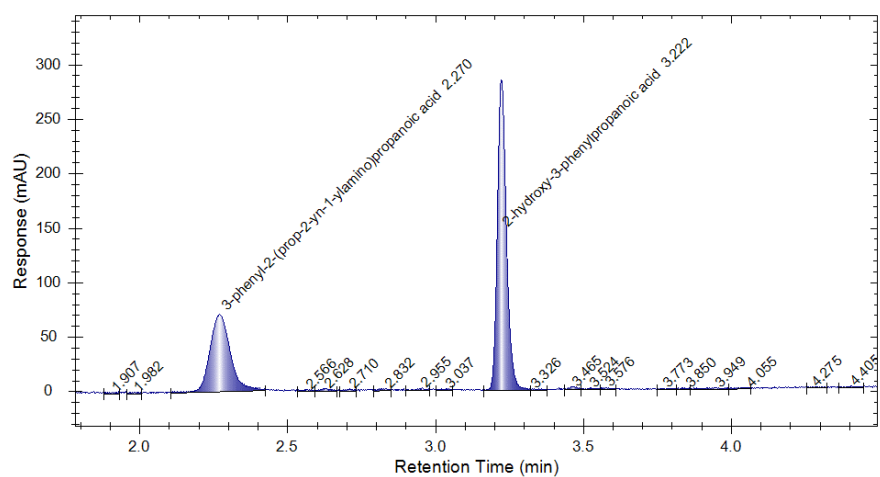
Achiral HPLC chromatogram of racemic 147 from reductive amination of 122 with 146 and sodium borohydride using Method 1



Achiral HPLC of 147 resulting from a biocatalytic reaction between keto acid 122 and amine 146 catalysed by En03 using Method 1.



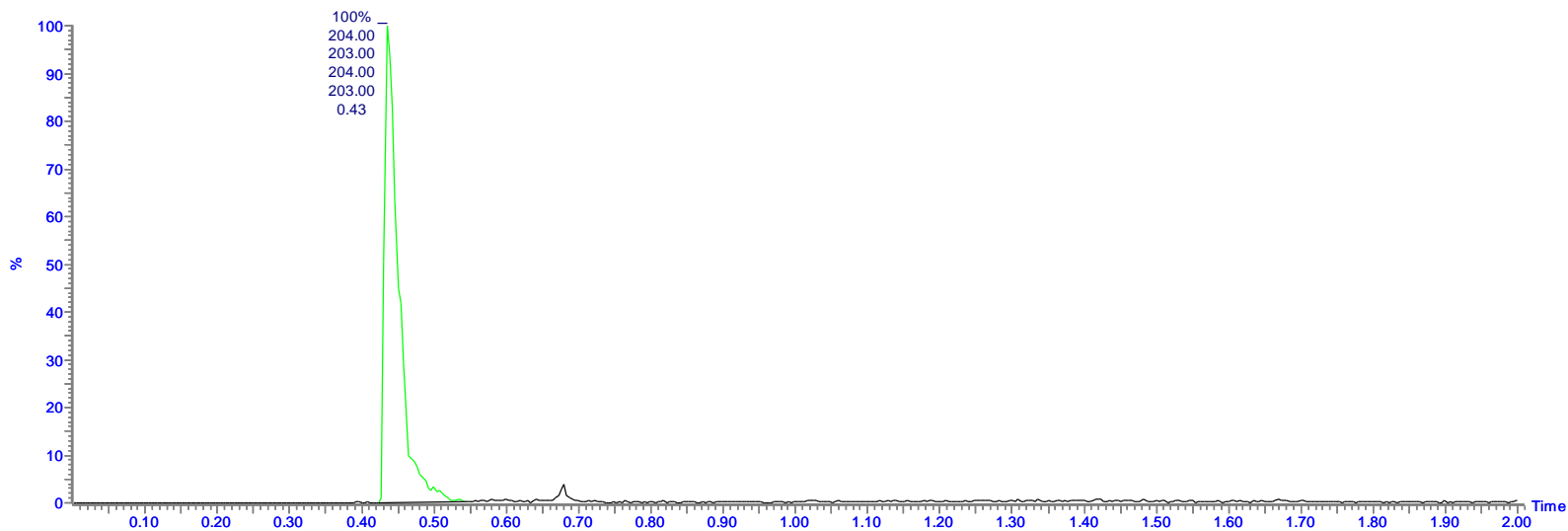
Achiral HPLC chromatogram of 147 using Method 1 generated from scale-up of reaction of keto acid 122 with 146 catalysed by En07.



LCMS chromatogram of 147 from reductive amination of 122 with 146 and sodium borohydride using Method 5

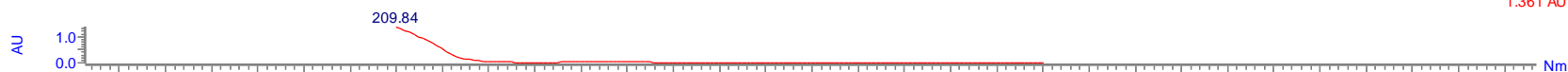
MS ES+ :226+204 1.0000Da

3.6e+007



SAMPLE: 1:11 Combine (1026)

3:UV Detector
1.361 AU



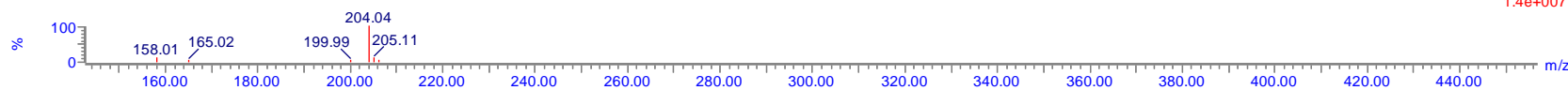
SAMPLE: 1:11 Combine (110:123-(82:85+149:152))

2:MS ES-
3.0e+004



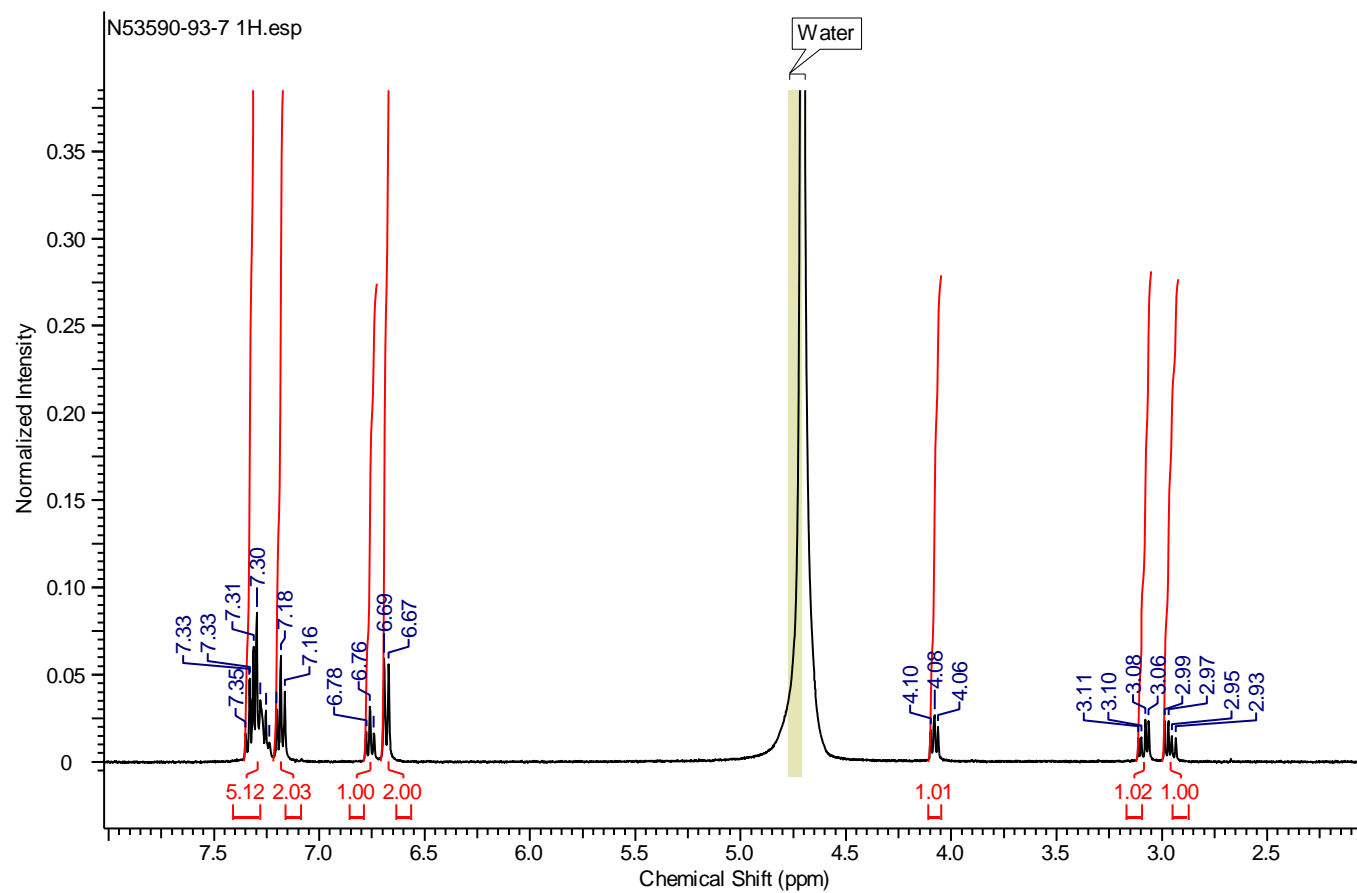
SAMPLE: 1:11 Combine (109:122-(82:85+169:172))

1:MS ES+
1.4e+007

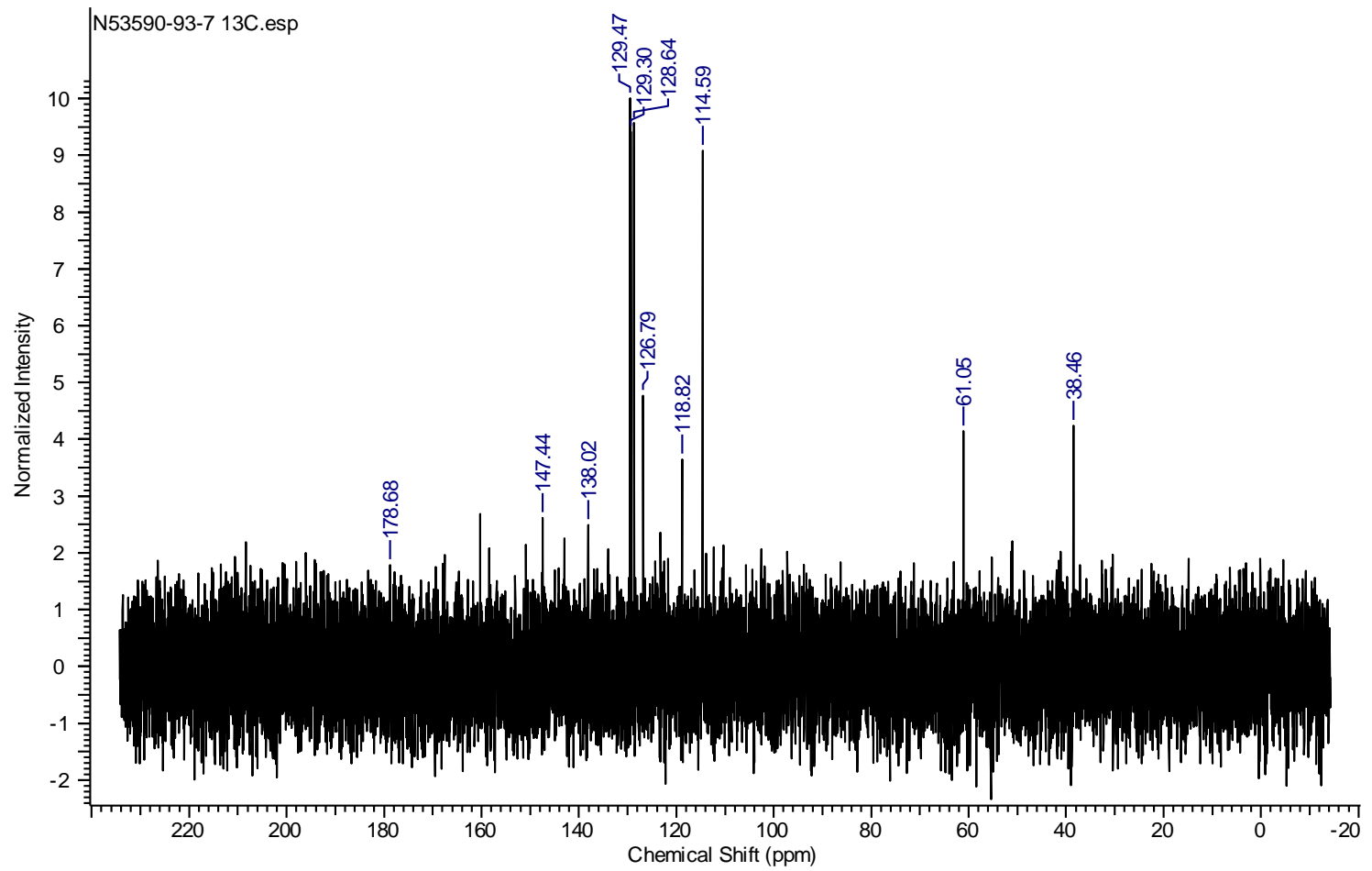


3-phenyl-2-(phenylamino)propanoic acid 149

¹H-NMR spectrum of 149 from reductive amination of 122 and 148 with sodium borohydride

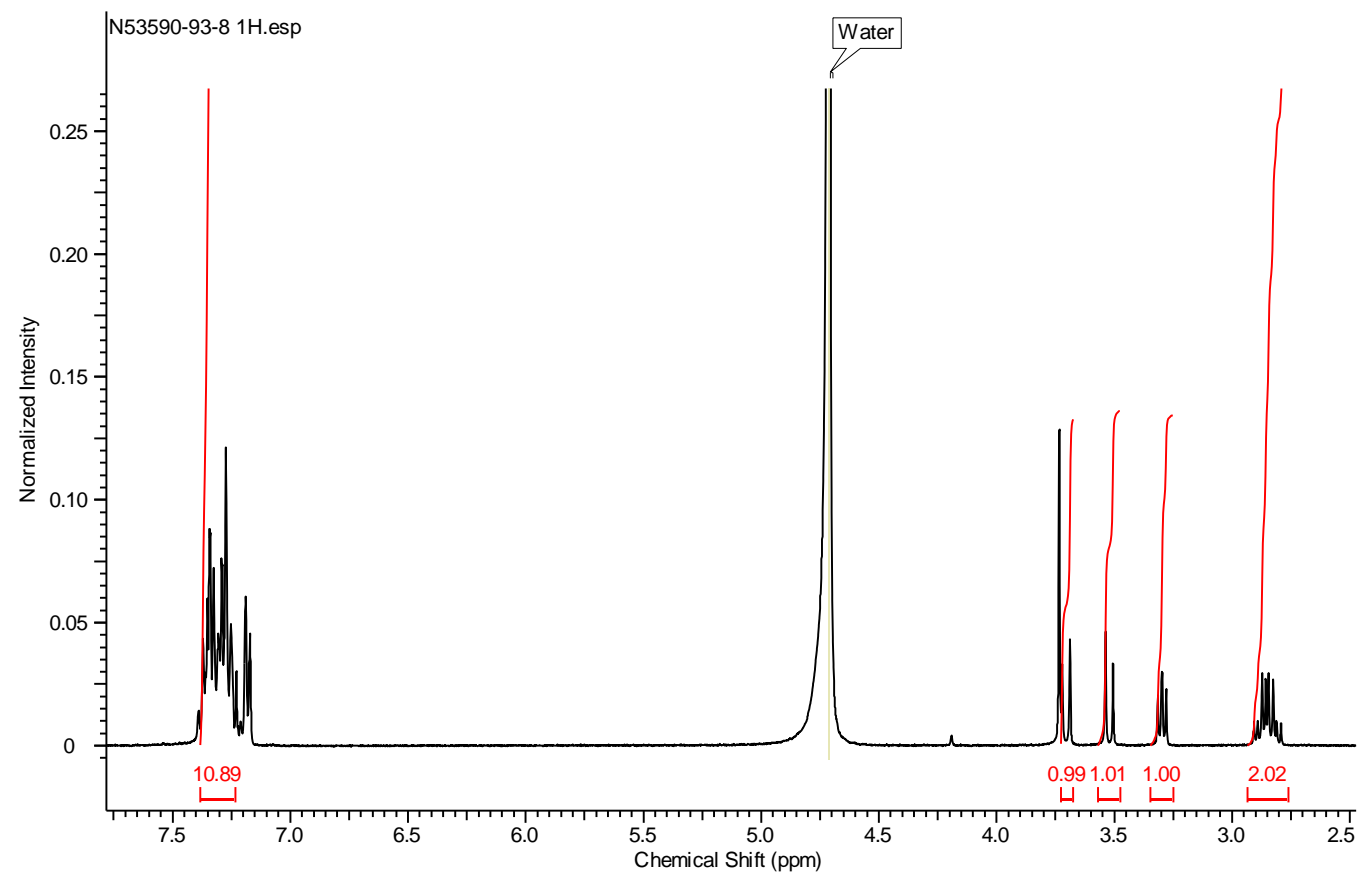


¹³C-NMR spectrum 149 from reductive amination of 122 and 148 with sodium borohydride

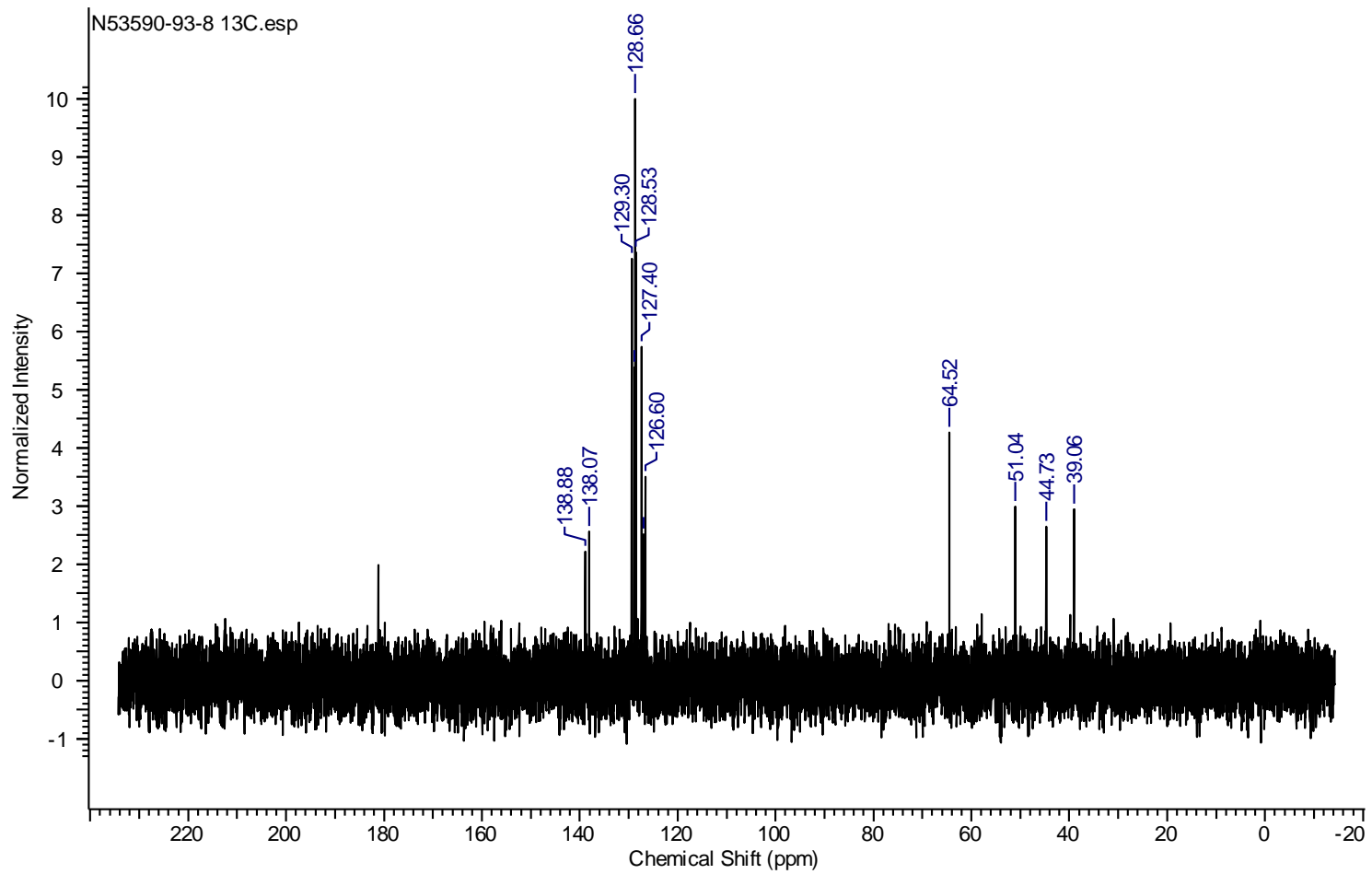


2-(Benzylamino)-3-phenylpropanoic acid 151

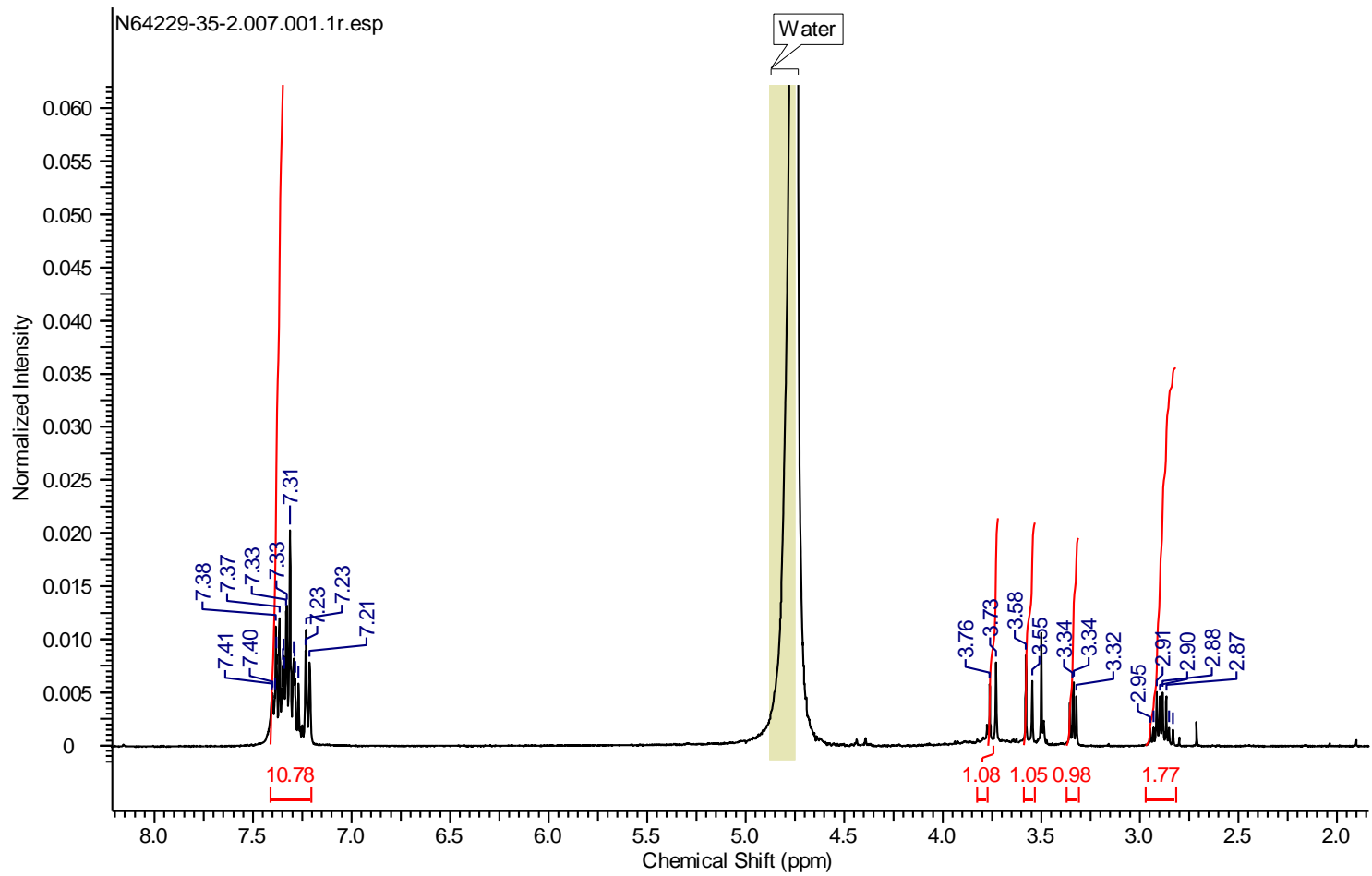
¹H-NMR spectrum 151 from reductive amination of 122 and 150 with sodium borohydride



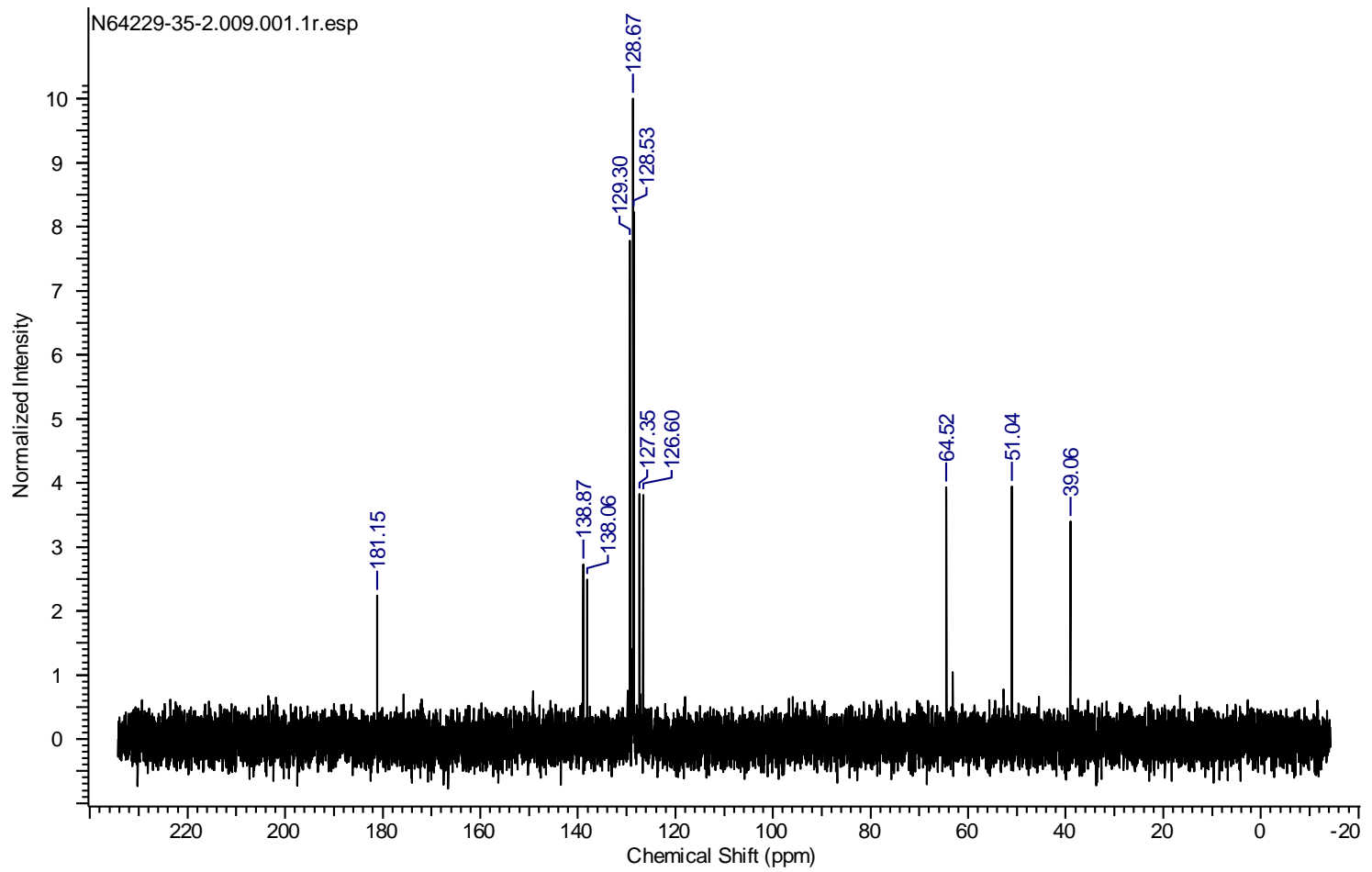
¹³C-NMR spectrum of 151 from reductive amination of 122 and 150 with sodium borohydride



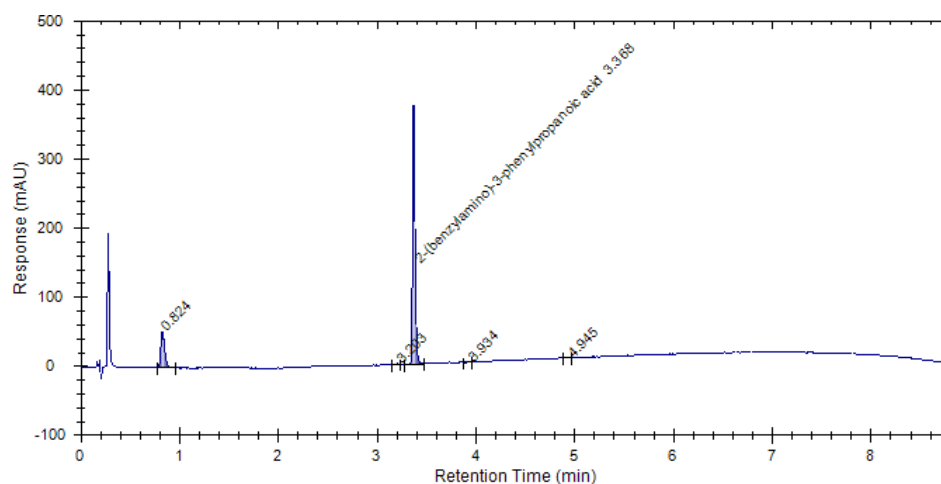
¹³C-NMR of 151 generated from scale-up of reaction of 122 and 150 catalysed by En04.



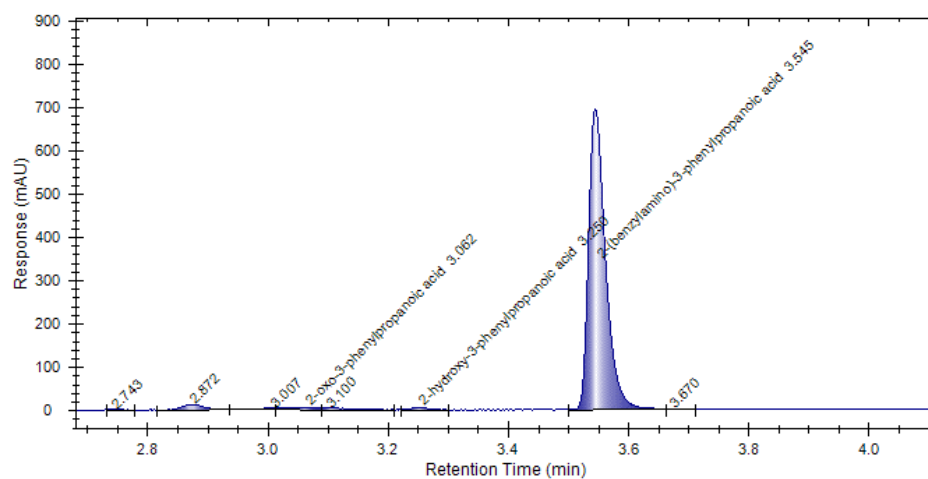
^{13}C -NMR of 151 generated from scale-up of reaction of 122 and 150 catalysed by En04.



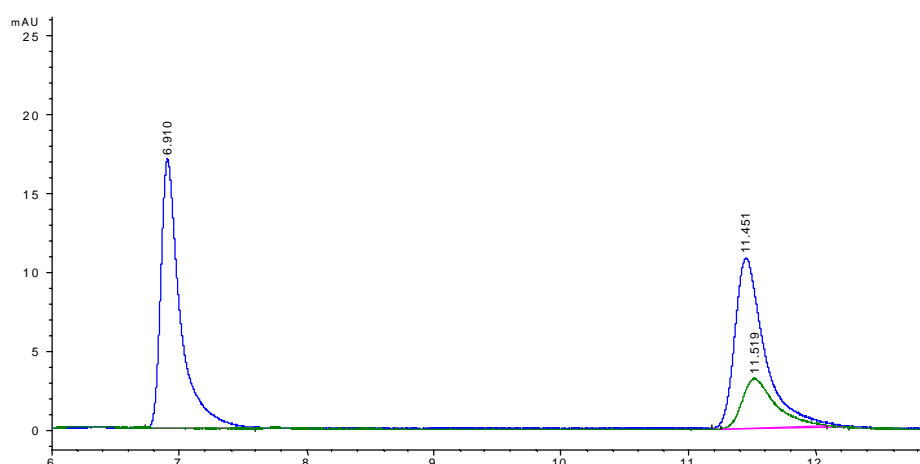
Achiral HPLC chromatogram of 151 from reductive amination of 122 and 150 with sodium borohydride using Method 1



Achiral HPLC chromatogram of 151 generated from scale-up of reaction of 122 and 150 catalysed by En04.

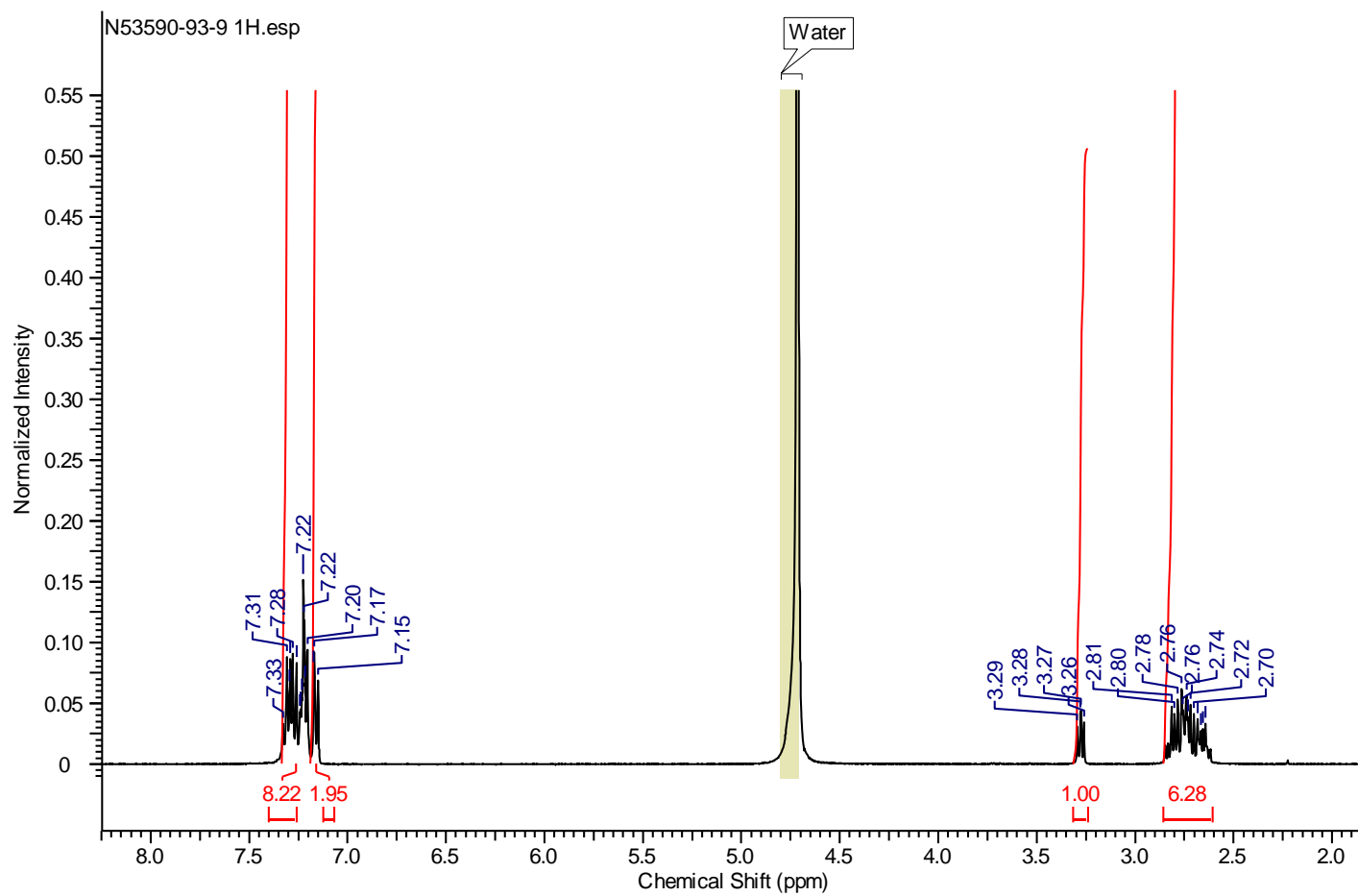


Chiral UPLC of 151 resulting from a biocatalytic reaction between 122 and 150 catalysed by En04 using Method 3 (green), overlaid with racemic 3g (blue)

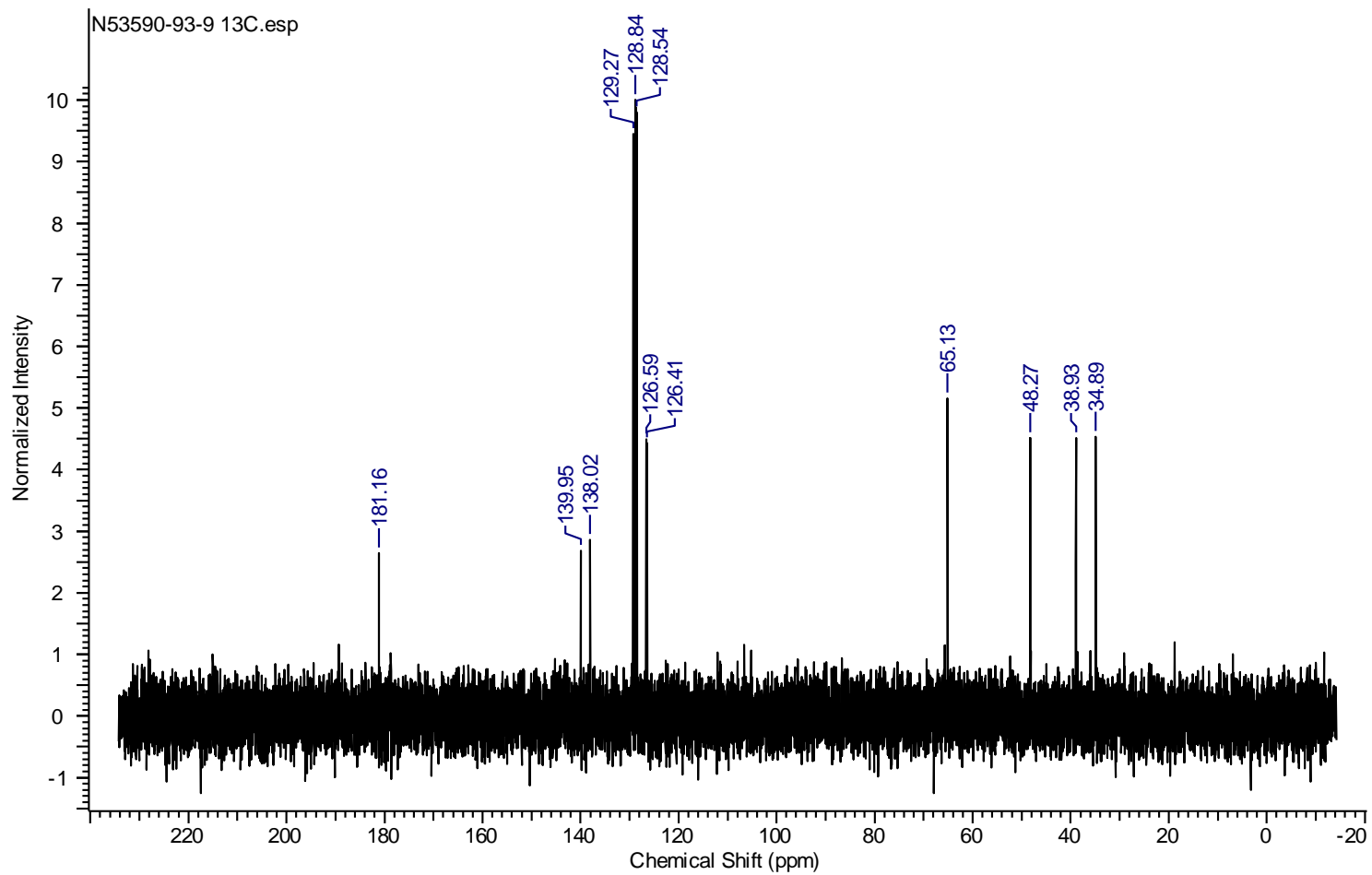


2-(Phenethylamino)-3-phenylpropanoic acid 153

¹H-NMR spectrum of 153 from reductive amination of 122 and 152 with sodium borohydride

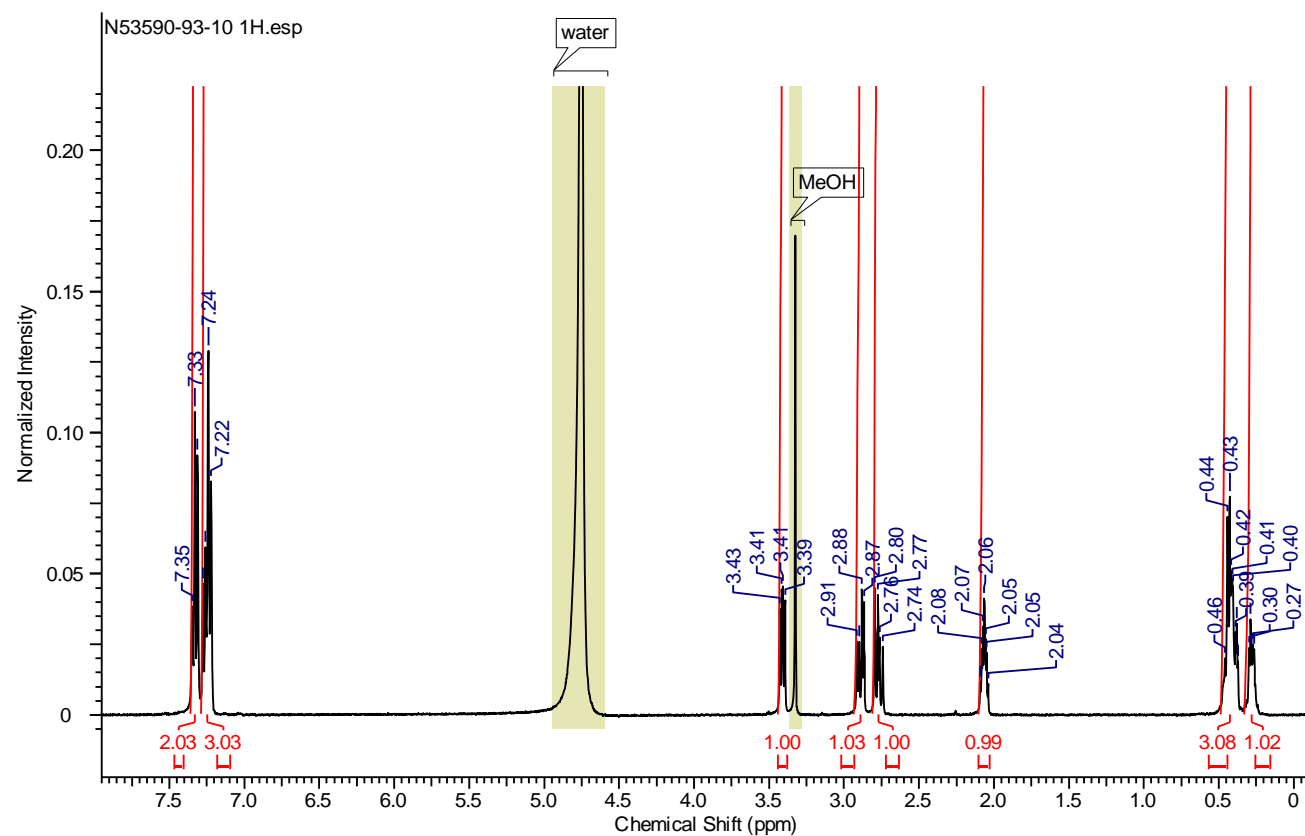


¹³C-NMR spectrum of 153 from reductive amination of 122 and 152 with sodium borohydride

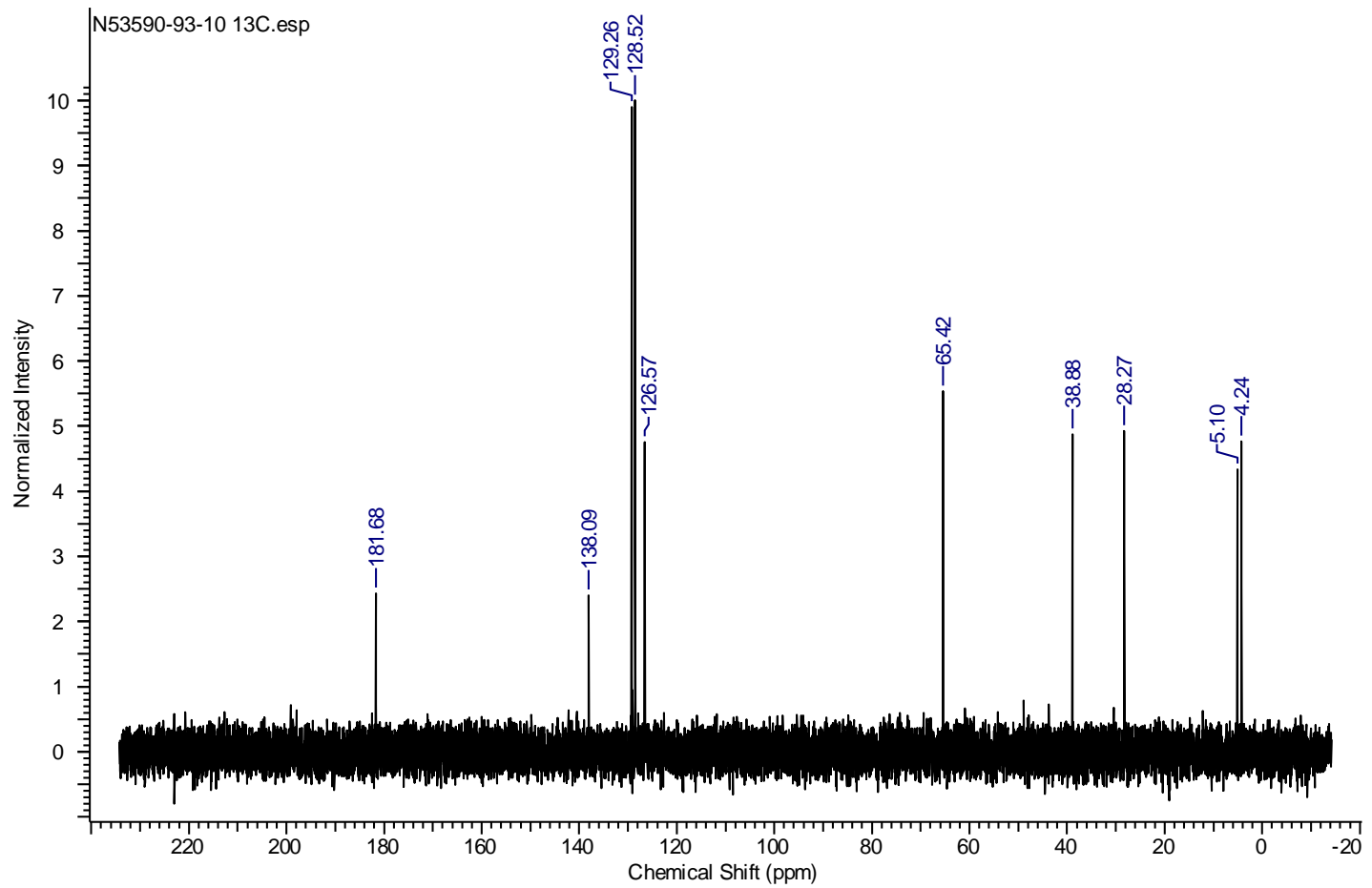


2-(Cyclopropylamino)-3-phenylpropanoic acid 155

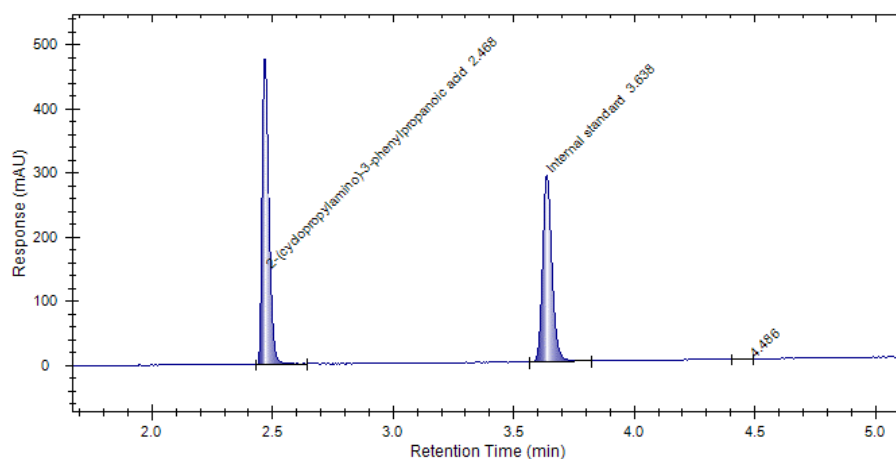
¹H-NMR spectrum of 155 from reductive amination of 122 and 154 with sodium borohydride



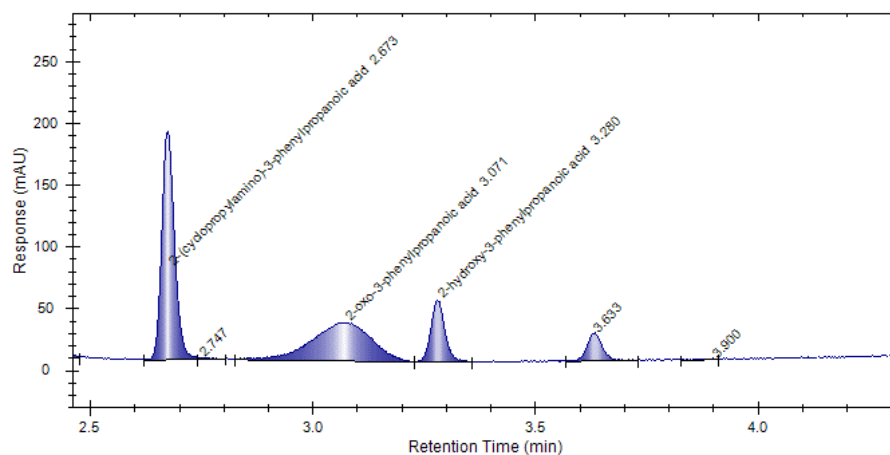
¹³C-NMR spectrum of 155 from reductive amination of 122 and 154 with sodium borohydride



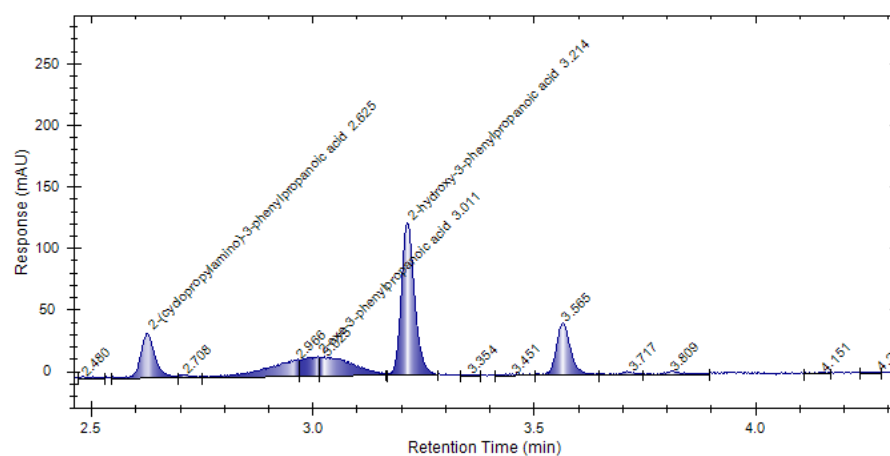
Achiral HPLC chromatogram of 155 from reductive amination of 122 and 154 with sodium borohydride using Method 1



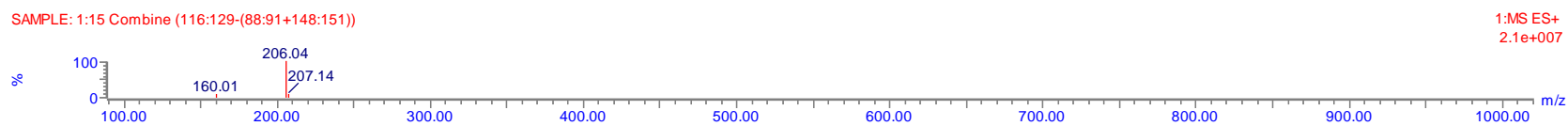
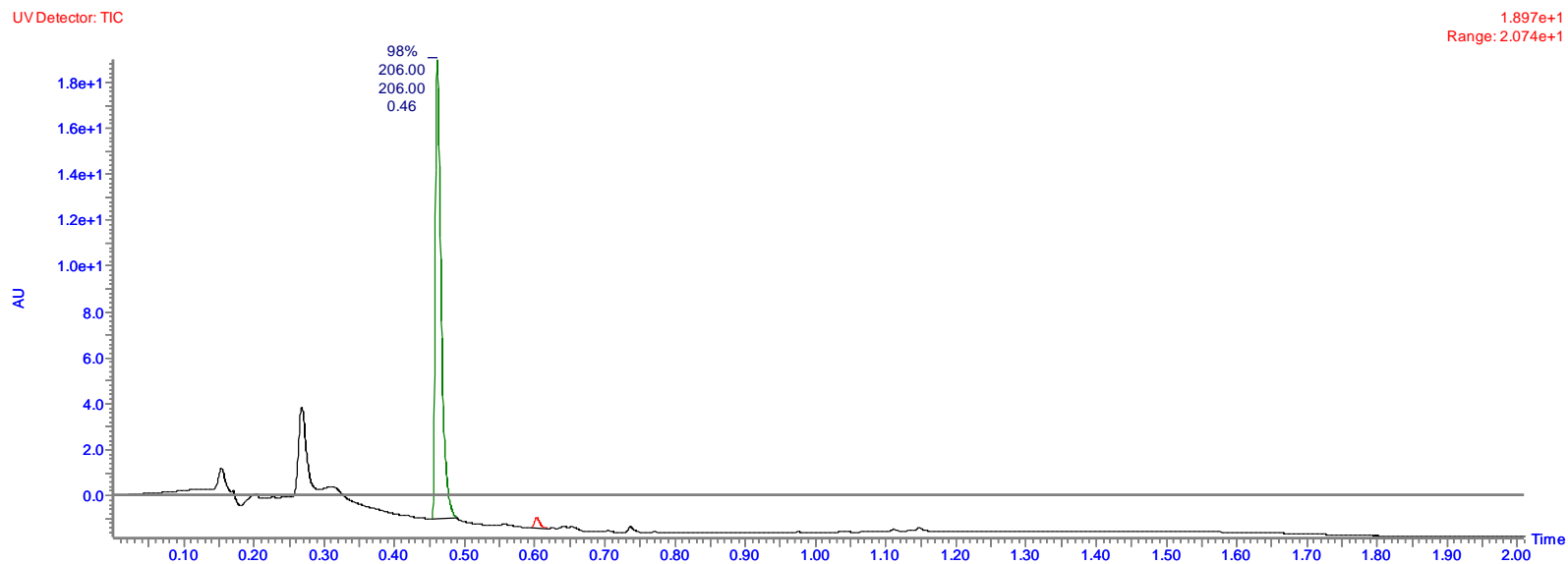
Achiral HPLC chromatogram of 155 generated from small scale reaction of 122 and 154 catalysed by En05 using Method 1



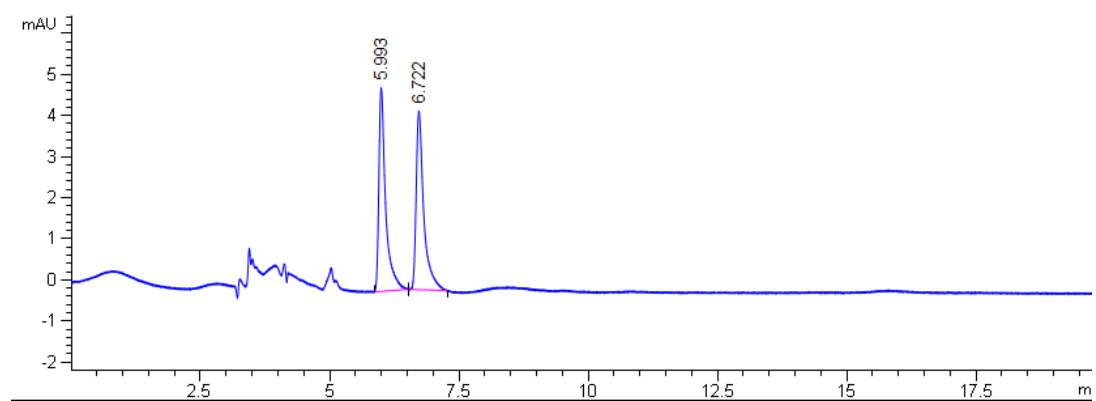
Achiral HPLC chromatogram of 155 generated from the scale-up of the reaction of 122 and 154 catalysed by En02 using Method 1



LCMS chromatogram of 155 from the reductive amination of 122 and 154 with sodium borohydride using Method 5

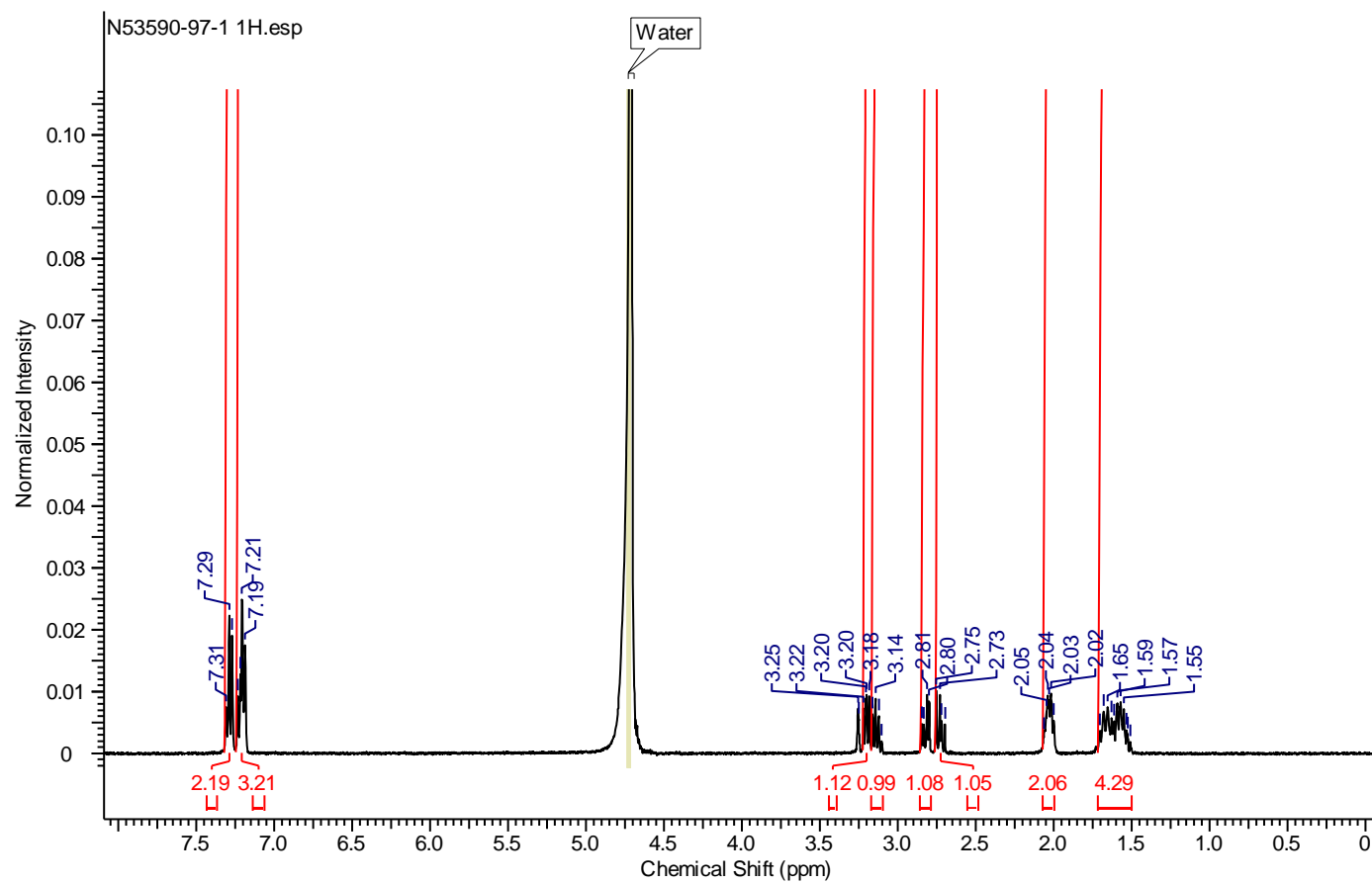


Chiral HPLC of racemic 155 from the reductive amination of 122 and 154 with sodium borohydride using Method 3

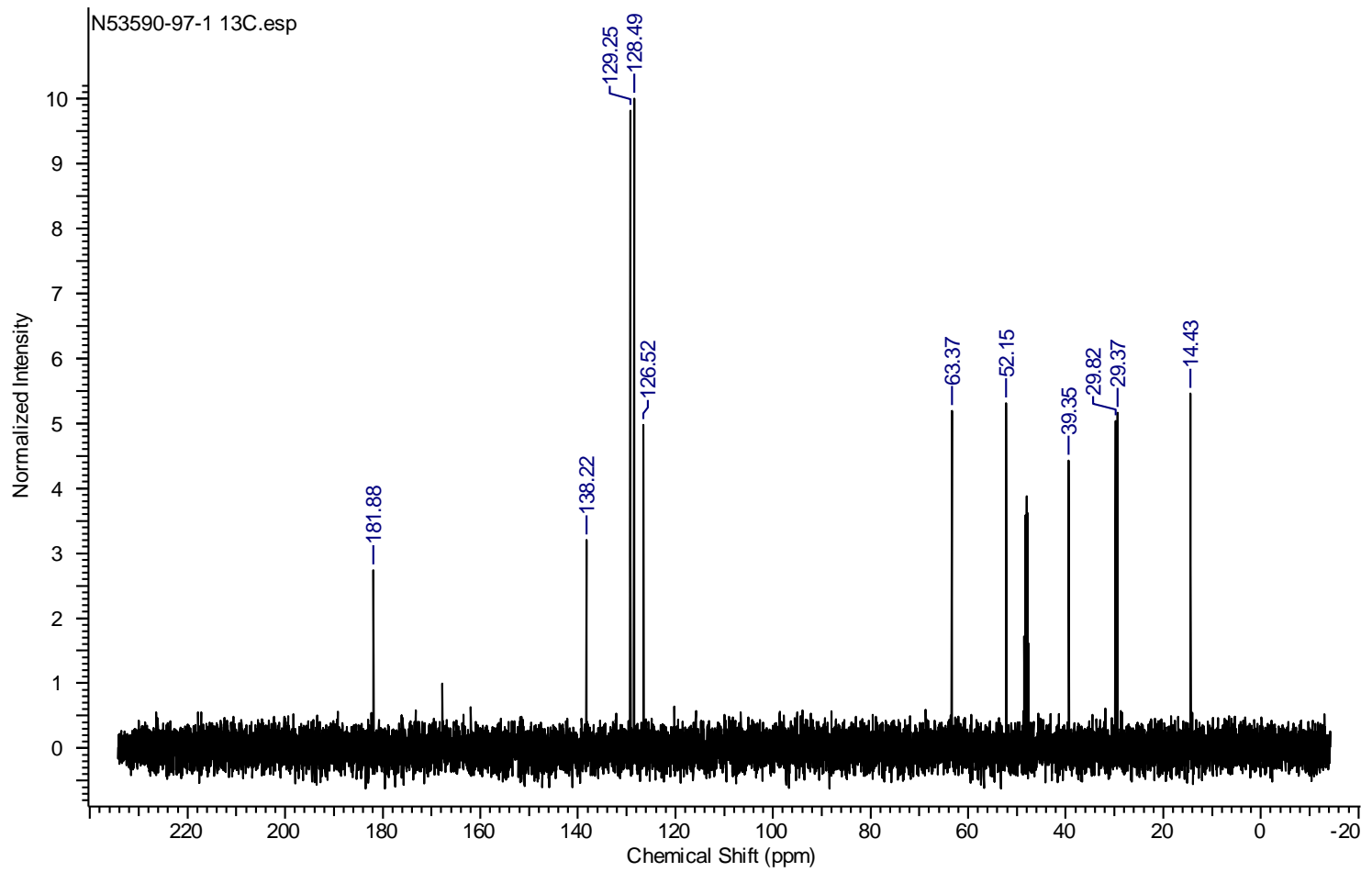


2-(Cyclobutylamino)-3-phenylpropanoic acid 157

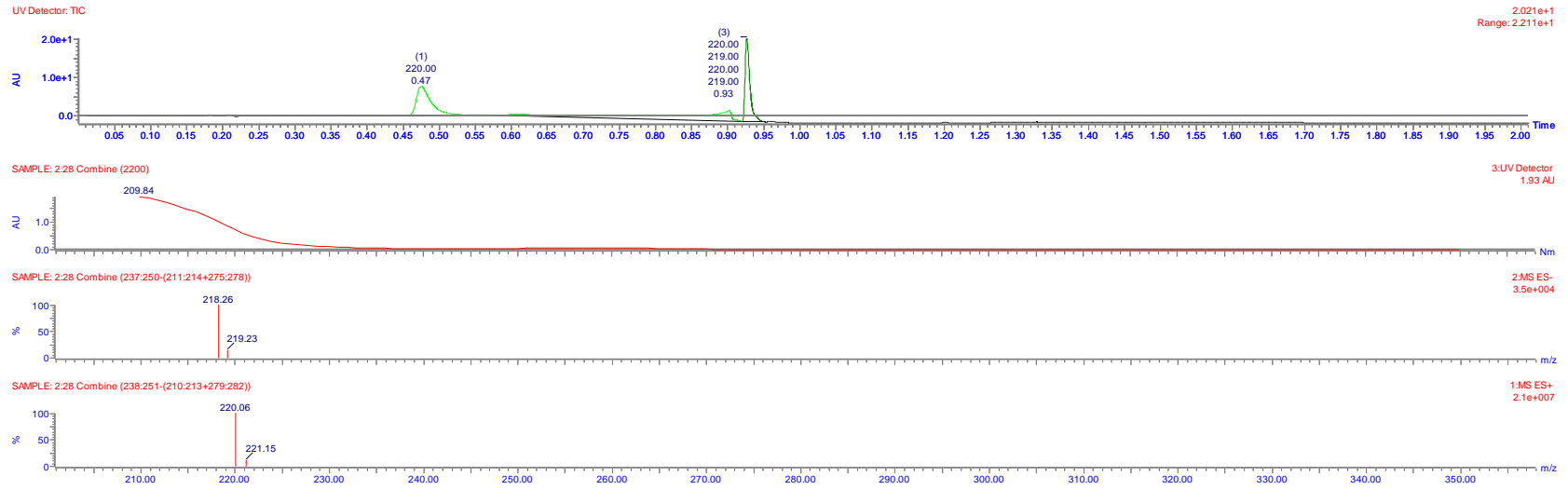
¹H-NMR spectrum of 157 from the reductive amination of 122 and 156 with sodium borohydride



^{13}C -NMR spectrum of of 157 from the reductive amination of 122 and 156 with sodium borohydride

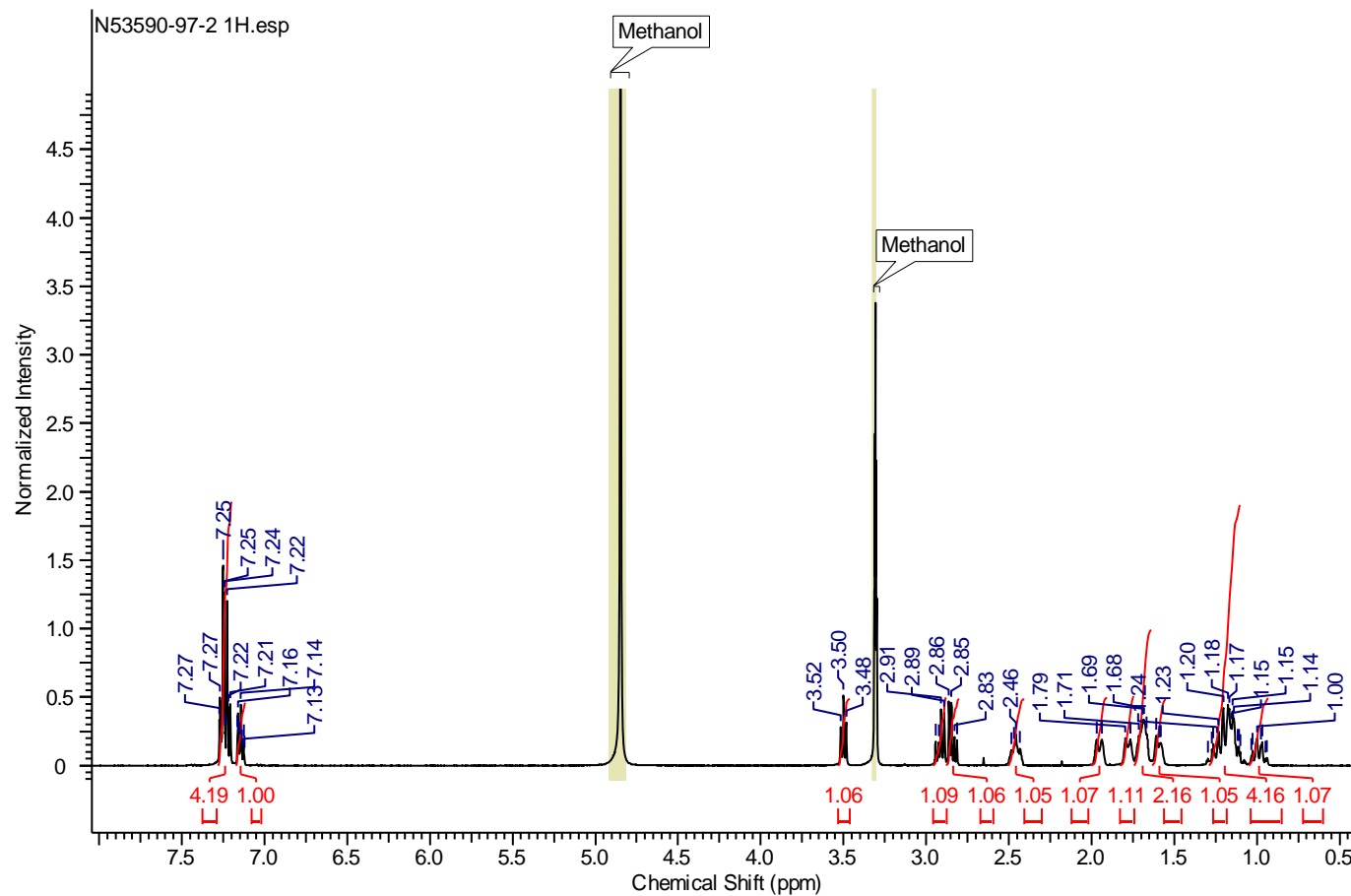


LCMS chromatogram of 156 from the reductive amination of 122 and 155 with sodium borohydride using Method 5

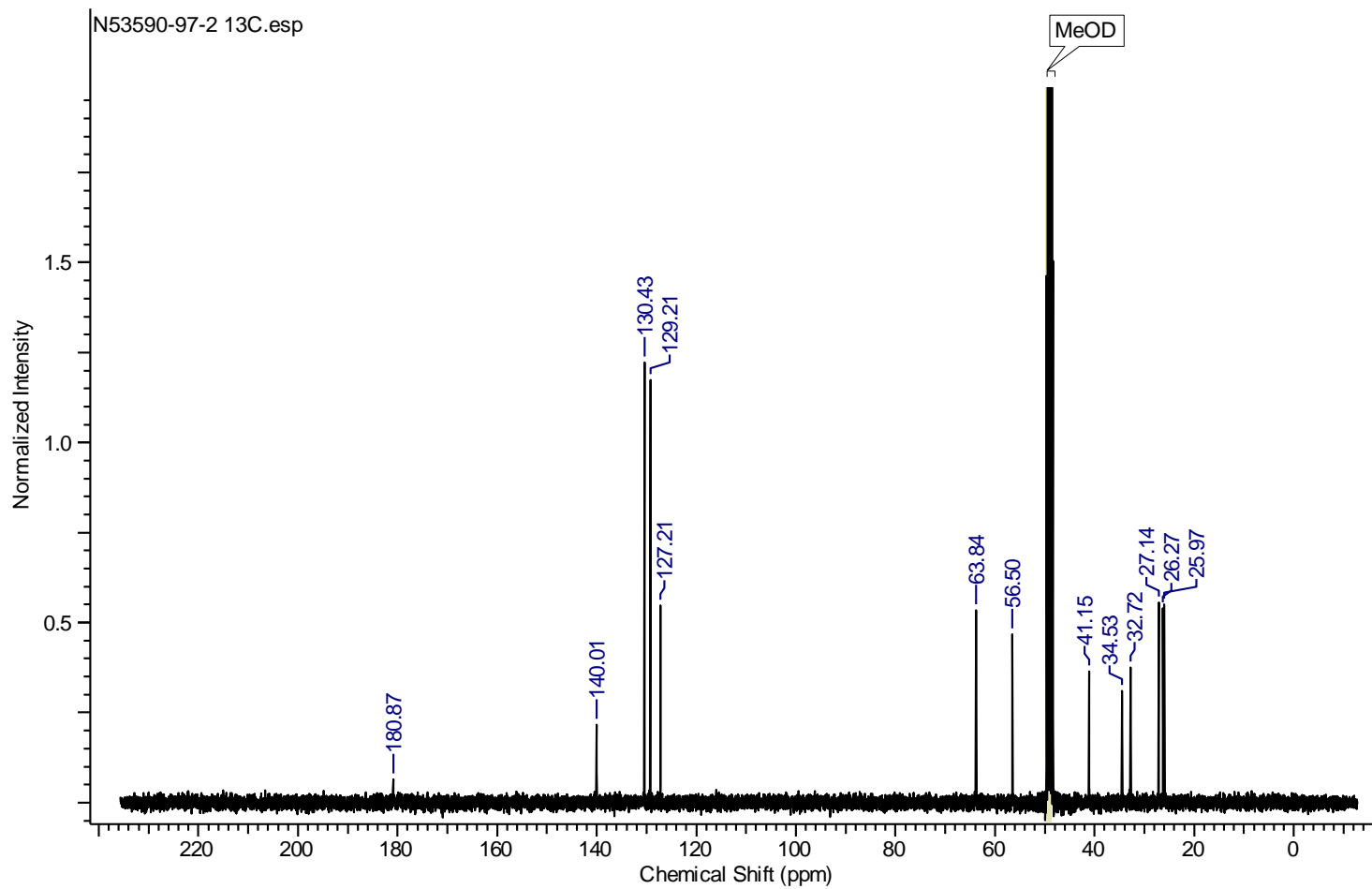


2-(Cyclohexylamino)-3-phenylpropanoic acid 159

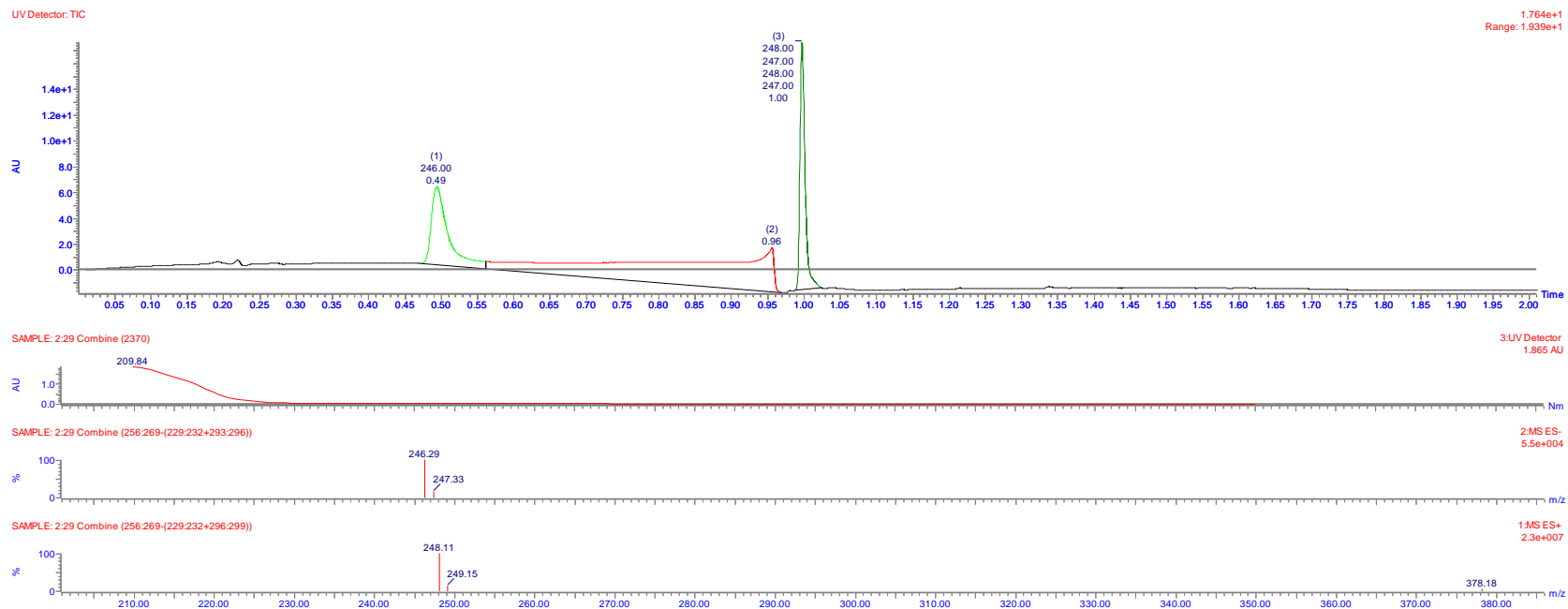
¹H-NMR spectrum of 159 from the reductive amination of 122 and 158 with sodium borohydride



¹³C-NMR spectrum of 159 from the reductive amination of 122 and 158 with sodium borohydride

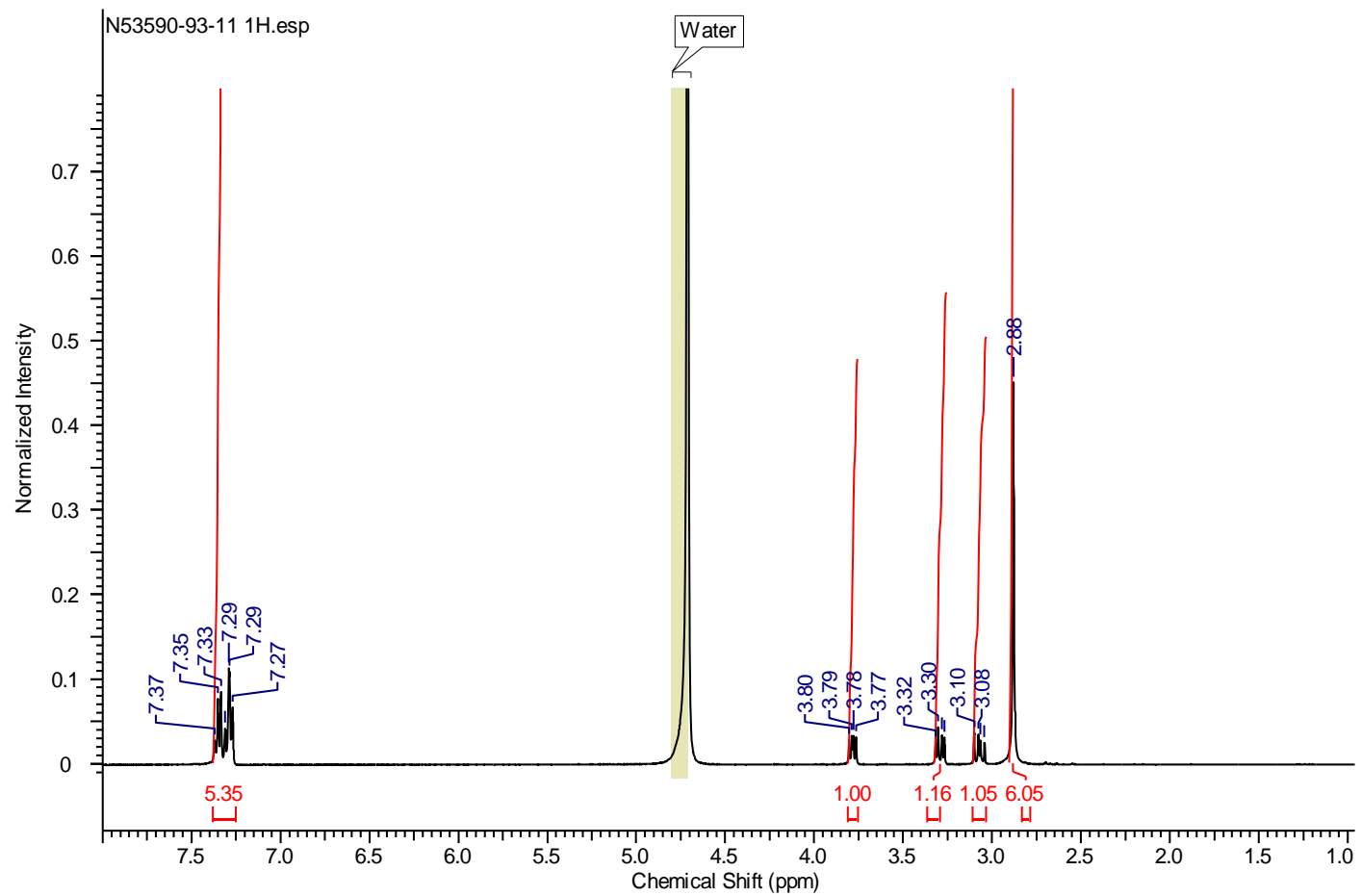


LCMS chromatogram of 158 from the reductive amination of 122 and 157 with sodium borohydride using Method 5

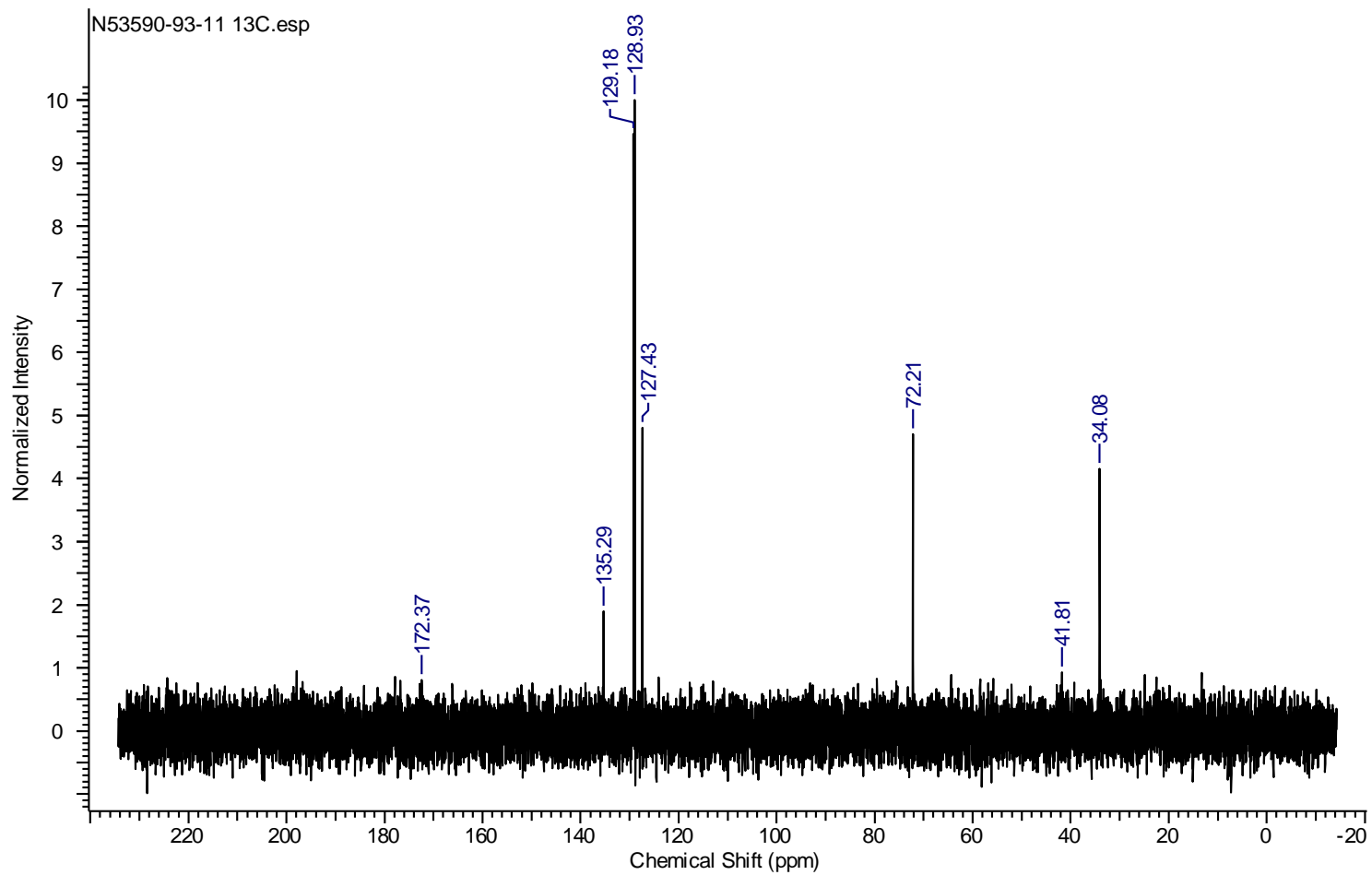


2-(Dimethylamino)-3-phenylpropanoic acid 160

¹H-NMR spectrum of 160 from the reductive amination of 122 and 127 with sodium borohydride

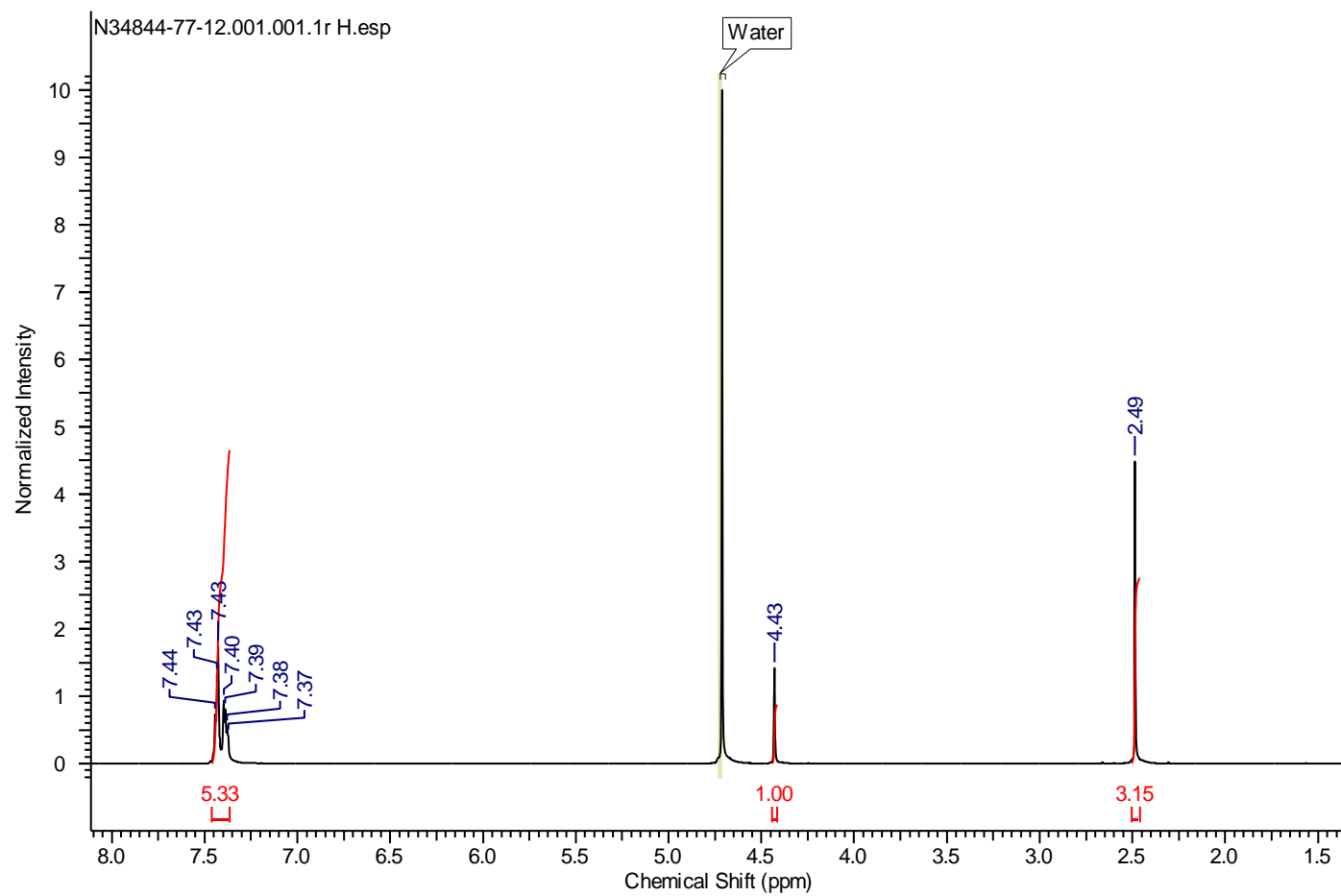


¹³C-NMR spectrum of 160 from the reductive amination of 122 and 127 with sodium borohydride

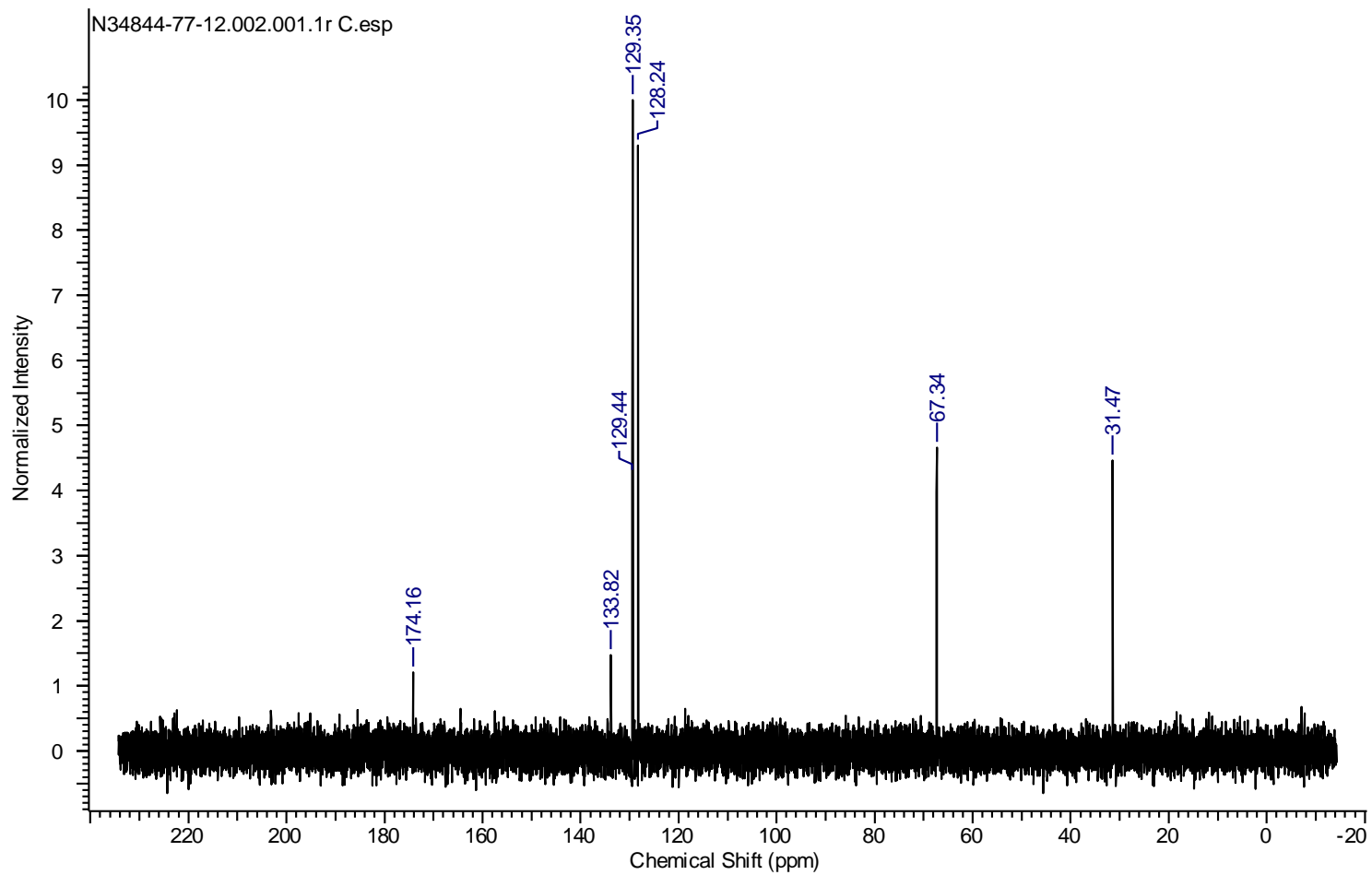


2-(Methylamino)-2-phenylacetic acid **162**

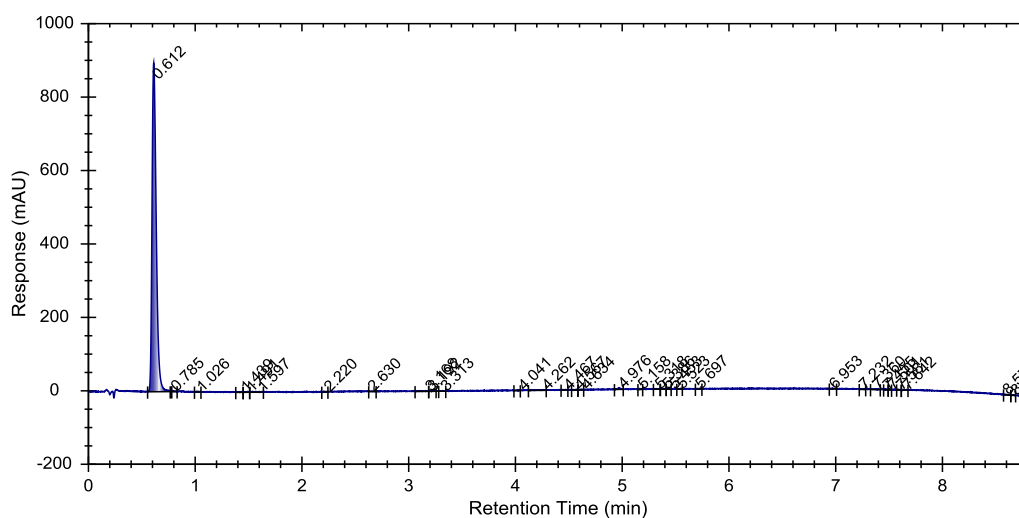
$^1\text{H-NMR}$ spectrum of **162** from the reductive amination of **161** and **76** with sodium borohydride



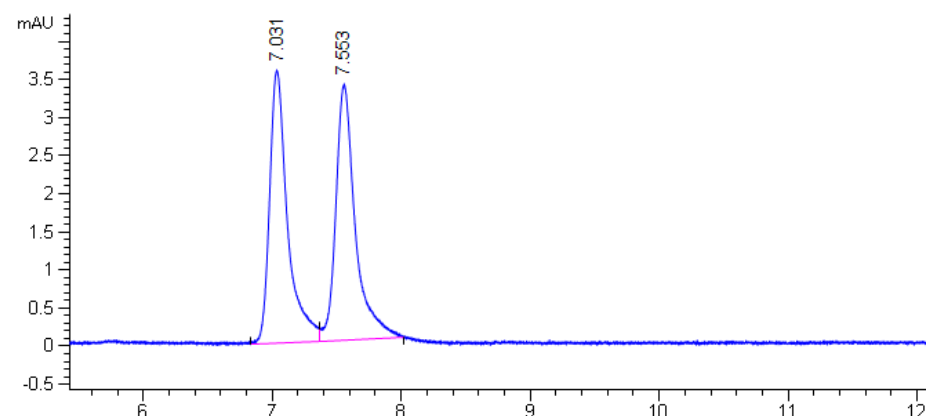
¹³C-NMR spectrum of 162 from the reductive amination of 161 and 76 with sodium borohydride



Achiral HPLC chromatogram of 162 from the reductive amination of 161 and 76 with sodium borohydride using Method 1



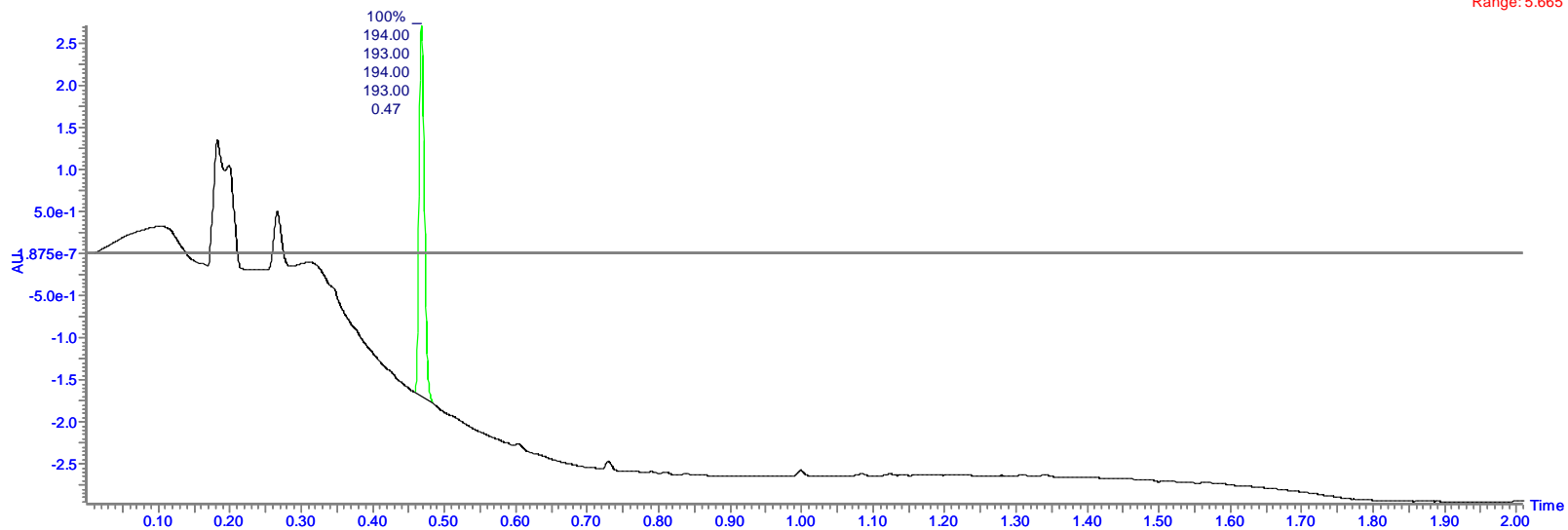
Chiral HPLC of racemic of 162 from the reductive amination of 161 and 76 with sodium borohydride using Method 3



LCMS chromatogram of 162 from the reductive amination of 161 and 76 with sodium borohydride using Method 4

UV Detector: TIC

2.712
Range: 5.665



SAMPLE: 1:13 Combine (117:130-(91:94+153:155))

2:MS ES-
8.3e+004



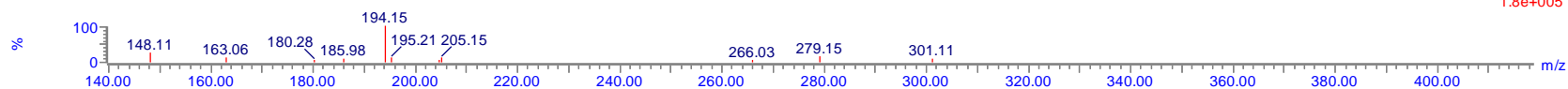
SAMPLE: 1:13 Combine (118:131-(91:94+153:156))

1:MS ES+
3.8e+006



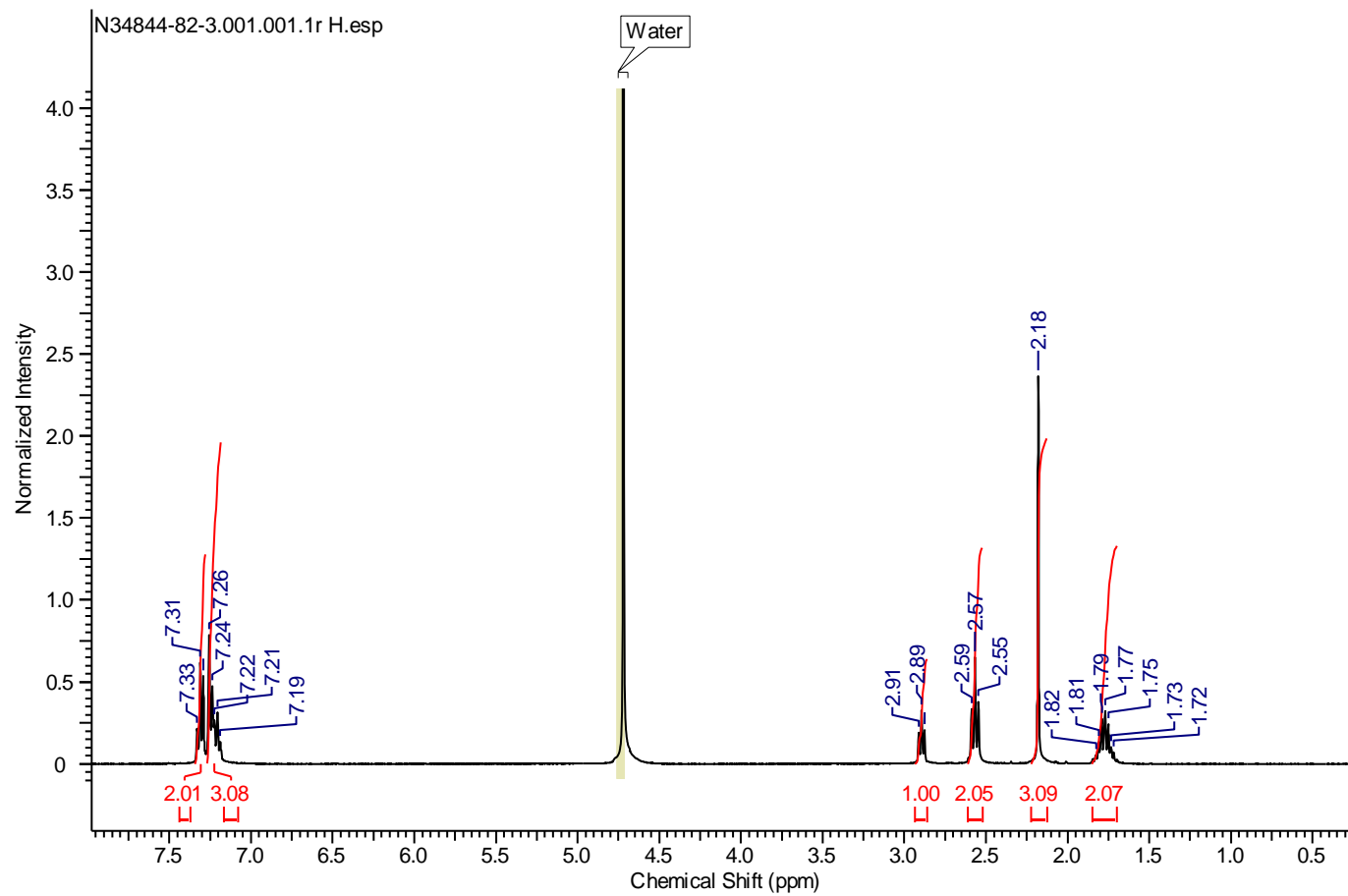
SAMPLE: 1:13 Combine (108:121-(82:85+145:148))

1:MS ES+
1.8e+005

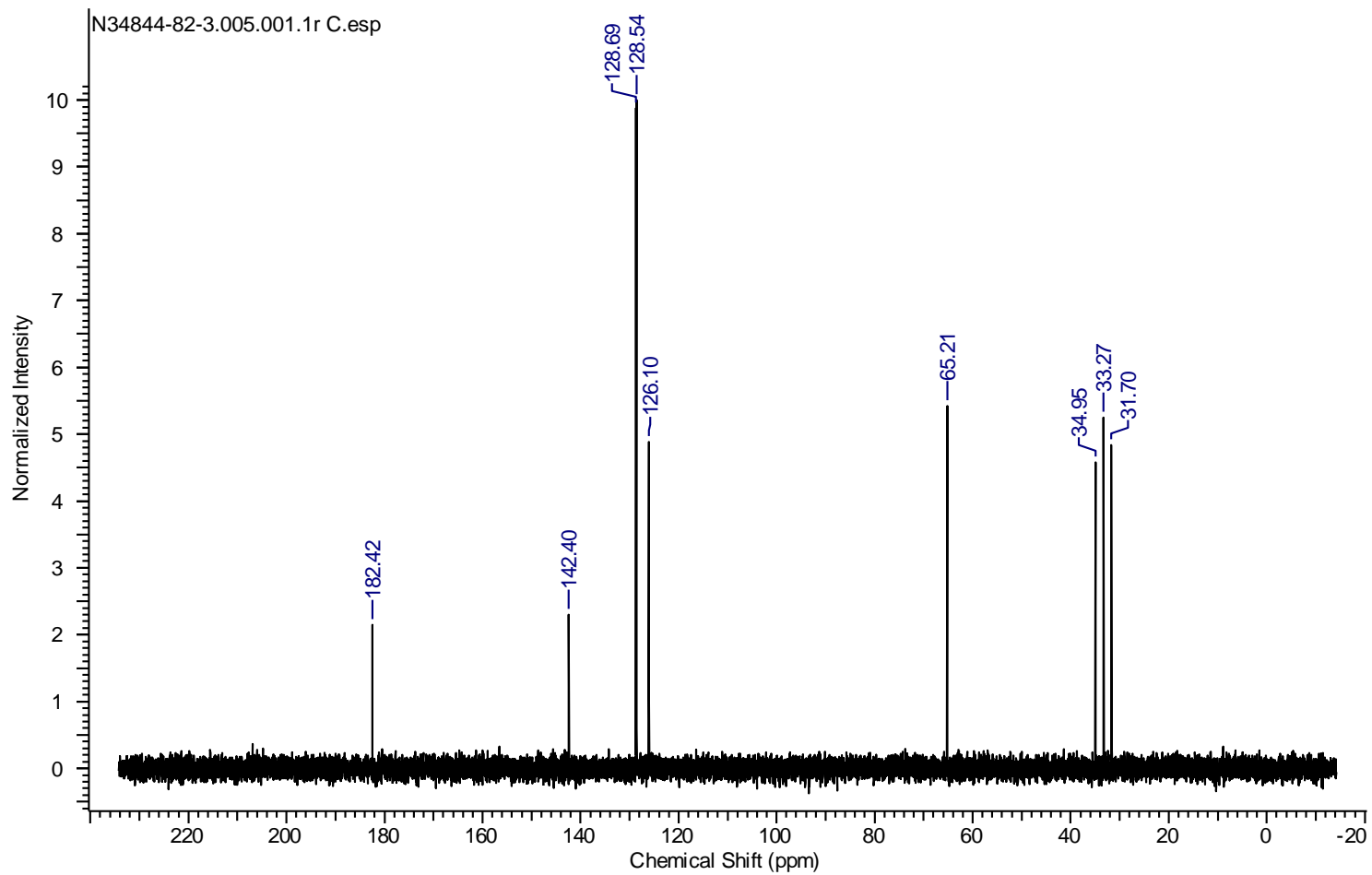


2-(Methylamino)-4-phenylbutanoic acid 164

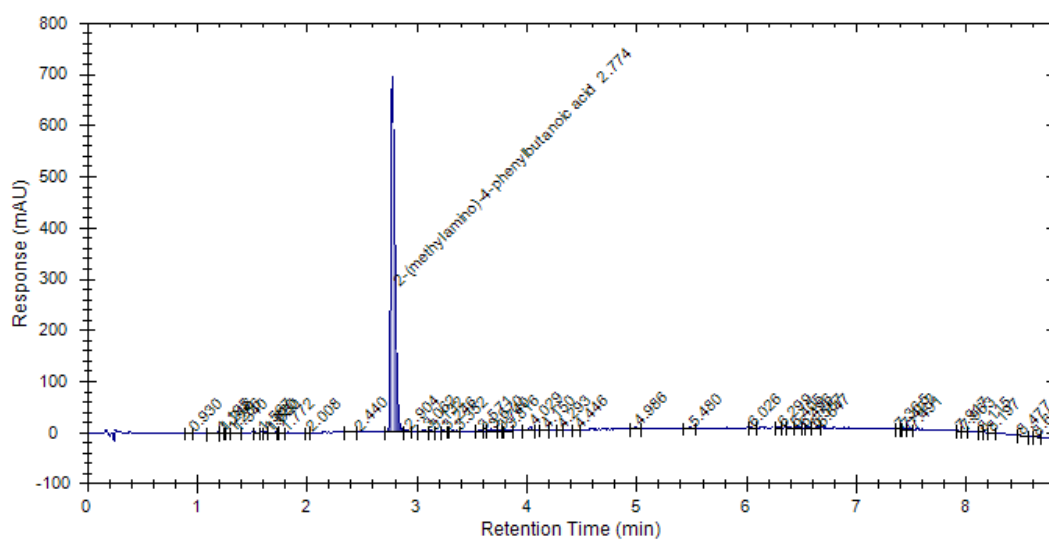
¹H-NMR spectrum of 164 from the reductive amination of 163 and 76 with sodium borohydride



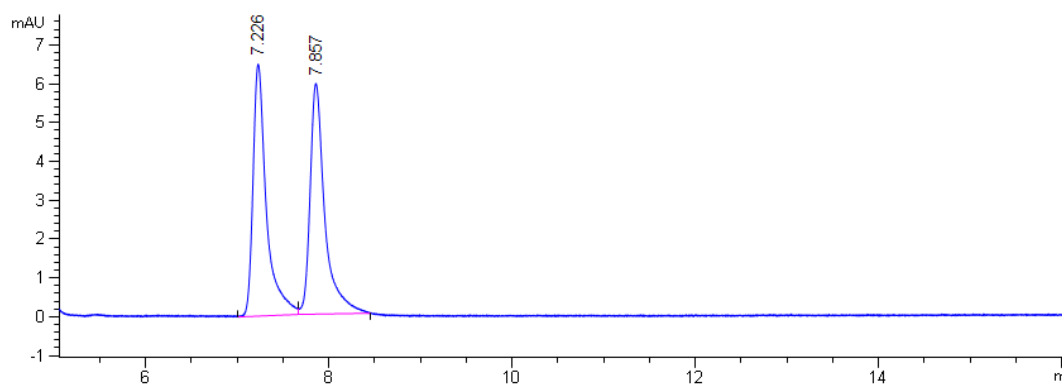
¹³C-NMR spectrum of 164 from the reductive amination of 163 and 76 with sodium borohydride



Achiral HPLC Chromatogram of 164 from the reductive amination of 163 and 76 with sodium borohydride using Method 1



Chiral HPLC of 164 using Method 3



LCMS chromatogram of 164 from the reductive amination of 163 and 76 with sodium borohydride using Method 5

